UNIVERSITAT de BARCELONA
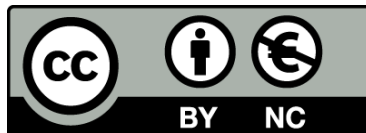
Cell death and cytokine-mediated inflammatory responses to glucose deprivation in cancer cells

Franziska Püschel

Cell death and cytokine-mediated inflammatory responses to glucose deprivation in cancer cells

Doctoral thesis for obtaining the
academic degree

Doctor of Philosophy

submitted by

Franziska Püschel

at the

Universitat de Barcelona

Faculty of Pharmacy

Program of Biomedicine

Institut d'Investigació Biomédica de Bellvitge (IDIBELL)

Supervisor: Dr. Cristina Muñoz-Pinedo
Tutor: Dr. Albert Tauler Girona

Barcelona, 2019

Affidavit

I hereby confirm that my thesis entitled 'Cell death and cytokine-mediated inflammatory responses to glucose deprivation in cancer cells' is the result of my own work. I did not receive any help or support from commercial consultants. All sources and / or materials applied are listed and specified in the thesis.

Furthermore, I confirm that this thesis has not yet been submitted as part of another examination process neither in identical nor in similar form.

_____   _____

 Place, Date   Franziska Püschel

_____   _____

Dr. Cristina Muñoz-Pinedo   Dr. Albert Tauler Girona
Supervisor   Tutor

Acknowledgement

First and foremost, I want to thank my supervisor Cristina Muñoz-Pinedo for offering me a PhD position in her lab and for giving me the possibility to work on this exciting project for the completion of my PhD thesis. I want to thank her for her continuous support, motivation and trust throughout the years. I also want to thank her for her steady positivity during the development of this project. She has not only been a great mentor and provided great guidance but also has been a great inspiration in many ways.

I want to thank my tutor Albert Tauler Girona for his mentorship and Francesc Viñals as well as Maria Jesus Pujol Sobrevia for being in my supervisory committee and for their feedback and evaluation of this project.

My gratitude also goes to the reviewer of this thesis, for taking their time and effort to evaluate this project and for being present at the final defence.

Furthermore, I want to thank Afshin Samali, the coordinator of the Marie Skłodowska-Curie Innovative Training Network (ITN) TRAINERS of the HORIZON2020 EU program, which provided the founding for this project. I want to thank him, for giving me the possibility to be one of the early stage career researchers (ESRs). I also want to thank all the principal investigators (PIs) and partners: Markus Rehm, Eric Chevet, Adrienne Gorman, Patricia Agostini, Simone Fulda, Leif Eriksson, Jackie de Belleroche, Andrey V. Kozlov, Aristotelis Chatziioannou and John Patterson for attending the six-monthly follow up meetings and for giving their feedback as well as for their inspiring ideas. I especially want to thank the project manager Sandra Healy for the great organisation. I also want to thank all the ESRs: Andreia Veríssimo Luís, Alexandra Papaioannou, Luigi Montibeller, Dimitrios Doultsinos, Aitor Almanza Goikoetxea, Antonio Carlesso, Brian Leuzzi, Chetan Chintha, Josip Skoko, Sanket Mohan More, Stuart Creedican, Nicole McCarthy and Maria Livia Sassano. I am very grateful for our six-monthly meetings around Europe. We did not only travel together to Galway, Paris, Rennes, Barcelona, Frankfurt, Brussels, London, Stuttgart and Dublin, spending an incredible amazing time together, but we also supported each other in our projects, discussed science and had the one or other memorable night out. During the years we became not only colleges but also friends and build up a network together with all the partners of TRAINERS, which I hope will be of our benefit in the future. Being part of the TRAINERS network was truly a great and rewarding experience.

Especially, I want to thank Eric Chevet for hosting me in his laboratory in the proteostasis and cancer team at the CLCC Eugène Marquis in Rennes, where I was able to perform my three-

5

6

Abbreviations

Abbreviation	Definition
ADCC	Antibody-dependent cellular cytotoxicity
AMPK	AMP-activated protein kinase
ATF4	Activating transcription factor 4
ATF6	Activating transcription factor 6
ATRA	All-trans retinoic acid
Breg	regulatory B cells
CAFs	Cancer-associated fibroblasts
CCL2/MCP-1	Chemokine (C-C motif) ligand 2, monocyte chemoattractant protein-1
CCL5/RANTES	Chemokine (C-C motif) ligand 5
CCL19	Chemokine (C-C motif) ligand 19
CCL20/ MIP-3α	Chemokine (C-C motif) ligand 20, macrophage inflammatory protein 3 alpha
CHOP	(C/EBP) homologous protein
CRC	Colorectal cancer
CREB	cAMP response-element binding
CTGF	Connective tissue growth factor
CTL-4	Cytotoxic T-lymphocyte-associated Protein 4
CXCL1	(C-X-C motif) ligand 1, GRO-α
CXCL2	(C-X-C motif) ligand 2, MIP2-α
CXCL3	(C-X-C motif) ligand 3, GRO-γ
CXCL5	(C-X-C motif) ligand 5, epithelial-derived neutrophil-activating peptide 78 (ENA78)
CXCL 12	(C-X-C motif) ligand 12
CXCR 1/2	C-X-C motif chemokine receptor 1
DC	Dendritic cells
DISC	Death inducing signal complex
DR4	TRAIL receptor 1, death receptor 4
DR5	TRAIL receptor 2, death receptor 5
DTT	Dithiothreitol
ECM	Extracellular matrix
EGFR	Epidermal growth factor receptor
eIF2α	Eukaryotic initiation factor 2α
EMT	Epithelial-mesenchymal transition
FADD	Fas-associated death domain
Fru	Fructose
GADD34	DNA-damage-inducible 34
GCN2	General control non-derepressible 2
Glc	Glucose

GlcNAc	N-Acetylglucosamine
Gln	Glutamine
HBP	Hexosamine biosynthetic pathway
HBSS	Hank´s Balanced Salt Solution
HRI	Heme-regulated eIF2α kinase
IKK	IκB kinase
IL-6	Interleukin-6
IL-8	Interneukin-8
IL-11	Interleukin-11
IFN γ	Interferon γ
IRE1	Inositol requiring kinase 1
ISR	Integrated stress response
JNK	c-Jun N-terminal Kinase
KRAS	Kirsten Rat Sarcoma
LKB1	Liver Kinase B1
MAMs	Mitochondria associated membranes
MAPK	Mitogen-activated protein kinase
MCS-F/(CSF-1)	Macrophage colony-stimulating factor, co-stimulatory factor 1
MDSC	Myeloid-derived suppressor cells
Me-Pyr	Methyl-pyruvate
miRNA	Micro RNA
mTOR	Mammalian target of rapamycin
mTORC 1/2	Mammalian target of rapamycin complex 1/2
NK cells	Natural killer cells
NRF2	Nuclear factor erythroid 2-related factor
NSCLC	Non-small-cell lung carcinoma
PARP	poly (ADP-ribose) polymerase
PBMCs	Peripheral blood mononuclear cells
PD-L1	Programmed death ligand 1
PDAC	Pancreatic ductal adenocarcinoma
PDGF	Platelet-derived growth factor
PERK	RNA-activated (PKR)-like endoplasmic reticulum kinase
PI	Propidium Iodide
PI3K	Phosphoinositide 3-kinase
PKR	Double-stranded RNA-dependent protein kinase
PMA	Phorbol 12-Myristate 13-Acetate
PTEN	Phosphatase and tensin homolog
RIDD	Regulated IRE1-dependent decay
ROS	Reactive oxygen species

siRNA	Small interfering RNA
SIRT1	Sirtuin 1
SPARC	Secreted Protein Acidic and Rich in Cysteine
TAMs	Tumor-associated macrophages
TANs	Tumor associated neutrophils
Tg	Thapsigargin
TILs	Tumor-infiltrating lymphocytes
TLR	Toll like receptor
TNFα	Tumor necrosis factor α
TNFR	TNF receptor family receptors
TRAF2	Tumour-necrosis factor-α (TNF-α)-receptor-associated factor 2
Treg	Regulatory T cells
tRNase	Transfer RNases
TSC2	Tuberin, Tuberous Sclerosis Complex 2
TSGs	Tumor suppressor genes
uORFs	upstream open reading frames
XBP1	X-box binding protein

Table of content

14

1. Summary

The reprograming of the cancer metabolism is considered as one of the hallmarks of cancer. Regarding that, new lines of research evolved in the last years which not only address the metabolism of cancer cells but also investigate the impact of the rewired cancer metabolism on the tumor microenvironment (TME). The TME is a heterogenic tissue, which consist not only of cancer cells but also of resident or infiltrating non-cancerous cells including for instance fibroblasts, cells of the vasculature and immune cells.

Metabolic alterations are primarily caused by oncogenic mutations in cancer cells, which modify the expression of metabolic enzymes and key regulatory proteins of biochemical reactions. Therefore, cancer cells use aerobic glycolysis instead of OXPHOS in the presence of oxygen, a phenomenon known as the ´´Warburg effect´´. The Warburg effect allows cancer cells to generate larger quantities of cellular building blocks such as proteins, nucleic acids and lipids, which are required for proliferation and cell growth. Moreover, cancerous cells are more dependent on glucose compared to non-transformed tissue, which in turn sensitises them to low glucose availability and makes cells more prone to cell death upon glucose deprivation. This opens up the door to new anti-cancer strategies based on the sensitivity of cancer cells to nutrient supply. In the last years new anti-metabolic drugs entered clinical trials, targeting the uptake and utilization of nutrients. In order to make these drugs more efficient and applicable in the clinic, it is necessary to fully investigate the cancer cell metabolism, especially how cancer cells die upon glucose deprivation and more importantly, the consequences on the surrounding tissue when modifying or interfering with the cancer metabolism.

The unfolded protein response (UPR) is an intracellular stress response that is known to be induced upon glucose deprivation in cancer cells. Cancer cells, which are exposed to glucose deprivation, fail to post translationally modify *de novo* synthesized proteins properly, which is possibly due to impaired glycosylation. Misfolded proteins are recognized by the ER intrinsic sensor proteins which induce the three UPR pathways: inositol requiring kinase 1 (IRE1), the activating transcription factor 6 (ATF6) and the protein kinase RNA-activated (PKR)-like endoplasmic reticulum kinase (PERK). The activation of the three branches of the UPR facilitates pro-survival responses mainly through the reduction of protein synthesis and through the upregulation of alternative metabolic pathways. However, chronic exposure to intra- or extracellular stresses result in a switch towards a pro-death UPR response, which goes along with the upregulation of the cell death machinery. The UPR is also described to be involved in pro-inflammatory responses based on the induction of cytokines and chemokines in several cell

lines. Therefore, the release of cytokines upon glucose deprivation could facilitate the infiltration or exclusion of specific immune cells.

This thesis aims to investigate how cancer cells die upon glucose deprivation and what are the adaptive responses cancer cells induce for survival. In detail, we hypothesized that the UPR, and other signaling pathways such as NF-κB and mTOR, which are modulated by glucose deprivation in cancer cells, promote the induction of cell death as well as the upregulation and secretion of cytokines. We further hypothesized that secreted cytokines promote the infiltration of immune cells from the surrounding tissue.

We found that HeLa cells, exposed to glucose deprivation, died in a TRAIL receptor 1- (DR4) and 2- (DR5) dependent manner. We also confirmed that HeLa cells undergo cell death in an UPR-dependent manner facilitated by the activating transcription factor 4 (ATF4). Moreover, ATF4 mediated the upregulation of the cell death receptor DR5 upon glucose deprivation in HeLa cells.

Furthermore, we found the release of pro-tumorigenic cytokines such as interleukin-8 (IL-8), interleukin-6 (IL-6) and the leukemia inhibitory factor (LIF) from glucose-deprived cancer cells. We also found that glutamine deprivation and the treatment with anti-metabolic drugs such as metformin promoted the release of IL-8 and IL-6, whereas the application of 2-deoxyglucose (2-DG) promoted the release of IL-8, IL-6 and LIF in several cancer cell lines. Investigating the regulation of cytokine induction upon glucose deprivation, we found that IL-6 and IL-8 but not LIF were regulated in an ATF4-dependent manner. We also investigated the role of the mTOR signaling pathway in cytokine induction by using the chemical inhibitors, rapamycin and Torin1. We found that rapamycin and Torin1 reduced IL-8 release upon glucose deprivation, whereas LIF release was only slightly reduced by rapamycin. Furthermore, we found that p65, the transcription factor of the NF-κB pathway, regulated the release of IL-8 and IL-6 as well as the mRNA of several other tested cytokines. However, LIF was not regulated in a p65-dependent manner upon glucose deprivation in HeLa and A549 cells. Moreover, the conditioned media of glucose-deprived A549 promoted the migration of macrophage-like THP-1 cells as well as of B cells and neutrophils isolated from human blood.

In conclusion, we found that nutrient deprivation as well as the application of anti-metabolic drugs induced the release of cytokines and chemokines from cancer cells. Moreover, conditioned media of starved A549 cells promoted the migration of some immune cells, which could have immunosuppressive functions in the TME. These findings are important, since interfering with the cancer metabolism by using anti-metabolic drugs could suppress their anti-tumorigenic effects by promoting more substantial pro-tumorigenic responses.

18

2. Introduction

Cancer is classically defined by the six hallmarks of cancer, which were acquired by oncogenic transformations and distinguishes them from non-cancerous cells. These hallmarks include, sustaining proliferation, resistance to cell death, evading growth suppressors, replicative immortality, and the ability to promote angiogenesis, invasion and metastasis (**Figure 1**) (Hanahan and Weinberg, 2011a). In general, cancer evolves due to genetic predeterminations or due to oncogenic mutations induced by environmental factors such as pollution or the exposure to toxins and ultraviolet (UV) light. Other causes are unhealthy life styles, poor diets and the lack of exercise, which are associated with obesity and in some cases predisposes to cancer (Stone et al., 2018). Other risk factors include smoking, which is associated with lung cancer (Hecht, 2002).
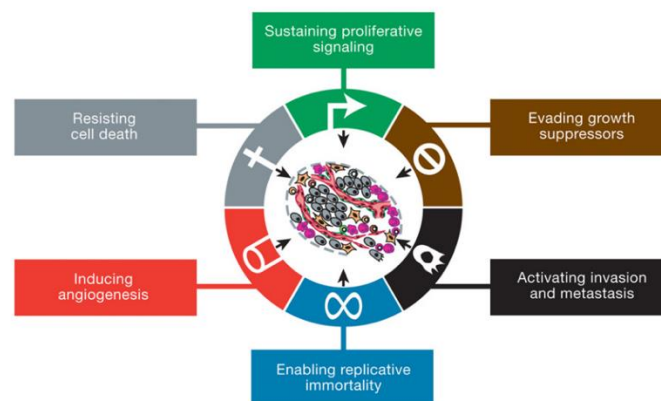
Figure 1 Hallmarks of cancer
Cancer is classified by six hallmarks including sustained proliferation, evading growth suppressors, activating invasion and metastasis, enabling replicative immortality, inducing angiogenesis and cell death resistance (Hanahan and Weinberg, 2011a).

The investigation of cancer and the development of new therapies are progressing rapidly in the last decades. However, common treatments like chemotherapy often fail and are insufficient due to the development of resistance or the relapse of patients years later. To overcome these drawbacks, there is a high demand for new strategies in order to improve patient survival. Currently, a new area in cancer research emerged, which gained strong interest in the last years, which is the personalized therapy. This form of therapy allows medical doctors to treat patients with adequate drugs according to their specific cancer type, based on mutational burdens and other patient specific characteristics. Another field is immunotherapy which focuses on the investigation of tumor-intrinsic immune cells and on the development of drugs that promote anti-tumorigenic responses. Regarding that, tumors are often considered as immunosuppressed

or as 'cold', meaning that anti-tumorigenic immune cells are inactivated or excluded from the tumor tissue. Hence, it is necessary to conduct further studies of the overall intra-tumoral interactions between cancer cells and immune cells.

Furthermore, the tumor tissue is also characterized by a hostile tumor microenvironment (TME), including regions of hypoxia, low nutrient supply as well as acidity. Tumor-intrinsic cell populations cope differently with these conditions, which promotes a variety of biological responses, such as migration, cytokine secretion or cell death. Moreover, these environmental alterations also affect the efficiency of chemotherapeutic drugs and influence patient responses to specific therapies. Cancer cells are more resistant to hostile environments compared to other cell populations, due to their oncogenic mutations. Oncogenic mutations allow cells to rewire their metabolism, which was first described by Otto Warburg (Warburg, 1956). Moreover, cancer cells are also able to induce cell-intrinsic stress signaling pathways, such as the unfolded protein response (UPR) upon perturbations in the endoplasmic reticulum (ER), to ensure survival. These adaptations give cancer cells advantages in terms of growth and survival compared to other tumor-intrinsic cell populations, such as immune cells. In this sense, many recent reports claim that in particular the adapted metabolism of cancer cells is associated with tumor immunosuppression (Chang et al., 2015).

Keeping this in mind, it is of high importance to understand how immune cells and cancer cells interact among each other under metabolic stress. Therefore, this thesis deals with the investigation of how cancer cells respond towards environments low in glucose with focus on the induction of the UPR and possible subsequent effects on cells of the immune system.

2.1 Cell metabolism

Anabolic biochemical reactions require energy and are utilized by the cell to synthesize complex macromolecules from smaller building blocks (Sullivan et al., 2016). Cells use catabolic biochemical reactions to produce energy by breaking down complex macromolecules into smaller units. Smaller units are metabolized and converted to adenosine triphosphate (ATP), which is the intracellular energy-unit. In order to fuel catabolic reactions, nutrients are uptaken from the extracellular environment in form of glucose, lipids or amino acids. These macromolecules are catabolized by the cell by various biochemical reactions to generate energy in form of ATP (Arnim McLaughlin, 2011).

In general, untransformed proliferating cells use glycolysis in the presence of oxygen to convert glucose to pyruvate, which is followed by oxidative phosphorylation (OXPHOS) in the mitochondria. Intermediate products derived from glycolysis and OXPHOS can be utilized for

anabolic biochemical reactions such as amino acid- and fatty acid- synthesis and *de novo* nucleic acid synthesis by the pentose phosphate pathway (PPP).

The balance between catabolic and anabolic pathways allow cells to convert extracellular nutrients into energy and to build up proteins, membranes as well as DNA and RNA for sustained proliferation and tissue growth. (Caro-Maldonado and Muñoz-Pinedo, 2011; Muñoz-Pinedo et al., 2012)

2.2 Glucose metabolism

Glycolysis, followed by OXPHOS, is the conventional biochemical pathway to produce ATP in the presence of oxygen in proliferating cells (**Figure 2**). Glucose uptake is facilitated by glucose transporters (GLUT), which are located in the cell membrane. Once uptaken, glucose is phosphorylated by the hexokinase (HK) to glucose-6-phosphate (G6P) in the cytoplasm of the cell. The glucose-6-phosphophate isomerase (GPI) converts G6P to fructose-6-phospate (F6P), which is further metabolized to two molecules of pyruvate, two molecules of ATP and two molecules of nicotinamide adenine dinucleotide (NADH). This pathway is known as glycolysis. In a next step is pyruvate, derived from glycolysis, converted by the pyruvate dehydrogenase complex (PDC) to acetyl-Coenzyme A (acetyl-CoA) that enters the tricarboxylic acid (TCA) cycle in the mitochondria, also known as Krebs cycle or citric acid cycle. In detail, acetyl-CoA enters the TCA cycle and is converted to various intermediate products as well as to three molecules of NADH and one molecule of reduced flavin adenine dinucleotide (FADH$_2$). Citrate is an intermediate products of the TCA cycle and can be exported from the mitochondria to the cytosol and converted to acetyl-CoA for lipid and amino acid synthesis (Levine and Puzio-Kuter, 2010).

During OXPHOS, protons (H$^+$) are pumped into the intermembrane space of the mitochondria, which is facilitated by the oxidation of NADH to NAD+ at the electron transport chain complexes I-IV. Electrons are accepted by oxygen (O$_2$) and protons are pumped back into the mitochondrial matrix through ATP synthase channels, using the concentration gradient of H$^+$, which catalyse the synthesis of ATP out of adenosine monophosphate (ADP) and phosphate. This process produces energy in form of 36 ATP molecules generated from one molecule of glucose. In the absence of oxygen pyruvate does not fuel the Krebs cycle but gets reduced to lactate by the lactate dehydrogenase (LDH) in the cytoplasm. This process is named anaerobic glycolysis, which yields lactate but only two molecules of ATP. However, this metabolic pathway is favoured by many cancer cells even in the presence of oxygen, known as the ´´Warburg Effect´´. (Cairns et al., 2011a; Ngo et al., 2015)

Introduction

Another way to metabolize glucose is the hexosamine biosynthetic pathway (HBP). In a first step is F6P and glutamine converted to glucosamine-6-phosphate (GlcN-6P) and glutamate (Glu), which is catalysed by the fructose-6-phosphate transaminase (GFAT) (Chiaradonna et al., 2018). The final product of the HBP is UDP-N-acetylglucosamine (UDP-N-GlcNAc). UDP-N-GlcNAc is transferred by O-GlcNAc transferases (OGT) to proteins, which is important for protein glycosylation. (Chiaradonna et al., 2018; Kim et al., 2018)

The PPP is a parallel biochemical pathway to glycolysis and needed for nucleic acid synthesis and the generation of nicotinamide adenine dinucleotide phosphate (NADPH). NADPH is a reducing molecule and needed for other cellular biosynthetic reactions such as fatty acids, cholesterol, nucleotides and amino acid synthesis. Glucose is converted to ribose-5-phosphate (R5P), which is a pentose sugar used for nucleic acid synthesis. (Laurence Cole, 2016)

In summary, glucose is uptaken from the cell and converted to intermediate products which fuel the TCA cycle for energy production in form of ATP, the HBP for post translational modifications of proteins and lipids, whereas the PPP is mainly used for nucleic acid synthesis. (**Figure 2**)
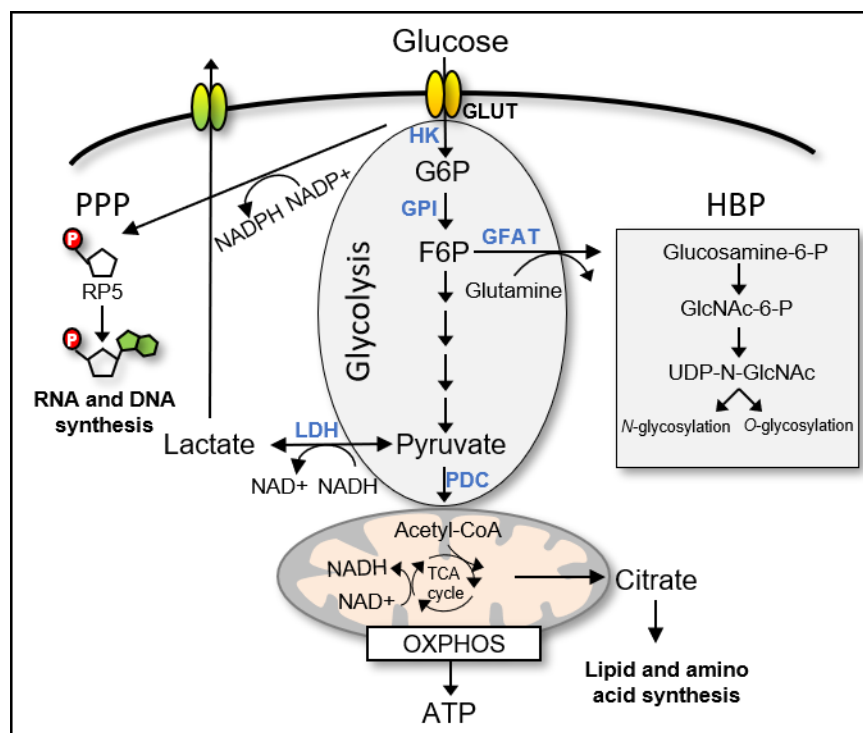
Figure 2 Glucose Metabolism
Glucose uptake is facilitated by glucose transporters (GLUT) in the cell membrane. During glycolysis in the cytoplasm is glucose converted to glucose-6-phosphate (G6P) by hexokinases (HK), and further converted to fructose-6-P (F6P) by the glucose-6-P isomerase (GPI). F6P is further metabolized to pyruvate including several intermediate steps. During the Warburg effect (aerobic glycolysis) pyruvate is reduced to lactate by the lactate dehydrogenase (LDH).

Pyruvate is converted to acetyl-CoA by the pyruvate dehydrogenase complex (PDC), which enters the tricarboxylic acid (TCA) cycle in the mitochondria. The TCA cycle produces various intermediate products and the generation of NADH. During OXPHOS at the mitochondrial respiratory chain complex is NADH oxidized to NAD+ and protons are pumped in the intermembrane space of the mitochondria. Protons are transported back by the ATP synthase I the mitochondrial matrix, generating adenosine triphosphate (ATP). Citrate, a TCA cycle intermediate product is exported to the cytosol where it is used for lipid, nucleic and amino acid synthesis. The hexosamine biosynthetic pathway (HBP) converts F6P and glutamine to glucosamine-6-phosphate, catalysed by the fructose-6-phosphate transaminase (GFAT). Glucosamine-6-phosphate is converted to UDP-N-GlcNAc, which is used for protein glycosylation. Glucose fuels the pentose phosphate pathway (PPP) parallel to glycolysis for the generation of nucleotides and nicotinamide adenine dinucleotide phosphate (NADPH). Glucose is converted to ribose-5-phosphate (R5P) by oxidation of NADH+ to NADPH.

2.3 Cancer metabolism

Tumor-associated alterations of the metabolism were announced as a hallmark of cancer (Hanahan and Weinberg, 2011b; Luo et al., 2009). Altered metabolic pathways allow cancer cells to adapt to their increased energetic needs in order to maintain fast proliferation rates.

The most important metabolic alteration is the increased uptake of nutrients, such as glucose and glutamine. These nutrients fuel anabolic biochemical reactions to produce cellular building blocks for instance for lipid membrane generation. (Deberardinis et al.; Heiden et al., 2009) Furthermore, metabolic alterations also lead to alterations in intracellular stress signaling pathways (Panieri and Santoro, 2016). Cancer cells acquired an altered metabolism mostly due to evolutionary induced oncogenic mutations, which promotes their competitiveness in hostile regions of the TME. These regions are marked by low oxygen and nutrient supply as well as by pH changes. One of the major oncogenic mutations that promote a rewiring of the metabolism, are mutations in the KRAS (Kirsten rat sarcoma) gene, which is a proto oncogene that belongs to the RAS family of GTPases. In its active state it binds guanosine triphosphate (GTP) and activates several downstream pathways like the mitogen activated kinase-like protein (MAPK) or the phosphatidylinositol 3-kinase (PI3K)/AKT/mTOR pathway. Its mutation occurs in cancers like colorectal cancer (CRC), pancreatic ductal cell carcinoma (PDCA) and most frequently in non-small cell lung cancer (NSCLC) (Kawada et al., 2017). One third of lung adenocarcinomas contain a KRAS mutation, which promotes proliferation, suppression of apoptosis and most importantly metabolic reprogramming (Pylayeva-Gupta et al., 2011; Rajalingam et al., 2007). With focus on lung cancer, it is described that homozygous Kras$^{G12D/G12D}$;p53$^{-/-}$ tumors increase the expression of glycolytic genes (Kerr et al., 2016). This is accompanied by enhanced nutrient uptake, increased autophagy and higher energetic and anabolic needs (Pylayeva-Gupta et al., 2011).

Introduction

Another oncogenic mutation is the deletion of phosphatase and tensin homolog (PTEN), which is a tumor suppressor and inhibitor of the PI3K pathway. A constitutively active PI3K pathway promotes increased tumor growth. The AKT serine/threonine kinase 1 (AKT) is the main downstream effector of PI3K and promotes glycolysis through the expression and the transport of glucose transporters to the membrane. (Elstrom et al., 2004) The downstream effector of AKT is the mTOR pathway, which regulates protein synthesis. AKT inactivates the negative regulator tuberous sclerosis complex 2 (TSC2), which results in a hyperactivation of the mammalian target of rapamycin (mTOR) signaling pathway and subsequently to increased protein and lipid synthesis (Cairns et al., 2011b; Robey and Hay, 2009)

2.3.1 The Warburg Effect

Proliferation and the energy metabolism of untransformed cells is controlled by growth and survival factors. Only when stimulated cells take up nutrients from the extracellular environment. In contrary to untransformed cells, cancer cells take up continuously high amounts of nutrients such as glucose (Hay, 2016) and glutamine (Altman et al., 2016) even without stimulation by growth factors.

The oncogenic mutations discussed before, and many others, are responsible for the altered metabolism and increased glucose uptake. Glucose is utilized as one of the main sources for energy production in tumor tissue, which allows cancer cells to increase their proliferation rates and fasten tumor growth. Differentiated non-tumorigenic tissue converts glucose to pyruvate by glycolysis which fuels the TCA cycle in the mitochondria, and which is finally oxidized by OXPHOS to CO_2 yielding 36 mol of ATP per mol glucose. This reaction needs oxygen as electron acceptor during OXPHOS. If oxygen is not available cells undergo anaerobic glycolysis in which pyruvate does not fuel the TCA cycle in the mitochondria but is redirected for the conversion into lactate by glycolysis. This reaction yields two molar equivalents of ATP per mol glucose and is therefore less energy producing.

Otto Warburg discovered in the 1920s that the metabolism of tumor cells mainly consists of aerobic glycolysis. That means that cancer cells convert glucose to pyruvate followed by the conversion to lactate by glycolysis even in the presence of oxygen. This metabolic reaction is called aerobic glycolysis or the ´´Warburg effect´´ (**Figure 3**). (Warburg, 1956; Warburg et al., 1927) First it was assumed that this was to be due to impaired mitochondrial functions, which was disproved in the last years. Nowadays the mitochondria is awarded with many important functions involved in cancer progression (Porporato et al., 2018).

In patients, the high glycolytic tumor activity can be visualized by ^{18}F-deoxyglucose positron emission tomography (FDG-PET). It is based on a radioactive fluorine-labelled glucose
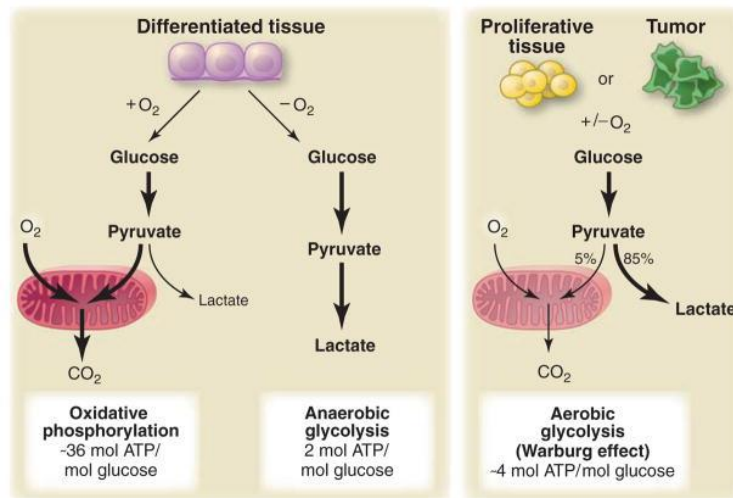
Figure 3 Schematic representation of metabolic differences between differentiated tissue and tumor tissue
Oxidative phosphorylation (OXPHOS): In the presence of oxygen, differentiated tissue converts glucose to pyruvate by glycolysis, which is further oxidized in the mitochondria to CO_2. OXPHOS requires O_2 as final electron acceptor. This results in the generation of energy in form of 36 mol ATP per metabolized mol glucose.
Anaerobic glycolysis: In the absence of oxygen in differentiated tissue glucose is metabolized in the cytoplasm to pyruvate, which is enzymatically converted to lactate by glycolysis. The conversion of pyruvate to lactate instead of its oxidation by OXPHOS yields only in two mol of ATP per mol glucose.
Warburg effect (aerobic glycolysis): Tumor tissue and proliferating tissue uses only small portions for OXPHOS and favour lactate generation by glycolysis independent of oxygen availability (Vander Heiden et al., 2009)

analogue, which is uptaken by the tumor tissue. Afterwards, radioactivity of certain tissue can be visualized. Nowadays this technique is an important clinical tool for cancer monitoring. (Almuhaideb et al., 2011)

The Warburg effect allows cancer cells to utilize nutrients for anabolic biosynthetic pathways by reducing the generation of energy in form of ATP. This is beneficial for the cells since consequentially cells produce higher amounts of macromolecules, which fuel cell growth and proliferation. Today's assumption is that the Warburg effect, along with a reprogrammed metabolism, is based on oncogenic transformation accompanied by loss-of-function of certain tumor suppressor genes, as well as altered growth factor signaling. (Vaupel et al., 2019)

2.4 AMPK and mTOR signaling

The altered metabolism of cancer cells goes along with an increased glucose dependency compared to untransformed tissue. Hence, glucose plays a crucial role in tumor progression and

Introduction

if glucose is limited in the extracellular environment, cells undergo cell cycle arrest and stop growing. When glucose deprivation is sustained, cell death promoting pathways are upregulated and cells undergo cell death. (El Mjiyad et al., 2011) However, cancer cells developed mechanisms which allow them to survive periods of low glucose availability mainly by the upregulation of alternative metabolic pathways for energy production. In order to sense low glucose level, cells possess glucose-sensing mechanisms. One of them is the activation of the AMP-activated protein kinase (AMPK) and subsequent inhibition of mTOR signaling. (**Figure 4**) A major consequence of low glucose availability is an ATP drop in the cell due to reduced OXPHOS, which is sensed by AMPK. Low glucose availability changes the adenosine monophosphate (AMP)/ATP ratio, which functions as a metabolic checkpoint. If the AMP/ATP ratio is increased AMPK is phosphorylated and activates downstream signaling pathways resulting in growth inhibition. (Gowans and Hardie, 2014) Moreover, recently it was shown that a cellular decrease in Fructose-1,6-bisphosphate (FBP), a glycolytic intermediate product, promotes AMPK activation independently of ATP (Lin and Hardie, 2018; Zhang et al., 2017a). The liver kinase B1 (LKB1), which is frequently deleted in non-small-lung cancer (NSCLC) (Ji et al., 2007), is an activator of AMPK. AMPK phosphorylation induces a metabolic switch in nutrient utilization, favouring fatty acid oxidation and catabolic processes such as autophagy (Hardie, 2007; Jeon, 2016; Salt et al., 1998). Interestingly, in cancer cells several oncogenic mutations suppress AMPK signaling, which promote cell growth even in nutrient poor environments (Lin and Grahame Hardie, 2018).

AMPK is also an inhibitor of the mTOR pathway, which is another key sensor of cellular nutrient availability and involved in the regulation of protein synthesis (Tokunaga et al., 2004). mTOR is the catalytic subunit of the functional distinct complexes mTORC1 and mTORC2. mTORC1 is activated by growth factors, energy level or amino acids, whereas mTORC2 is regulated by growth factors. Activated mTORC1 phosphorylates the p70 ribosomal protein S6 Kinase (p70S6K), which subsequently phosphorylates ribosomal protein S6 (S6). Furthermore, mTORC1 also phosphorylates the elongation initiation factor (EIF)-4E Binding Protein 1 (4EBP-1). Dephosphorylation of these proteins results in decreased protein, nucleotide and lipid synthesis as well as cellular growth arrest. (**Figure 4**) mTORC2 activates among others protein kinase B (AKT) as well as Protein-Kinase C (PKC) and controls cell structure. (Conciatori et al., 2018)

The mTOR pathway is constitutively active in proliferating cells, promoting protein synthesis and cell growth. However, activation of AMPK by glucose deprivation leads to an inactivation

of mTOR and subsequently an attenuation of protein synthesis to restore energy. (El Mjiyad et al., 2011)

Inhibition of mTOR signaling is a potent anti-cancer target and several mTOR inhibitors were developed in the last years. Among them is rapamycin (Sirolimus) a macrocyclic antibiotic, that is described to specifically inhibit mTORC1 (Ballou and Lin, 2008), whereas Torin1, an ATP-competitive inhibitor, blocks both mTOR complex 1 and 2 (Thoreen et al., 2009).
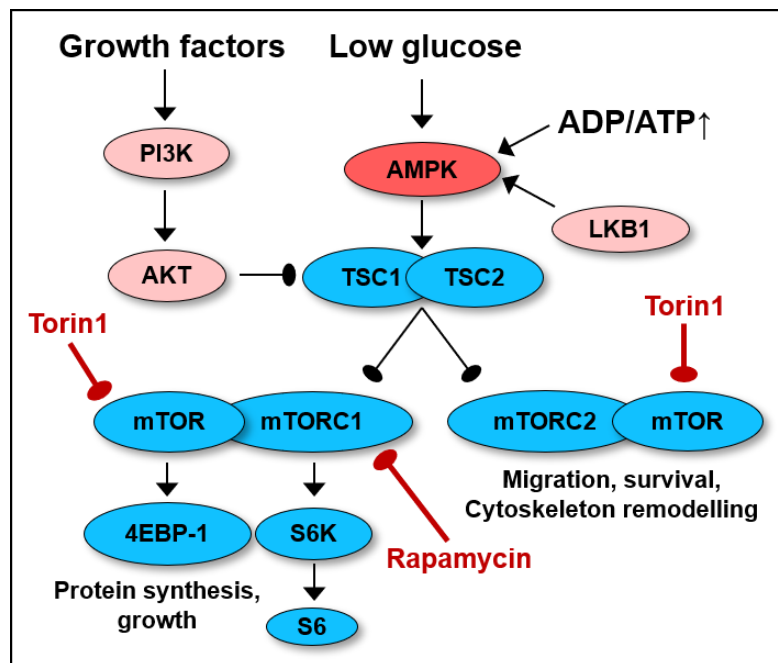
Figure 4 Schematic presentation of AMPK/mTOR signaling
Growth factors promote phosphatidylinositol 3-kinase (PI3K) signaling through AKT, that inactivates the tuberous sclerosis complex 1 and 2 (TSC1) and (TSC2). TSC1 and 2 inhibit the mammalian target-of-rapamycin (mTOR), which is present in the mTOR complex 1 and 2. Activation of mTORC1 leads to the phosphorylation of S6K and subsequently S6 as well as 4EBP-1 and promotes protein synthesis. Phosphorylation of mTORC2 regulates migration, survival and cytoskeleton remodelling.
The AMP-activated protein kinase (AMPK) is activated by low glucose level sensed by an ATP drop. Phosphorylated AMPK activates TSC1 und 2 and inhibits mTOR signaling. Rapamycin is a mTOR inhibitor which blocks mTORC1 whereas Torin1 blocks mTORC1 and 2.

2.5 The impact of glucose deprivation on cancer cells

Cancer cells are highly dependent on glucose and their metabolic requirements makes them more susceptible towards glucose deprivation compared to untransformed cells. Several pathological scenarios within the body tissues or in a tumor result in nutrient and glucose deprivation. Among them are vessel occlusions, which result in transient ischemia and fast tumor growth, which results in poor vascularisation and therefore in low nutrient supply of certain regions of the tumor. Moreover, the application of anti-angiogenic or anti-metabolic drugs, which either inhibit the formation of vessels or the uptake and metabolization of nutrients also promote starvation in the tumor tissue.

Glucose availability is not only essential for proper metabolic functions and macromolecule generation, but it is also involved in epigenetic gen regulation. Glucose is converted to acetyl-CoA from citrate, a mitochondrial intermediate product from the TCA cycle, which is involved in acetylating histones in the nucleus and therefore in gene regulation (Wellen et al., 2009). Acetyl-CoA and other metabolites also function as co-factors for epigenetic enzymes, which regulate DNA-methylation (Donohoe and Bultman, 2012). This could be a regulatory mechanism in order to reduce gene expression upon nutrient limitation to reduce the energy expenditure of the cell.

Furthermore, low glucose level result in a drop in the ATP level of some cells, which is a consequence of reduced OXPHOS. Reduced ATP level result in AMPK activation and mTOR inhibition as described before, to reduce the energetic needs of the cell. Moreover, glucose deprivation leads to an impaired glycosylation, which is an important posttranslational modification of many proteins. This is due to a reduced HBP which is not sufficiently fuelled by glucose. The HBP converts glucose in UDP-GlcNAc, a substrate for intracellular *O*-linked-glycosylation as well as for extracellular glycoconjugates (Vasconcelos-dos-Santos et al., 2015). Impaired *N*-linked glycosylation at the ER leads to an accumulation of glycosylated proteins in the ER, which promotes the induction of the UPR.

Taken together, glucose deprivation has severe effects on the homeostasis of metabolic pathways as well as on the regulation of gene transcription and on qualitative protein folding that promotes, upon sustained starvation, cell death. However, cancer cells upregulate adaptive signaling pathways to cope and resolve the cellular stress induced by glucose deprivation. Regarding that, one of the most important stress signaling pathways, which is induced upon glucose deprivation, is the UPR.

2.6 Anti-metabolic drugs

Since glucose and other nutrients play an essential role in proliferation and growth, targeting the cancer metabolism is seen as a promising anti-cancer therapy. Anti-metabolic drugs are in development based on the Warburg effect and the increased glycolytic activity of cancer cells. Amongst them is 2-deoxyglucose (2-DG), an anti-glycolytic drug that is uptaken by the cell and promotes the inhibition of the glycolytic enzymes HK and GPI (WICK et al., 1957) (**Figure 2**). Hence, 2-DG treatment results in an ATP drop (Karczmar et al., 1992) and in the inhibition of glycosylation. Several forms of protein glycosylation are described in the literature; however, the two most important forms are *O*-linked-glycosylation and *N*-linked glycosylation. *O*-linked-glycosylation is the form by which an *O*-linked N-acetylglucosamine (GlcNAc), derived from the HBP modification is transferred to a serine or threonine protein residue. UDP-GlcNAc is the product of the HBP. *N*-linked glycosylation is mostly carried out at the ER by the transfer of oligosaccharides to asparagine residues. *N*-linked glycosylation is prevented by tunicamycin treatment, a known UPR inducer and is thought to be the most vulnerable glycosylation form, that is impaired by glucose deprivation (Kang and Hwang, 2006). 2-DG blocks *N*-linked glycosylation and consequently, non-glycosylated proteins accumulate in the ER and facilitate the induction of the UPR (León-Annicchiarico et al., 2015a), as well as the sensitization of tumors cells towards cell death (Muñoz-Pinedo et al., 2003)

Another anti-metabolic drug is metformin which is commonly used for treatment of patients with type II diabetes; however, it gained strong interest in the last years as an anti-cancer drug (Libby et al., 2009) especially for NSCLC (Levy and Doyen, 2018) and pancreatic cancer (Zhou et al., 2017). Metformin inhibits complex I of the respiratory chain in the mitochondria during OXPHOS (Owen et al., 2000), which results in an ATP drop . An increased ADP/ATP ration activates AMPK, which subsequently inhibits mTOR signaling and cell growth (Zhou et al., 2001). There are many more modes of actions described for metformin both systemically as well as at cellular level including the activation of the UPR, which will be described in the following chapter. However, impacts at cellular level are cell type and concentration dependent. However, the detailed mechanism of its anti-cancer effect is not completely understood yet. (Rena et al., 2017)

2.7 The Unfolded Protein Response

The UPR is a stress response induced in the ER due to an overload of misfolded or unfolded proteins. The UPR triggers the transcriptional machinery, promoting the induction of target proteins, which are involved in the resolution of the stress. These proteins promote, among others, the upregulation of alternative metabolic signaling pathways or the Endoplasmic-reticulum-associated protein degradation (ERAD) to reduce the protein load and to restore cell homeostasis. Furthermore, a sustained activation of the UPR promotes the induction of pro-apoptotic proteins, promoting to cell death.

In general, the UPR is induced due to intrinsic or extrinsic perturbations of the cell. Intrinsic perturbations include oncogenic mutations, which promote sustained cell growth, proliferation and differentiation. This is accompanied by increased protein synthesis that leads to a protein overload of the ER and can induce the UPR.

Extrinsic perturbations include microenvironmental stresses such as non-physiological temperatures, alterations in pH and acidification and reactive oxygen species (ROS) production. The application of drugs and toxins are also described to function as ER stressors. In detail, microenvironmental perturbations occur in a tumor due to its rapid tumor growth, which is accompanied by nutrient and oxygen depletion, causing local microenvironmental stress including hypoxia, starvation and acidosis. Another extrinsic perturbation is ROS. The ER lumen is under normal conditions highly oxidized compared to the cytoplasm in order to facilitate the formation of disulphide bounds for proper protein folding. Moreover, an oxidized environment prevents the accumulation of unfolded protein aggregates in the ER lumen (Almanza et al., 2019; Zeeshan et al., 2016a). Therefore, high ROS level disturb cellular signaling pathways and functions and promote the UPR. Other extrinsic perturbations of the cell include drugs such as tunicamycin or thapsigargin. Thapsigargin targets the Sarco/ER Ca^{2+} -ATPase (SERCA) which pumps Ca^{2+} in the ER for proper protein folding. Thapsigargin treatment results in a Ca^{2+} decrease in the ER lumen and subsequently in the accumulation of unfolded proteins. Tunicamycin blocks the *N*-linked glycosylation by inhibiting the GlcNAc phosphotransferase (GPT). As a consequence, oligosaccharides cannot be transferred to nascent polypeptides, which results in impaired protein glycosylation at the ER. Proteins are recognized as misfolded or unfolded and induce the UPR. (Hemming, 1985) 2-DG, which is an anti-glycolytic drug (see also chapter 3.7), blocks glycosylation due to its interference with the glucose metabolism (Simons et al., 2009). Other UPR inducing drugs are Dithiothreitol (DTT), which inhibits protein disulphide bond formation (Cleland, 1964) and Brefeldin A, which prevents the trafficking of proteins from the ER to the Golgi apparatus (Liu et al., 1992).

Intrinsic and extrinsic perturbations lead to a protein overload or an accumulation of misfolded or unfolded proteins in the ER. If the accumulation of un- and misfolded proteins in the ER exceeds the threshold, the UPR sensors are activated. These sensors induce transcriptional or translational genes and proteins, which are involved in the clearance of the unfolded/misfolded proteins from the ER. Furthermore, the induction of the UPR also increases the capacity of the ER to fold proteins correctly in order to regain cell homeostasis (Almanza, Püschel et al., 2019). The major sensor for un- and/or misfolded proteins in the ER lumen is the ER resident chaperone, heat shock protein A5 (heat shock protein family A (Hsp70) member 5) also known as glucose-regulated protein 78 (GRP78) or binding immunoglobulin protein (BiP). Under unstressed conditions BiP is bound by the luminal domains of the three key transmembrane ER stress sensors: inositol requiring kinase 1 (IRE1), the activating transcription factor 6 (ATF6) and the protein kinase RNA-activated (PKR)-like endoplasmic reticulum kinase (PERK) (Figure 5). If there is an accumulation of unfolded or misfolded proteins in the ER, BiP binds to these proteins and dissociates from the luminal domain of IRE1, ATF6 and PERK. IRE1 activation can further be regulated by the ER luminal co-chaperone ERdj4/DNAJB9, which represses IRE1 activation by promoting a complex between the luminal domain of IRE1 and BiP (Amin-Wetzel et al., 2017).

To sum it up, dissociation of BiP from the UPR key stress sensor proteins elicits the UPR response by activating the three UPR branches of the UPRosome, which will be explained in detail below. (reviewed in Almanza, Püschel et al., 2019)
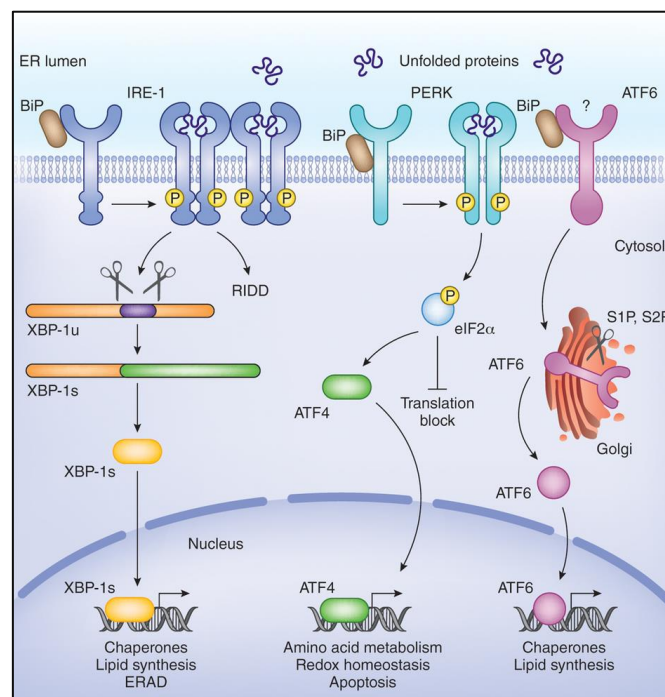
Figure 5 The Unfolded Protein Response
The UPR is induced upon accumulation of unfolded proteins in the ER lumen. BiP dissociates from the UPR stress sensors: IRE1, PERK and ATF6. IRE1 oligomerizes and auto-phosphorylates to activate the cytosolic RNase domain. The RNase domain cleaves dual stem loops within the XBP1 mRNA. Spliced XBP1 (XBP1s) translocates to the nucleus and functions as transcription factor for chaperons, genes involved in ERAD and lipid synthesis. The RNase activity of IRE1 degrades other mRNAs through the regulated IRE1-dependent decay (RIDD). ATF6 translocates to the Golgi apparatus upon activation where it is cleaved. Cleaved ATF6 translocates to the nucleus where it functions as a transcription factor for chaperones and genes involved in lipid synthesis. PERK autophosphorylates upon activation and phosphorylates eIF2α, that leads to an attenuation of protein synthesis. However, ATF4 is selectively induced and leads to the induction of genes involved in amino acid metabolism, redox homeostasis and apoptosis. (Janssens et al., 2014)

2.7.1 ATF6 signaling

ATF6 is a leucine zipper protein and can be encoded in humans by ATF6 A for ATF6α or ATF6 B for ATF6β. After dissociation from BiP, ATF6 gets translocated from the ER membrane to the Golgi apparatus where it is cleaved by the Golgi-resident protease membrane bound transcription factor peptidase, site-1 (MBTPS1) and site-2 (MBTPS2). A ~400 amino acid long fragment gets released, which corresponds to the ATF6 cytosolic N-terminal portion (ATF6N). ATF6N contains a transcription activation domain (TAD), a bZIP domain, a DNA-binding domain and a nuclear localization signal. In the nucleus it functions as a transcription factor, involved in the expression of its target genes (**Figure 5**). Moreover, ATF6 can also induce the transcription of XBP1 and CHOP to enhance UPR signaling (Yoshida et al., 2001).

2.7.2 IRE1 signaling

The IRE1 branch is the most conserved arm of the UPR and plays crucial roles in many processes including development, immunity, inflammation and metabolism. In humans two paralogues exist for IRE1 (IRE1 α and β) encoded by endoplasmic reticulum to nucleus signaling 1 and 2 (*ERN1* and *ERN2*) genes. IRE1α is expressed in all tissues however, IRE1β expression is restricted to the gastrointestinal tract and the pulmonary mucosal epithelium.

IRE1 activation results in its oligomerization at the luminal sensor domain and the activation of the cytosolic effector domains, which contain the kinase and RNase subdomains. Oligomerization facilitates the trans-autophosphorylation in the activation loop of the kinase domain, specifically at the Ser724, Ser726 and Ser729. Phosphorylation is necessary to activate the cytosolic RNase domain, as well as for the recruitment of the TNF receptor-associated factor 2 (TRAF2) and for the activation of the c-Jun N-terminal Kinase (JNK) pathway (Urano, 2000). The RNase domain catalyses the splicing of a 26-nucleotide intron from unspliced mammalian X-box binding protein 1 (XBP1) mRNA. The splicing of the 26 base intron from the XBP1

mRNA produces spliced XBP1 (XBP1s), which functions as a transcription factor (Sidrauski and Walter, 1997). XBP1s is a basic leucin zipper (bZIP) transcription factor. The unspliced form of XBP1 (XBP1u) is not able to function as a transcription factor due to the lack of a transactivation domain. The XBP1u C-terminal region contains a P (proline), E (glutamic acid), S (serine) and T (threonine) motif, which is responsible for the destabilization and short half-life of the protein. The N-terminal domain of XBP1u also contains a hydrophobic region that targets XBP1u to the ER membrane and a domain that promotes efficient XBP1 splicing and cleavage by preventing XBP1 translation (Yanagitani et al., 2009). XBP1 promotes the transcription of chaperones, foldases and components of ERAD (**Figure 5**). Moreover, XBP1 can interact with other transcription factors like AP1, oestrogen receptor α (ERα), cAMP response element-binding protein (CREB)/ATF and the hypoxia inducible factor 1 α subunit (HIF1α). XBP1s is also involved in the regulation of metabolic pathways such as lipid biosynthesis, glucose metabolism, DNA repair, differentiation and development.

The RNase activity of IRE1 also targets other mRNA transcripts promoting their degradation through the regulated IRE1-dependent decay (RIDD), which as a consequence reduces protein synthesis (Hollien et al., 2009). Thereby, IRE1 cleaves mRNA transcripts containing the consensus sequence (CUGCAG) accompanied by a stem-loop structure. The cleaved RNA fragments are rapidly degraded by cellular endoribonucleases. (Almanza, Püschel et al., 2019)

2.7.3 PERK signaling

The third branch of the UPR is the PERK signaling pathway. PERK is ubiquitously expressed in the body and contains a cytosolic kinase domain and an ER luminal sensor domain. PERK is activated due to BiP dissociation from its luminal domain, oligomerization and trans-autophosphorylation and the subsequent phosphorylation on Ser51 of the eukaryotic initiation factor α (eIF2α). eIF2α is a subunit of the eIF2 heterotrimer, which regulates the initiation step of protein synthesis. It promotes the binding of the initiator tRNA to the 40S ribosomal subunits. However, phosphorylated eIF2α (peIF2α) inhibits the eukaryotic translation initiation factor 2B (eIF2B) activity and thereby attenuates protein synthesis and reduces protein load in the ER. However, transcripts containing short upstream open reading frames (uORFs), like the activating transcription factor 4 (ATF4), which is a member of the cAMP response-element binding (CREB) family of transcription factors, are translated (**Figure 5**). Under normal conditions these transcripts are inefficiently translated from the protein coding AUG sequence. However, attenuation of translation from uORFs shifts translation initiation towards the protein coding AUG, leading to a more efficient synthesis of selectively ATF4 (Harding et al., 2000).

Introduction

ATF4 is the major transcription factor of the CAAT/enhancer-binding protein (C/EBP) homologous protein (CHOP)/GADD153 by binding to the C/EBP-ATF site in its promotor (Kato and Nishitoh, 2015). The induction of genes induced by ATF4 and CHOP can result in ATP depletion, oxidative stress and cell death (Han et al., 2013). Growth arrest and DNA-damage-inducible 34 (GADD34) is a negative regulator of eIF2α. GADD34 interacts with the catalytic subunit of type 1 protein serine/threonine phosphatase (PP1), which dephosphorylates eIF2α. GADD34 is transcriptionally induced by ATF4 and CHOP and facilitates a negative feedback loop that antagonizes p-eIF2α-dependent translation inhibition and restores protein synthesis. Protein translation attenuation serves the cell to restore protein load in the ER and to save energy (Kato and Nishitoh, 2015). ATF4 translation further promotes gene transcription involved in amino acid transport and metabolism, protection from oxidative stress, protein homeostasis and autophagy.

ATF4 can also be induced by one of the four integrated stress response (ISR) family members: PERK, double-stranded RNA-dependent protein kinase (PKR), heme-regulated eIF2α kinase (HRI), and general control nonderepressible 2 (GCN2). The kinases catalytic domains of the four regulators are homolog and promote in the phosphorylation of eIF2α as described before. However, their activation domains are distinctive and so are the activation stimuli. GCN2 is mainly activated by amino acid deprivation. However, recent reports also suggest that glucose deprivation elicits the same response. Though, this could be mediated by a higher amino acid consumption as a secondary effect of glucose deprivation (Ye et al., 2010). In detail, GCN2 binds to deacylated transfer RNases (tRNAs) via a histidyl-tRNA synthetase-related domain (Vazquez de Aldana et al., 2015), which facilitates its activation. PKR, is activated by double-stranded RNA (dsRNA) upon viral infections (Clemens and Elia, 2009). HRI is mainly expressed in erythroid cells, regulating differentiation, and protects cells against accumulation of toxic globin aggregates (Han et al., 2001). (Pakos-Zebrucka et al., 2016)

Mild ER stress activates signaling pathways to resolve the stress. However, if the stress is chronic and irreversible, the primary adaptive UPR response switches towards an pro-death response (Oakes, 2017). The phosphorylation status of eIF2α possibly codetermines the pro-survival and pro-death switch. A delayed negative feedback loop through GADD34, ATF4 and CHOP signaling promotes the transcription of genes involved in the cell death response. (Almanza, Püschel et al, FEBS Journal, 2019)

2.8 Cell death

Cells induce alternative metabolic pathways and adaptive stress signaling pathways when lacking nutrients, as described before. However, if nutrient deprivation is sustained, cell cycle arrest is induced followed by the upregulation of pro-death proteins (Sun and Lee, 2008).

Under physiological conditions cell death is an important cellular mechanism, which aims at maintaining tissue homeostasis. Under pathological conditions cells undergo cell death to eliminate infected, transformed or defective cells.

After the first description of cell death in 1960 several cell death forms have been described. The two main cell death forms are known as necrosis and apoptosis and have been classified by their morphological and biochemical criteria. (Favaloro et al., 2012)

Apoptosis, also called 'programmed cell death', is a highly regulated and energy dependent cell death mechanism, which was first described by Kerr, Wyllie and Currie in 1972 as an active, inherently programmed phenomenon (J. F. R. KERR*, 1972). If the cell receives apoptosis inducing signals, for instance through cytokines or cell death promoting proteins, the cell induces the condensation of the chromatin, cytoplasmic shrinking and the blebbing of the membrane (Chen and Lai, 2009). In contrast to necrosis, apoptosis is not induced by mechanic damage of the cell, but by cellular signaling factors that activate the intrinsic (mitochondria-mediated) or extrinsic (death receptor mediated) apoptotic pathway.

The extrinsic apoptotic pathway is mediated by cell death receptors including: tumor necrosis factor receptor (TNFR), Fas (APO-1, CD95) or the Tumor necrosis factor-related apoptosis-inducing ligand receptor (TRAIL/Apo-2) (Wang and El-Deiry, 2003). The TRAIL receptor is a type II transmembrane protein and in human exist four homologous receptors including TRAIL receptor 1/DR4 and TRAIL receptor2/DR5 (Pan et al., 1997). Reports proved that the TRAIL ligand has the potent ability to induce apoptosis in tumor cells but not most of untransformed cells (Ashkenazi et al., 1999). Once cell death receptors are activated by their ligand or by ligand independent mechanism, the death inducing signal complex (DISC) is formed at the cytoplasmic membrane. DISC consist of the Fas-associated death domain (FADD) and the procaspase-8 and -10, which interact with FADD. Caspases are a family of proteases that use their proteolytic activity in order to coordinate cell death (Earnshaw et al., 1999). Oligomerization of procaspase-8 induces its autoproteolytic cleavage and facilitates cleavage and activation of caspase-3 (Galluzzi et al., 2018).

The intrinsic apoptotic pathway is regulated by BCL-2 family proteins like Bax and Bak. Bim, NOXA and Puma are the major BH3-only proteins that interact with Bax and Bak. Bax and Bak form pores in the outer mitochondrial membrane that promotes mitochondrial outer

membrane permeabilization (MOMP) followed by cytochrome C release. Cytochrome C interacts with Apaf-1 and procaspase-9 forming the apoptosome. The apoptosome formation is followed by caspase-3 and caspase-7 activation and the induction of proteins involved in the execution of cell death (Elmore, 2007).

2.8.1 UPR-mediated cell death induction upon glucose deprivation

If the cell is exposed to chronic and severe ER stress, cells induce pro-death signaling pathways (**Figure 6**). It is described that the UPR regulates the pro-apoptotic BH3-only proteins PUMA, NOXA and BIM, which are involved in the intrinsic apoptotic pathway. ER stress induced by thapsigargin or tunicamycin facilitates the upregulation of DR5 mRNA and protein in cancer cell lines, mediated by the transcription factor CHOP (**Figure 6**) (Lu et al., 2014; Yamaguchi and Wang, 2004; Zinszner et al., 1998). Furthermore, the PERK-ATF4-CHOP axis was shown to induce the induction and activation of DR5 in an ligand independent manner which results in caspase-8 activation (Lu et al., 2014; Martín-Pérez et al., 2012).

Regarding the mitochondrial apoptotic pathway it is reported that CHOP induces Bim (Puthalakath et al., 2007). Furthermore, NOXA is known to be involved in starvation induced cell death (Ramírez-Peinado et al., 2011). Our group also proved that ATF4 mediates necrosis in rhabdomyosarcoma cells upon glucose deprivation (León-Annicchiarico et al., 2015b).

Though, how glucose deprivation induces apoptosis in an UPR dependent manner was still not completely understood and will be the first objective of this thesis. (Iurlaro and Munoz-Pinedo, 2016)
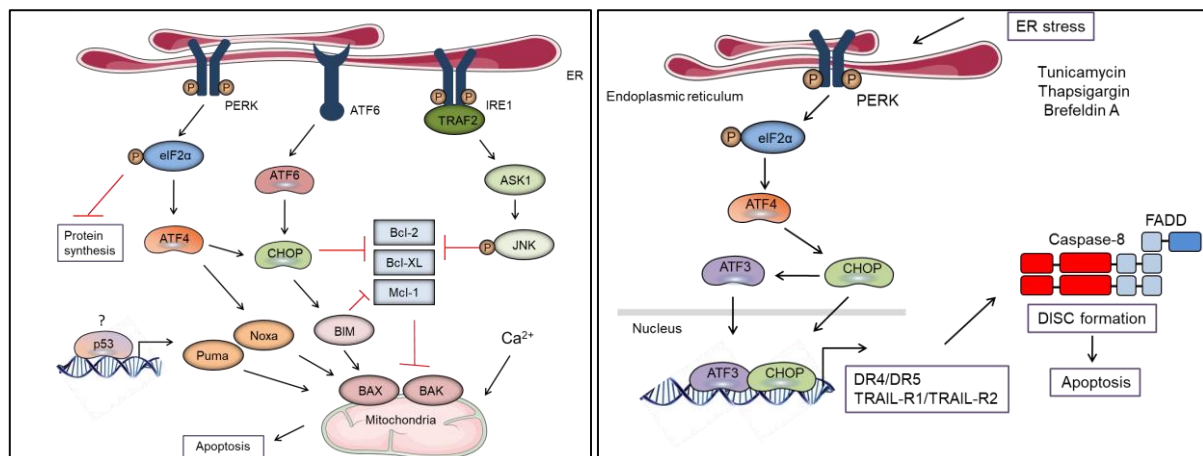
Figure 6 Endoplasmic reticulum stress induced cell death
Left: UPR induction activates and phosphorylates PERK and its downstream target eIF2α. ATF4 is selectively translated and induces CHOP and NOXA, which results in apoptosis. CHOP induces Bim and inhibits anti-apoptotic Bcl-2 proteins. It is still under investigation how p53 induction upon ER stress facilitates induction of NOXA and Puma. IRE1α induction

mediates TRAF2 recruitment and mediates ASK1 and subsequently JNK induction. JNK can promote apoptosis by inhibiting Bcl-2 and Bcl-XL proteins. Right: Sustained ER stress activates PERK, which promotes ATF4 and CHOP induction. CHOP can bind the promotor of DR5 and DR4 and upregulate their expression. This promotes caspase-8 activation, DISC formation and cell death. (modified from Iurlaro and Muñoz-Pinedo, 2016)

2.9 Tumor heterogeneity

The tumor microenvironment (TME) consist not only of cancer cells but also of other cell types including cancer-associated fibroblasts (CAFs) and myofibroblasts, which form the tumor stroma. Other cell population include cells of the lymphatic and vascular network, blood cells, adipose cells and immune cells. Furthermore, the extracellular matrix (ECM), which is the extracellular space between cells, consists of extracellular components like collagen, fibronectin and Secreted Protein Acidic and Rich in Cysteine (SPARC), growth factors, cytokines and hormones, which together build an environment that facilitates tumor growth (Kim et al., 2011). The distinct cell populations, together with the ECM, form the tumor tissue. Each of these cell populations have their specific functions in order to maintain tumor growth, which will be explained in detail in the following chapter. Furthermore, cells communicate among each other through cell-cell interactions, mediated by soluble secreted factors in form of cytokines, chemokines or metabolites, as well as through membrane interactions. (Wu and Dai, 2017)

High numbers of CAFs are associated with poor patient outcome in breast, lung and pancreatic cancer (Räsänen and Vaheri, 2010). These cells express high levels of chemokines including CXC motif ligand (CXCL)12 (Orimo et al., 2005), chemokine CC motif ligand (CCL)2 or CCL8. Secretion of these chemokines promotes the infiltration of inflammatory cells in the tumor microenvironment. (Chen et al., 2015)

Cells of the tumor vasculature are responsible for the supply of oxygen and nutrients in the tumor. Unequally distributed vasculature or more distant regions from the vasculature generate distinct TME regions in terms of nutrient and oxygen supply. Cancer cells in different regions in the tumor tissue adapt to these changes through alterations in gene expression, which induce alternative metabolic pathways and the secretion of cytokines such as the platelet-derived growth factor (PDGF), transforming growth factor α (TNFα) or VEGF, which promote the re-vascularization of the tumor tissue. Moreover, cancer cells also secrete inflammatory cytokines, which promote the infiltration of immune cells in the tumor tissue. Tumor-intrinsic immune cells become 'reprogrammed' and release cytokines which provide a pro-tumorigenic environment and promote tumor growth and metastasis (Atretkhany et al., 2016b). (**Figure 7**)

Introduction
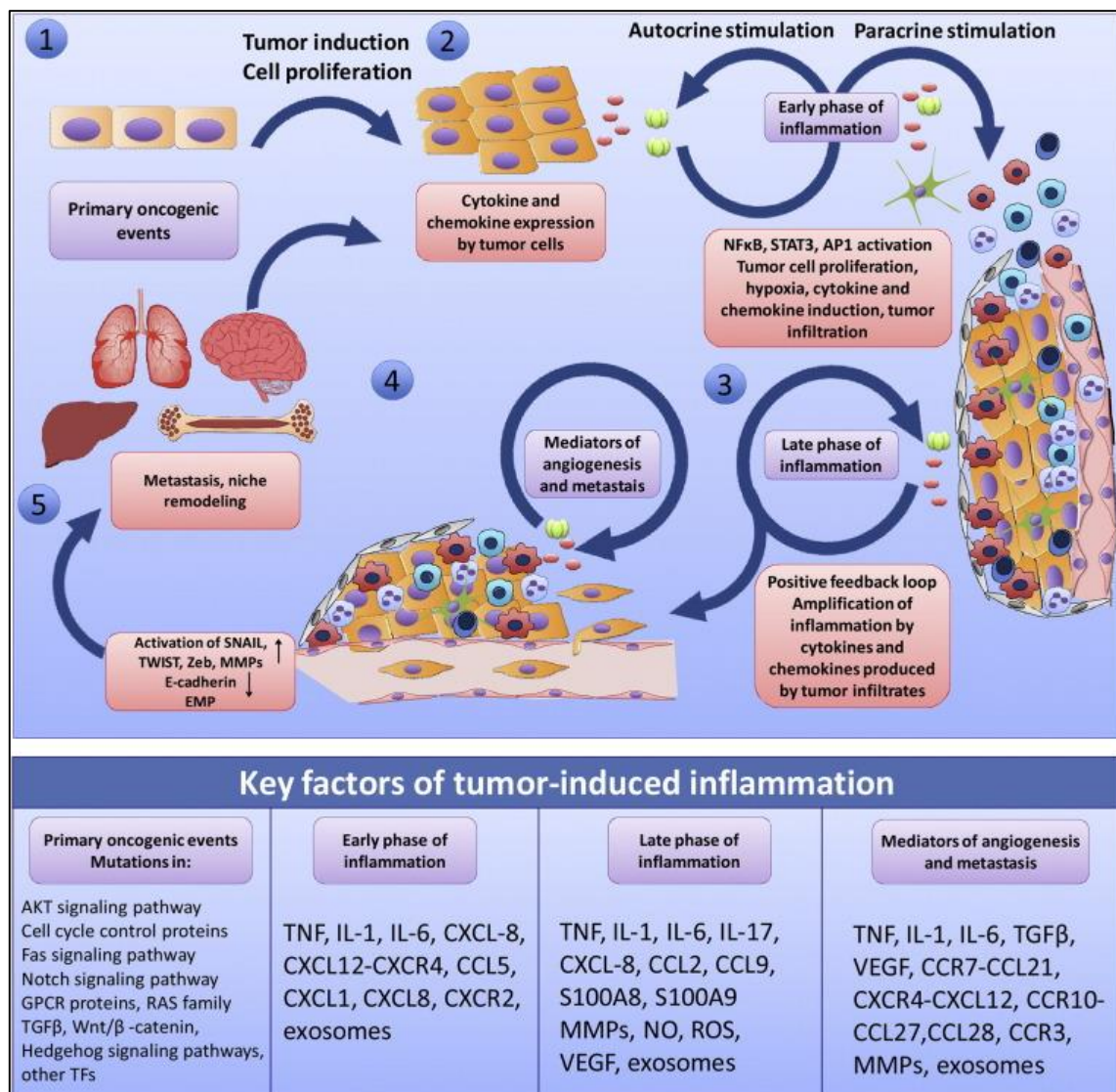
Figure 7 Schematic presentation of tumor-induced inflammation
Tumorigenesis is initiated by oncogenic mutations with impacts on proliferation, apoptosis and other pro-tumorigenic processes. (2) Oncogenic mutations promote altered cytokine and chemokine expression, increased proliferation and survival. Secreted pro-inflammatory cytokines from cancer cells activate in an autocrine manner transcription factor such as NF-κB, STAT3, AP1 families of transcription factors. Cytokines also function in a paracrine manner through stimulating distant tissue. This results in increased vascular endothelium permeability and the upregulation of adhesion molecules. The release of chemokines favours immune cell infiltration. (3) Tumor-infiltrating immune cells and stromal cells are possibly ´reprogrammed´ by the tumor cells and release cytokines which provide a pro-tumorigenic environment, which stimulates tumor growth and anti-immune responses. Tumor cells release proinflammatory cytokines, chemokines, ROS and nitrogen oxide, which amplify the inflammatory response. (4) Infiltrating myeloid cells produce metalloproteases, which are needed for tumor niche remodelling including: angiogenesis, acquisition of invasive properties of tumor cells and metastasis. Epithelial-mesenchymal transition (EMT) is promoted through activation of E-cadherin repressors: SNAIL, TWIST and Zeb transcription factors. Transcription factors like NFκB, HIF, Notch, Wnt/β-catenin are also promoting EMT an metastasis. (5) In the last step of tumor progression, tumor cells release exosomes and chemokines to metastasize towards distal sites. (Atretkhany et al., 2016a)

38

2.9.1 Immune cell composition in cancer

In general, immune cells can be classified in innate immune cells, including macrophages, neutrophils, dendritic cells (DC), myeloid-derived suppressor cells (MDSC) and natural killer (NK) cells and in cells from the adaptive immune system, including T and B cells.

Immune cells were primary thought to be anti-tumorigenic in order to prevent malignancy by recognition of antigens at the cell surface of cancer cells. However, the tumor-immune environment is rather characterized by 'limited antigen recognition` and ´immune suppression´. One reason is that cancer cells are highly impacted by their mutational load, which favours the expression of oncogenes and tumor suppressor genes (TSGs). Regarding that, epidermal growth factor receptor (EGFR) mutated lung tumors are associates with high expression levels of the programmed death ligand (PD-L1), which is associated with immune escape (Tung et al., 2018).

Recent findings confirm that cells of the innate immune response, such as macrophages and neutrophils, promote cancer cell growth. In detail, MDSC are derived from myeloid origin and include myeloid progenitor cells and immature -macrophages, -dendritic cells, or monocytes. These cells secret cytokines and chemokines with immunosuppressive functions and are therefore considered as pro-tumorigenic (L.J. et al., 2012). Moreover, some myeloid cells are known to have immunosuppressive effects on T cells. These cells release factors such as VEGF, which promotes the re-vascularization of the tumor. (Motz and Coukos, 2011; Stockmann et al., 2008) Furthermore, MDSC migrate towards the tumor from the circulating blood and differentiate into type II tumor-associated macrophages (TAMs). TAMs promote tumor growth through secretion of cytokines like interleukin-6 (IL-6), which promotes tumor growth, chemo-resistance and is protective against cell death in several cancers (Bollrath et al., 2009; Grivennikov et al., 2009; Ruffell and Coussens, 2015). Furthermore, TAMs can prevent the immune attack from natural killer (NK) cells, which are described to be anti-tumorigenic due to their ability in killing cancer cells (Marcus et al., 2014; Noy and Pollard, 2014). TAMs can be classified into M1 and M2 subpopulations. Class M1 macrophages are activated by interferon γ (INF γ), which is released by Th1 subcellular populations. M1 cells are characterized by expression of the major histocompatibility complex (MHC) class II, secretion of interleukin-12 (IL-12) and TNFα. M2 macrophages induce differentiation upon stimulation with cytokines such as IL-4 and IL-13. (Qian and Pollard, 2010) The M2 phenotype is described to promote tumorigenesis due to the secretion of immune suppressive cytokines. However, the classification of M1 and M2 macrophages is controversially discussed. It is rather seen as a 'functionally diverse group' than a 'unique activation state' (Metchnikoff, 2015).

Introduction

Tumor associated neutrophils (TANs) are associated with poor patient prognosis in several cancers (Gentles et al., 2015). The major chemokines promoting neutrophil migration are: CXCL1 (GRO-α), CXCL3 (GRO-γ), CXCL5 (ENA-78) and IL-8, which are released by other immune cells as well as by cancer cells themselves (Atretkhany et al., 2016a). Neutrophil recruitment is associated with poor prognosis in patients due to their T cell suppressive effects. (Templeton et al., 2014). After being recruited to the tumor tissue, cells secrete cytokines and factors that promote tumor growth, including IL-6, VEGF and reactive oxygen species (ROS) (Coffelt et al., 2016).

B cells occur in all stages of tumor development. Up to date their role in tumor progression is still under investigation and controversial (Tsou et al., 2016). However, some studies have shown that patients with a high number of follicular B cells and tumor infiltrating plasma cells have a better long-term survival in NSCLC. This is mediated by secreted antibodies and immunoglobulins which are associated with tumor lysis through antibody-dependent cellular cytotoxicity (ADCC) (Germain et al., 2014; Lohr et al., 2013; Wang et al., 2018). Moreover, B cell infiltration is also associated with activation and formation as well as with memory formation of T cells, promoting anti-tumorigenic effects. On the other hand, it is reported that B cells promote *de novo* carcinogenesis by promoting innate immune cell infiltration (De Visser et al., 2005). Other reports show that regulatory B cells (Breg) secrete factors like IL-10 and TGFβ, which are associated with immunosuppression. Moreover, B cells can also upregulate ligands like PD-L1 and the cytotoxic T-lymphocyte-associated Protein 4 (CTL-4), which inhibit T and NK cells response and promote the tumor responses mediated by regulatory T cells (Tregs), MDSCs and TAMs (Wang et al., 2018; Zhang et al., 2015).

2.9.2 Tumor-intrinsic immune cells in lung cancer

Lung tumors contain approximately 2/3 of tumor-infiltrating lymphocytes (TILs) and 1/3 of TAMs (Kataki et al., 2002). CD4^{+}, CD8^{+} and CD20^{+} lymphocytes are associated with good prognosis in lung cancer patients (Bremnes et al., 2016). In contrary Th2, Th17 and Foxp3^{+} Treg cells are associated with poor prognosis (Marshall et al., 2016). In approximately 35 % of lung cancer incidences proliferating B cells are observed, which could have an impact on the patient outcome (Gottlin et al., 2011). In NSCLC, neutrophils are the pre-dominant immune cell population. However, the immune cell composition differs between adenocarcinoma and squamous carcinomas. Squamous carcinomas have a reduced macrophage but a higher neutrophil content compared to adenocarcinomas (Kargl et al., 2017).

2.9.3 Immune cell metabolism in the tumor microenvironment

The decreased pH in some regions of the tumor environment results among other factors from increased lactate secretion. This creates together with hypoxia and nutrient starvation a hostile tumor microenvironment (Reznik et al., 2018). The flexibility of malignant cells, which involves the ability to adapt to hostile environments through oncogenic mutations and TSGs, gives cancer cells an advantage to other cell populations in the TME (Vander Heiden and DeBerardinis, 2017). Alterations of cancer cell-intrinsic signaling pathways promote for instance cytokine and metabolite release from cancer cells. Subsequently this also affects the metabolism of non-malignant cells in the stroma. Regarding that, cancer cells can adapt their metabolism and deplete the tumor environment of nutrients like glucose (Busk et al., 2011; Chang et al., 2015), which leads to immunosuppression of some immune cells (Badur and Metallo, 2018). For instance, low glucose level in the TME promote T cell inactivation due to their high glycolytic needs and results in the downregulation of key signaling pathways like Nuclear factor of activated T-cell (NFAT) signaling (Ho et al., 2015). Furthermore, glucose deprivation also affects B cells which are described to be dependent on glucose in order to proliferate and differentiate towards antibody producing cells. B cells have on the one hand anti-tumorigenic effects but also promote an immunosuppressive milieu due to their various subtypes. (Caro-Maldonado et al., 2014; Singer et al., 2018; Wang et al., 2018)

Some cancer cells secrete high amounts of lactate based on their increased aerobic glycolytic activity. Lactate in the extracellular milieu can have immunosuppressive effects on infiltrated immune cells. For instance, lactate inhibits the cytotoxic activity of CD8$^+$ T cell, which are considered as anti-tumorigenic (Fischer et al., 2007). Moreover, lactate blocks the production of IFNγ of tumor-infiltrating NK cells, which is associated with loss of immunosurveillance (Brand et al., 2016). Lactate also affects macrophages of the innate immune system by inducing an M2-like phenotype (Colegio et al., 2014). Furthermore, increased acidity is associated with negative effects on cells of the innate and adaptive immune response due to the downregulation of cytokines and therefore lactate inhibits the cytotoxic effector function of several immune cells. (Fischer et al., 2000; Singer et al., 2018)

Keeping this in mind, glucose deprivation does not only affect cancer cells but also the activity of tumor-associated immune cells.

2.9.4 The role of the UPR in the tumor microenvironment

The UPR is not only a stress response in non-malignant cells in order to regain cell homeostasis upon extra- or intracellular perturbations, but also displays a pro-tumorigenic role in some

cancers. This is associated with cancer cell survival, as well as with drug resistance (Almanza et al., 2019). Moreover, several reports indicate that the UPR is involved in immunosuppression and an important regulator of the inflammatory response (Grootjans et al., 2016). The induction of the UPR results in cytokine secretion and modulation of immune cells within the TME, which promotes tumor growth (Cubillos-Ruiz et al., 2017; Mogilenko et al., 2019). Regarding that, it was recently published that IRE1 is responsible for myeloid recruitment in glioblastoma (Obacz et al.,2019). Moreover, it is described that pharmacological induction of ER stress promoted distinct macrophage populations (Zhang, et al, 2019) as well as cancer cells (Logue et al., 2018) to release inflammatory cytokines with pro-tumorigenic functions.

To sum it up, glucose deprivation induces the UPR and this could promote the secretion of pro-inflammatory cytokines in an UPR-dependent manner, impacting the TME.

2.10 Cytokines and chemokines in the tumor microenvironment

Distinct cell populations in the TME communicate with each other through cell-cell interactions, mediated by soluble signaling proteins. Depending on the cell type, these factors are cell type-specific and function in autocrine or paracrine manners. Secreted factors can be metabolites, such as lactate or pyruvate, as well as cytokines. Cytokines are small proteins (~5-20 kDa), which are secreted mainly by immune cells in order to facilitate inflammatory responses. These signaling molecules have paracrine or autocrine functions and bind through receptor-ligand interactions to their corresponding receptor at the cell surface. Cytokines can be further subclassified in chemokines, which promote infiltration of immune cells from the circulating blood towards an inflamed tissue, based on a concentration gradient. (Lee and Margolin, 2011; M.D. et al., 2014)

2.10.1 The involvement of NF-κB signaling in cytokine induction

The Nuclear Factor-kappa B (NF-κB) pathway is involved in cell survival, proliferation, angiogenesis and the inflammatory response. Furthermore, it is the major signaling pathway for the induction of pro-inflammatory cytokines and chemokines, which is well described for many diseases (Liu et al., 2017). This pathway can be induced, among others, downstream of interleukin-1 (IL-1), by the TNFR or by the Toll-like microbial pattern recognition receptors (TLRs). In detail, inactive IκBα is bound to the transcription factor p65/RelA. IκB gets activated upon phosphorylation by a multi-subunit IκB kinase (IKK) complex that results in its proteasomal degradation. Therefore, p65 can translocate to the nucleus and induce the transcription of pro-inflammatory cytokines (Liu et al., 2017).

With regard to the UPR, it is described that NF-κB can be induced downstream of the UPR through the formation of an IRE1-TRAF2 complex, interacting with IKK, which results in IκBα phosphorylation. Moreover, phosphorylation of eIF2α results in a global attenuation of protein synthesis, which also prevents *de novo* IκBα synthesis. As a consequence, p65 translocate to the nucleus and induces transcriptionally cytokine genes (Figure 8). (Schmitz et al., 2018; Zhang and Kaufman, 2008a)

In cancer, the NF-κB pathway is activated by many chemotherapeutic drugs or ionic radiation, which in some cases promotes drug resistance (Wolf et al., 2014). Furthermore, NF-κB signaling promotes tumor development in a murine mouse adenocarcinoma model Kras[LSL-G12D];Trp53[f/f] promoting a pro-inflammatory TME (Meylan et al., 2009).
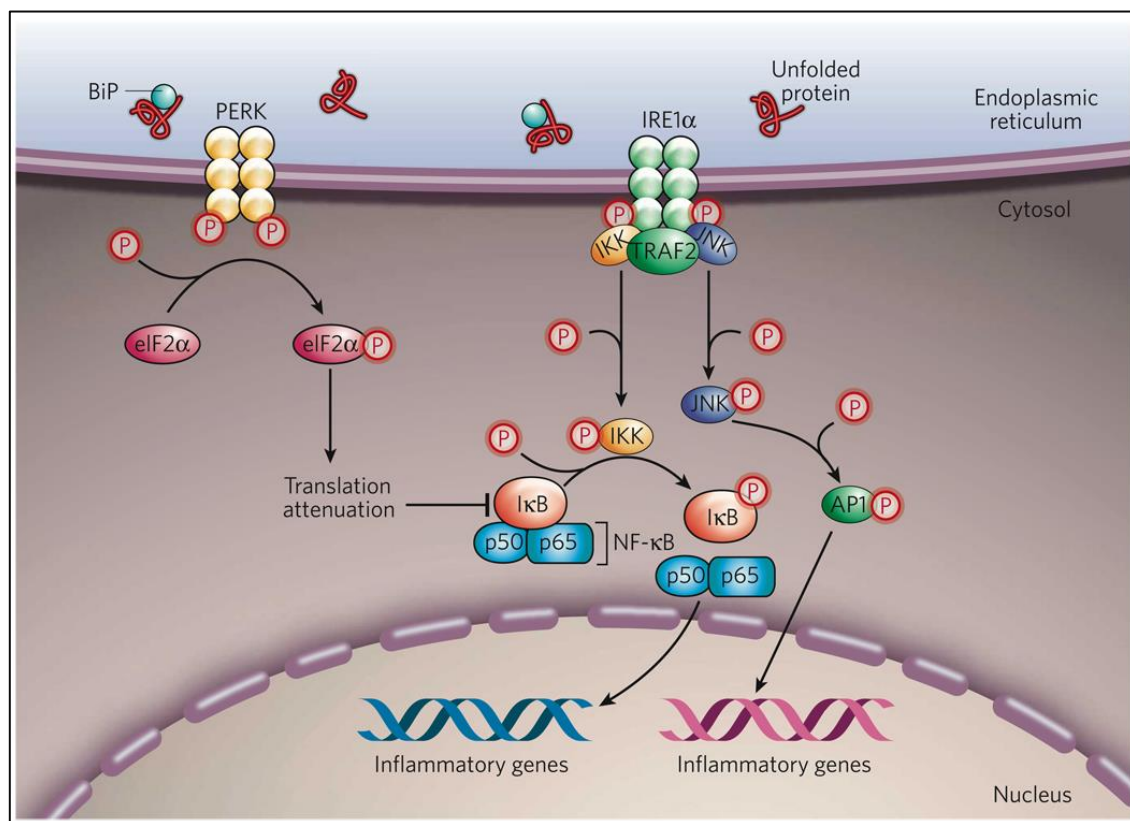
Figure 8 Schematic presentation of UPR-mediated NF-κB activation
Activation of PERK results in eIF2α phosphorylation, which mediates protein translation attenuation. IκBα has a shorter half-life than p65, which results in a shift towards higher p65 protein level. Free p65 can translocate to the nucleus. The cytoplasmic domain of IRE1α can recruit TRAF2. The complex IRE1α-TRAF2 complex can interact with IKK or JNK promoting its activation. Activated JNK phosphorylates activator protein 1 (AP1), which can also mediate transcription of inflammatory genes. Activated IKK mediates the degradation of IκBα and subsequently p65 can translocation to the nucleus, inducing inflammatory gene transcription.(Zhang and Kaufman, 2008b)

2.11 Cancer-associated cytokines

Focusing on cancer, recent findings award cytokines important functions in tumor progression. Cancer related cytokines can be subclassified in pro- or anti-tumorigenic, depending on their functions. For instance, chemokines like CXCL1/2/3 are known chemoattractants for neutrophils, macrophages and MDSCs in the TME, which are associated with poor prognosis. Other cytokines are associated with immunomodulatory functions, angiogenesis or tumor growth. An overview of the cytokines which were examined in this thesis and examples of their general and tumorigenic functions are summarized in **Table 1**.

Within this thesis we will focus on the regulation of mainly three pro-tumorigenic cytokines: IL-8, IL-6 and the leukaemia inhibitory factor (LIF) since these cytokines are well described to have pro-tumorigenic functions in several cancers and are associated with poor patient survival.

Table 1 Cancer-associated cytokines and their functions

Cytokine	Function
CXCL1	Neutrophil recruitment, metastasis (Sawant et al., 2016)
CXCL2	Chemoattractant for myeloid cells (Massagué et al., 2012)
CXCL3	Leukocyte recruitment (Gui et al., 2016)
CXCL5	Tumor progression, neutrophil recruitment and angiogenesis (Hu et al., 2018)
CCL2	Monocyte attractant (Yoshimura, 2018), tumor growth (Zhang et al., 2010)
CCL19	T and B cell migration, pro-tumorigenic in cervical cancer (Zhang et al., 2017b)
CCL20	Chemoattractant for lymphocytes (Hieshima et al., 1997), pro-tumorigenic (Samaniego et al., 2018)
IL-6	Proliferation and activation of T cells, regulation of acute phase response (Hunter and Jones, 2015), proliferation, metastasis and angiogenesis (Kumari et al., 2016; Lee and Margolin, 2011)
IL-8	Chemoattractant for neutrophils, angiogenesis, tumor progression (Lee and Margolin, 2011)
LIF	Self-renewal of cancer-initiating cells (Peñuelas et al., 2009), expansion and activation of MDSCs (Won et al., 2017), infiltration of TAMs (Mónica Pascual-García et al., 2019)
MCS-F	Proliferation and differentiation of monocytes and macrophages, recruitment of TAMs (Chockalingam and Ghosh, 2014)

2.11.1 Interleukin-8

IL-8 is a proinflammatory cytokine, which was initially described to attract neutrophils to the site of inflammation (Baggiolini et al., 1989). Many reports associate IL-8 serum level of patients with poor prognosis and several reports link its chemotactic functions to neutrophil, monocytes and MSDC infiltration in tumors (Alfaro et al., 2016) as well as with angiogenesis in cancer. In NSCLC, IL-8 promotes proliferation in an EGFR dependent manner by promoting the activation of MAPK p42/44 (ERK1/2). Other studies prove that the IL-8 mRNA expression in lung tumors versus non-malignant lung tissue is associates with a shorter overall survival,

44

relapse and tumor progression (Yuan et al., 2000). Furthermore, increased IL-8 serum level after PD1/PD-L1 therapy are associated with worse response towards therapy (Sanmamed et al., 2017). IL-8 and IL-6 serum level in patients are in coherence with poor patient survival in stage I lung cancer patients. Moreover, IL-8 promotes the formation of neutrophil extracellular traps (NETs) of MSDCs (Alfaro et al., 2016). NETs consist out of DNA and DNA binding proteins, which have bacteriostatic properties. Binding of IL-8 at the CXCR1 or CXCR2 receptors activates among others PI3K, PKC and MARK signaling cascades. (Raghuwanshi et al., 2012)

2.11.2 Interleukin-6

IL-6 is a glycosylated polypeptide chain with a size of 25 kDa. It was first discovered as a cytokine involved in B cell maturation towards antibody producing plasma cells (Kishimoto, 2003). Nowadays it is considered as a pleiotropic cytokine involved in inflammation, immune response, and haematopoiesis (Tanaka et al., 2014). IL-6 is not exclusively release from immune cells but also from stromal and cancer cells in the TME. (Kumari et al., 2016)

In a tumor setting IL-6 is described to promote differentiation and proliferation of tumor cells, which correlates with the aggressiveness of the tumor. Regarding that, clinical studies found that IL-6 is increased in the patient serum of many cancers, including lung tumors, which is associated with poor prognosis and poor response to therapy (Chang et al., 2013). IL-6 can also induce HIF1α and activate neutrophils. Furthermore, IL-6, secreted from stromal cells, stimulates the secretion of VEGF from multiple myeloma cells (Dankbar et al., 2000). IL-6 also has an important role in cell metabolism. Mice that lack IL-6 are intolerant to glucose and insulin resistant (Wunderlich et al., 2010). In muscle cells it was shown that IL-6 promotes increased fatty acid oxidation, glucose uptake, translocation of glucose transporters to the cell membrane, as well as the increased activation of AMPK (Carey et al., 2006). Targeting IL-6 with receptor-tyrosine inhibitors (TKIs) is seen as a promising approach to prevent IL-6 paracrine signaling networks in cancer (Lin et al., 2002).

2.11.3 Leukemia inhibitor factor

The leukemia inhibitory factor (LIF) belongs to the IL-6 superfamily. LIF is a glycosylated monomeric protein with a size of 20-25 kDa. It binds to the Leukemia inhibitory factor receptor (LIFR) followed by the recruitment of the gp130 receptor, which forms together with LIFR a heterogenic complex. Dimerization induces several signaling pathways including JAK/STAT3, PI3K/AKT, ERK1/2 and mTOR signaling (Li et al., 2014).

Introduction

LIF is a pleiotropic cytokine, involved in several physiological processes including embryonal implantation, neuronal development, stem cell self-renewal and in the regulation of the immune system. (Janssens et al., 2015; Metcalfe, 2011; Taga and Kishimoto, 1997; 2015) Furthermore, LIF also has some metabolic implications. Regarding that it is reported that LIF promotes the glucose uptake in skeletal muscle cells (O'Neill et al., 2015) and it alternates the energy metabolism of cardiomyocytes (Odegaard et al., 2005).

With focus on cancer, LIF is involved in the proliferation of breast, kidney, ovarian as well as prostate cancer cells (Kellokumpu-Lehtinen et al., 1996a; McLean et al., 2018). LIF promotes the invasion of fibroblasts and creates an invasive tumor environment, which can result in primary metastasis (Albrengues et al., 2014). With regard to tumor resident immune cells, LIF is involved in the differentiation of murine M1 myeloid leukemia cell and macrophages (Gearing et al., 1987), as well as in the prevention of CD8+ T cell tumor-infiltration and promotes the infiltration of TAMs (Pascual-García et al.,2019). Therefore, high LIF level predict poor prognosis of patient. (Kellokumpu-Lehtinen et al., 1996b; Won et al., 2017; Zeng et al., 2016)

To sum it up, cytokines released from cancer or other tumor-resident cells can regulate a broad range of functions in autocrine and paracrine manners. Through ligand-receptor interactions cytokines induce several downstream signaling pathways, ranging from STAT, NF-κB, PI3K or MAPK signaling to cell death signaling. Therefore, the investigation of the tumor-intrinsic events promoting their secretion and of the regulatory mechanisms behind regulating their release, is important to develop effective anti-cancer drugs.

3. Hypothesis and objectives

Since cancer cells are highly dependent on glucose and mainly use aerobic glycolysis for energy production, known as the Warburg effect, targeting the glucose metabolism is a promising anti-cancer approach. However, to develop functional drugs it is important to understand in detail the adaptive survival mechanism induced by cancer cells upon glucose deprivation as well as the mechanisms promoting cell death. Due to the discovery that the TME plays a significant role in tumor progression, it is also necessary to investigate the impacts of glucose-deprived cancer cells on the surrounding tissue.

Regarding that, it is known that glucose deprivation induces the UPR, which is not only a pro-death but also a pro-survival response. We hypothesize that sustained glucose deprivation induces among other stress signaling pathways the UPR, which mediates apoptosis in a TRAIL death receptor dependent manner. Moreover, we further hypothesize that cancer cells induce in an earlier response adaptive mechanism, which allow them to escape nutrient stress in order to regain cell homeostasis. We suggest that one of the adaptive responses is the secretion of cytokines and chemokines with functional roles in migration, cell death and immune cell infiltration.

In detail, we want to investigate how cancer cells die in an UPR-dependent manner upon glucose deprivation and whether secreted cytokines from glucose-deprived cancer cells promote the migration of macrophages, neutrophils and lymphocytes. Experiments will be performed in different lung cancer cell lines including adenocarcinoma and squamous carcinoma cells as well as in a cervical cancer cell line.

1. Investigation of cell death induction upon glucose deprivation in cancer cells

    – Uncovering the cell death mechanism induced by cancer cells upon glucose deprivation.
    – Revealing the mechanistical pathway involved in glucose deprivation-induced cell death.

2. Investigation of cytokine release upon glucose deprivation from cancer cells and functional analysis

    – Identification of cytokines released from starved cancer cells and from cancer cells treated with anti-metabolic drugs.
    – Revealing the regulatory mechanism of cytokine release upon glucose deprivation with a focus on the UPR, NF-κB signaling and the mTOR pathway.
    – Functional analysis of the effect of conditioned media derived from glucose-deprived cancer cells on cancer cells, THP-1 cells and primary immune cells isolated from human blood.

4. Material

Table 2 Products and reagents

Products/Reagents	Manufactures	Cat. Number
Blocking Buffer ODDYSSEY	LI-COR	927-40000
Bovine Serum Albumin	SIGMA	A7030
Boyden 3.0 μm Transparent PET Membrane (24-well)	Millipore	PITP01250
Boyden 8.0 μm Transparent PET Membrane (24 well)	Falcon	353097
Crystal Violet	Sigma	61135
D-(−)-Fructose	Sigma	F0127
D-(+)-Glucose	Sigma	G7021
D-(+)-Mannose	Sigma	M6020
Dextran	Sigma	31392-50G
Dharmafect	Fisher	W9945D
Dimethyl sulfoxide (DMSO)	SIGMA	D2650
DMEM, high glucose	Life Technologies	41965-062
DMEM, no glucose	Life Technologies	11966-025
DMEM, no L-glutamine	Life Technologies	11960044
dNTP Mixes	Fermentas	R1121
Dulbecco's Phosphate Buffered Saline 10X w/o Calcium w/o Magnesium (PBS)	Biowest	X0515-500
ECL Western Blotting Substrate	Promega	W1001
EDTA	SIGMA	E5134
ELISA 96-well Plates	Sigma	M9410-1CS
Ethanol	Alcoholes Gual	47000ER
Fast EvaGreen Master Mix for qPCR (500rxn)	Biogen Cientifica S.L.	31003-1
FBS	Life Technologies	10270106
Ficoll (Lymphocytes isolation solution, 1.077 g/ml)	Rafer	LN0250
Film Curix RP2 Plus Medical X-Ray film 100 NIF 18 x 24	Agfa	ENKMV
Glycine	SIGMA	161-0718
HBSS	Gibco	24020083
HBSS (w/o Magnesium and Calcium)	Sigma	H9394-500ML
Immobilon-FL PVDF (fluorescence)	Merck Millipore	IPFL00010
Immobilon-PSQ Membrane, PVDF	Millipore	ISEQ00010
L-Glutamine	Life Technologies	25030-024
Methanol	Alcoholes Gual S.A.	UN1230
MicroAmp® Optical 96-Well Reaction Plate	Life Technologies	N8010560G
Nitrocellulose Membrane	Bio-rad	162-0112
Paraformaldehyde	VWR	1.04005.1000

Percoll	Sigma	P4937-100ML
PfuTurbo Hotstart DNA Polymerase	Agilent Tech	600320
Ponceau S.	SIGMA	P3504
Potassium chloride	SIGMA	P9541
Precision Plus Protein™ Dual Colour	Bio-rad	161-0394SP
Propidium iodide	SIGMA	81845
Protein Concentrator PES, 3K MWCO, 2-6 mL	Thermo Fisher Scientific	88515
Protein Concentrator PES, 3K MWCO, 5-20 mL	Thermo Fisher Scientific	88526
Recombinant Human IL-8	R&D System	208-IL-010
Recombinant Human LIF	R&D System	7734-LF-025
Recombinant Human TNFα	Peprotech	300-01A
RIPA Lysis and Extraction Buffer	Thermoscientific	89900
RPMI	Thermo Fisher	21875034
Sodium bicarbonate	SIGMA	S5761
TaqMan® Gene Expression Master Mix	Applied biosystems	4369016
TaqMan® Gene Expression Master Mix	Applied Biosystems	4369016
TEMED	SIGMA	T7024
Triton® X-100	VWR	108603
Trypan Blue solution	SIGMA	93595
Trypsin-EDTA (0.05 %), phenol red	Life Technologies	25300-062
Tween® 20	SIGMA	P1379

Table 3 Commercial kits

Kit	Manufacture	Cat. Number
ELISA Ancillary Reagent Kit 2	R&D System	DY008
ELISA CCL20	NOVUS	NBP2-31049-1 KIT
ELISA DuoSet Human CXCL1	R&D System	DY275-05
ELISA DuoSet Human CXCL5	R&D System	DY254-05
ELISA Duoset Human IL-6	R&D System	DY206-05
ELISA Duoset Human IL-8	R&D System	DY208-05
ELISA DuoSet Human LIF	R&D System	DY7734-05
ELISA DuoSet Human M-CSF	R&D System	DMC00B
ELISA Duoset Human TNFα	R&D System	DY210-05
High Capacity cDNA Reverse Transcription Kit	Applied Biosystems	4368814
Pierce™ BCA Protein Assay Kit	Thermo Scientific	23225
Proteome Profiler Human Chemokine Array	R&D System	ARY017
Proteome Profiler Human XL Cytokine Array	R&D System	ARY005
RNeasy MINI KIT	QIAGEN	74104

5. Methods

5.1 Cell lines and human derived primary cultures

Human blood samples (buffy coats) were obtained from the Banc de Sang i Teixits - BST (Blood and Tissue Banc). Experiments were approved by the Clinical Research Ethical Committee from the Hospital of Bellvitge (Comitè d'Ètica d'Investigació Clínica - CEIC). Isolation of peripheral blood mononuclear cells (PBMCs) and neutrophils was performed immediately after arrival of buffy coats, and primary cultures did not exceed 24 h including experiments. Primary cells were cultured in pyruvate-free Dulbecco's Modified Eagle's Medium (DMEM) containing 25 mM glucose, complemented with 10 % FBS (heated at 57ºC for 30 min) and 2 mM fresh L-glutamine at 37ºC and 5 % CO_2 atmosphere.

Different cancer cell lines (lung: A549, H1299, H460, H520, SW900; cervix: HeLa; and leukemia: HL60) were cultured in the same DMEM supplemented as for primary cells. Cells were maintained at 37ºC and 5 % CO_2 atmosphere and adherent cells were splitted twice a week when reached 90 % confluence using a 0.05 % trypsin EDTA solution. THP-1 (leukemia) cells were grown in RPMI supplemented with 10 % FBS and 2 mM L-glutamine and diluted once a week with fresh RPMI in a ration of 1:20. All cells were grown in antibiotic-free medium. (**Table 4**)

Table 4 Cell lines

Cell Lines	Source	Cat. Number
HeLa	Douglas Green Lab	N/A
HeLa	Joan Gil Lab	ECACC
A549	Maria Molina Lab	ATCC-CCL-185
H1299	Ana Montes	N/A
H460	Laboratory of Vanessa Soto Cerrato	N/A
H520	Laboratory of Vanessa Soto Cerrato	N/A
THP-1	Laboratory of Isabel Fabregat	N/A
HL60	Esteban BallestarLab	N/A

5.2 Cell treatments

5.2.1 Dialyzing FBS

For FBS dialysis, the dialyzing membrane was washed according to manufacturer recommendations and filled with 100 mL of heat-inactivated FBS. The pipe was washed twice for 1 h and once overnight (O/N) in 1 L of PBS at 4ºC while stirring. Dialyzed FBS (dFBS) was sterile filtered using a 22 µm syringe filter. (Püschel and Muñoz-Pinedo, 2019)

5.2.2 Glucose and glutamine deprivation, total starvation

Treatment was performed by plating 300.000 (6-well plate) or 150.000 (12-well plate) cells 24 h prior to treatment. At a confluence of 80 % cells were washed twice with pyruvate-free DMEM, 0 mM glucose and 0 % FBS. Cells were treated with pyruvate-free DMEM containing 0 mM glucose, 10 % dFBS and 1 % L-glutamine, while the control cells were supplemented with 25 mM glucose or at concentrations indicated in the figures. (Püschel and Muñoz-Pinedo, 2019)

5.2.3 Drug treatment

For other treatments, cells were incubated in pyruvate-free DMEM with 25 mM glucose, 10 % FBS and 2 mM L-glutamine, unless indicated differently. Specifically, cells were treated with drugs summarized in **Table 5**. For glutamine free treatments, cells were washed twice with glutamine- and pyruvate-free DMEM containing 10 % FBS and incubated with this medium. For HBSS (Hank's Balanced Salt Solution) treatments, cells were washed twice with HBSS (with calcium, magnesium and 5.55 mM glucose) and incubated in HBSS. Control cells were incubated in regular culture media.

Table 5 Drugs

Drugs	$C_{Treatment}$	Manufacture	Cat.Nº	Function
2-Deoxyglucose	5-25 mM	Sigma	D6134	Glycolysis Inhibitor
AMG PERK 44	1-2 µM	TOCRIS	5517	PERK Inhibitor
DTT	1 mM	Sigma	D9779	UPR stressor
GSK2656157	0.5-1 µM	Chemigen	HY-13820	PERK Inhibitor
ISRIB	0.1-0.25 µM	Sigma	SML0843	eIF2α Inhibitor
Metformin	10-50 mM	Sigma	D150959	Metabolic drug
PMA	100 nM	Sigma	P1585	THP-1 Differentiation
Rapamycin	10-100 nM	Calbiochem	53123-88-9	mTOR inhibitor
Torin1	0.1-1 µM	Selleckchem	S2827	mTOR inhibitor
Thapsigargin	4 µM	Sigma	T9033	UPR stressor
QVD	10 µM	Sigma	A1901	Caspase Inhibitor
Ac-Y-VAD-cmk	10 µM	apeXbio	SML0429	Caspase-1 Inhibitor
Z-VAD	20 µM	apeXbio	A1902	Caspase Inhibitor
MKC-8866	10 µM	Fosun Orinove PharmaTech Inc	Eric Chevet Lab	IRE1 inhibitor

5.3 Secreted chemokine and cytokine arrays

For the cytokine array, A549 cells were treated for 24 h with pyruvate-free DMEM containing 25 mM or 0 mM glucose, 10 % dFBS and 2 mM L-glutamine as described before. After 24 h, the supernatant was collected and centrifuged for 5 min at 3000 g at 4ºC. The supernatants of three independent experiments were combined and the *Proteome Profiler Human XL Cytokine Array Kit* (**Table 3**) was performed according to manufacture instruction. For the chemokine array (**Table 3**), A549 cells were transfected for 40 h with siRNA against a non-targeting sequence (C) or against ATF4 (sequence #1) (**Table 6**). Cells were trypsinized and plated at confluences of 40 % (Glc+) and 60 % (Glc-) so that confluences were the same at the day of supernatant collection. The following day cells were treated with glucose deprivation for 24 h as described before. The supernatants were collected and centrifuged for 5 min at 3000 g at 4ºC. The supernatants of three independent experiments were combined and the *Human Chemokine Antibody Array* was performed according to manufacturer instructions. Membranes were developed by chemiluminescence (ECL) reaction using freshly prepared ECL reagent and *ChemiDoc®* development. Mean density of spots were analysed by quantification with ImageJ. Fold induction is shown by normalization of the mean intensity of the control (Glc+) versus the intensity of the Glc- treatment.

5.4 Transfection with small interfering (si)RNAs

Cells were plated in 6-well plates at a concentration of 450.000 cells/well (50 % confluence) in 2 mL fresh culture medium. Cells were transfected 5 h later, when adhered. Transfection solution (150 uL culture DMEM without supplements per well) was preincubated with 1 uL/mL DharmaFECT for 5 min. A final concentration of 50 nM siRNA (**Table 6**) was added and incubated for another 20 min. Complete transfection solution was added to cells. 40 h post-transfection medium was replaced with treatment media as described before.

Table 6 siRNA sequences

Target	Sequence 5'-3'
ATF4#1	CCAGAUCAUUCCUUUAGUUUA
ATF4#2	GCCUAGGUCUCUUAGAUGA
XBP1#1	GGAAGCCAUUAAUGAACUA
XBP1#2	AGAAGGCUCGAAUGAGUG
p65#1	GAUUGAGGAGAAACGUAAA
p65#2	GCCCUAUCCCUUUACGUCA
IL8#1	ACCACCGGAAGGAACCAUC
IL8#2	GCCAAGGAGUGCUAAAGAA

IL8#3	CCAAGGAGUGCUAAAGAACUUAGAU
LIF#1	GGUCUUGGCGGCAGGAGUU
ATF6	GGCAGGACUACGAAGUGAUGATT
IRE1	GCGUCUUUUACUACGUAAUCU
DR4	CACCAAUGCUUCCAACAAU
DR5	GCUGUGGAGGAGACGGUGAUU

5.5 Western blot

Supernatants were removed and cells were scraped on ice using RIPA lysis buffer supplemented with protease inhibitor (Roche) and phosphatase inhibitors (Roche) and stored at -20ºC. Cell lysates were sonicated, and quantification was carried out by *Pierce BCA Protein Assay Kit©*. The standard curve was prepared by using 2 mg/mL bovine serum albumin (BSA). The optical density was measured at an absorbance of 562 nm by *BioTek's PowerWave XS* microplate spectrophotometer. For gel electrophoresis 40 µg protein of each sample was loaded in a final volume of 40 µL 4X Laemmli Buffer (**Table 8**). Samples were denaturated at 95ºC for 10 min prior to loading the gel. Proteins were separated by Sodium Dodecyl Sulphate Polyacrylamide Gel Electrophoresis (SDS-PAGE).

The percentage of the polyacrylamide gel was chosen according to the size of the protein of interest: 7 % resolving gel was prepared for proteins with the size of 80-180 kDa and 12 % resolving gel for proteins between 15-60 kDa. Gel preparation is shown in **Table 7**.

Table 7 Gel preparation

Percent Gel [%]	dest. H_2O [mL]	Acrylamide [mL]	Gel buffer [mL]	10 % SDS [mL]	APS [mL]	TEMED [µL]
Stacking	6.425	0.975	2.5	0.1	0.1	0.01
7	5.675	1.725	2.5	0.1	0.1	0.01
12	4.4	3	2.5	0.1	0.1	0.01
15	3.65	3.75	2.5	0.1	0.1	0.01

The gel chamber was filled with 500 mL running buffer (**Table 8**). Proteins were transferred to a nitrocellulose membrane for 1 h, 100 V at RT by using 1 L of transfer buffer (**Table 8**). Membranes were blocked in 5 % non-fat dry milk and TBS-T for 1 h at RT.

Table 8: Western blot buffer and solutions

Buffer	Concentrations
Ammonium persulphate (APS)	0.1 g/ml in H_2O
Laemmli (4X) Loading Buffer	63 mM Tris-HCl; 10 % glycerol; 2 % SDS; 0.01 % bromophenol; 5 % β-mercaptoethanol; in dest. H_2O
Ponceau Staining Solution	1.31 mM Ponceau; 5 % acetic acid; in dest. H_2O
Resolving Buffer	1.5 M Tris; SDS 0.4 % in dest. H_2O pH 8.8

RIPA Buffer	25 mM Tris-HCl pH 7.6, 150 mM NaCl, 1 % NP-40, 1 % sodium deoxycholate, 0.1 % SDS
Running Buffer 10X	0.249 M Tris-Base; 1.92 M glycine; 1 % SDS in dest. H_2O; pH 8.3
Stacking Buffer	0.5 M Tris ;0.4 % SDS
TBS 10X	0.1 M Tris-HCl; 1.5 M NaCl; in dest. H_2O; pH 7.5.
Transfer Buffer 10X	25 mM Tris-HCl; 0.2 M glycine; 3.46 mM SDS; 20 % methanol; in dest. H_2O
TBS-T	0.1 % Tween in TBS (1X).

Membranes were incubated with the primary antibody, see **Table 9**, overnight at 4ºC in blocking buffer (5 % BSA in TBS-T), and washed afterwards three times for 10 min in TBS-T. The secondary antibodies are listed in **Table 10**. We used either a horseradish peroxidase (HRP) or a fluorescent secondary antibody (Li-COR Biosciences). The first was diluted 1:5000 in TBS-T and the latter 1:15-20.0000 in (1:1) TBS:Odyssey blocking buffer (Li-COR Biosciences) and incubated with the membrane for 1 h at RT. Membranes were washed 3 times for 10 min each in TBS-T and signal was obtained by chemiluminescence (ECL) reaction using freshly prepared ECL reagent and *ChemiDoc®* development. When fluorescent secondary antibodies were used the third wash was performed with TBS and the membrane was developed with the *Odyssey Infrared Imaging System.*

Table 9 Primary antibodies

Primary antibody	Dilution	Produced in	MW (kDa)	Manufacture	Cat. Number
Actin	1:2000	mouse	42	Merck Millipore	MAB1501R
ATF4/Creb2	1:1000	rabbit	49	Cell Signaling	11815
Caspase-3 (full length and cleaved)	1:1000	rabbit	17, 35	Cell Signaling	9662
CHOP/GADD153	1:500	mouse	30	Cell Signaling	2895
4EBP-1 total	1:1000	rabbit	15-20	Cell Signaling	9452
AMPK–phospho (Thr172)	1:1000	rabbit	62	Cell Signaling	2535
PARP	1:1000	mouse	116	Cell Signaling	9542
PARP Cleaved	1:1000	rabbit	89	Cell Signaling	9541
Phospho-eIF2α(Ser51)	1:1000	rabbit	38	Cell Signaling	1673398S
eIF2α	1:1000	rabbit	36	cell signaling	1675324S
S6 (Phospho) Ser235/236	1:1000	rabbit	32	Cell Signaling	2211
p65 (C-20)	1:1000	rabbit	65	Cell Signaling	D14E12

Table 10 Secondary antibody

Secondary antibody	Conjungated with	Manufacture	Cat. Number
rabbit	HRP	Zymax	81-6120
mouse	HRP	Zymax	81-6520
rabbit	IRDye 800CW	LI-COR Biosciences	926-32213
mouse	IRDye 680CW	LI-COR Biosciences	926-68022

5.6 ELISA

Cells were treated in a 6-well plate with 2 mL treatment media or in a 12-well plate with 1 mL treatment media. Supernatants were collected and centrifuged at 3000 g at 4°C to remove dead cells and cell debris and stored at -80ºC. Supernatants were diluted when necessary to be in the optimal optical range and analysed by ELISA using the *DuoSet ELISA Development Systems©* (**Table 3**) according to manufacturer's instructions. Optical densities were measured at a *BioTek'sPowerWave XS* microplate spectrophotometer at 450 and 540 nm. Final cytokine concentrations (pg/mL) were normalized to the protein concentration of each sample, measured as described before for WB and is displayed as pg/mg of protein in the final figures. Protein from a 6-well plate was lysed using 50 µL RIPA Buffer (12-well plate, 25 µL RIPA Buffer).

5.7 Gene expression analysis by RT-PCR and qPCR

Cells were washed once with PBS and trypsinized using a 0.05 % trypsin EDTA Solution. Cells were pelleted at RT, 450 g for 5 min. Cell pellet was washed once with PBS, centrifuged again at 450 g for 5 min, and lysed in 350 µL RLT buffer (Quiagen) completed with β-mercapthoethanol (10 µL/mL) of the *RNeasy MINI KIT©* (Quiagen). Cell lysate was mixed with 350 µL 70 % ethanol and transferred to a mini spin column placed in a 2 mL collection tube. RNA extraction was performed according to manufacturer instructions. Total RNA was quantified at the *NanoDrop* and 1 µg per condition of total RNA was retro-transcribed to cDNA using the *High-Capacity cDNA Reverse Transcription Kit (Thermo Fisher)* (**Table 11 and 12**).

Table 11 Reverse transcription

Reagent	Volume [µL]
Buffer 10X	2
25X dNTP Mix (100 mM)	0.8
10X RT Random Primers	2
MultiScribe RNase	1
RNase Inhibitor	1
RNase-free water	3.2

Table 12 Reverse transcription cycle

	Step 1	Step 2	Step 3	Step 4
Temperature (ºC)	25	37	85	4
Time (min)	10	120	5	∞

5.7.1 qPCR

For qPCR 10 ng of cDNA, 1 µM of primer (**Table 13**) and the Syber-Green Mastermix (Thermo Fisher) was used per reaction. Amplification was performed in a 384-well plate using the *Light Cycler480©* according to the following protocol: denaturation 1 cycle at 95ºC; amplification: 45 cycles: 95ºC 4s, 62ºC 30s, 72ºC 30s, see also **Table 14**. For the analysis, the ΔCp of the mRNA of interest was calculated by using L32 as the housekeeping gene. The fold increase of $2^{\wedge}(-\Delta\Delta Cq)$ was calculated by normalization to the control sample of cells cultured in the presence of glucose at indicated time points.

Table 13 pPCR primer

	Primer sequence 5'-3'	
	Forward	**Reverse**
CCL2	CAGCCAGATGCAATCAATGC	GCACTGAGATCTTCCTATTGGTGAA
CCL20	CCAAGAGTTTGCTCCTGGCT	TGCTTGCTGCTTCTGATTCG
CCL19	CCAGCCCCAACTCTGAGTG	ATCCTTGATGAGAAGGTAGTGGA
CHOP	AAGGCACTGAGCGTATCATGT	TGAAGATACACTTCCTTCTTGAACA
CXCL1	ACTGAACTGCGCTGCCAGTG	GGCATGTTGCAGGCTCCTCA
CXCL2	CACACTCAAGAATGGGCAGA	CTTCAGGAACAGCCACCAAT
CXCL3	TCCCCCATGGTTCAGAAAATC	GGTGCTCCCCTTGTTCAGTATCT
CXCL5	TGGACGGTGGAAACAAGG	CTTCCCTGGGTTCAGAGAC
CXCL8	ATACTCCAAACCTTTCCACCC	TCTGCACCCAGTTTTCCTTG
CTGF	TTGGCCCAGACCCAACTA	GCA GGA GGCGTTGTCATT
MCS-F	GTTTGTAGACCAGGAACAGTTGAA	CGCATGGTGTCCTCCATTAT
IL6	CAACCTGAACCTTCCAAAGATG	ACCTCAAACTCCAAAAGACCAG
TNFα	ACTTTGGAGTGATCGGCC	GCTTGAGGGTTTGCTACAAC
Erdj4	TGGTGGTTCCAGTAGACAAAGG	CTTCGTTGACTGACAGTCCTGC
Herpud1	ACTTGCTTCCAAAGCAGGAA	CTCTTGTGCACTTGGTGGTG

Table 14 qPCR cycle program

Steps	Cycle [n]	Temperature [ºC]
Pre-incubation	1	95
Amplification	45	95,62, 72
Melting Curve	1	95
Cooling	1	∞

5.7.2 RT-PCR

For RT-PCR cells were collected, and RNA was extracted and retro-transcribed as described in chapter 6.7. Amplification of cDNA, using the primers in **Table 15**, was performed in a Thermal Cycler according to the following protocol: 95ºC 5 min, 95ºC 1 min, 55ºC 1 min, 72ºC 1 min for 34 cycles, 72ºC 1 min, 72ºC 5 min, see **Table 16**. Samples were separated using an acrylamide gel and subsequent ethidium bromide (EtBr) staining. Separation was visualized using a ChemiDoc.

Table 15 RT-PCR primer

| | Primer sequence 5'-3' | |
	Forward	Reverse
XBP1	TTACGAGAGAAAACTCATGGCC	GGGTCCAAGTTGTCCAGAATGC

Table 16 RT-PCR cycle Program

	Cycle [n]	Temperature [ºC]
Pre-incubation	1	95
Amplification	34	95, 55, 72
Melting Curve	1	72
Cooling	1	∞

5.8 Cell death analysis by propidium iodide incorporation and FACS analysis

Supernatant were collected and cells were collected by trypsinization using a 0.05 % trypsin EDTA solution at RT. Cells and supernatant were combined and centrifuged for 5 min at 350 g at RT. Cell pellet was resuspended in 300 µL PBS containing 0.5 µL/mL propidium iodide (PI). Samples were analysed with the *Gallios Flow Cytometer Beckman Coulter©*. The quantification was done using the FlowJo software by gating PI positive population. (Püschel and Muñoz-Pinedo, 2019)

5.9 Preparation of conditioned medium from cancer cells

A549 and H460 cells were treated with DMEM containing 25 mM or 0 mM glucose, 2 mM L-glutamine and 0 % dFBS (A549) or 2 % dFBS (H460). After 24 h, supernatants were collected and centrifuged for 5 min at 3000 g at 4°C to remove remaining dead cells and cell debris.

1. Conditioned media of A549 cells was prepared by concentrating supernatants 5X using protein concentrator with a cut-off of 3 kDa by centrifugation at 3000 g. Aliquots were stored at -80ºC (yellow). The filtrate was kept at -80ºC likewise (blue).

2. Conditioned washed media was prepared by concentrating supernatants 20X, using protein concentrators with a cut-off of 3 kDa and centrifugation at 3000 g and 4°C. The 20X concentrated conditioned media was refilled with fresh dFBS- and glucose-free DMEM and once again concentrated 20X. Concentrated conditioned media was diluted with fresh dFBS- and glucose-free DMEM to a final 5X concentration of the initial volume of the supernatant and stored at -80ºC. 25 mM glucose (+) was added for experiments when indicated.
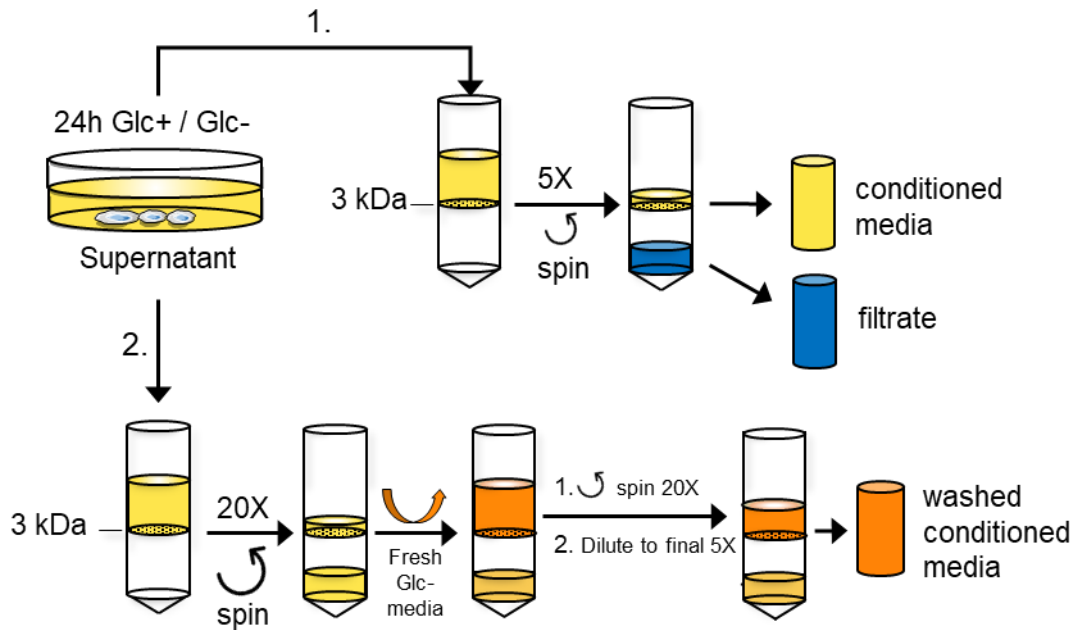
Schematic representation of conditioned media preparation.

5.10 Purification of PBMC from human blood

Cells were purified from whole blood buffy coats. Buffy coats (ca. 10 mL) were diluted in a 1:1 ratio in 1X PBS and layered on top of 15 mL Ficoll in a 50 mL tube. After centrifugation for 30 min at 750 g the layer containing PBMCs was transferred into a new 50 mL tube. Cells were washed twice in 50 mL 1X PBS by centrifugation at 250 g, 6 min and RT. Cells were resuspended in pyruvate-free DMEM containing 25 mM glucose, 0 % FBS and 2 mM L-glutamine.

5.11 Purification of primary neutrophils

Cells were purified from whole blood buffy coats. Buffy coats were diluted 1:4 in 0.9 %-NaCL before adding a 3 % Dextran-0.9 % NaCl solution in a ratio of 1:1. After sedimentation for 30-40 min the upper layer, which contained the cells of interest, was centrifuged for 6 min at 250 g without breaks and resuspended in calcium- and magnesium-free HBSS containing

0.25 % BSA (HBSS-BSA). The percoll gradient consisted out of a 42 % (top) layer and a 51 % (down) layer of a 90 %-percoll solution in HBSS-BSA. The cell suspension was layered on top and centrifuged for 10 min at 250 g and RT without breaks. The layer between the 51 % and 42 % percoll gradient was removed and washed twice in HBSS-BSA at 250 g and RT for 5 min. Cells were resuspended in pyruvate-free DMEM containing 25 mM glucose, 0 % dFBS and 2 mM L-glutamine.

5.12 Differentiation of THP-1 and HL60 cells

Undifferentiated THP-1 cells were incubated for 48 h with 100 nM Phorbol 12-Myristate 13-Acetate (PMA) in culture media until adherent and allowed to recover for 24 h in fresh culture media before using differentiated THP-1 cells for experimental analysis.

Undifferentiated HL60 cells were incubated with 1.25 % DMSO and trans-retinoic acid (ATRA). After 3 days cells were diluted 1:1 with fresh culture media containing 1.25 % DMSO and were incubated for another 4 days before using differentiated HL60 cells for experimental analysis.

5.13 Chemotactic assay

A549 and differentiated THP-1 cells (50.000 cells) were plated on top of an 8 µm Falcon® boyden insert (200 µl) in a 24-well plate and conditioned media (500 µl) was placed in the bottom chamber and cells were allowed to migrate for 20 h. For analysis boyden inserts were removed and washed 2 times with PBS 1X and cells, which were attached to the membrane of the boyden, were stained for 3 h with crystal violet. Remaining crystal violet was removed using a cotton swap and 5 pictures of each boyden were taken using an inverted microscope. Cells were counted using ImageJ and average cell number was calculated.

PBMCs (500.000 cells) were plated on top of a 3 µm Millicell® boyden insert (200 µl) and indicated conditioned media (500 µl) was placed in the bottom chamber with a re-addition of 1 % dFBS. Cells migrated for 20 h. Migrated cells were collected and centrifuged at 250 g for 5 min at RT and were resuspended in 100 µL 1X PBS containing markers for CD56, CD3 and CD19, listed in **Table 14**. After 20 min at RT, 1 mL of PBS was added to the cell suspension and centrifuged for 5 min, 250 g at RT. Cells were resuspended in 300 µL PBS and analysed by FACS. Analysis was performed by FlowJo.

Table 14 Primary antibodies immune cells

Primary antibody	Conjugated with	Manufacture	Cat. Number
CD3	APC	Becton Dickinson	345767
CD19	PE-Cy™7	BD Pharmingen™	552854
CD56	AF488	BD Pharmingen	557699

Neutrophils and HL60 cells (500.000 cells) were plated on top of a 3 µm Millicell® boyden insert (200 µl) in a 24-well plate. The bottom chamber contained the conditioned media (500 µl) with 0 % (for neutrophils) and 2 % (for HL60 cells) dFBS. Cells migrated for 2 h and were counted using a Neubauer chamber.

5.14 Statistical analysis

The significance of the data was calculated using the two-tailed, paired Student's T-test unless indicated differently. Two-way ANOVA followed by Sidak's multiple comparison test was performed using Prism Graph/Pad. Error bars represent the standard error of the mean (SEM). The significance was indicated as following: *$p < 0.05$ one (*)* asterisk*; $p < 0.01$ two (**) asterisk; $p < 0.001$ three (***) asterisks.* N.S means not significant.

6. Results - Part I

6.1 Glucose deprivation induces cell death in a TRAIL receptor 1 (DR4) and receptor 2 (DR5) dependent manner mediated by ATF4

Cancer cells are highly dependent on glucose and sustained low level of glucose promote cell death. In a tumor, environmental low glucose level emerges due to several scenarios such as fast tumor growth, which is associated with transient ischemia due to insufficient vascularization or by the application of anti-angiogenic or -metabolic drugs. The former prevents vessel formation and therefore the nutrient flux in the tumor and the latter prevents nutrient uptake or its metabolization. However, very little was known about the regulatory mechanisms that induce cell death upon glucose deprivation.

Therefore, the first result chapter of this thesis examines the mechanistic pathways which promote cell death upon glucose deprivation in cancer cells. The experiments were performed in cooperation with Raffaella Iurlaro (Iurlaro, 2015) and recently published (Iurlaro, Püschel et al., 2017)
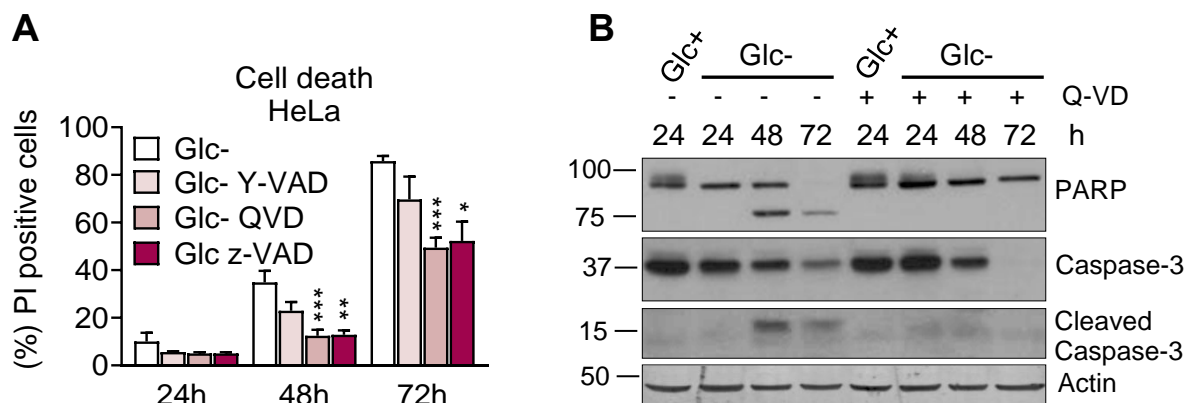
Figure 9 Glucose deprivation induces apoptosis in HeLa cells
A) HeLa cells were treated between 24 and 72 h with 0 mM glucose (Glc-) or Glc- in combination with Y-VAD (10 µM), QVD (10 µM) and Z-VAD (20 µM) and cell death was detected by propidium iodide (PI) incorporation and FACS analysis. Data represent mean ±SEM (n=6-8). Asterisks denote significant differences versus control cells (Glc-) for each time point.
B) A representative western blot of PARP and Caspase-3 cleavage after treatment of HeLa cells with 25 mM (Glc+) or with 0 mM (Glc-) glucose and QVD (10 µM) between 24 and 72 h is shown. WB was taken from doctoral thesis of Raffaella Iurlaro (Iurlaro, 2015) and (Iurlaro, Püschel et al., 2017)

First, we examined if HeLa cells undergo cell death in an apoptotic manner upon glucose deprivation. Therefore, HeLa cells were treated between 24 and 72 h with the pan-caspase inhibitors QVD and Z-VAD, as well as with the caspase-1 inhibitor Y-VAD in combination

with glucose deprivation. QVD and Z-VAD but not Y-VAD protected significantly from cell death after 48 and 72 h of glucose deprivation, indicating that cells die in an apoptotic manner (**Figure 9A**). This result was further confirmed PARP and caspase-3 cleavage after 48 and 72 h of glucose deprivation, which are downstream effectors of the apoptotic pathway. Moreover, cleavage of PARP and caspase-3 was prevented when treated in combination with QVD, see **Figure 9B**.
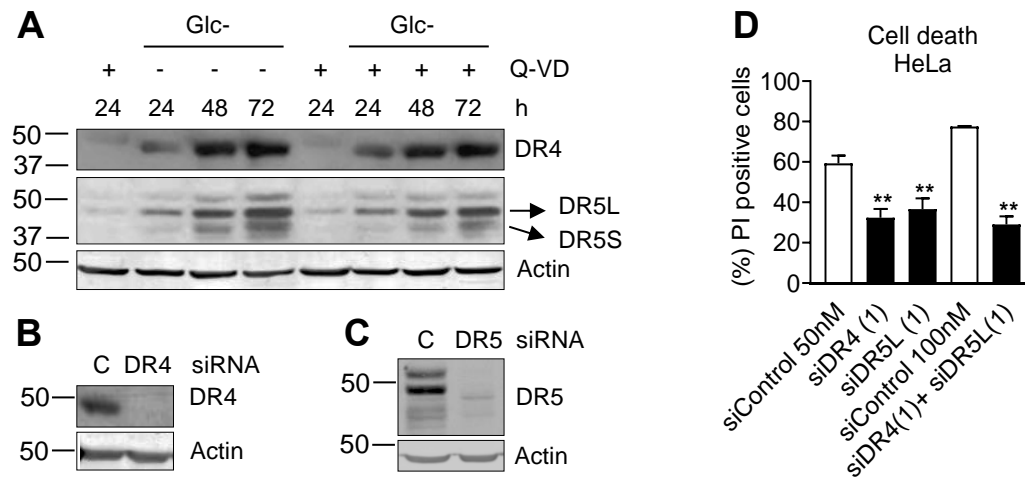
Figure 10 HeLa cells die in an DR4 and DR5 dependent manner.
A) HeLa cells were treated between 24 and 72 h with 25 mM (Glc+) or with 0 mM (Glc-) glucose in the presence or absence of QVD (10 µM). A representative western of DR4 and DR5 protein expression is shown. (L) long; (S) short. Western blot taken from doctoral thesis of Rafaella Iurlaro and (Iurlaro, Püschel et al., 2017)
B-C) HeLa cells were transfected for 24 h with control siRNA (labeled as ''siControl'') or with siRNA for DR4 (labeled as ''siDR4 (1)'') and DR5 (labeled as ''siDR5 (1)''). Cells were treated for 48 h post transfection with 0 mM glucose. A representative western blot for DR4 (B) and DR5 (C) knockdown is shown.
D) HeLa cells were transfected as described in B. and treated for 48 h with 0 mM glucose. Cell death was measured by PI incorporation and FACS analysis. Data represent mean ±SEM (n=4). Asterisks denote significant differences versus the control siRNA.

Apoptosis is carried out by the intrinsic- or extrinsic-apoptotic pathway. Examination of the extrinsic-apoptotic pathway showed that glucose deprivation promotes the protein expression of the cell death receptors DR4 and DR5 respectively, in a time dependent manner, starting at 24 h. (**Figure 10A**). To verify if these receptors are involved in cell death induction, DR4 and DR5 were silenced using siRNA (**Figure 10B-C**) and cell death was measured by PI incorporation and FACS analysis. We found that HeLa cells are significantly protected from cell death upon glucose deprivation when DR4 and DR5 were silenced. Double knockdown of DR4 and DR5 did not synergistically increase cell death protection (**Figure 10D**).

Several studies before linked the induction of DR4 and DR5 to the UPR (Iurlaro and Munoz-Pinedo, 2016). Taking this into consideration, we examined if the UPR is induced upon glucose deprivation in HeLa cells. Therefore, we analysed ATF4 and CHOP protein expression as downstream effectors of the PERK branch of the UPR. We found that ATF4 and CHOP are upregulated on protein level upon 24 h of glucose deprivation (**Figure 11A-B**). Knockdown of ATF4 using siRNA prevented DR5 but not DR4 protein induction upon glucose deprivation. Surprisingly, knockdown of CHOP did not affect DR5 protein expression as described before by other stimuli (Lu et al., 2014). However, DR4 protein expression was slightly regulated by CHOP (**Figure 11A-B**).
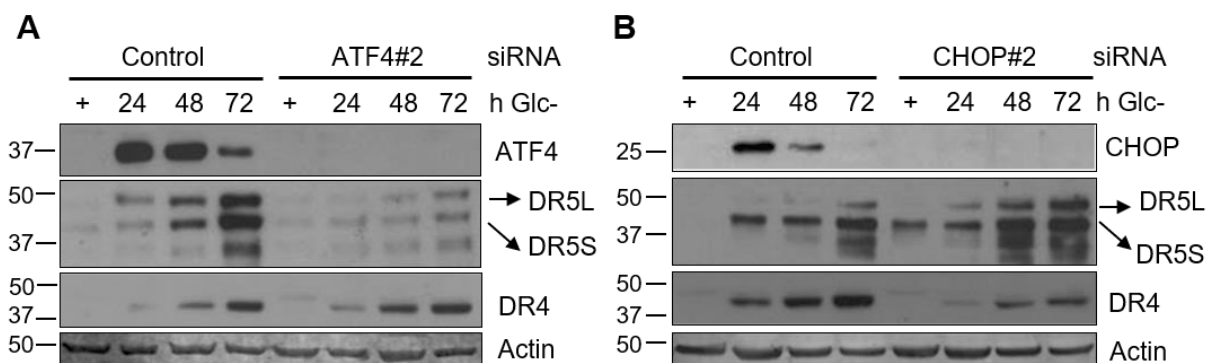
Figure 11 ATF4 but not CHOP regulates DR5 protein expression
A, B) HeLa cells were transfected for 24 h with control siRNA (labelled as ''Control''), siRNA for CHOP and ATF4 (labelled as ''ATF4#2'' and ''CHOP#2'' and treated post transfection for indicated times with 25 mM (+) or 0 mM (Glc-) glucose. A representative western blot of protein level of CHOP, DR5, DR4 and ATF4 is shown. (L) long; (S) short. (A and B are taken from doctoral thesis of Raffaela Iurlaro and (Iurlaro, Püschel et al., 2017)

Moreover, knocking down ATF4 with two different siRNA sequences (A#1 and A#2) prevented cell death induction, whereas CHOP knockdown only protected minor from cell death. (**Figure 12A-D**).

To sum it up, we found that HeLa cells undergo cell death upon glucose deprivation in an apoptotic manner, which is mediated by the induction of DR4 and DR5. We also found that ATF4 but not CHOP regulates DR5 protein expression. These results were further confirmed in DR4, DR5 and CHOP deficient cells (see also Appendix (Iurlaro, Püschel et al., 2017b))
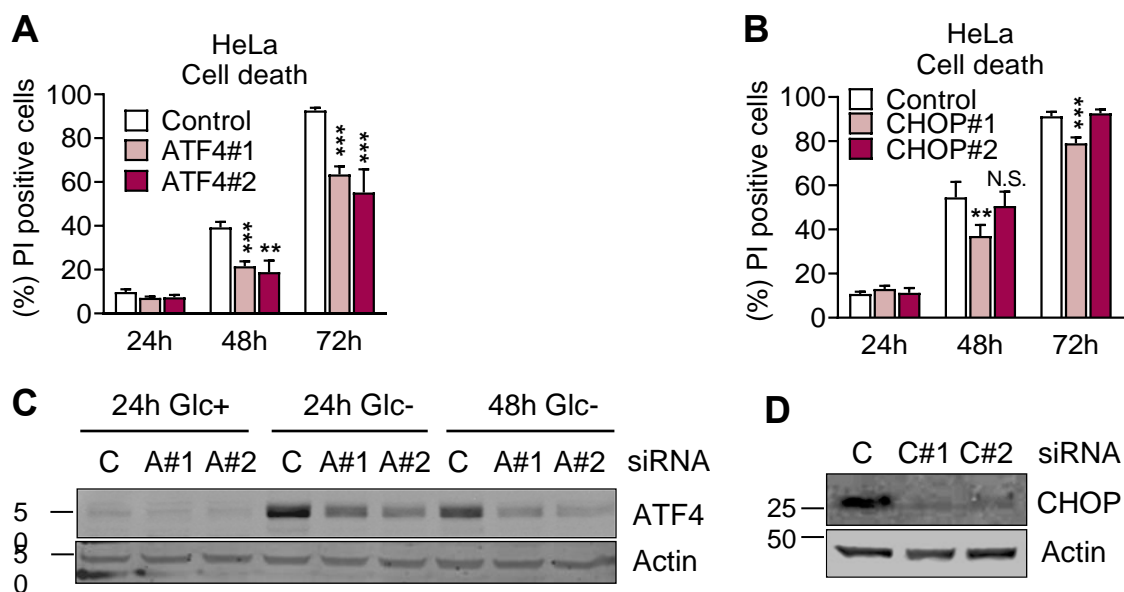
Figure 12 ATF4 mediates cell death upon glucose deprivation

A,B,C,D) Cells were transfected for 24 h with control siRNA (labelled as 'Control' or 'C') and with siRNA against CHOP (labelled as 'CHOP' or 'C#1' for sequence 1 and ''CHOP'' or 'C#2' for sequence 2) and against ATF4 (labelled as 'A#1' and 'A#2'). Cells were treated for indicated times with 0 mM (Glc-) or with 25 mM (Glc+) glucose when indicated. Cell death was analysed by PI incorporation and FACS analysis. Data represent mean ±SEM (n=7). Asterisks denote significant differences against the control siRNA of each time point.

C) HeLa cells were transfected as described in A. Representative western blot of ATF4 induction upon glucose deprivation (Glc-) or in the presence of glucose (Glc+) are shown.

D) HeLa cells were transfected as described in A. Representative western blot of CHOP induction after 48 h of glucose deprivation.

7. Results - Part II

7.1 Starvation and anti-metabolic drugs induce the secretion of cytokines and chemokines

In the previous section we showed that cancer cells, under sustained glucose deprivation, undergo apoptotic cell death. However, we also hypothesized that cancer cells induce an adaptive response, which allows cells to regain homeostasis when exposed to nutrient stress. Concerning that, it is described that hypoxia, which can result among others from fast tumor growth and its poor vascularization, promotes the secretion of cytokines like VEGF (Forsythe et al., 1996). VEGF is a cytokine that induces angiogenesis and therefore promotes the re-vascularisation of the tumor (Carmeliet, 2005). Furthermore, transient ischemia, which involves nutrient and oxygen deprivation, is associated with increased inflammation (Lee et al., 2000). This suggests that cancer cells induce cytokine release upon nutrient stress, which promote cell-cell interaction in the tumor for survival.

Regarding that it is not only important to understand how cells undergo cell death upon glucose deprivation but also how cells adapt to nutrient limitations and how this affects the overall survival of the tumor in order to discover suitable therapies for patients.

Therefore, the second part of the results presented in this thesis address the question of how cancer cells adapt to nutrient deprivation and what are the underlying mechanisms and consequences for the tumor and its surrounding tissue. We specifically investigated if cancer cells release cytokines upon starvation and which were the functional consequences of these cytokines for cancer as well as for immune cells.

7.1.1 Glucose deprivation promotes the secretion of cytokines

In the first chapter, we demonstrated that glucose deprivation promotes cell death. Cell death has been linked to cytokine release and inflammation. The most prominent cell death form that induces inflammation is necrosis. One of the consequences of necrotic cell death is the release of cellular contents, which contain ´danger signals´, promoting the activation of the immune system (Matzinger et al., 2002). However, also apoptosis is associated with inflammation since dying cells, which are not immediately cleared by immune cells, release cellular contents by a process named ´secondary necrosis´. In this process the cell membrane becomes permeable for macromolecules and inflammation is triggered due to released cell contents (Kono and Rock, 2008). This is an important defence reaction of the body against pathogens or to induce wound healing and tissue repair upon damage. However, not only released cellular contents promote

inflammation but also the release of cytokines. Regarding that it is reported that IL-8 is released upon TNFα treatment and Fas-ligation mediating apoptosis (Hagimoto et al., 1999).

In our experimental settings we wanted to exclude cell death involvement in cytokine induction upon glucose deprivation. Therefore, cell death was analysed in several cancer cell lines from different origins: NSCLC adenocarcinoma cells: A549 and H1299, squamous lung carcinoma cells: SW900 and H520 and large cell lung cancer cells: H460. We found that none of the tested cell lines underwent cell death at 24 h of glucose deprivation (**Figure 13A-E**). Cell death occurred after 48 h of glucose deprivation in A549, H460, H1299, SW900 and HeLa cells. H520 cells did not undergo cell death up to 72 h of glucose deprivation and are therefore more resistance towards glucose deprivation compared to the other cell lines (**Figure 13E**). Therefore, experiments measuring cytokine release upon glucose deprivation were performed at 24 h to exclude cell death involvement.
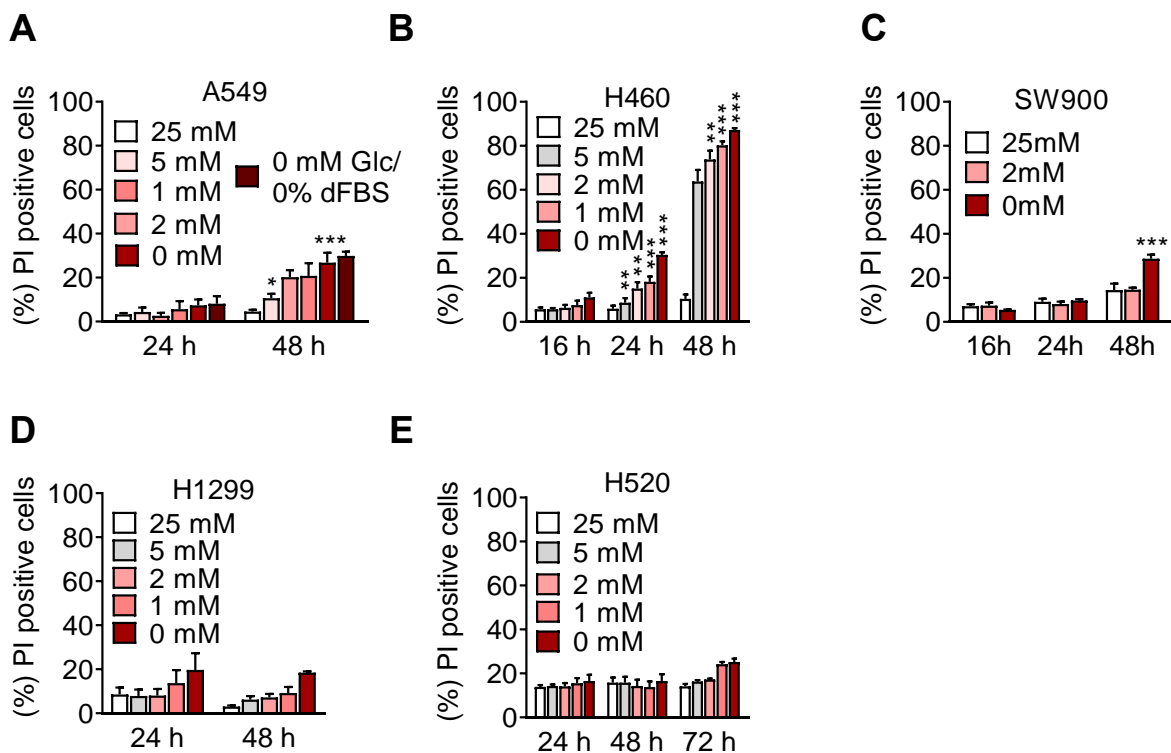
Figure 13 Glucose deprivation induces cell death in lung cancer cells
A-E) Different cell lines were treated with indicated glucose concentrations and 10 % FBS at indicated time points. Cell death was analyzed by PI incorporation and FACS analysis. Data represent mean ±SEM (n=3-4). Asterisks denote significant differences between treated cells and the control sample in Glc+ (25 mM).

To investigate if glucose deprivation induces the release of cytokines, the *Proteome Profiler Human XL Cytokine Array* (R&D System*)* was performed. This array analysed 105 selected human cytokines simultaneously. Therefore, A549 cells were treated for 24 h with 10 % FBS

in the presence (25 mM) or absence (0 mM) of glucose. The supernatants of three independent experiments were collected, combined and analysed according to manufacturer's instructions.
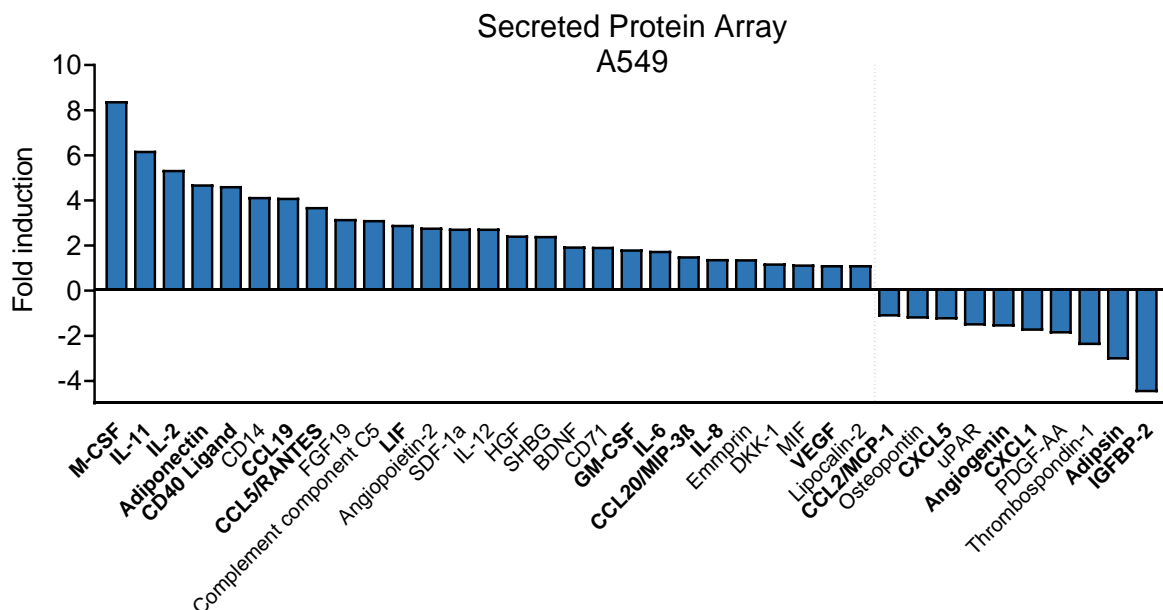
Figure 14 Proteome Profiler Human XL Cytokine Array of A549 cells
A549 cells were treated for 24 h with dFBS-free media containing 25 (Glc+) or 0 mM (Glc-) glucose. Supernatants of three independent experiments were collected and combined. *Proteome Profiler Human XL Cytokine Array Kit* was performed according to manufacturer instructions. Mean densities of membrane spots were analysed by ImageJ and selected proteins are shown. Fold induction of each cytokine was calculated versus Glc+.

We found various up- and downregulated cytokines and chemokines involved in various cellular processes. Amongst them, we found release of chemokines such as IL-8, CCL5/RANTES, CCL20 (MIP-3β) and CCL19, as well as immune cytokines including IL-6, IL-2, IL-11, M-CSF and CD40-ligand. Cytokines with alternative functions like LIF, VEGF or adiponectin were released as well (**Figure 14**). This confirms that not only inflammatory ones but also cytokines with other functions are secreted from lung cancer cells. Importantly, the release of some chemokines like CXCL5 and CCL2 as well as cytokines like IGFBP-2, adipsin, angiogenin and PDGF-AA, which have functions in insulin signaling, and angiogenesis were downregulated.

These results indicate, that glucose deprivation does not only induce, but also reduce, the release of various cytokines with different biological functions. However, most of the released cytokines were identified to be pro-inflammatory. This suggests, that cytokines induced upon glucose deprivation may alter the immune landscape in the tumor.

Results-Part II

Since there is currently a major interest in inflammatory processes associated with the cancer metabolism and patient outcome, the further course of this project focuses on the induction and release of inflammatory cytokines, which are associated with immune infiltration in cancer.
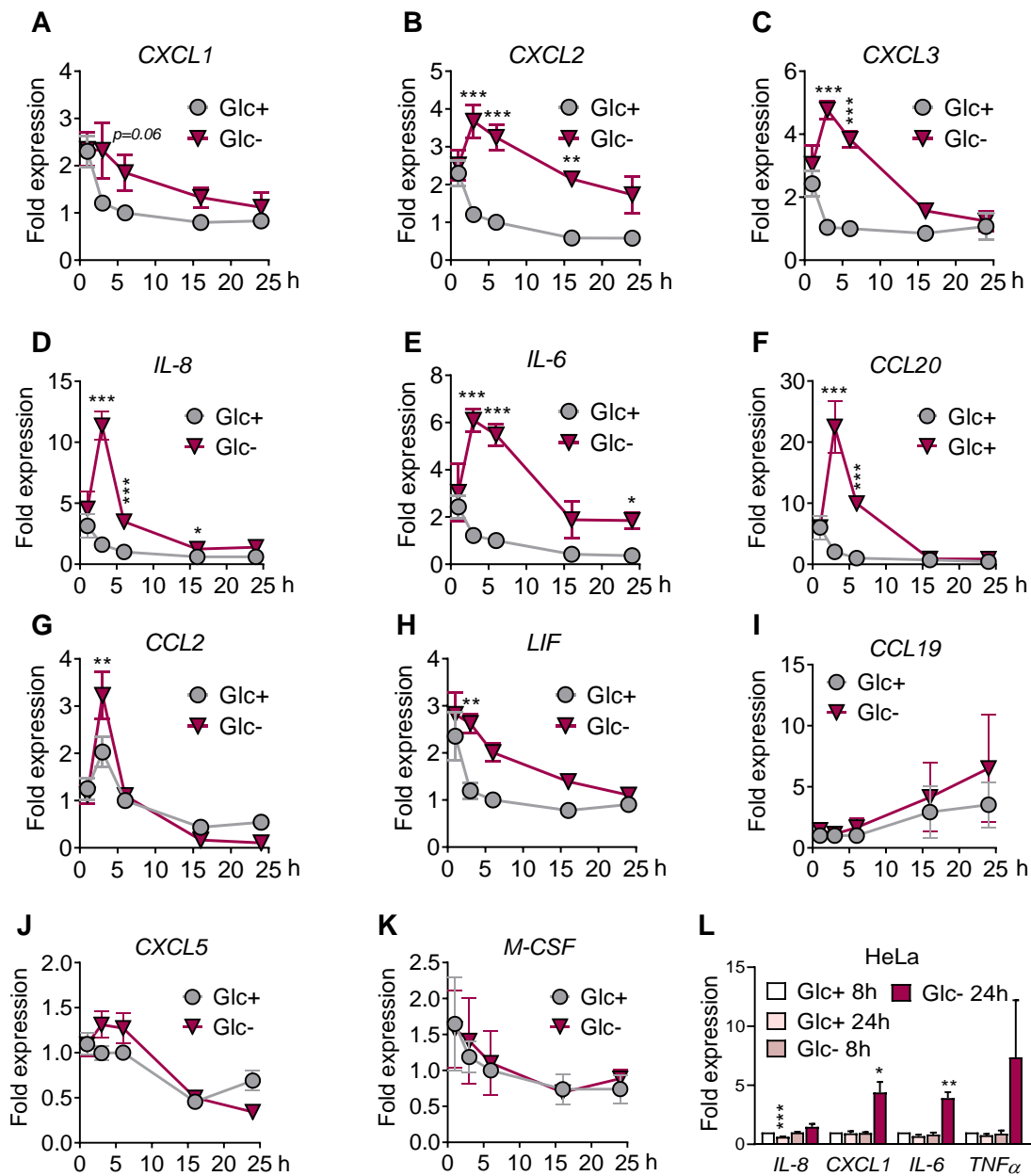
Figure 15 Glucose deprivation induces immune cytokine and chemokine mRNA expression in A549 cells

A-H) A549 cells were treated for 1, 3, 6, 16 and 24 h with media containing 25 (Glc+) or 0 mM (Glc-) glucose. qPCR of CXCL1 (A), CXCL2 (B), CXCL3 (C), IL-8 (D), IL-6 (E), CCL20 (F), CCL2 (G), LIF (H), CCL19 (I) and CXCL5 (J) and M-CSF (K) is shown. Fold expression was calculated by normalizing to cells treated for 6 h with Glc+. Data represent mean ±SEM (n=3-9). Asterisks denote significant differences versus the control samples in Glc+ of each time point analysed by two-way ANOVA.

L) HeLa cells were treated for 8 or 24 h with media containing 25 (Glc+) or 2 mM (Glc-) glucose. qPCR for indicated genes is shown. Fold expression was calculated by normalizing to

the control sample Glc+ at 8 h. Data represent mean ±SEM (n=3). Asterisks denote significant differences between treated cells and samples treated for 8 h with Glc+.

We validated the induction and release of some of the identified cytokines by ELISA and qPCR in A549 and HeLa cells. We confirmed that the mRNA of CXCL2, CXCL3, IL-8, IL-6, CCL20, CCL2, LIF and slightly CXCL1 was induced at short time points with a peak at 3 h upon glucose deprivation (**Figure 15A-H**). Cytokine mRNA level returned to basal level within 24 h with exception for CXCL2 and IL-6 (**Figure 15B,E**). We could not confirm an mRNA induction of CCL19, CXCL5 and M-CSF upon glucose deprivation in A549 cells (**Figure15 I-K**). We further confirmed mRNA induction of IL-8, IL-6, CXCL1 and TNFα in HeLa cells after 24 h of glucose deprivation (**Figure 15L**). In summary, these results prove that glucose deprivation induces the mRNA of inflammatory cytokines upon glucose deprivation.

We further validated the cytokine release upon glucose deprivation from several cancer cell lines of different origin and carcinoma type by ELISA. A549, H460, SW900 and HeLa cells released IL-8 at basal level. However, IL-8 release was increased upon glucose deprivation in these cell lines, see **Figure 16A-D**. As a control for IL-8 release, we treated A549 and HeLa cells for 24 h with TNFα (10 ng/mL). TNFα induced approximately a 10-fold higher release of IL-8 in A549 cells and a 5-fold higher release in HeLa cells compared to glucose deprivation (**Figure 16E-F**).
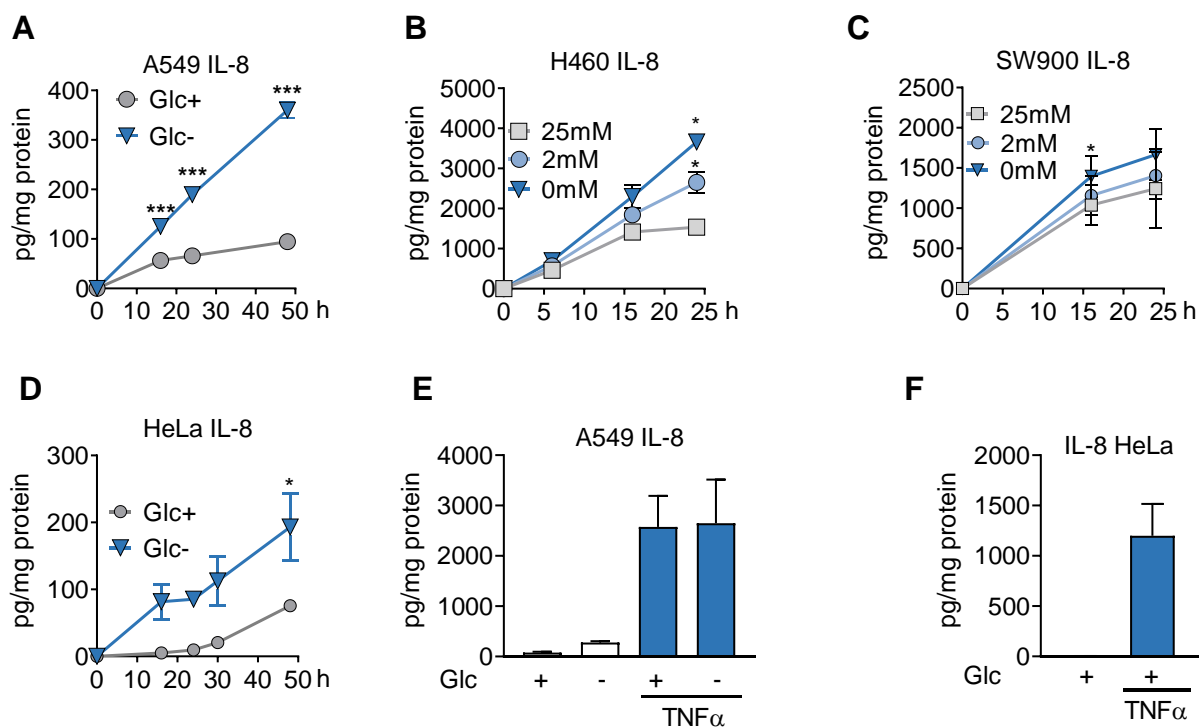
Figure 16 Glucose deprivation induces IL-8 release in cancer cells
A,E) A549 cells were treated with 25 (Glc+), 0 mM (Glc-) or with TNFα (10 ng/mL) for 24 h
or as indicated and IL-8 release was measured by ELISA. Data represent mean ±SEM (n=3-4).
Asterisks denote significance versus the Glc+ control sample for each time point analysed by
two-way ANOVA.
B-C) H460 and SW900 cells were treated with 25 mM (Glc+), 0 mM (Glc-) or 2 mM glucose
between 16 and 48 h (as indicated) and IL-8 release was analysed by ELISA. Data represent
mean ±SEM (n=3-4). Asterisks denote significance versus the Glc+ control sample for each
time point analysed by two-way ANOVA.
D,F) HeLa cells were treated as in A. or for 24 h with TNFα (10 ng/mL) and IL-8 release was
measured by ELISA. Data represents Mean ±SEM (n=3-4).

IL-6 was released at basal levels from H460, SW900 and HeLa cells and in accordance with

IL-8 did glucose deprivation promote the release of IL-6 from A549, H460, SW900 and HeLa

cells. (**Figure 17A-D**)

Regarding CXCL1 we found that A549 and HeLa cells released CXCL1 at basal level, whereas

secretion was not induced upon glucose deprivation (**Figure 18A-B**). HeLa cells induced TNFα

at mRNA level, however TNFα release was not detected by ELISA in HeLa cells (**Figure 18B**).

Furthermore, M-CSF and CCL20 release were induced in the protein array however its release

was not detected by ELISA in A549 cells (**Figure 18C-D**).
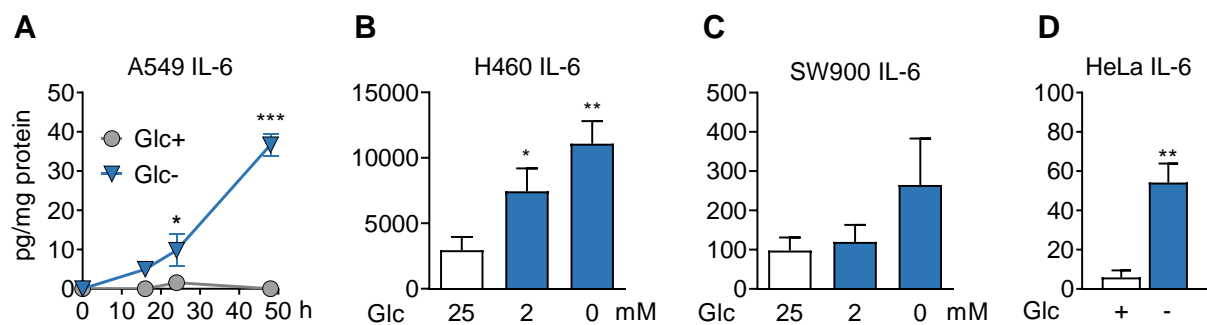
Figure 17 Glucose deprivation promotes IL-6 release from cancer cells
A) A549 cells were treated with 25 mM (Glc+) or 0 mM (Glc-) glucose for indicated times and
ELISA for IL-6 is shown. Data represent mean ±SEM (n=4). Asterisks denote significance
versus the Glc+ control sample for each time point analysed by two-way ANOVA.

B-D) H460, SW900 and HeLa cells were treated with 25, 2 or 0 mM glucose for 24 h and IL-6
release was analysed by ELISA. Data represent mean ±SEM (n=3). Asterisks denote
significance versus the 25 mM glucose control sample. Data are presented in pg/mg protein.
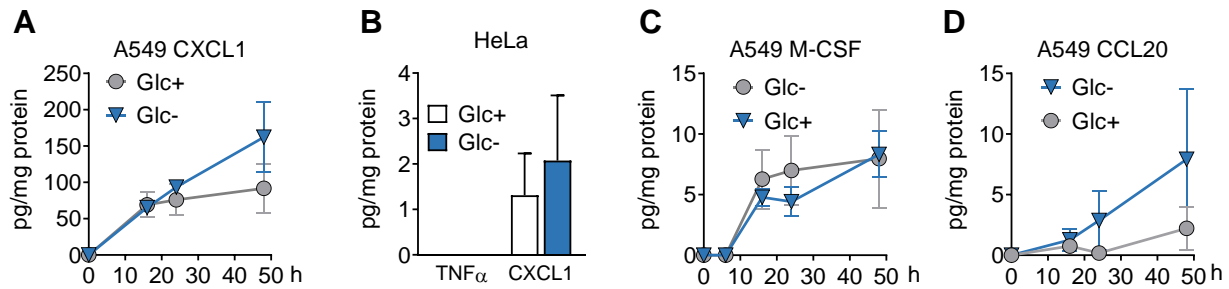
Figure 18 Glucose deprivation does not induce CXCL1, TNFα, M-CSF and CCL20 release in tested cell lines

A, C, D) A549 cells were treated for indicated times with 25 (Glc+) or 0 mM (Glc-) glucose and ELISA for CXCL1 (n=5) (A), M-CSF (n=6) (C) and CCL20 (n=2) (D) is shown. Data represent mean ±SEM. Data are presented in pg/mg protein.

B) HeLa cells were treated with 25 (Glc+) or 0 (Glc-) mM glucose for 24 h and cytokine release was analysed by ELISA for TNFα and CXCL1. Data represent mean ±SEM (n=3-5). Data are presented in pg/mg protein.

We validated cytokine release in H1299 and H520 cells. However, these cells neither released

IL-8 nor IL-6 upon glucose deprivation in our setting (**Figure 19A-D**).
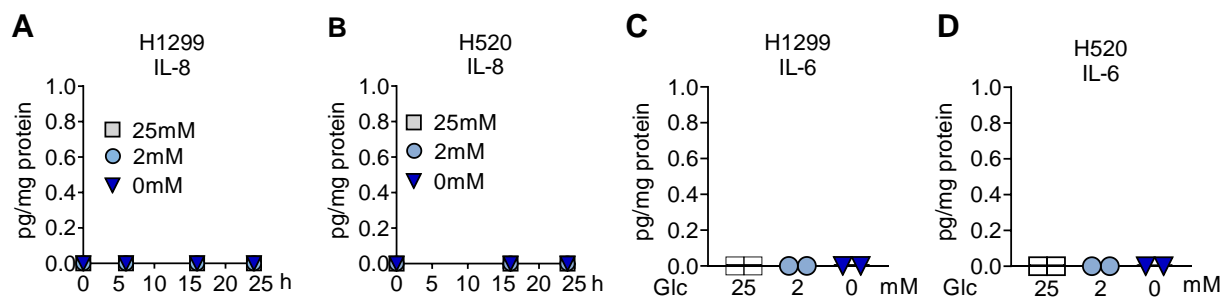
Figure 19 H1299 and H520 cells do not release IL-8 and IL-6

A-B) H1299 and H520 cell were treated with 0, 2 or 25 mM glucose for indicated time points and IL-8 release was measured by ELISA. Data represent mean ±SEM (n=2-3)

C-D) H1299 and H520 cell were treated with 0, 2 or 25 mM glucose for 24 h and IL-6 release was measured by ELISA. Data represent mean ±SEM (n=2).

In the secreted protein array (**Figure 14**), we also detected LIF secretion, which was recently

associated with tumor progression and poor patient survival in several cancers (Pascual-García

et al., 2019). Therefore, we validated LIF release from several cancer cell lines. We found that

LIF was secreted in a time and dose dependent manner from the lung cancer cell lines A549,

H460, SW900 and H1299 cells (**Figure 20A-D**) but not from HeLa or H520 cells.

(**Figure 20E-F**)

In conclusion, we found that glucose deprivation promotes the induction and release of IL-6,

IL-8 and LIF at times when cell death was not induced. Within our analysis we could not find

a correlation between different carcinoma types (adeno- and squamous carcinoma) and cytokines release. Moreover, quantity and cytokine type are cell type dependent.
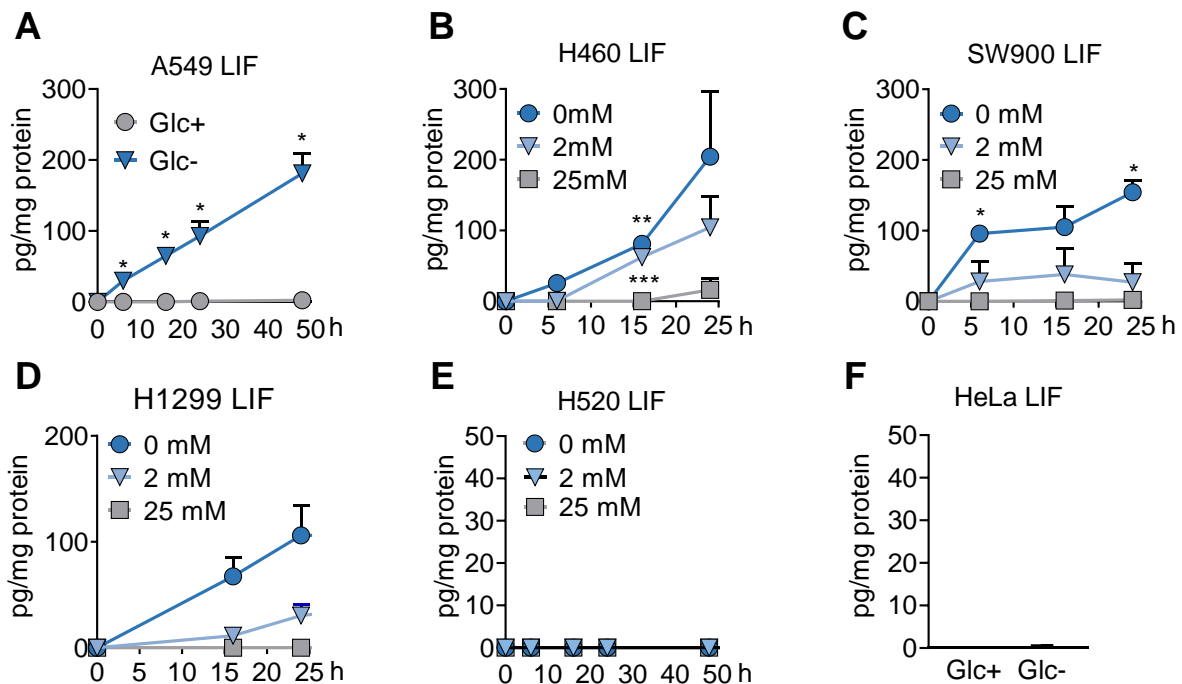
Figure 20 Glucose deprivation induces LIF release in cancer cells
A-E) Cells were treated for indicated times with 25 mM (Glc+), 2 mM or 0 mM (Glc-) glucose and LIF release was analysed by ELISA for A549 (A), H460 (B), SW900 (C), H1299 (D) and H520 (E) cells. Data represent mean ±SEM (n=4) for A549, (n=4) for H460, (n=3) for SW900, (n=5) for H1299 and (n=2) for H520. Asterisks denote significance versus the 25 mM glucose control sample of each time point.
F) HeLa cells were treated for 24 h with Glc+ or Glc- and LIF release was analysed by ELISA. Data represent mean ±SEM (n=2).

7.1.2 IL-8 but not LIF accumulates intracellular in A549 cells upon glucose deprivation

In a next step, we analysed if cytokines are intracellularly stored in A549 cells under normal culture conditions and get released upon glucose deprivation, or if cytokines get *de novo* synthesized upon glucose deprivation. First, we analysed IL-8 and LIF protein level in the cell lysate and in the supernatant of A549 cells over time and at different glucose concentrations.

We detected IL-8 in the cell lysate of A549 cells in the presence and absence of glucose, however the intracellular IL-8 level was higher in glucose-deprived cells (**Figure 21A-B**). This suggests, that the intracellular IL-8 level is increased in the absence of glucose. We also found that intracellular IL-8 level and IL-8 release increased in a dose and time dependent manner, meaning that lower glucose level induce higher intracellular IL-8 accumulation and release (**Figure 21B-C**).
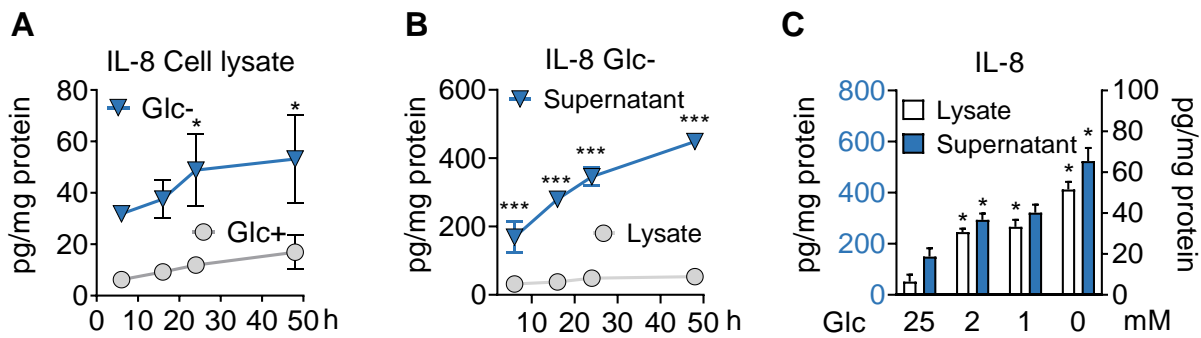
Figure 21 IL-8 accumulates in the cell lysate of A549 cells upon glucose deprivation

A) A549 cells were treated between 6 and 48 h with 0 mM (Glc-) or 25 mM (Glc+) glucose and IL-8 level in the cell lysate were analysed by ELISA. Data represent mean ±SEM (n=3). Asterisks denote significant differences between the control sample of each treatment.

B) A549 cells were treated with Glc- for indicated times and IL-8 was analysed by ELISA in the supernatant and in the cell lysate. Data represent mean ±SEM (n=3). Asterisks denote significant differences between the control sample at 6 h Glc+ and each treatment.

C) A549 cells were treated for 24 h at indicated glucose concentrations. IL-8 in cell lysate and supernatant was analysed by ELISA. Data represent mean ±SEM (n=3). Asterisks denote significant differences between the control sample (25 mM) and each condition.

We found that LIF release is dose- and time-dependent with the highest secretion at a concentration of 0 mM glucose (**Figure 22A-B**). In contrary to IL-8, we could not detect LIF in the presence of glucose (25 mM) intra- or extracellularly (**Figure 22A,C**). LIF was only detectable in the cell lysate after 24 h of glucose deprivation at very low level (**Figure 22C**).
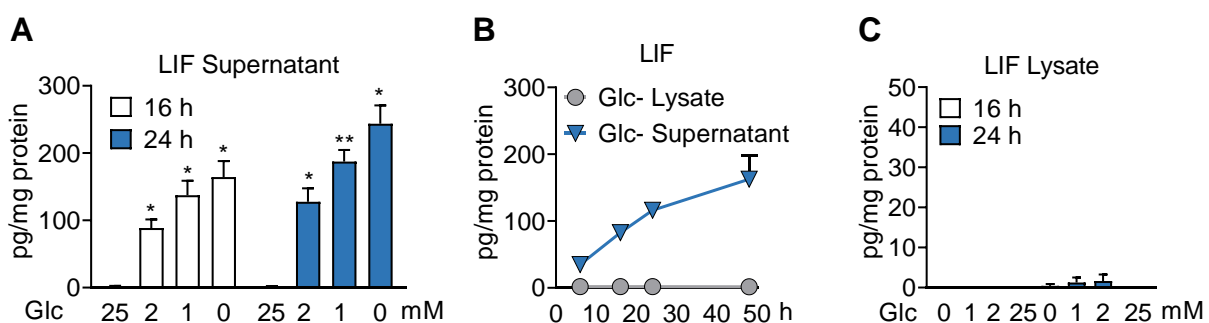
Figure 22 LIF is not detectable in the cell lysate of A549 cells.

A) A549 cells were treated for 16 and 24 h at indicated glucose concentrations and LIF release was analysed by ELISA. Data represent mean ±SEM (n=3). Asterisks denote significant differences between the sample treated with 25 mM glucose.

B) A549 cells were treated for indicated times with glucose-free media and LIF was analysed by ELISA in the supernatant and the cell lysate. Data represent mean ±SEM (n=2).

C) A549 cells were treated for 16 and 24 h with indicated doses of glucose and LIF was analysed in the cell lysate by ELISA. Data represent mean ±SEM (n=3).

7.1.3 Addition of nutrients to glucose-deprived media has differential impacts on cytokine release

Glucose is not exclusively important for energy production, but it is also needed for glycosylation of newly synthesized proteins in the ER. Therefore, glucose deprivation leads to less energy production as well as to impaired glycosylation in the cell. However, depending on the cancer cell type, cells increase the uptake of alternative nutrients to maintain energy homeostasis and glycosylation upon glucose deprivation (Chaveroux et al., 2016a). Other nutrients include for instance amino acids, fatty acids, lactate as well as glucose derivates such as mannose or fructose. These nutrients can be converted into glucose or fuel glycolysis through alternative metabolic pathways (Sharma et al., 2014).

Therefore, we wanted to further understand if the addition of alternative selected nutrients reverses the release of cytokines upon glucose deprivation. Hence, we substituted glucose-deprived media with nutrients, which are described to substitute for glucose at different stages of specific metabolic pathways. These nutrients include: Mannose (Man) and fructose (Fru), which fuel the glycolytic pathway, either directly or after conversion to glucose. Methyl-pyruvate (Me-Pyr) is a mitochondrial substrate for the generation of ATP in cells. Lactate, which is a product of anaerobic glycolysis, was recently described to be uptaken and catabolized in the Krebs cycle by lung cancer cells (Faubert et al., 2017). N-Acetylglucosamine (GlcNAc), which is a product of the hexosamine biosynthetic pathway, can be utilized by cells for *N*- and *O*-glycosylation. 2-DG, an anti-metabolic drug and inhibitor of glycosylation, has been shown to substitute for glucose in cells in certain contexts (Giammarioli et al., 2012; Lee et al., 2018). We treated A549 cells for 24 h with glucose free media, which was replenished with one of the nutrients described above. First, we measured cell death by FACS and PI-incorporation and found that addition of mannose and fructose significantly protected cells from death after 48 h of treatment (**Figure 23**). This suggests, that cells use mannose and fructose to overcome glucose deficiency and maintain energy level. Surprisingly, addition of 2-DG slightly protected A549 cells from cell death, which was shown before (Lee et al., 2018). However, lactate, Me-Pyr and GlcNAc did not protect cells from cell death. (**Figure 23**)
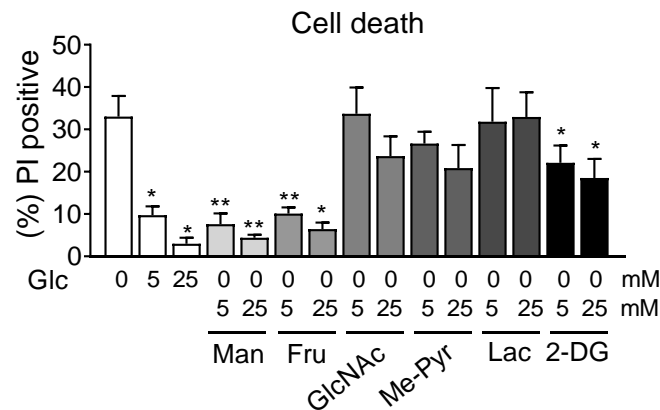
Figure 23 Addition of mannose, fructose and 2-DG protects from glucose deprivation induced cell death
A549 cells were treated for 48 h with indicated concentrations of glucose (Glc), mannose (Man), fructose (Fru), N-Acetyl-glucosamine (GlcNAc), methyl-pyruvate (Me-Pyr), lactate (Lac) and 2-deoxyglucose (2-DG). Cell death was analysed by PI incorporation and FACS analysis. Data represent mean ±SEM (n=4). Asterisks denote significant differences versus the 0 mM glucose control sample.

Once we analysed cell death upon addition of alternate nutrients, we also measured the mRNA expression of IL-8, CXCL3, CXCL2 and LIF after 6 h, as well as the cytokine release of IL-8 and LIF after 24 h of glucose deprivation.

CXCL2 mRNA expression was partially prevented by addition of Man, 2-DG and high doses of Me-Pyr (**Figure 24A**). In contrary, CXCL3 mRNA expression was only prevented by addition of high doses of Me-Pyr. Furthermore, low concentrations of 2-DG slightly increased and high doses slightly decreased CXCL3 mRNA level, however not significantly. These results suggest that cytokine mRNA induction is not regulated in the same manner for all cytokines and is dependent on the involvement of distinct metabolic pathways.

IL-8 mRNA induction and release was prevented by addition of high doses of Me-Pyr to glucose-deprived media, similar to the mRNA of CXCL2 and CXCL3 (**Figure 24A-C**). Surprisingly, low doses of 2-DG induced IL-8 mRNA but not its release (**Figure 24D**). Moreover, IL-8 release but not mRNA induction was prevented by Man and and partially Fru. This data suggests, that IL-8 mRNA and protein induction are regulated differently, since the addition of nutrients have opposing effects on mRNA level and secretion (**Figure 24C-D**).

Regarding LIF we found that mRNA induction upon glucose deprivation was not prevented by the addition of any of the tested nutrients, suggesting that LIF mRNA induction is specific to the lack of glucose and it cannot be reversed by the addition of alternative substrates for the glucose metabolism (**Figure 24 E**). In contrary, LIF secretion was partially prevented by addition of Fru, lactate and high doses of Me-Pyr and completely prevented by addition of Man and 2-DG (**Figure 24F**).
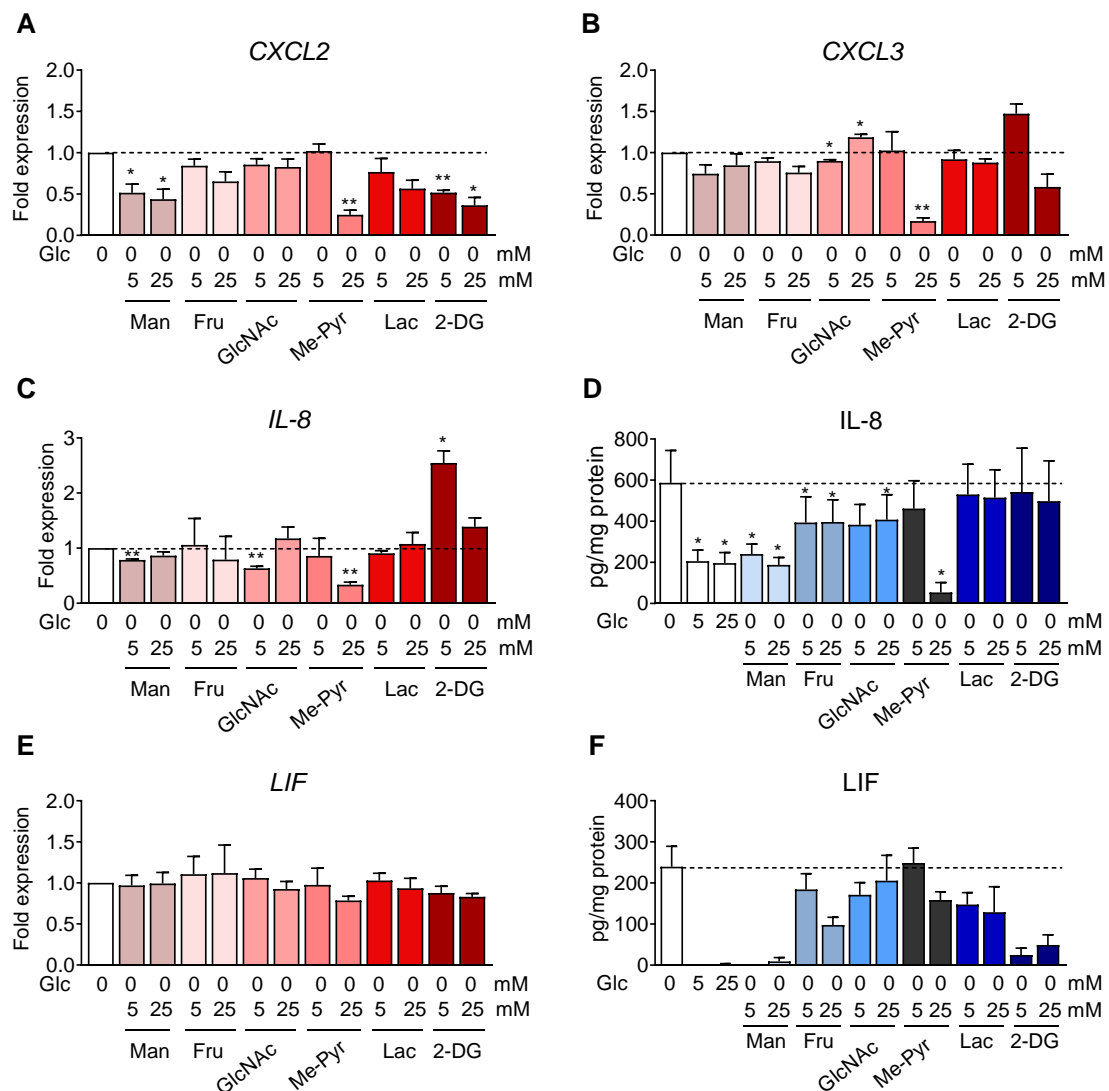
Figure 24 Mannose reduced IL-8 and LIF release upon glucose deprivation in A549 cells

A,B,C,E) A549 cells were treated for 6 h with indicated concentrations of glucose (Glc), mannose (Man), fructose (Fru), N-Acetyl-glucosamine (GlcNAc), methyl-pyruvate (Me-Pyr), lactate (Lac) or 2-deoxyglucose (2-DG). qPCR for CXCL2 (A), CXCL3 (B), IL-8 (C) and LIF (E) is shown. Data are represented as mean ±SEM (n=3). Asterisks denote significant differences versus the control 0 mM glucose sample.

(D,F) A549 cells were treated for 24 h as described in A. and ELISA for IL-8 (D) and LIF (F) is shown. Data are represented as mean ±SEM (n=4). Asterisks denote significant differences versus the control 0 mM glucose sample.

In conclusion, nutrient addition to glucose-deprived media did not exert the same effect on cell death as on cytokine release. This suggests, that these two processes are regulated by independent pathways. Moreover, these results demonstrate that the addition of some nutrients like Man or Fru can reverse the release of IL-8 and LIF upon glucose deprivation. However, the effects on mRNA expression and protein release do not correspond, which is possibly due to impaired post translational modifications. Moreover, addition of nutrients to glucose-deprived media had distinct outcomes on specific cytokines, meaning that cytokines are not regulated likewise. In this sense, LIF seems to be regulated at mRNA level in a completely different manner compared to the other tested cytokines.

7.1.4 Glutamine deprivation and anti-metabolic drugs induce cytokines

The further course of this project will focus on the induction and release of IL-6, IL-8 and LIF, due to their importance in lung and other cancer types (Kumari et al., 2016) as well as due to their high mRNA induction and release upon glucose deprivation in our model.

In the previous chapters we proved that glucose deprivation leads to the induction and release of cytokines that partially can be reversed by addition of intermediate nutrients of specific metabolic pathways. In the following chapter we investigate if glutamine deprivation or total starvation as well as treatment with anti-metabolic drugs such as 2-DG and metformin induces the same response on cytokine release as glucose deprivation.

In a first experiment we analysed cell death and we found that none of the conditions described before induced cell death within 24 h (**Figure 25**). Therefore, A549 cells were treated for 24 h upon glutamine deprivation and total starvation. Total starvation was mimicked by treating cells with Hank's salt balanced solution (HBSS), a saline buffer containing 5.55 mM glucose.
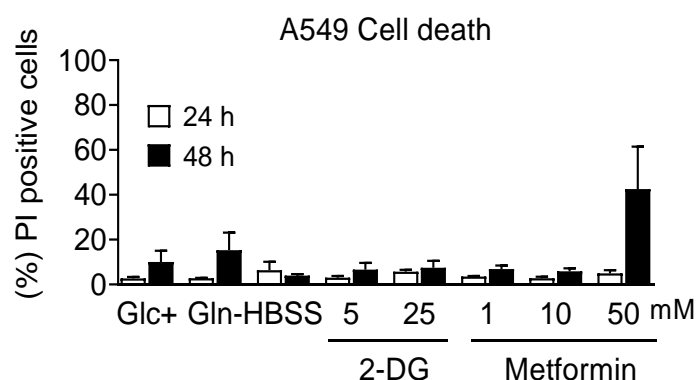
Figure 25 Cell death in A549 cells upon treatment with metabolic drugs and starvation
A549 cells were treated with media containing 25 mM glucose (Glc+), 0 mM glutamine (Gln-), Hank's Balanced Salt Solution (HBSS), 2-Deoxyglucose (2-DG) or metformin at indicated

time points. Cell death was analysed by PI incorporation and FACS analysis. Data represent mean ±SEM (n=3).

We found that IL-6 and IL-8, but not LIF were induced (**Figure 26A**) and secreted (**Figure 26B**) upon glutamine deprivation. In contrary, HBSS did not induce the release of none of the tested cytokines, however the mRNA of IL-8 was partially induced (**Figure 26A**). These results show, that glutamine deprivation but not total starvation promotes cytokine release.
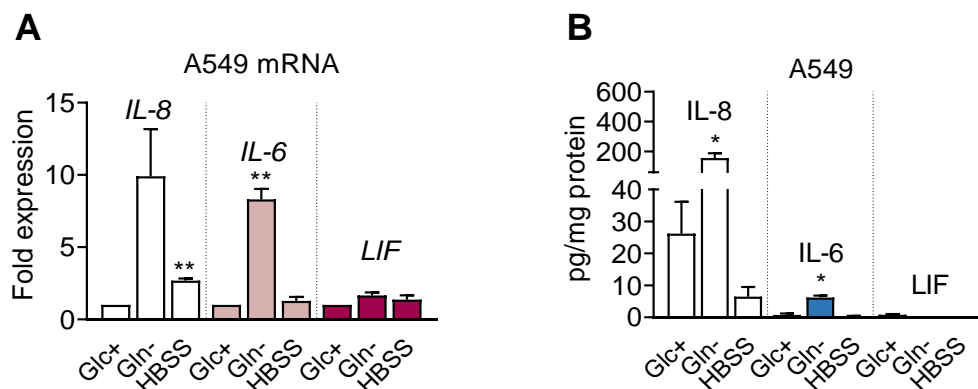
Figure 26 Glutamine deprivation induces IL-8 and IL-6 but not LIF mRNA expression and release
A) A549 cells were incubated in 25 mM glucose (Glc+), 0 mM (Gln-) glutamine medium or HBSS for 6 h. mRNA expression is shown for IL-8, IL-6 and LIF analysed by qPCR. Values were normalized to Glc+ control of each mRNA. Data represent mean ±SEM (n=3). Asterisks denote significant differences versus the Glc+ sample of each cytokine.
B) A549 cells were incubated in Glc+, Gln- medium or HBSS for 24 h. ELISA is shown for IL-8, IL-6 and LIF. Data indicate mean ±SEM (n=4). Asterisks denote significant differences versus the Glc+ control sample of each cytokine.

Anti-metabolic drugs, that target glucose or glutamine deprivation are currently under investigation in the clinic. Considering that nutrient deprivation induces cytokines, we assumed that anti-metabolic drugs could promote the release of cytokines likewise, which could affect the efficiency and mode of action of these drugs. 2-DG is a glucose derivate that blocks glycolysis and glycosylation in the cell. As a consequence, glucose is not metabolized, and glycolysis and protein glycosylation are impaired.

We found that the mRNA of IL-6 and IL-8 was induced in A549 cells upon treatment with 2-DG (**Figure 27A**). Furthermore, IL-8 was release from HeLa and A549 cells but not from H460 cells, whereas IL-6 release was induced in all tested cell lines (**Figure 27B-C**). LIF was not induced at mRNA level in A549 cells (**Figure 27A**) but it was released upon 2-DG treatment from all tested cell lines except from HeLa cells in a dose dependent manner (**Figure 27D**).
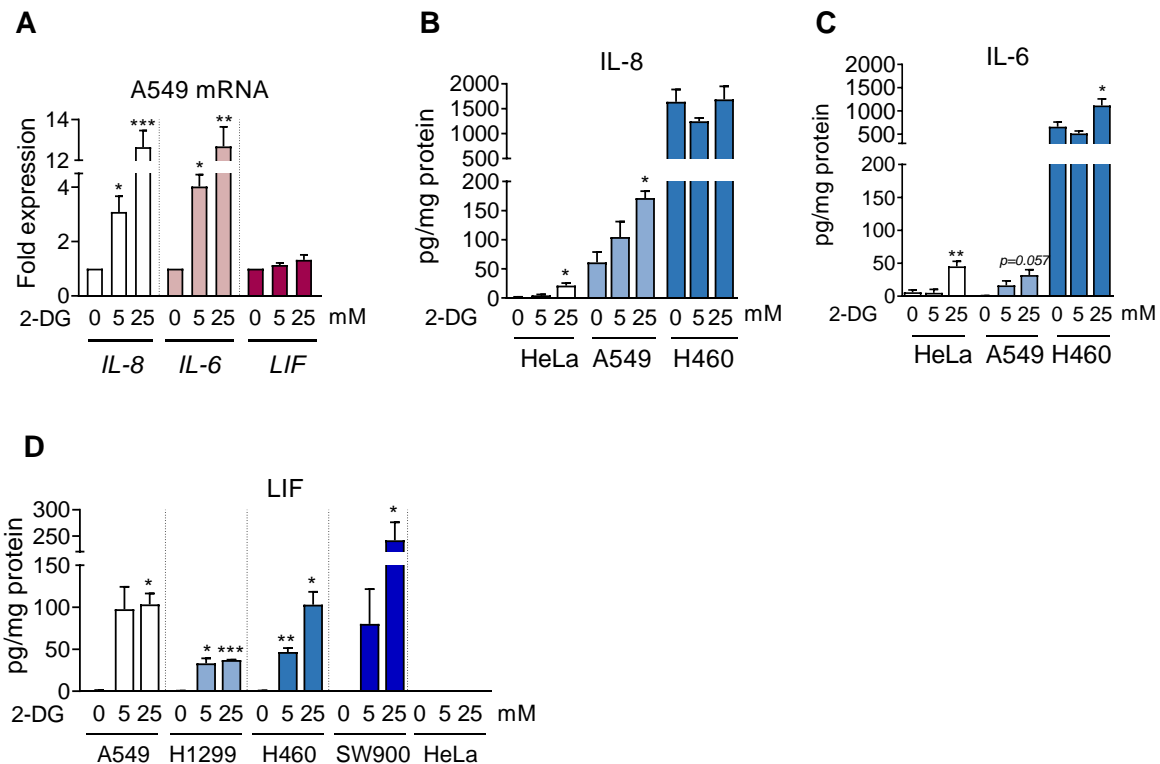
Figure 27 2-DG induces cytokine release in cancer cells
A) A549 cells were treated for 6 h with indicated concentrations of 2-deoxyglucose (2-DG). mRNA expression for IL-8, IL-6 and LIF was analysed by qPCR. Data represent mean ±SEM (n=3-4). Asterisks denote significant differences versus the control (0 mM) sample of each cytokine. Data obtained from (Jaime Redondo, Master thesis, 2018)
B-D) HeLa, A549, H460, SW900, H1299 cells were treated for 24 h as described in A. and IL-8 (B), IL-6 (C) and LIF (D) release was analyzed by ELISA. Data represent mean ±SEM (n=3-4). Asterisks denote significant differences versus the control (0 mM) sample.

Metformin, a diabetic drug, interferes with the mitochondria by blocking complex I of the respiratory chain. Recently it was shown that metformin affects the growth of lung tumors and it is also involved in pro-tumorigenic cytokine production (Levy and Doyen, 2018; Yaniv et al., 2018). We found that metformin induced the mRNA of IL-8, IL-6 but not LIF in A549 cells (**Figure 28A**). IL-6 and IL-8 release was induced in A549 and H460 but not SW900 cells (**Figure 28B-C**). In contrary, LIF release was not induced by any of the tested cell lines upon metformin treatment (**Figure 28E**).
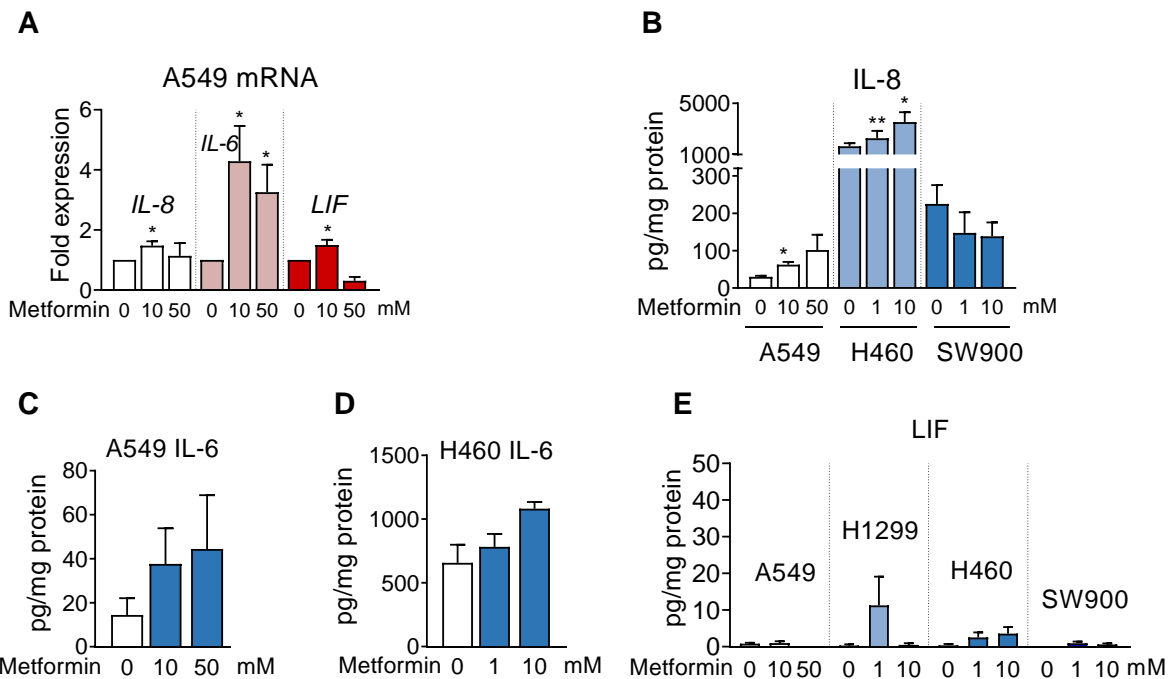
Figure 28 Metformin induces IL-8 and IL-6 release from cancer cells
A) A549 cells were treated for 6 h with indicated metformin concentrations and mRNA expression for IL-8, IL-6 and LIF was analysed by qPCR. Data represent mean ±SEM (n=4). Asterisks denote significant differences versus the control (0 mM) sample of each cytokine. (Jaime Redondo, Master thesis, 2018)
(B-E) A549, H460, SW900 and H1299 cells were treated for 24 h as described in A. and IL-8 (B), IL-6 (C-D) and LIF (E) release was analysed by ELISA. Data represent mean ±SEM (n=3). Asterisks denote significant differences versus the control (0 mM) sample.

To sum it up, we found that glutamine deprivation and treatment with 2-DG and metformin, but not total starvation, induces IL-8 and IL-6 in a cell type dependent manner. LIF in contrary, was only found to be induced and released upon 2-DG treatment. This suggests that LIF release is possibly a specific response to the glucose deprivation or impaired glycosylation, whereas IL-6 and IL-8 release is induced by a general interference with the cellular metabolism.

7.2 The UPR is induced upon glucose deprivation in A549 cells

In the first result chapter, it was described that cancer cells undergo cell death upon glucose deprivation in an UPR dependent manner. However, the UPR is described to be primary a pro-survival response in order to adapt to extra- or intracellular stresses. In this context, it is described that the UPR is induced upon glucose deprivation in cancer cells as that this response is involved in cytokine induction upon several stimuli (Iwasaki et al., 2014; Logue et al., 2018; Zhang et al., 2013a; Zhu et al., 2017). Therefore, we hypothesized that the UPR is involved in cytokine induction upon glucose deprivation in our model.

In the first result chapter we found that ATF4 and CHOP are induced upon glucose deprivation in HeLa cells. Since the following experiments were performed in A549 cells, we first validated if the three branches of the UPR are induced upon glucose deprivation.

To investigate if the ATF6 arm of the UPR is activated, cells were transfected with an ATF6-Flag plasmid and ATF6 cleavage was detected between 6 and 16 h by western blot upon glucose deprivation. As a control, cells were treated for 24 h with Dithiothreitol (DTT), a known UPR inducer (**Figure 29A**).

IRE1 endoribonuclease activity was validated by XBP1 splicing and analysed by PCR. XBP1 splicing was detected between 3 and 48 h of glucose deprivation (**Figure 29B**). As a control, cells were treated for 24 h with thapsigargin (Tg), a known UPR inducer. This result was further validated by qPCR, showing increased XBP1s mRNA level upon 6 h of glucose deprivation (**Figure 29C**). Furthermore, we also showed an induction of IRE1 but not ATF6 at mRNA level (**Figure 29C-D**). RIDD activity was analysed by transfecting A549 cells with a plasmid expressing a cytoplasmatic-defective IRE1 mutant (dominant-negative (DN)) (Drogat et al., 2007; Nguyen et al., 2004) as well as with a plasmid expressing the truncated IRE1 mutant variant (*Q780). *Q780 is one of the described somatic mutation (Greenman et al., 2007) in the cytosolic domain of IRE1 (Lhomond et al., 2018). Cells were pre-treated for 2 h with actinomycin, which blocks gene transcription and afterwards incubated in media without glucose. SPARC1 is a known RIDD target (Dejeans et al., 2012) and its mRNA was degraded upon treatment with glucose deprivation between 2 and 6 h (WT). However, mRNA degradation was prevented when cells were previously transfected with the plasmid expressing the DN or mutated *Q780 form of IRE1 (**Figure 29E**). This proves that glucose deprivation promotes RIDD activity in these cells.

To sum it up, we proved that the ATF6 branch and the IRE1 endoribonuclease activity is fully functional in A549 cells upon glucose deprivation.

Activation of the PERK arm of the UPR was shown by ATF4 and CHOP induction at mRNA and protein level starting at 3 h of glucose deprivation (**Figure 29F-I**). As a control, cells were treated for 24 h with Tg.
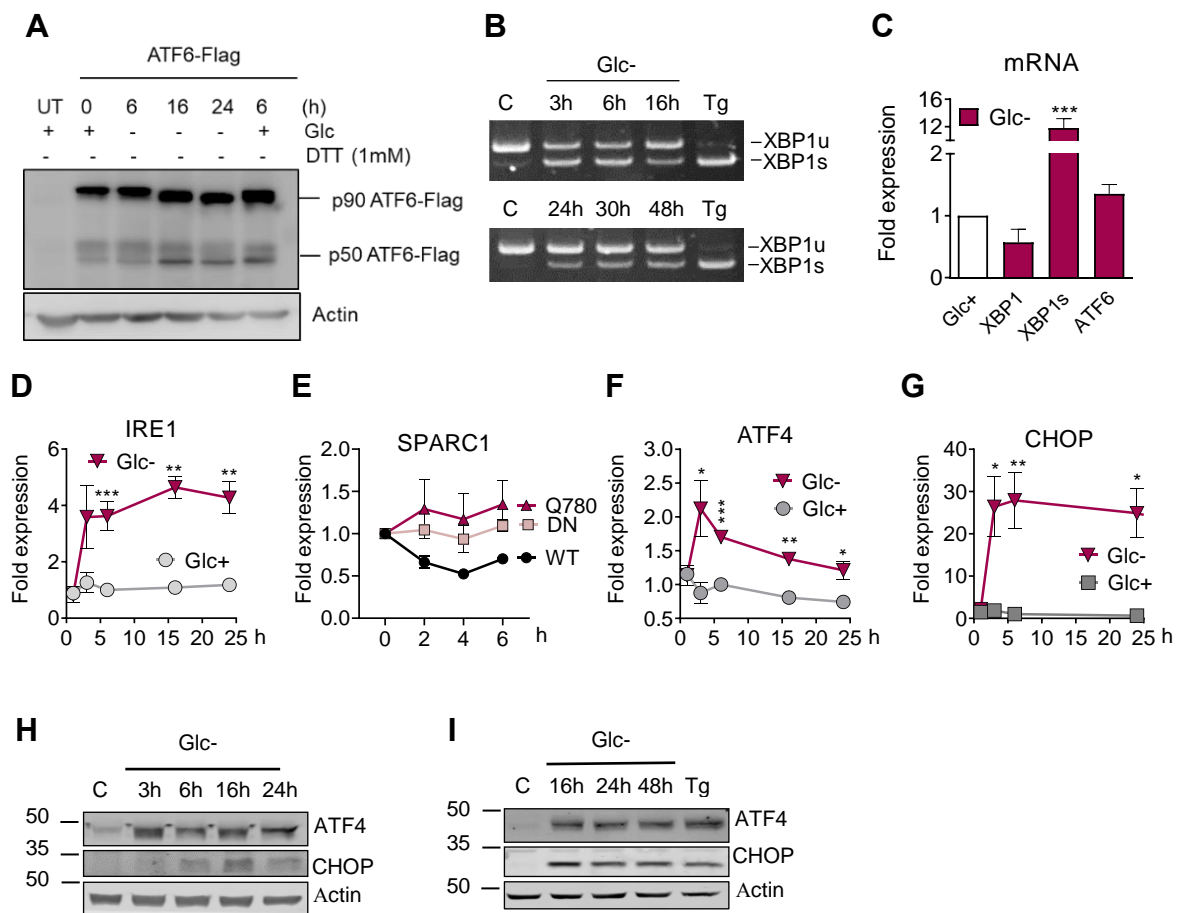
Figure 29 Glucose deprivation activates the UPR in A549 cells

A) A549 cells were transfected for 24 h with an ATF6-Flag overexpressing plasmid and treated for indicated times with 25 mM (+), 0 mM (-) or 1 mM Dithiothreitol (DTT). Representative western blot for Flag is shown. UT: not transfected.

B) A549 cells were treated with 25 mM Glc+ (C), 0 mM (Glc-) or with Tg for indicated times and lysed for mRNA extraction. Retro-transcription was performed followed by RT-PCR for XBP1. Tg: Thapsigargin (4 µM, 24 h); XBP1u (unspliced) and XBP1s (spliced). Representative PCR is shown out of (n=3).

C) A549 cells were treated for 6 h with Glc+ or Glc- and qPCR analysis for XBP1, XBP1s and ATF6 is shown. Data represent mean ±SEM (n=4). Asterisks denote significant differences versus the Glc+ control sample.

(D,F-G) A549 cells were treated as described in C. for indicated times and IRE1 (D), ATF4 (F) and CHOP (G) mRNA was analysed by qPCR. Values were normalized versus the 6 h Glc+ sample.

E) A549 cells were transfected for 24 h with plasmids expressing mutated forms of IRE1 (*Q780, DN) or an empty plasmid (WT). Cells were pretreated for 2 h with actinomycin before being incubated in glucose free media for 2, 4 and 6 h. mRNA was extracted and qPCR for SPARC1 was performed. Values were normalized versus the control sample time=0 of each treatment.

H-I) A549 cells were treated for indicated time points with Glc+ (labelled as 'C'), 0 mM (Glc-) or for 24 h with 4 µM Tg. A representative western blot (n=3) for ATF4 and CHOP is shown.

7.2.1 ATF4 mediates IL-8 and IL-6 but not LIF cytokine release

Some reports demonstrate that the PERK and IRE1 branch of the UPR are involved in cytokine release in breast cancer cells and monocytes (Logue et al., 2018; Zhang et al., 2013b). ATF4 and CHOP as well as the IRE1 arm of the UPR were induced at short time points (3 h) upon glucose deprivation, which is in accordance with the cytokine mRNA expression. Therefore, we hypothesised that the UPR is involved in cytokine induction. We first investigated if ATF4 as one of the transcription factors of the PERK branch of the UPR, is involved in the cytokine induction upon glucose deprivation.
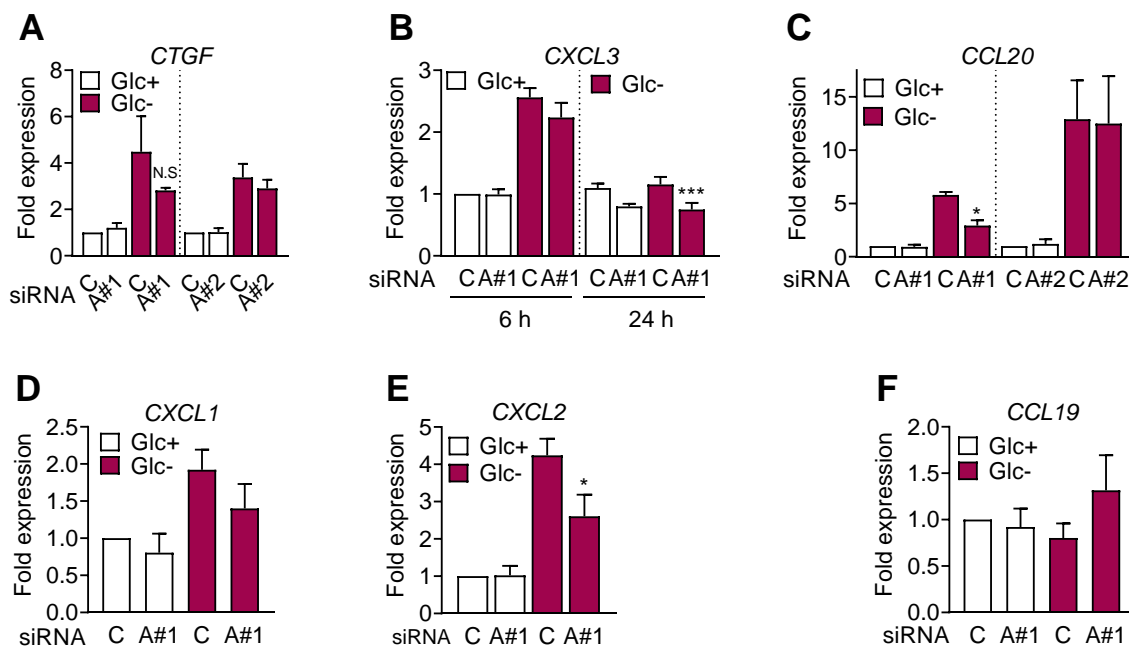
Figure 30 ATF4 regulates cytokine mRNA induction
A-F) A549 cells were transfected for 40 h with non-targeting siRNA (labelled as 'Control siRNA') or with siRNA against ATF4 (labeled as 'A#1' for sequence 1 or 'A#2' for sequence 2) which were treated post transfection for 6 h with media containing 0 mM or 25 mM glucose. mRNA expression was analysed by qPCR for CTGF (A), CXCL3 (B), CCL20 (C), CXCL1 (D), CXCL2 (E) and CCL19 (F). Data are represented as mean ±SEM (n=3-4) Asterisks denote significant differences of ATF4-transfected cells versus the control siRNA in each culture medium.

First, we silenced ATF4 using siRNA and analysed the mRNA expression of several cytokines, which we proved before to be induced upon glucose deprivation (**Figure 15**). CTGF, CXCL3, CCL20 and CXCL2 (**Figure 30A-D)** are partially induced by ATF4, whereas CXCL1 and CCL19 mRNA was not regulated by ATF4 upon glucose deprivation (**Figure 30D-F**).

We further confirmed, that knockdown of ATF4 in HeLa cells (**Figure 31A**) lead to a reduction in IL-8, IL-6 and CXCL1 mRNA expression (**Figure 31B-D**).
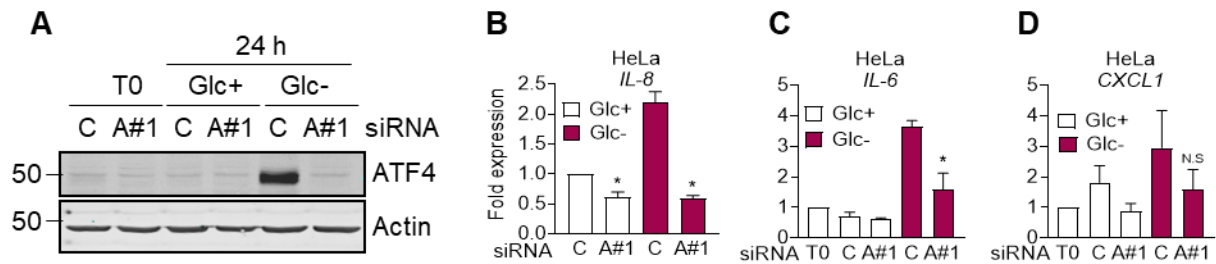
Figure 31 ATF4 mediates cytokine induction upon glucose deprivation in HeLa cells
A) HeLa cells were transfected for 24 h with non-targeting siRNA (labelled as ''C" for Control siRNA) or siRNA against ATF4 (labelled "A#1" for ATF4 sequence 1). After 24 h cells were washed and incubated in 25 (Glc+) or 2 mM (Glc-) glucose. A representative western blot of ATF4 is shown.
B-D). HeLa cells were transfected and treated (24 h) as in A. qPCR for IL-8 (B), IL-6 (C) and CXCL1 (D) is shown. Data represent mean ± SEM (n=3). Fold expression was calculated by normalizing to the control siRNA in Glc+ conditions or to time=0 (before treatment). Asterisks denote significant differences of ATF4-transfected cells versus the control siRNA in each culture medium.

Furthermore, these results were confirmed in A549 cells by silencing ATF4 with two siRNA sequences (A#1 and A#2), as shown in **Figure 32A**, which reduced IL-8 (**Figure 32B-C**) and IL-6 mRNA induction and secretion (**Figure 32D-E**). However, LIF mRNA expression and secretion was not altered (**Figure 32F-G**), suggesting that ATF4 is not regulating LIF mRNA induction or release.
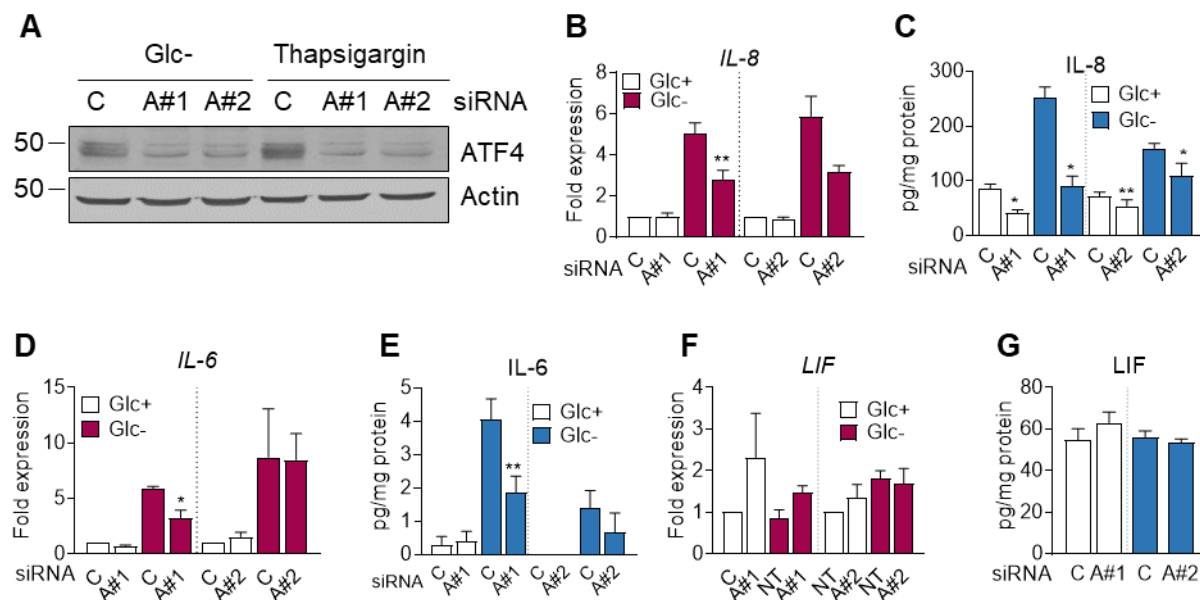
Figure 32 ATF4 mediates IL-8 and IL-6 but not LIF release
A) A representative western blot for ATF4 of A549 cells transfected for 40 h with non-targeting siRNA (labelled as "C" for Control siRNA) or siRNA against ATF4 (labelled as 'A#1' for sequence 1 or 'A#2' for sequence 2) is shown, which were treated for 24 h with media containing 0 mM glucose (Glc-) or with thapsigargin (4 µM).
B-G) A549 cells were transfected as described in A. and treated with 25 mM (Glc+) or 0 mM (Glc-) glucose for 6 h (B, D, E) or 24 h (C, E, G). qPCR data for CXCL8 (B), IL-6 (D) and LIF

(F) were normalized to the control siRNA of Glc+. ELISA is shown for IL-8 (C), IL-6 (E) and LIF (G). Data represent mean ±SEM (n=3-5). Asterisks denote significant differences of ATF4-transfected cells versus the control siRNA in each culture medium.

In order to investigate which other chemokines are regulated by ATF4, we performed a chemokine antibody array, which analyses the secretion of 31 know chemokines. Therefore, A549 cells were transfected with control siRNA and siRNA against ATF4 (sequence#1) and treated for 24 h in the presence or absence of glucose.

We found that ATF4 regulated the release of CXCL5 in the presence and absence of glucose in this array even the overall release was lower in Glc- than in the presence of glucose (**Figure 33A-B**). We validated these results by qPCR and ELISA and fond that ATF4 regulated CXCL5 at mRNA level but not its release (**Figure 33C-D**). Surprisingly, CCL2 which is a chemokine involved in macrophage attraction, is highly secreted at basal levels from A549 cells, whereas its release was prevented upon glucose deprivation in this array. Surprisingly, ATF4 knockdown reversed CCL2 release slightly (**Figure 33B**). We validated CCL2 mRNA expression by qPCR and found that silencing of ATF4 indeed promoted CCL2 mRNA induction upon glucose deprivation (**Figure 33E**). IL-8 release, as proved earlier (**Figure 32B-C**), was regulated by ATF4 in this array (**Figure 33B**).

In conclusion we found, that ATF4 is involved in the cytokine regulation upon glucose deprivation, however in a cytokine specific manner. With focus on IL-8, IL-6 and LIF we found that IL-6 and IL-8 but not LIF are positively regulated by ATF4.

A

Control siRNA   ATF4 siRNA#1

☐ IL-8   ☐ CXCL5   ◯ CCL2

B

Chemokine Array

C

D

E
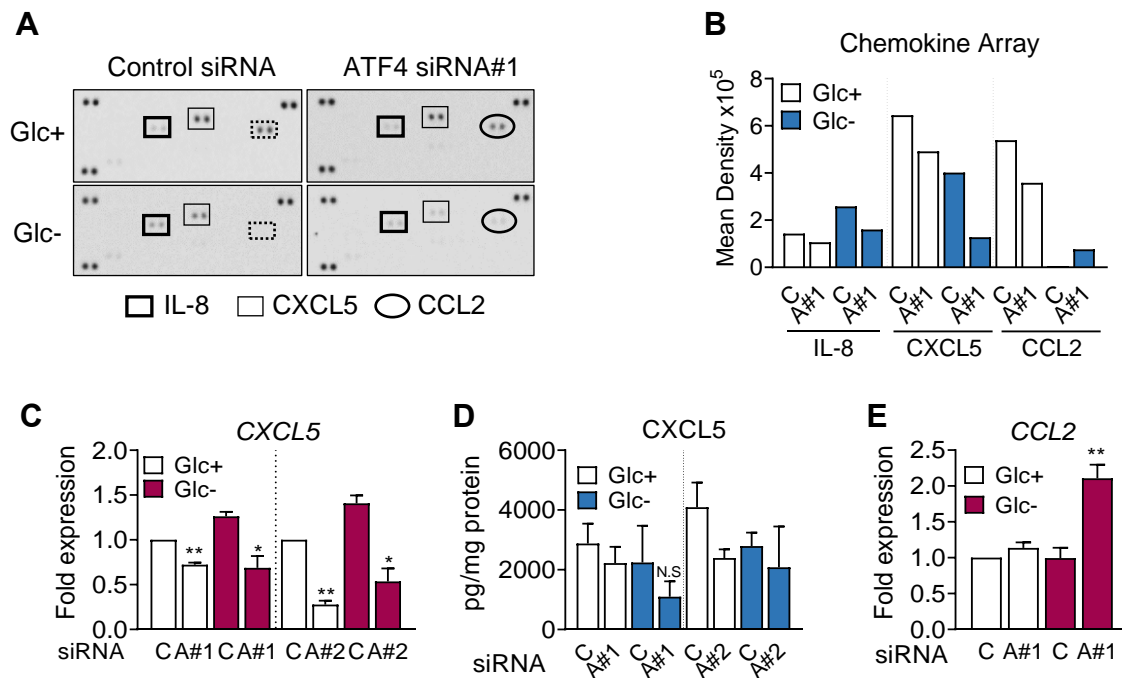
Figure 33 ATF4 regulates CXCL5 positively and CCL2 negatively at mRNA level.

A) A549 cells were transfected for 40 h with non-targeting siRNA (labelled as 'Control siRNA' or C) or with siRNA against ATF4 (labelled as 'ATF4 siRNA#1' for sequence 1). Cells were treated post transfection for 24 h with media containing 0 mM or 25 mM glucose. Supernatants of three independent experiments were collected and combined. *Human Chemokine Antibody Array* was performed according to manufactures instructions. Membranes are shown.

B) Mean densities of membranes spots in A. were quantified by ImageJ.

C, E). A549 cells were transfected and treated as in A. and mRNA expression was analysed by qPCR after 6 h for CXCL5 (C) and CCL2 (E). Data represent mean ±SEM (n=3-4). Asterisks denote significant differences of ATF4-transfected cells versus the control siRNA of each culture medium.

(D) A549 cells were treated and transfected as described in A. and ELISA for CXCL5 is shown. Data represent mean ±SEM (n=3). Asterisks denote significant differences of ATF4-transfected cells versus the control siRNA in each culture medium.

7.2.2 The IRE1 branch of the UPR is not involved in IL-8 and LIF induction upon glucose deprivation

Focusing on the IRE1 branch of the UPR, we found that the Inhibitor of the IRE1 RNase activity (MKC-8866) reduced XBP1s mRNA level, however it did not regulate the mRNA of IL-8 and LIF (**Figure 34A**). Furthermore, knockdown of IRE1 did not change IL-8 and LIF mRNA expression. However, it must be considered that IRE1 knockdown was not very efficient in this cell line. (**Figure 34B-D**) Furthermore, IL-8 but not LIF release was only minorly reduced (not

significant) (**Figure 34E-F**). Therefore, we performed further experiments silencing XBP1, which is spliced by IRE1 and functions as a transcription factor of the UPR.
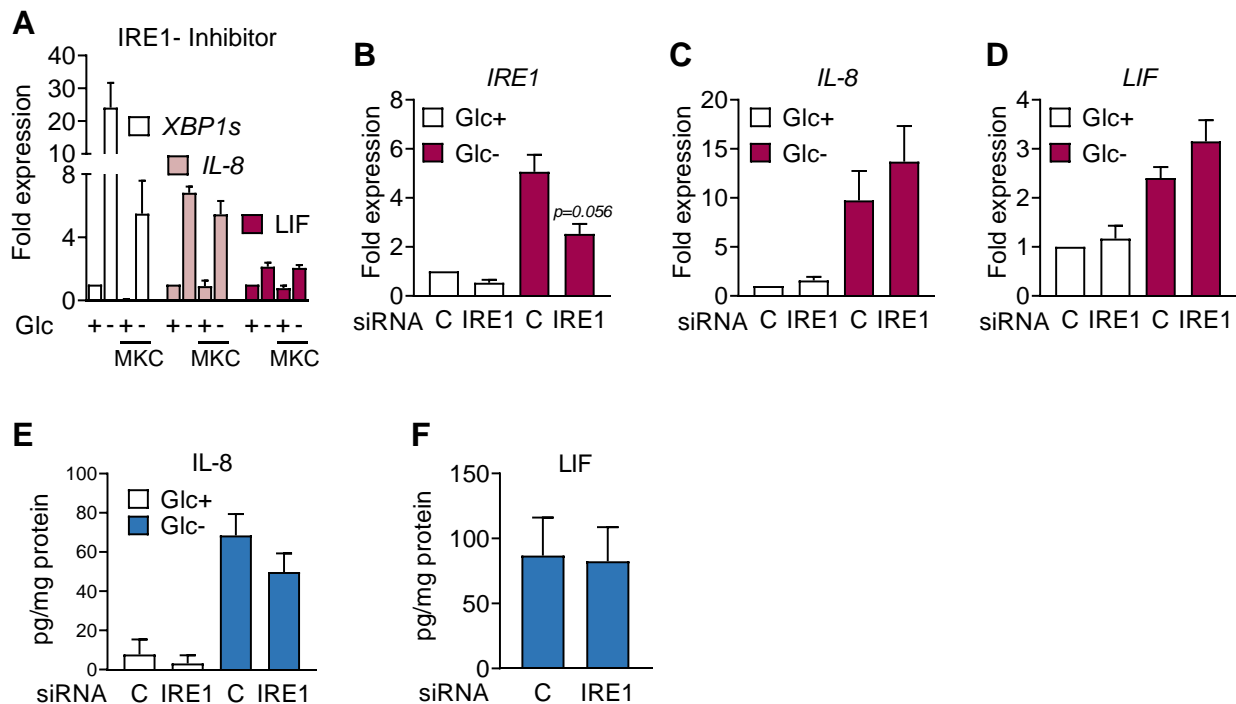
Figure 34 IRE1 is not involved in IL-8 and LIF regulation upon glucose deprivation

A) A549 cells were pre-treated with the IRE-1 inhibitor MKC-8866 (MKC, 10 µM) for 16 h and for another 6 h in combination with media containing 25 mM (Glc+) or 0 mM (Glc-) glucose. XBP1s, IL-8 and LIF mRNA was analysed by qPCR. Values are normalized to the Glc+ control sample. Data show mean ±SEM (n=3).

B-D) A549 cells were transfected for 24 h with non-targeting control siRNA (labeled as 'C') or siRNA for IRE1. qPCR for IRE1 (B), IL-8 (C) and LIF (D) after 6 h treatment with either 25 mM (Glc+) or 0 mM (Glc-) glucose is shown. Values were normalized to the control siRNA in Glc+. Data represent mean ±SEM (n=4). Asterisks denote significant differences of IRE1-transfected cells versus the control siRNA in each culture medium.

E-F) A549 cells were transfected and treated for 24 h as described in B. ELISA for IL-8 (E) and LIF (F) is shown. Data represent mean ±SEM (n=3).

Silencing of XBP1 with two siRNA sequences (X#1 and X#2) lead to a reduction of the mRNA of XBP1s and Erdj4, which is a known downstream target of XBP1s (**Figure 35A-B**). However, the two sequences had inconsistent effects on Herpud1, which is another known downstream target of XBP1s (**Figure 35C**). We found a similar inconsistent regulation of the two siRNA sequences on the mRNA and release of IL-8 and LIF. X#1 reduced IL-8 mRNA and protein expression, whereas X#2 had no significant effect on IL-8 induction and release (**Figure 35D-E**). Regarding LIF, X#1 induced LIF release, whereas X#2 had controversial effects on mRNA and protein release of LIF (**Figure 35F-G**).

Results-Part II

To sum it up, our results regarding the role of XBP1 in the induction of cytokines are controversial and depending on the siRNA sequence. However, since IRE1 knockdown and its RNase inhibitor MKC-8866 did not regulate IL-8 and LIF, neither at mRNA nor at protein level, we conclude that the IRE1 arm of the UPR is not involved in cytokines induction.
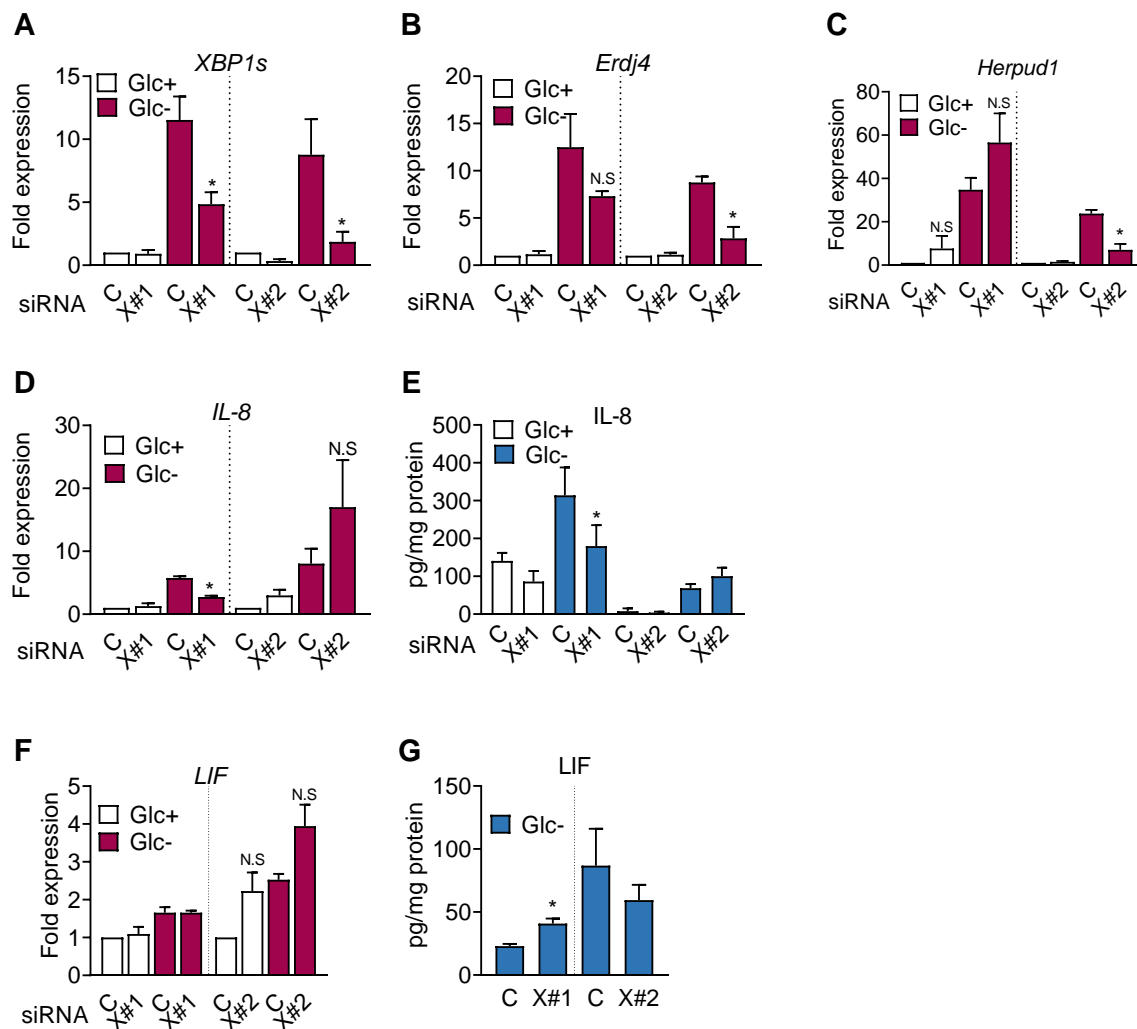
Figure 35 XBP1 does not regulate IL-8 and LIF upon glucose deprivation
A-D,F) A549 cells were transfected for 40 h with non-targeting control siRNA (labeled as 'C') or siRNA for XBP1 (labeled as X#1 for sequence 1and X#2 for sequence 2). Cells were treated for 6 h as described in B. and qPCR for XBP1s (A), Erdj4 (B), Herpud1 (C) and IL-8 (D) and LIF (F) is shown. Values were normalized to the control siRNA in Glc+. Data represent mean ±SEM (n=3) for X#1 and (n=4) for X#2. Asterisks denote significant differences of XBP1 transfected cells versus the control siRNA in each culture medium.
E,G) A549 cells were transfected as described in A and treated for 24 h with 25 mM (Glc+) or 0 mM (Glc-). ELISA for IL-8 (E) and LIF (G) is shown. Data represent mean ±SEM (n=3-4). Asterisks denote significant differences of XBP1 transfected cells versus the control siRNA in each culture medium.

7.2.3 ATF6 does not regulate IL-8 induction upon glucose deprivation

Silencing of ATF6, using siRNA in A549 cells, induced IL-8 and LIF mRNA expression. (**Figure 36A-C**) However, LIF but not IL-8 release is slightly decreased upon ATF6 knockdown, see **Figure 36D-E**. Therefore, we conclude that the ATF6 branch of the UPR could possibly be involved in the regulation of LIF but not IL-8 upon glucose deprivation.
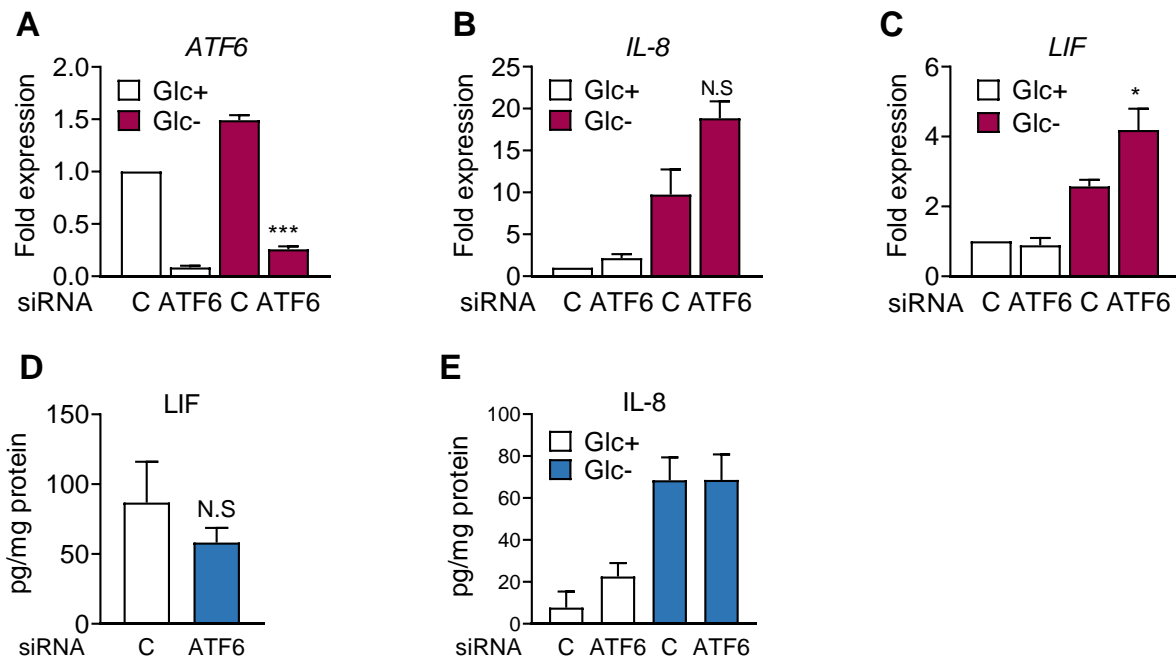
Figure 36 ATF6 does not regulate IL-8 upon glucose deprivation
A-C) A549 cells were transfected for 24 h with non-targeting control siRNA (labelled as 'C') or siRNA for ATF6. Cells were treated for 6 h with 25 mM (Glc+) or 0 mM (Glc-) glucose and qPCR for ATF6 (A), IL-8 (B) and LIF (C) is shown. Data represent mean ±SEM (n=4). Asterisks denote significant differences of ATF6-transfected cells versus the control siRNA in each culture medium.
D-E) A549 cells were transfected as in A. and treated with 25 mM (Glc+) or 0 mM (Glc-) glucose for 24 h. ELISA for LIF8 (D) and IL-8 (E) are shown. Data represent mean ±SEM (n=3). Asterisks denote significant differences of ATF6-transfected cells versus the control siRNA in each culture medium.

We conclude that the IRE1 branch of the UPR is not involved in cytokine induction in our model. The ATF6 branch possibly plays a minor role in LIF release. Nevertheless, we proved that ATF4 is involved in cytokine induction and release upon glucose deprivation since most of the tested cytokines are positively regulated by ATF4.

7.2.4 PERK induces LIF release upon glucose deprivation

ATF4 is induced by the ISR, which is mediated by one of the four kinases PERK, GCN2, PKR and HRI. To further test if PERK is involved in cytokine induction, we inhibited PERK with two known chemical inhibitors GSK2656157 (GSK) and AMG PERK 44. Both inhibitors lead to a partially decreased in ATF4 protein expression (**Figure 37A-B**).

Regarding IL-8, the inhibitor GSK2656157 had no effect on IL-8 release (**Figure 37C**), however the inhibitor AMG PERK 44 induced IL-8 release in glucose repleted and depleted conditions, see **Figure 37D**.

In case of LIF, both inhibitors decreased its release upon glucose deprivation (**Figure 37E-F**). Since we could not show a regulation of LIF by ATF4, this result suggests an ATF4-independent but PERK-dependent regulation of LIF release.
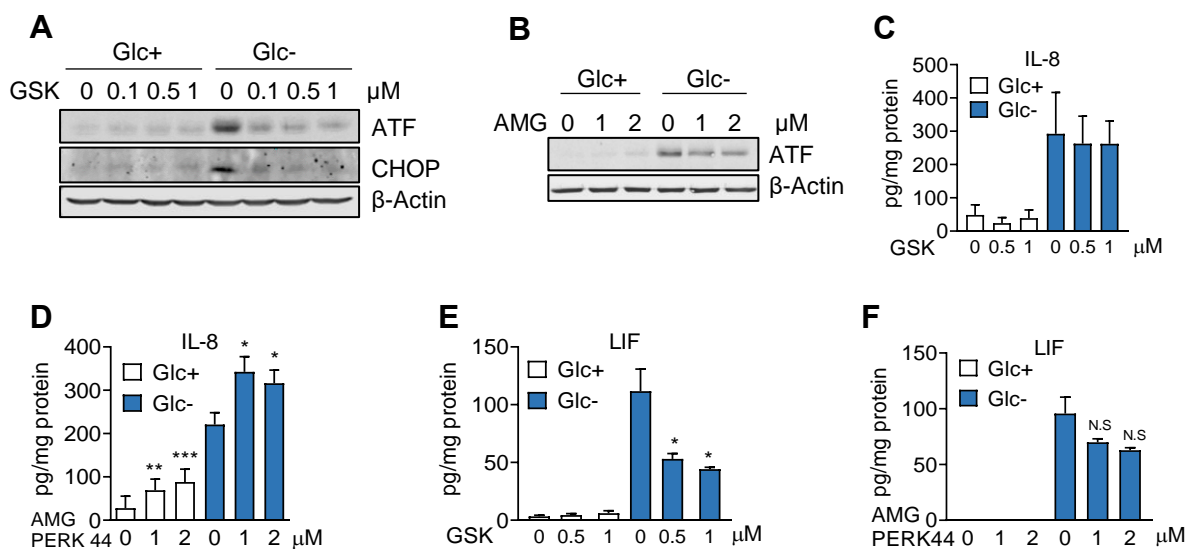
Figure 37 The PERK- Inhibitor GSK2656157 and AMG PERK 44 prevent LIF but not IL-8 release upon glucose deprivation
A) A549 cells were treated for 1 h with GSK2656157 (GSK) at indicated concentrations. Afterwards cells were washed and treated with media containing 25 mM (Glc+) or 0 mM (Glc-) glucose in combination with GSK2656157 at indicated concentrations for 24 h. A representative western blot of ATF4 and CHOP is shown (n=3).
B) A549 cells were treated for 24 h with indicated concentrations of AMG PERK 44 (AMG). Western blot of ATF4 and CHOP is shown (n=1).
C,E) A549 cells were treated as described in A. and cytokine level were measured by ELISA for IL-8 (C) and LIF (E) are shown. Data represent mean ±SEM (n=4). Asterisks denote significant differences between the control sample of each condition.
D, F) A549 cells were treated as described in B. and cytokine level measured by ELISA of IL-8 (D) and LIF (F) are shown. Data represent mean ±SEM of IL-8 (n=4) and LIF (n=3). Asterisks denote significant differences between the control sample of each condition.

Activation of the ISR results in the phosphorylation of eIF2α, which subsequently leads to the specific translation of ATF4. The eIF2α inhibitor ISRIB reverses the effects of eIF2α phosphorylation.

We treated A549 cells, in the presence or absence of glucose in combination with ISRIB for 24 h and analysed IL-8, IL-6 and LIF release. We found a slight increase in IL-8 release in the absence of glucose (**Figure 38A**), similar to treatment with the AMG PERK 44 inhibitor. IL-6 release was not changed upon treatment with ISRIB, as shown in **Figure 38B**. However, LIF release was slightly decreased, which is in coherence with the results of the tested PERK inhibitors (**Figure 38C**).
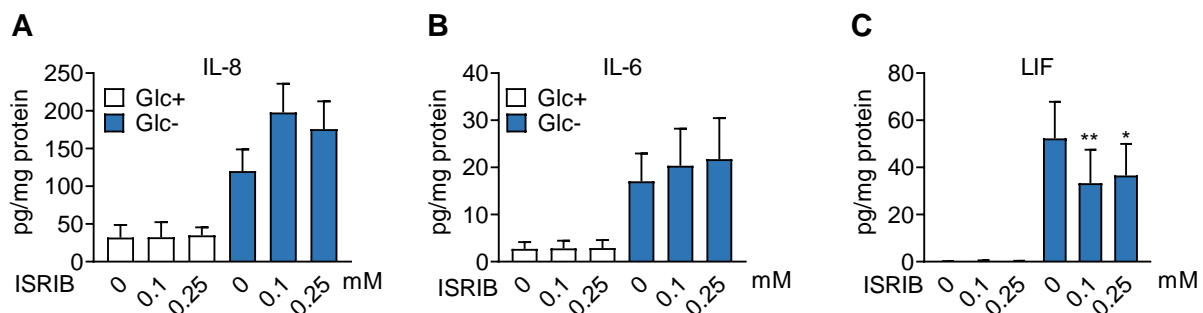
Figure 38 ISRIB partially prevents LIF release upon glucose deprivation
A-C) A549 cells were treated for 24 h with indicated concentrations of ISRIB. ELISA for IL-8 (A), IL-6 (B) and LIF (C) is shown. Data represent mean ±SEM (n=3). Asterisks denote significant differences between the control sample of each condition.

Altogether, the involvement of PERK in the induction of IL-8 remains unclear since results upon treatment with the PERK-inhibitors GSK2656157 and AMG PERK44 remained controversial. However, LIF release was partially prevented upon treatment with GSK2656157, AMG PERK44 as well as with ISRIB, which suggests a PERK-dependent but ATF4-independent regulation of LIF.

Results-Part II

7.3 mTOR signaling is involved in IL-8 but not LIF induction

The mTOR pathway is the major regulator of protein synthesis and reported to be inactivated upon glucose deprivation in an AMPK dependent manner (Gwinn et al., 2008). This allows
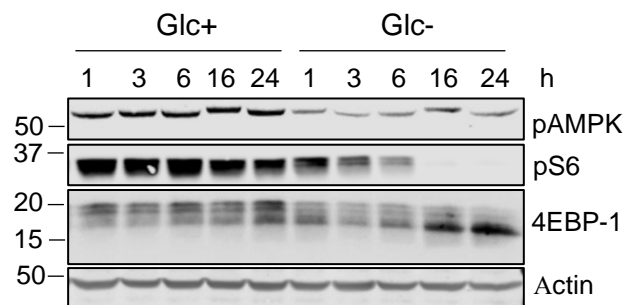
Figure 39 Glucose deprivation inactivates mTOR upon glucose deprivation
A549 cells were treated for indicated times with 25 mM (Glc+) or 0 mM (Glc-) glucose. A representative western blot is shown for pAMPK, pS6 and 4EBP-1 (n=2)

cells to reduce their energy needs based on decreased protein synthesis. We proved that glucose deprivation results in mTOR inactivation in A549 cells as shown by pS6 and 4EBP-1 dephosphorylation (**Figure 39**). However, in our model multiple repetitions of this experiment indicated that AMPK was not phosphorylated upon glucose deprivation in these cells, which lack LKB1 expression. As shown in **Figure 39,** AMPK phosphorylation was lower in cells treated without glucose compared to cells grown with glucose. This suggests that mTOR inactivation is facilitated in an AMPK-independent manner.

Previous reports describe an involvement of mTOR inactivation in IL-8 secretion upon glutamine deprivation (Shanware et al., 2014). To examine if mTOR inactivation participates in cytokine induction in our model, we used two mTOR inhibitor: rapamycin, which blocks mTORC1, and Torin1, which blocks mTORC1 and 2. As shown in **Figure 40A-B**, both inhibitors prevent mTOR signaling as shown by dephosphorylation of S6 and 4EBP-1.

We found that Torin1 but not rapamycin induced IL-8 release in the presence of glucose, suggesting that inhibition of both mTOR complexes is essential to promote IL-8 secretion. However, treatment with rapamycin and Torin1 in the absence of glucose reduced IL-8 release (**Figure 40C-D**). LIF release was not induced by the two inhibitors in the presence of glucose; however, treatment with rapamycin in the absence of glucose slightly reduces LIF release, suggesting that mTORC1 is partially involved in LIF release (**Figure 40E-F).**
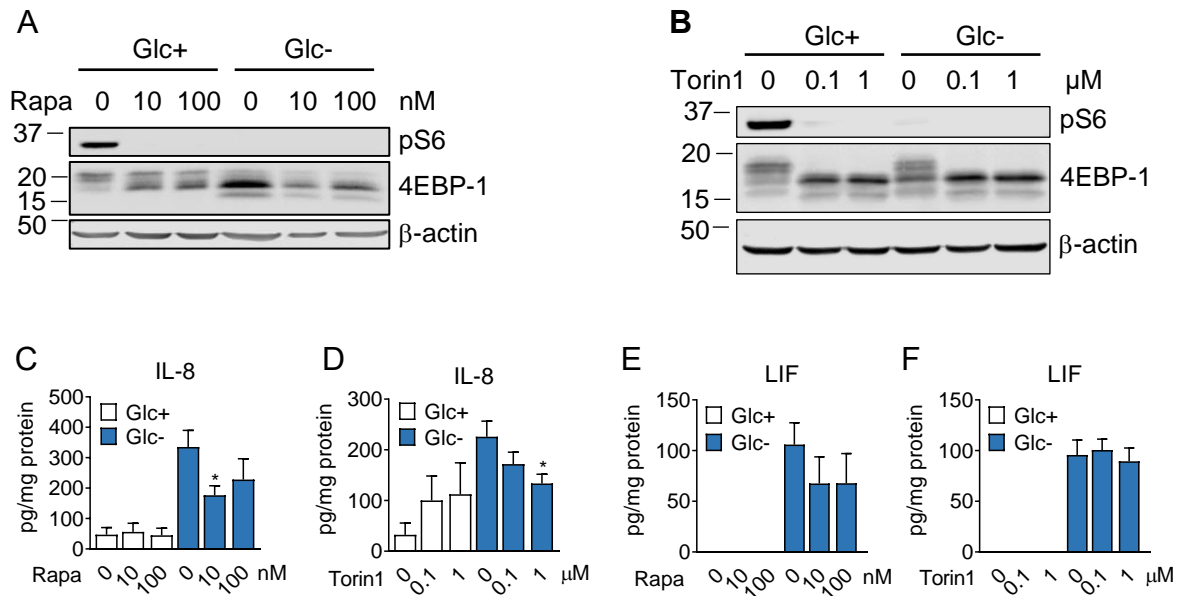
Figure 40 mTOR partially participates in cytokine release
A) A549 cells were treated for 24 h with 10 or 100 nM of rapamycin (Rapa) in the presence of 25 mM (Glc+) or 0 mM (Glc-) glucose. A representative western blot of pS6 and 4EBP-1 is shown.
B) Cells were treated for 24 h with 0.1 or 1 μM Torin1 in the presence of 25 mM (Glc+) or 0 mM (Glc-) glucose. A representative western blot for pS6 and 4EBP-1 is shown (n=3).
C-D) A549 cells were treated with rapamycin and Torin1 as described in A and B and IL-8 release was analysed by ELISA. Data represent mean ±SEM of rapamycin (n=3) and Torin1 (n=4-5). Asterisks denote significant differences between the control sample of each condition.
E-F) A549 cells were treated as described in A and B and LIF release was analysed by ELISA. Data represent mean ±SEM of rapamycin (n=2) and Torin1 (n=3). Asterisks denote significant differences between the control sample of each condition.

In a nutshell, we found that mTOR inactivation using Torin1 slightly promoted IL-8 but not LIF release in the presence of glucose. However, co-treatment of cells with the two mTOR inhibitor in the absence of glucose partially prevented IL-8 release. This suggests that upon glucose deprivation some mTOR activity remains active that is sufficient to promote IL-8 release. However, complete inhibition of mTOR signalling by using inhibitors in the absence of glucose prevented cytokine release.

7.4 The transcription factor p65 mediates IL-8 and IL-6 induction upon glucose deprivation

The NF-κB pathway is known as a major inducer of pro-inflammatory cytokines in several settings. The canonical pathway can be induced by several mechanism including among others TLRs, cell death receptors or pathogen infection. Moreover, several reports indicate that the UPR promotes NF-κB induction (Schmitz et al., 2018). Therefore, we hypothesized that the NF-κB pathway, with its major transcription factor p65, is involved in cytokine induction and release upon glucose deprivation.

To prove this, we silenced p65, using siRNA (**Figure 41A**), and we found that p65 significantly reduced CXCL1, IL-6 and IL-8 mRNA expression in HeLa cells (**Figure 41B-D**).
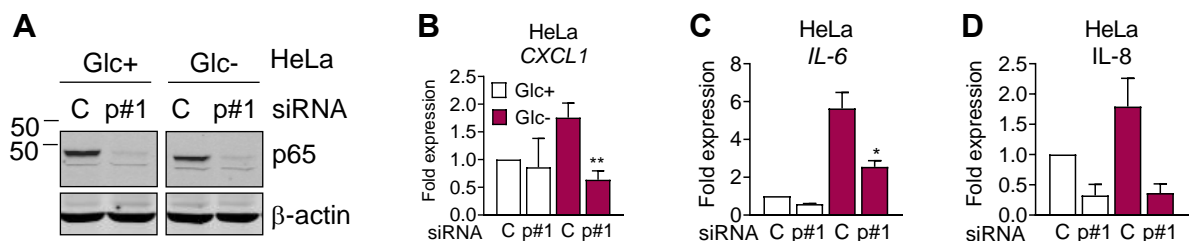
Figure 41 p65 regulates cytokine mRNA expression in HeLa cells
A) HeLa cells were transfected for 24 h with siRNA for p65 (labelled as p#1 for sequence 1) and treated for 24 h with 25 mM (Glc+) or 0 mM (Glc-) glucose. A representative western blot for p65 is shown.
B-D) HeLa cells were transfected and treated for 6 h as described in A. qPCR for CXCL1 (B), IL-6 (C) and IL-8 (D). Values are normalized versus the control siRNA in Glc+. Results show mean ±SEM (n=4) experiments. Asterisks denote significant differences of p65-transfected cells versus the control siRNA in each culture medium.

Moreover, silencing of p65 with two siRNA sequences (p#1 and p#2) in A549 cells (**Figure 42A**) lead to a reduction in IL-8 and IL-6 mRNA expression and release upon glucose deprivation (**Figure 42B-E**). We also confirmed the mRNA regulation by p65 of M-CSF, CXCL1 and CXCL2 and CCL20 (**Figure 42H-K**). However, cytokines like CXCL3, CXCL5 and CTGF are not regulated by p65 at mRNA level in A549 cells (**Figure 42L-N**). LIF mRNA expression was only reduced with the first siRNA sequence, however none of the two siRNA sequences reduced LIF release. (**Figure 42F-G**)

Focusing on IL-8, IL-6 and LIF, these results prove that p65 is involved in the mRNA expression and protein release of IL-8 and IL-6 but not LIF, in our model.
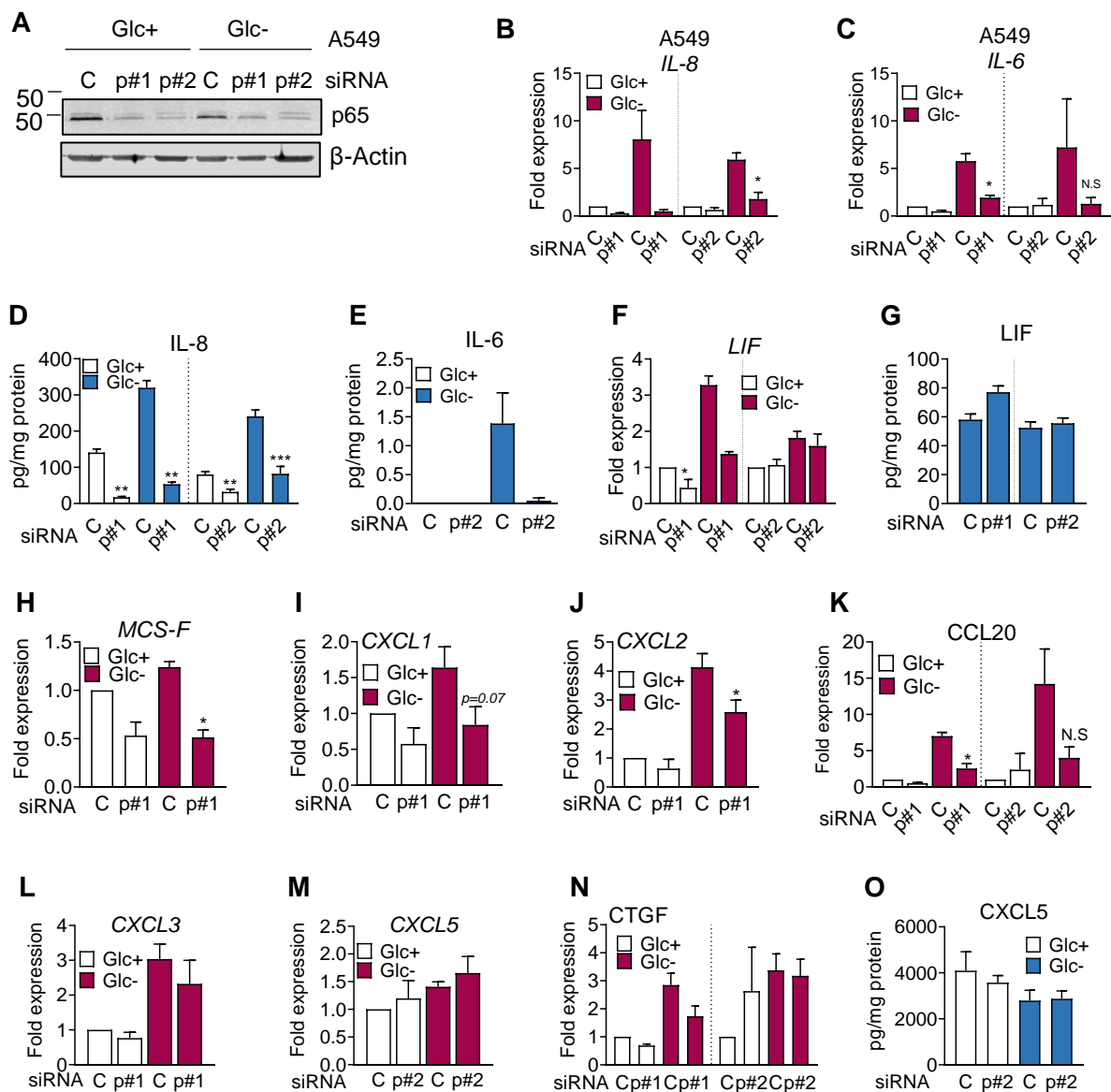
Figure 42 p65 regulates IL-8 and IL-6 but not LIF upon glucose deprivation
A) A549 cells were transfected for 40 h with control non-targeting siRNA (labelled as ''C'')
and siRNA for p65 (labelled as ''p#1'' for sequence 1 and ''p#2'' for sequence 2). A
representative western blot of p65 is shown in A. Cells were subsequently treated for 6 h
(panels B, C, F, H-N) or for 24 h (panels D, E, G and O) with media containing 25 mM (Glc+)
or 0 mM (Glc-) glucose. qPCR for IL-8 (B), IL-6 (C), LIF (F), MCS-F (H), CXCL1 (I),
CXCL2 (J), CCL20 (K), CXCL3 (L), CXCL5 (M) and CTGF (N) is shown. Values were
normalized versus control siRNA in Glc+. IL-8 (D), IL-6 (E), LIF (G) and CXCL5 (O) release
was analyzed by ELISA after treating cells for 24 h. Results show mean ±SEM (n=3-4).
Asterisks denote significant differences of p65-transfected cells versus the control siRNA in
each culture medium.

97

7.5 Functional effects of conditioned media from A549 cells on cancer and immune cells

Tumors are heterogenic and not only composed of cancer cells but also of others such as fibroblasts and immune cells. These cells interact continuously via cell-cell interactions within the tumor environment. Moreover, the tumor environment is also marked by hostile regions with, for instance, high acidity as well as oxygen and nutrient shortage, which results from fast tumor growth and poor vascularization. Tumor cells developed adaptive mechanisms in order to cope with these environments and maintain tumor progression. Many reports describe that cancer cells acquire features that allow them to modify the activity of surrounding cells. For instance, cancer cells which lack oxygen secrete cytokines like VEGF that promotes the revascularization of the tumor. Moreover, cancer cells also secrete metabolites or exosomes, in order to communicate with other cells in the surrounding tissue. But most interestingly, cancer cells are able to modify the activity of tumor resident immune cells through the secretion of specific immune modulating proteins or metabolites derived from their altered metabolism. (O'Sullivan et al., 2019; Wellenstein and De Visser, 2018)

Keeping this in mind, we proved that cancer cells release cytokines in an environment low in nutrients. These released cytokines could promote cell-cell responses between cancer and immune cells, favouring tumor progression. To further analyse which possible functions these cytokines have in a tumor setting, we analysed cell death and chemotaxis of cancer cells and of different immune cell populations, when treated with conditioned media of starved cancer cells. For the performance of the following experiments we generated supernatants from A549 cells which were treated for 24 h in the presence or absence of glucose and without dFBS. These supernatants were concentrated five times and will be designated as 'conditioned media' (presented with yellow bars) in the further course of this thesis.

Furthermore, from the supernatant derived from A549 cells, we also generated as second fraction, which was washed once with fresh glucose-free media using protein concentrators with a permeable membrane (cut-off 3 kDa). This process allowed us to remove metabolites or other ´waste products´ of the cell. This fraction only contains the secreted proteins with a size ≥3 kDa. This fraction will be designated as ´washed conditioned media´ and is presented in orange bars in the figures.

Moreover, when concentrating the supernatants, we also kept the filtrate, which is the 'exhausted' media of the cells, which does not contain proteins but secreted metabolites or other waste products of the cell. This fraction is presented in blue bars in the figures.

To sum it up, we generated three fractions: The full conditioned media containing secreted proteins and waste products (yellow), the washed conditioned media containing only secreted proteins (orange) and the filtrate containing only the waste products (blue) of the cell. (see also material and methods)

The following experiments were performed using the three fractions of the conditioned media of A549 cells to distinguish between effects of secreted protein, as well as of possible effects of secreted metabolites. The detailed preparation is described in **chapter 5.9** and shown in **Figure 43**.
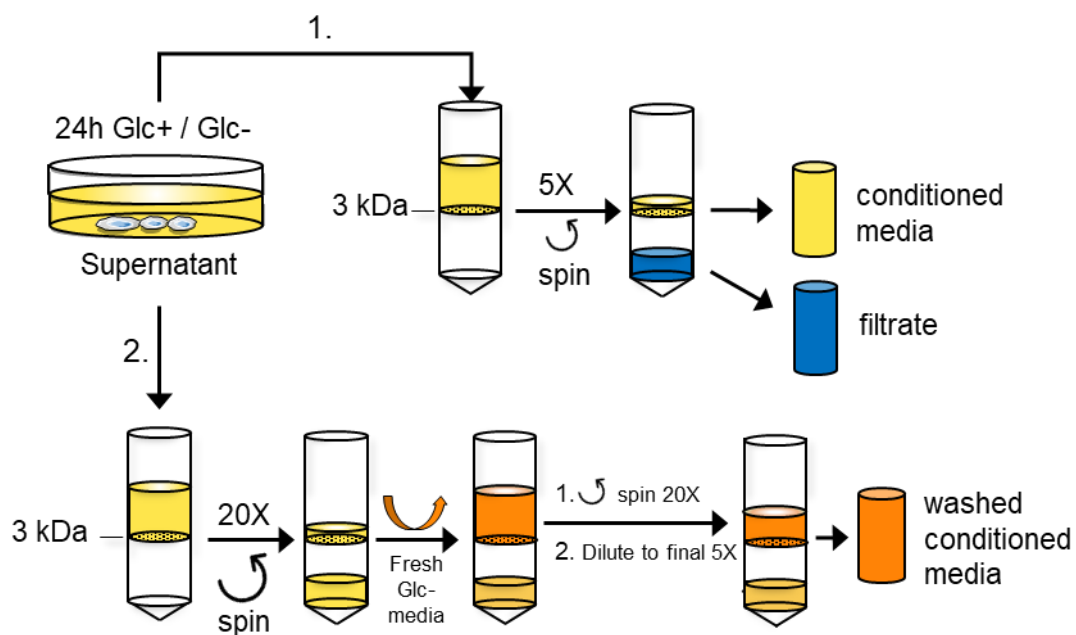
Figure 43 Scheme for preparation of conditioned media of A549 cells
1. Cells were treated for 24 h with 25 mM (Glc+) or 0 mM (Glc-) glucose and without dFBS. Supernatant (yellow) was 5X concentrated using protein concentrators (cut-off 3 µM) and concentrated conditioned media (yellow) and filtrate (blue) was stored.
2. Supernatant was 20X concentrated and diluted with fresh Glc- medium (orange). Media was concentrated again 20X and diluted with fresh Glc- media to a final 5X concentration. For experiments, 25 mM glucose was supplemented when indicated.

7.5.1 Effects of conditioned media of starved A549 cells on cell death
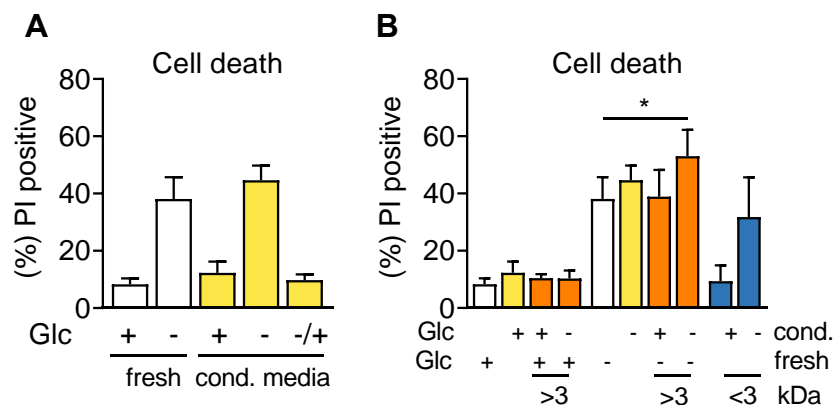
Figure 44 Secreted proteins from starved A549 cells slightly increase cell death upon glucose deprivation
A-B) A549 cells were treated for 48 h with fresh media (white bars) containing 25 mM (+) or 0 mM (-) glucose or with conditioned media (yellow bars) from other A549 cells. (-/+) indicates that 25 mM glucose was added to conditioned media of starved A549 cells. The washed conditioned media (orange bars) was substituted with glucose (+) when indicated. Cell death was analyzed by PI staining and FACS analysis. Data represent mean ±SEM (n=3) for A. and (n=5) for B. Asterisks denote significant differences between Glc- media (white bar) and washed conditioned media (orange).

First, we investigated the effects of the conditioned media of A549 cells on cell death of other A549 cells. Therefore, A549 cells were plated the day before and treated with regular media and the three fractions of the conditioned media as described before. Cells undergo cell death after 48 h of glucose deprivation when treated with regular glucose free media. There was no change in cell death observed when cells were treated with the conditioned media of other starved A549 cells (**Figure 44A**, yellow bars). However, the washed conditioned media, which only contained the secreted proteins from glucose-deprived cells (orange bars), slightly increased cell death in the absence of glucose (**Figure 44B**). This suggests that secreted proteins from starved A549 cells slightly promote cell death of other A549 cells upon glucose deprivation.
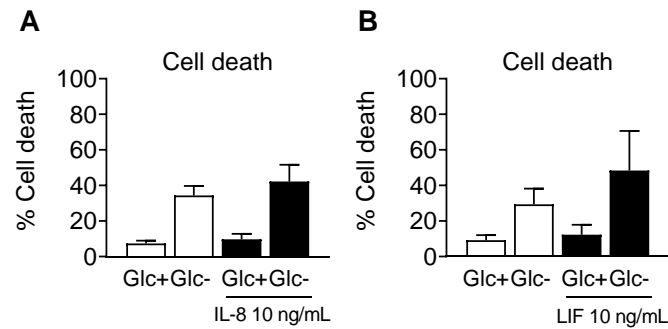
Figure 45 Recombinant IL-8 or LIF do not induce cell death
A) A549 cells were treated with media containing 25 mM (Glc+) or 0 mM (Glc-) glucose for 48 h. IL-8 (10 ng/mL) or LIF (10 ng/mL) were added when indicated. Data represent mean ±SEM IL-8 (n=4) and LIF (n=2).

To examine weather IL-8 or LIF are mediators of cell death induction, we treated cells with recombinant IL-8 or LIF in the presence or absence of glucose. However, neither recombinant IL-8 (**Figure 45A**) nor LIF (**Figure 45B**) induced cell death. This suggests that extracellular IL-8 or LIF does not promote cell death in our model.

However, the impact of cytokines on cell death could be mediated intracellularly. Therefore, A549 cells were transfected with three different sequences of siRNA for IL-8. IL-8 mRNA expression and release was reduced upon glucose deprivation when transfected with siRNA (**Figure 46A-B**). Cells were treated for 48 h post transfection in the presence or absence of glucose. We observed that two out of three IL-8 siRNA sequences partially protected from cell death, as shown in **Figure 46C**. Furthermore, we knocked down LIF with one siRNA sequence and mRNA as well as LIF release was reduced (**Figure 46D-E**). However, we did not detect an effect on cell death upon LIF knockdown (**Figure 46F**).

Previously, we described that cancer cells die upon glucose deprivation in an DR5-dependent manner. Here, we found that DR5 mRNA expression was slightly decreased upon IL-8 knockdown (**Figure 46G**). This could suggest that IL-8 promotes cell death in a DR5-dependent manner, however more tests including the analysis of DR5 protein level upon IL-8 knockdown, have to be performed.
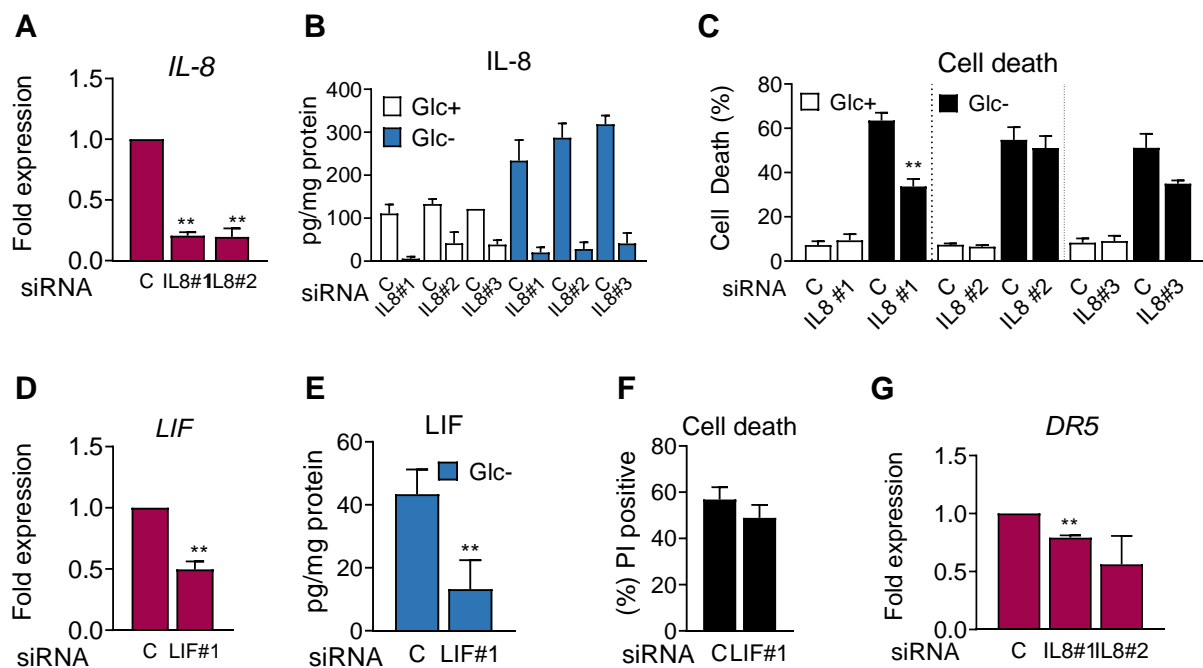
Figure 46 Knockdown of IL-8 protects from cell death upon glucose deprivation
A, D, G) A549 cells were transfected for 40 h with a non-targeting control siRNA (labelled as 'C') or with siRNA for IL-8 (labelled as IL8#1 for sequence 1, IL8#2 for sequence 2 or IL8#3 for sequence 3) and for LIF (labelled as LIF#1 for sequence 1). Cells were treated for 6 h with media containing 0 mM (Glc-) glucose and mRNA for IL-8 (A), LIF (D) and DR5 (G) was analysed by qPCR. Data represent ±SEM (n=3) for IL8#1, (n=3) for IL8#2 and (n=3) for LIF#1. Asterisks denote significant differences between the non-targeted siRNA and the targeted siRNA in Glc-
B, E) A549 cells were transfected as in A. and treated for 24 h with media containing 25 mM (Glc+) or 0 mM (Glc-) and ELISA for IL-8 (B) and LIF (E) was performed. Data represent ±SEM (n=4) for IL8#1, (n=3) for IL8#2, (n=2) for IL8#3 and (n=3) for LIF#1. Asterisks denote significant differences between the non-targeted siRNA and the targeted siRNA in each condition.
C,F) A549 cells were transfected as in A. and treated for 48 h with Glc+ or Glc- media. Cell death was analysed by PI incorporation and FACS analysis. Data represent ±SEM (n=3) for IL8#1, (n=3) for IL8#2 and (n=3) for IL8#3 and (n=4) for LIF#1.

7.5.2 Conditioned media of A549 cells promotes the migration of cancer cells

Another previously performed secreted protein array in the group (data not shown) detected secreted cytokines involved in extracellular matrix reorganisation, which are associated with metastasis. Hence, we suggested that an environment low in nutrients promotes the migration of cancer cells through cytokine release and cell-cell communication.

Effects on the migration of A549 cells were analysed by performing chemotactic assays using boyden chambers with a permeable membrane of 8 µM. A549 cells were plated in the upper

part of the boyden chamber and the regular control media as well as the conditioned media of other A549 cells were plated in the bottom chamber. Cells migrated for 20 h towards the media in the bottom chamber.

We found that A549 cells increased migration towards the conditioned media (yellow bars) of other A549 cells. However, no difference was observed between the conditioned media of cells cultured in the presence or absence of glucose. On the contrary, cells have the tendency to migrate less towards the media of starved A549 cells. This effect was reduced by readding 25 mM glucose to the conditioned media (-/+) of starved A549 cells. (**Figure 47A**) This tendency was also observed when cells migrated towards the washed fractions of the conditioned media (orange bars), suggesting that A549 migrate is stronger in the presence of glucose.

In order to examine if IL-8 or LIF promote migration, A549 cells were allowed to migrate towards regular media containing recombinant IL-8 or LIF. In our model we could not show an effect of these cytokines on migration (**Figure 47B**). This suggests that either other secreted cytokines or a combination of several cytokines promote migration.
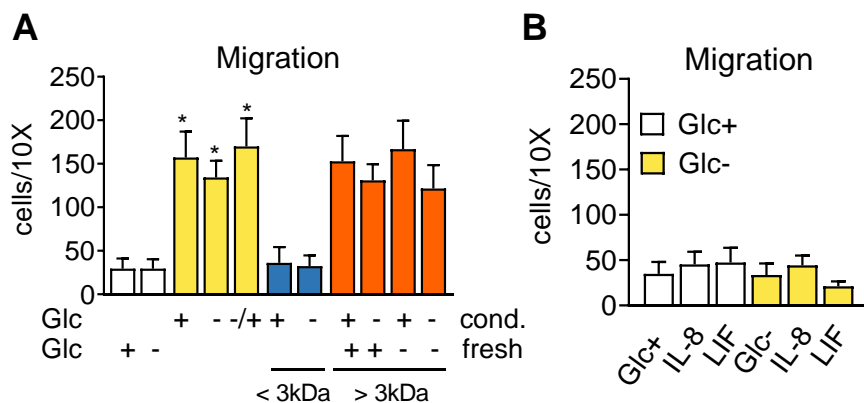
Figure 47 Conditioned media of A549 cells induces migration of other A549 cells
A) A549 cells were plated on top of a boyden insert. Cells were allowed to migrate for 20 h towards fresh (white bars) glucose-containing (25 mM, +) or glucose-free medium (0 mM, -), or towards conditioned (cond) media (yellow bars) from A549 cells grown in glucose-containing or glucose-free medium for 24h. (-/+) indicates conditioned, glucose-free medium to which 25 mM glucose was added before the experiment. Boyden membranes were stained with crystal violet and cells were counted using an inverted microscope (10X) and five pictures per condition were taken. Data represent mean ±SEM (n=3). Asterisks donate significant differences between the Glc+ control samples (white bar) and each treatment.
B) A549 cells were plated on top of a boyden insert and were allowed to migrate towards glucose-containing media (Glc+) or glucose-free (Glc-) media with the addition if IL-8 (10 nM) or LIF (100 ng/mL). Data represent mean ± SEM (n=4).

7.5.3 LIF induces IL-8 release in A549 cells in the presence and absence of glucose

In further experiments we investigated if cytokines can induce the secretion of other cytokines through paracrine or autocrine cell-cell effects. In this context, several reports indicate that LIF induces IL-8 (Tiziana Musso et al., 1995) and IL-6 (Gruss et al., 1992) release in myeloid cells and others (Villiger et al., 1993).

Thus, we treated A549 cells in the presence or absence of glucose with recombinant IL-8 for 24 h and measured LIF release by ELISA. LIF release was not altered by treatment with recombinant IL-8 in A549 cells (**Figure 48A**). To further validate this finding, cells were transfected for 40 h with three IL-8 siRNA sequences (as described before) and cells were treated for 24 h upon glucose deprivation. As expected, knockdown of IL-8 had no effect on LIF secretion (**Figure 48B**); Furthermore, we treated cells with recombinant LIF, which indeed induced IL-8 release in the presence and absence of glucose (**Figure 48C**). We also confirmed that IL-6 release was increased in the presence of LIF upon glucose deprivation, though not significantly (**Figure 48D**). To further validate this finding, cells were transfected with siRNA for LIF (**Figure 46D-E**) and treated for 24 h upon glucose deprivation. We found that knockdown of LIF led to a significant decrease of IL-8 release upon glucose deprivation in A549 cells (**Figure 48E**). In conclusion, we found that LIF induces IL-8 in the presence and absence of glucose.
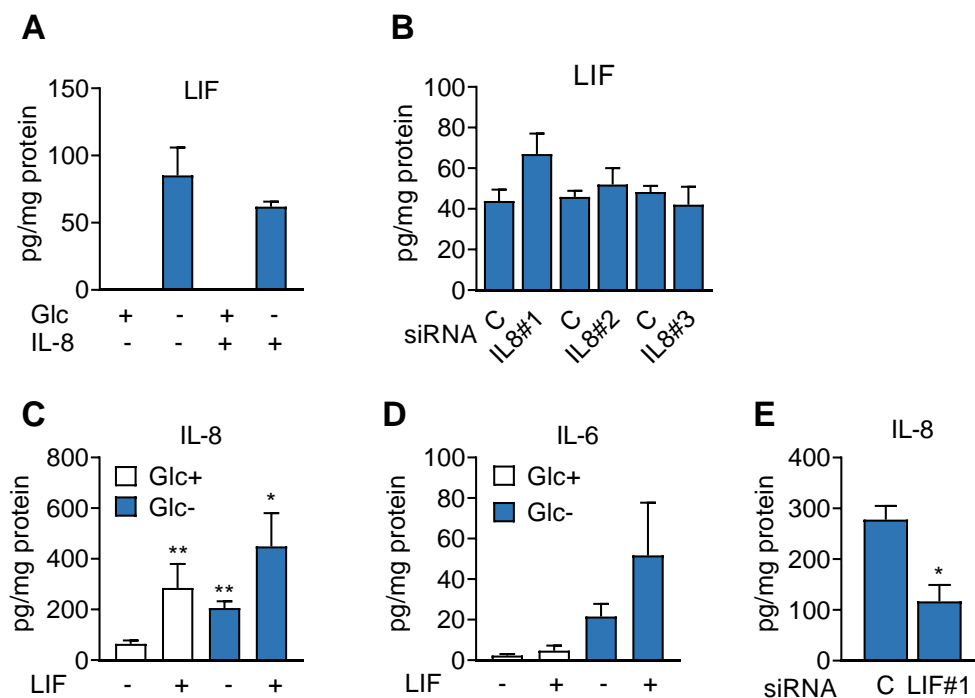
Figure 48 Recombinant LIF induces IL-8 release
A) A549 cells were treated with 25 or 0 mM glucose in the presence or absence of IL-8 (10 ng/mL). LIF release is shown by ELISA. Data represent mean ± SEM of (n=2).
B,E) A549 cells were transfected for 40 h with a non-targeting control siRNA (labelled as 'C') or with siRNA for LIF (labelled as LIF#1 for sequence 1) or for IL-8 (labelled as IL8#1 for sequence 1, IL8#2 for sequence 2 or IL8#3 for sequence 3). Cells were treated for 24 h with 0 mM glucose and ELISA is shown for LIF (B) and IL-8 (E). Data are represented as mean ± SEM IL-8 (n=3) and LIF (n=2-4). Asterisks donate significant differences between the control sample.
C-D) A549 cells were treated with 25 or 0 mM glucose in the presence or absence of LIF (10 ng/mL). IL-8 (C) and IL-6 (D) release is shown by ELISA. Data represent mean ±SEM IL-6 (n=3) and IL-8 (n=6). Asterisks donate significant differences between the Glc+ control sample and each treatment.

7.5.4 Conditioned media of A549 cells induces migration of primary B cells and macrophage-like THP-1 cells

In the previous chapter we showed that secreted cytokines from A549 cells have effects on other A549 in terms of cell death, migration and cytokine induction. Hence, we wanted to test if the conditioned media of A549 cells also affects the migration of immune cells. Regarding that, many studies suggested, that cancer cells have immunosuppressive effects by depleting the surrounding tissue of nutrients or by cytokine release. One of the consequences is that some immune cells, like T cells, lose their anti-tumor activity (Chang et al., 2015). In addition, it is also described that some tumors are marked by an increased infiltration of myeloid cells including macrophages and neutrophils, which are associated with poor patient prognosis. Hence, we suggested that an environment low in nutrients induces cytokine secretion from cancer cells and attracts immune cells from the surrounding tissue.

In the following chapter, we investigated if different immune cell population migrate towards the conditioned media of A549 cells when treated in the presence or absence of glucose. The following experiments were performed with macrophage-like THP-1 cells or with primary PBMCs and primary neutrophils purified from buffy coats obtained from human blood. We analysed the migration of these cells by performing chemotactic assays using boyden chambers as described for A549 cells in **chapter 7.7**. Cells were allowed to migrate between 2 and 20 h depending on the cell population (see also material and methods).

First 500.000 PBMCs were plated on the upper part of a boyden chamber and were allowed to migrate for 20 h towards the conditioned media of A549 cells. Afterwards, the conditioned media in the bottom chamber, which contained the migrated cells, was collected and cells were stained with fluorophore-tagged antibodies for CD3$^+$ (T cells), CD56$^+$ (NK cells) and CD19$^+$ (B cells). NKT cells were identified as CD56$^+$ and CD3$^+$ populations. The cell number of

migrated cells was quantified by FACS. The percentage of migration was calculated by analysing the total amount of PBMCs of each population present in the donor blood sample.

We found that T cells and NKT cells did not migrate towards the full conditioned media of A549 cells (**Figure 49A-B**). However, NKT cells and T cells had the tendency to migrate stronger towards the washed conditioned media of starved A549 cells (orange bars) compared to the filtrate (blue bars), independent of glucose availability. Moreover, in accordance with NKT cells, NK cells also induced migration towards the washed conditioned media of starved A549 cells (**Figure 49C**).

This suggests, that secreted proteins from starved cancer cells promote migration, however metabolites and the depletion of other nutrients in the filtrate attenuated this effect.

The strongest migratory effect was obtained for B cells, which migrated significantly stronger towards the media of glucose-deprived A549 cells (**Figure 49D**, yellow bar). Moreover, this migration was even stronger towards the washed conditioned media of starved A549 cells (orange bars). This again suggests, that metabolites or other factors in the exhausted media dampen the migration of cells.
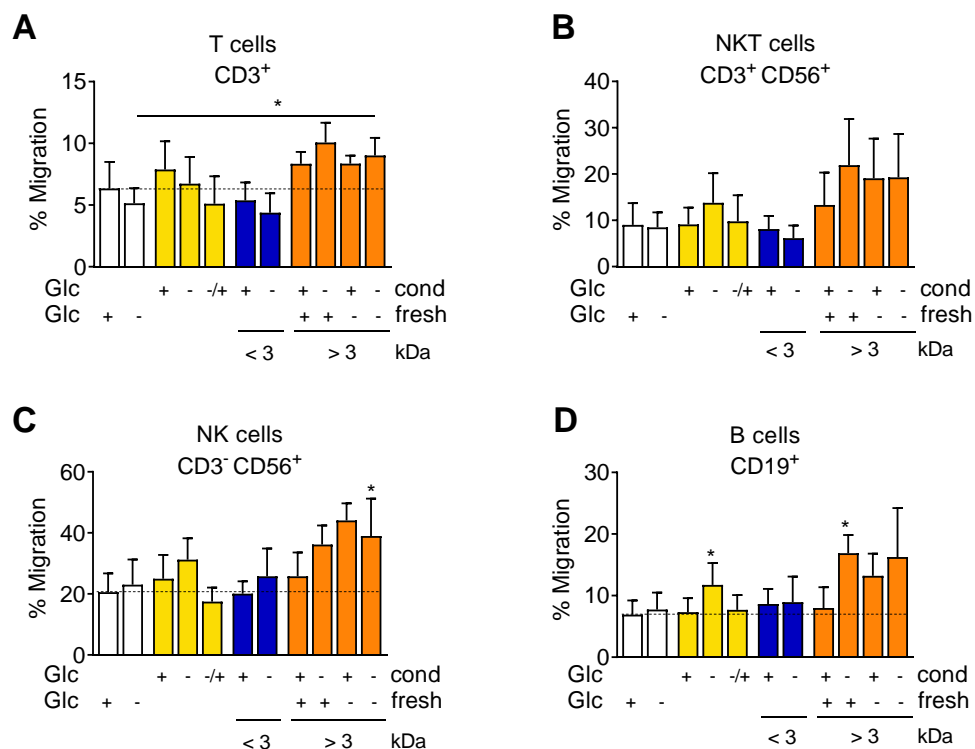
Figure 49 NK an B cells migrate towards conditioned media of starved A549 cells

A-D) Human PBMCs were allowed to migrate for 20 h towards fresh glucose (+)-containing (25 mM) or glucose (-)-free medium (white bars), to conditioned (cond) media (yellow bars) from A549 cells grown in glucose-containing or glucose-free medium for 24 h, to washed conditioned media (orange), and towards the filtrate (blue). Migrated cells were stained for

indicated markers and were analysed by FACS. Data represent mean ±SEM (n=5). Asterisks denote significant differences between cells migrated towards regular media (Glc+) except for A.

To explore if IL-8 or LIF are involved in the migration of these immune cells, we added recombinant IL-8 and LIF in the bottom chamber of the chemotaxis assay and analysed migration in the presence and absence of glucose. IL-8 and LIF had no effect on the migration of T cells, NKT cells and B cells, see **Figure 50A-B, D.** However, we found that IL-8, but not LIF, slightly induced (not significant) the migration of NK cells in glucose-deprived conditions (**Figure 50C**).
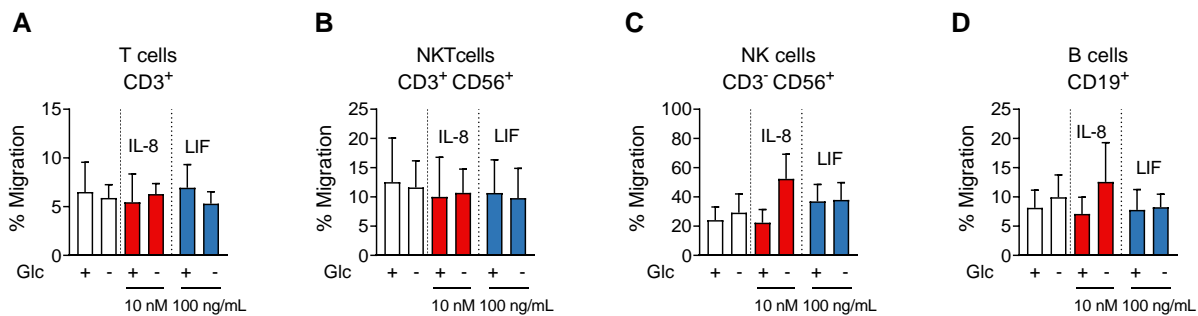
Figure 50 Recombinant IL-8 and LIF does not induce migration of PBMCs
A) PBMCs were allowed to migrate for 20 h towards regular media containing 25 or 0 mM glucose in combination with recombinant IL-8 (10 nM) or LIF (100 ng/mL). (%) migrated cells were analysed by FACS staining with indicated antibodies. Data represent mean ±SEM (n=3)

Next, we analysed if macrophage-like THP-1 cells migrated towards the conditioned media of A549 cells. Therefore, THP-1 cells were differentiated towards their macrophage-like phenotype by using PMA. Differentiated THP-1 cells (50.000 cells) were plated on the upper part of a boyden chamber and let migrate for 20 h towards the conditioned media of A549 cells. We found that THP-1 cells migrated stronger towards the conditioned media of starved A549 cells compared to conditioned media containing glucose (**Figure 51A**). Re-adding glucose to the conditioned media of starved A549 cells (+/-) did not reverse this effect. This proves that migration is due to secreted proteins in the media and not due to the absence of glucose. This was further confirmed due to the fact, that the washed conditioned media (orange) of starved A549 cells induced the migration, even after re-addition of glucose to the conditioned media, see **Figure 50B**. This proves that secreted proteins are responsible for the migration of THP-1 cells independently of glucose availability. To examine if IL-8 or LIF promoted migration, we added recombinant IL-8 and LIF in the bottom chamber to regular media in the presence or absence of glucose. Cells had the tendency (not significant) to migrate stronger towards the media containing IL-8 in the presence and absence of glucose and slight towards LIF in the absence of glucose. (**Figure 50C**)
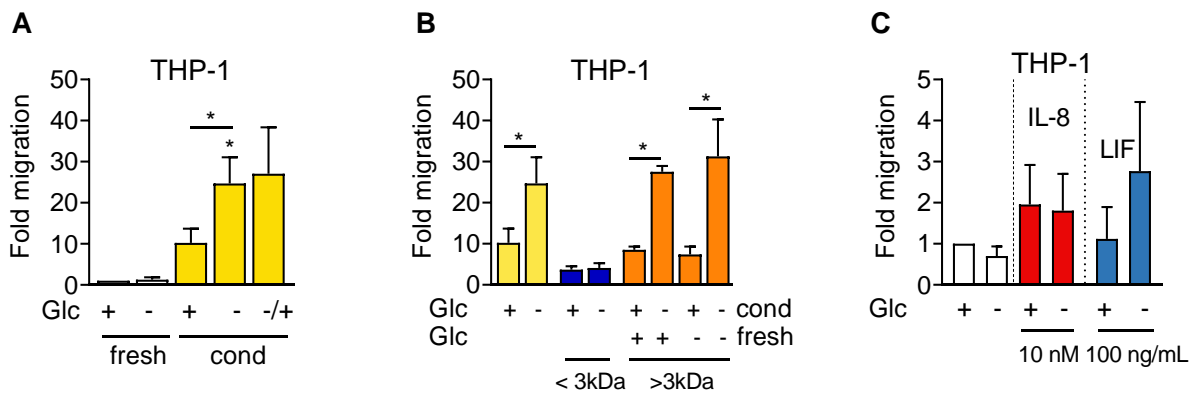
Figure 51 Macrophage-like THP-1 cells migrate towards conditioned media of starved A549 cells

A-B) THP-1 cells were differentiated with 100 nM PMA for 24 h and let recover for 48 h. Cells were plated on top of a boyden insert and were allowed to migrate for 20 h towards regular control media (white bars), conditioned (cond) media of A549 cells (yellow bars), washed conditioned media (orange bars) and filtered conditioned media (blue bars). Migrated cells were stained on the boyden membrane using crystal violet. Five pictures per membrane were taken using an inverted microscope and counted with ImageJ. Fold migration versus control Glc+ media is shown. Data represent mean ±SEM A. (n=3), B (n=3-4). Asterisks denote significant differences of cells migrated towards regular Glc+ and conditioned media Glc- in A. or as indicated.

C) THP-1 cells were differentiated and plated on top of a boyden insert as described in A. Cells migrated towards media with 25 mM (Glc+) or 0 mM (Glc-) substituted with recombinant IL-8 (10 nM) or LIF (100 ng/mL). Cells were analysed as described in A. Data represent mean ±SEM (n=3).

7.5.5 Primary neutrophils migrate towards the conditioned media of starved A549 cells

Lastly, we investigated the effects of the conditioned media of starved A549 cells on the migration of neutrophils. First, we performed chemotactic experiments using neutrophil-like HL60 cells, which were differentiated towards neutrophils using DMSO and ATRA.

HL60 cells migrated stronger towards the conditioned media of starved H460 cells but not A549 cells. (**Figure 52A-B**) We further validated these experiments by using primary human neutrophils isolated from human blood, using dextran sedimentation followed by a percoll gradient. Primary neutrophils migrated stronger towards the media of starved A549 cells (yellow bars) in comparison to the control media (**Figure 52C**). Experiments with washed conditioned media (orange) confirmed that migration was due to secreted protein from A549 cells and not due to metabolites in the media, since the filtrate (blue bars) did not induce migration.
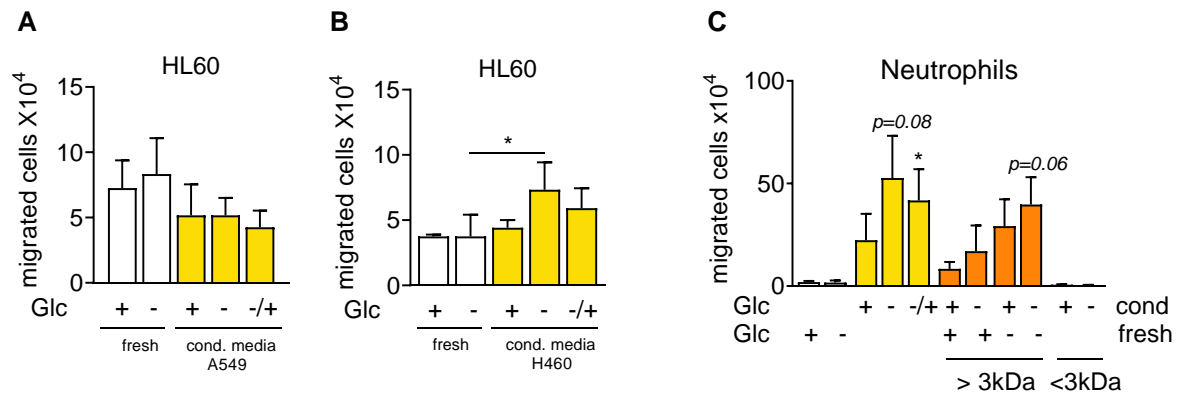
Figure 52 HL60 and primary neutrophils migrate towards conditioned media of starved A549 cells

A-B) HL60 cells were differentiated using 1.25 % DMSO and ATRA and cells migrated towards fresh control media (white bars) and conditioned media (yellow bars). Migrated cells were counted using a Neubauer chamber. Data represent mean ±SEM (n=3). Asterisks denote significant differences of cells migrated towards fresh Glc- media.

C) Primary neutrophils were extracted from human blood using a percoll gradient and were allowed to migrate towards fresh control media (white bars), conditioned media of A549 cells (yellow bars), washed conditioned media (orange bars) and filtered conditioned media (blue bars) for 2 h. Cells were analysed as described in A. Data represent mean ±SEM (n=4). *p-value* designates significance between the control Glc+ versus the indicated treatment.

8. Discussion

Cells need nutrients like carbohydrates, proteins and fatty acids not only for energy production but also for the *de novo* synthesis of proteins, nucleic acids and lipids for cell growth. Nutrient uptake is mediated by transporters embedded in the cell membrane followed by their conversion by anabolic and catabolic biochemical reactions. Glucose is one of the major nutrients needed for energy generation in form of ATP, as well as for the post translational modification of *de novo* synthesized proteins by glycosylation. Cancer cells are highly dependent on glucose compared to untransformed cells due to oncogenic mutations and a rewired metabolism. This altered metabolism is characterized by using mainly aerobic glycolysis instead of OXPHOS for energy production, which is known as the 'Warburg effect' (Hsu and Sabatini, 2008).

In the last decades, the altered cancer metabolism and its pro-tumorigenic impact on the TME arouse larger interest. The TME consists out of heterogenic cell populations, which interact among each other through cell-cell responses mediated by secreted cellular factors like cytokines or metabolites. Since plenty of discoveries show that tumors are often associated with inflammation (Balkwill and Mantovani, 2001; Landskron et al., 2014) many research groups investigate the impact of secreted cytokines and metabolites on intra-tumoral immune cells. Tumors that are characterized by immune cell exclusion or inactivation are designated as 'cold' or immunosuppressed tumors. This phenotype can be facilitated by the upregulation of certain immunosuppressive cell surface proteins like PD-L1 or CTL-4, as well as through secretion of cytokines by cancer cells. Furthermore, recent reports claim that oncogenic mutations and the increased nutrient uptake of cancer cells are accompanied by metabolic competition in the surrounding tissue or by the secretion of metabolites such as lactate to promote immune suppression in the TME (Chang et al., 2015). On the other hand, myeloid cells like macrophages or neutrophils, which are metabolically more resistant, are described to infiltrate tumors and to promote its progression through secretion of cytokines like IL-6, TNFα and VEGF (Murdoch et al., 2008). Therefore, it is suggested that the altered metabolism of cancer cells is associated with the immune landscape of the tumor and patient outcome.

In a tumor, transient nutrient deprivation occurs as a consequence of rapid tumor growth, resulting in poor vascularization of the tumor core, or through the application of anti-metabolic or anti-angiogenic drugs. In the body, ischemic tissue employed mechanisms that promote wound healing and the restoration of the nutrient flux. These mechanisms include angiogenesis and inflammation, which have been classically attributed to hypoxia or to necrotic inflammatory signals, respectively. Sustained lack of nutrients results in cell death; however, since multiple reports show that tumors are often associated with inflammation, we

Discussion

hypothesized that nutrient deprivation promoted the secretion of cytokines with chemotactic functions promoting immune cell infiltration in the tumor.

First, we investigated how cancer cells die upon environments low in glucose and how the UPR is involved in this response. Second, we investigated if cells secrete cytokines and chemokines upon nutrient deprivation or by the application of anti-metabolic drugs. We further investigated the specific signaling pathways that promoted the induction and release of these cytokines. In a last step we explored the functional consequences of secreted cytokines on cancer cells themselves as well as on immune cells. We focused specifically on IL-6, IL-8 and LIF due to their importance in inflammation, tumor progression and patient outcome in the clinic.

8.1 Glucose deprivation induces ATF4-mediated apoptosis through TRAIL-receptor 1 (DR4) and 2 (DR5)

Sustained ER stress induces a switch from the pro-survival UPR response towards a pro-death response. Several reports indicate that the transcription factor ATF4 mediates necrosis (León-Annicchiarico et al., 2015b) as well as apoptosis (Shin et al., 2015) upon glucose deprivation. Moreover, it is reported that the cell death receptors DR4 and DR5 are induced upon ER stress stressors, including thapsigargin and 2-DG (Chen et al., 2007; Liu et al., 2009; Yamaguchi and Wang, 2004).

Our results proved that glucose deprivation promotes apoptosis in HeLa cells. Furthermore, DR4 and DR5 protein expression was induced in cancer cells and knockdown of the death receptors protected from cell death (**Figure 10, 53**). Several studies before showed that DR5 is regulated by CHOP in several cancer cell lines. In our model we could not prove that DR5 is regulated by CHOP, however we found that ATF4 knockdown completely prevented DR5 protein induction (**Figure 11**). This is supported by other reports that show an UPR-dependent but CHOP-independent regulation of DR5 (Martín-Pérez et al., 2012). Furthermore, we found that CHOP slightly regulated DR4 protein level, however CHOP knockdown did not protect from cell death. Regarding ATF4, we proved that knockdown protected from cell death, which is in line with DR5 protein expression. This suggests that cells die in an DR5-dependent manner mediated by ATF4. However, within these experiments we could not confirm, if ATF4 directly induced DR5 transcriptionally or if its regulation is translationally. Therefore, in further experiments the mRNA level of DR5 and DR4 upon silencing of ATF4 and glucose deprivation have to be analysed by qPCR.

Within this project we did not analyse the involvement of the other branches (IRE1 and ATF6) of the UPR response in the induction of cell death upon glucose deprivation. Regarding that it is described that the IRE1 branch transiently mediates DR5 mRNA decay, which delays the cell

112

death response and allows the cell to recover (Lu et al., 2014). Furthermore, some reports, as well as preliminary data from our group, suggest a crosstalk between the three UPR branches. Regarding that it is described that the PERK branch enhances IRE1 signaling (Tsuru et al., 2016) upon treatment with thapsigargin. Possible crosstalk's between the UPR branches could fine tune cell death induction and need to be more profoundly investigated.

To sum it up, we conclude that sustained glucose deprivation switches the UPR towards a pro-death response, which induces the upregulation of DR5 and DR4. We proved that DR5 but not DR4 induction was mediated by ATF4. This project was recently published (Iurlaro, Püschel et al., 2017).
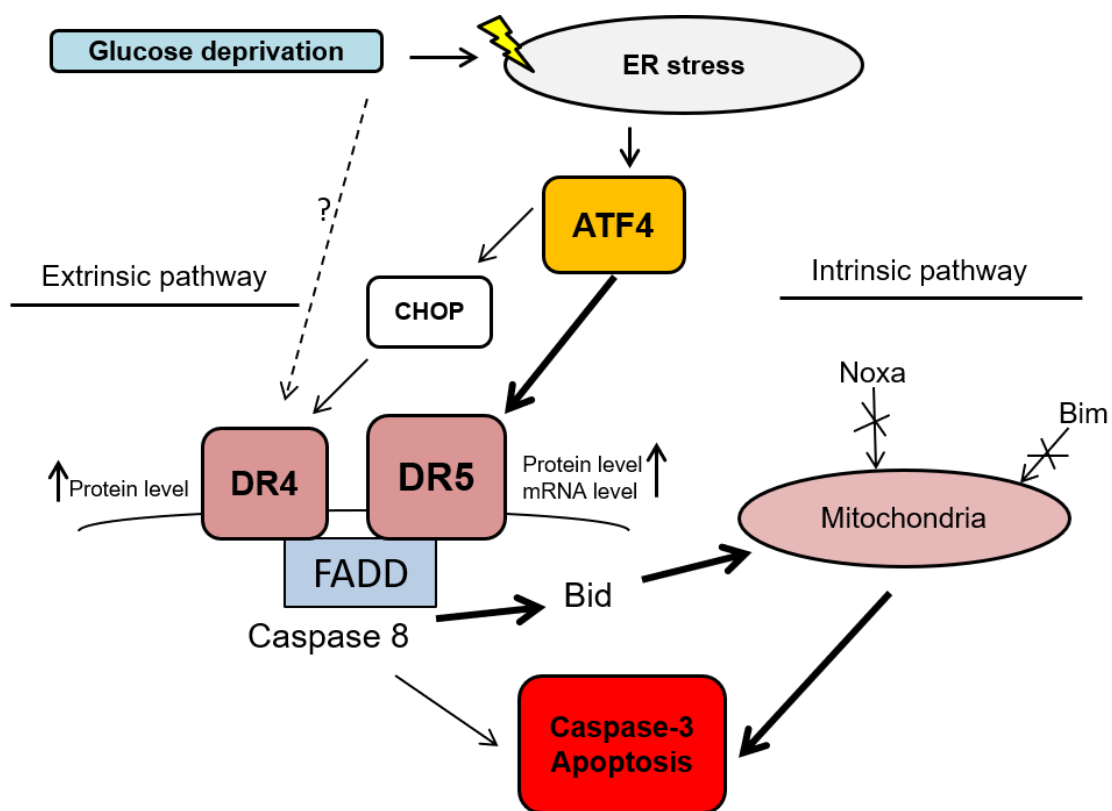
Figure 53 Schematic presentation of glucose deprivation induced apoptosis
Glucose deprivation induces ER stress in cancer cells, which promotes the induction of ATF4 and CHOP. CHOP slightly regulated DR4 protein level, whereas ATF4 regulated DR5. Cancer cells died in a apoptotic DR5-dependent manner mediated by ATF4 upon glucose deprivation. Silencing of Noxa and Bim had no effect on cell death induction upon glucose deprivation. (Iurlaro, Püschel et al., 2017b)

Discussion

8.2 Glucose deprivation induces cytokine release

Several reports show that the UPR induces cytokines in cancer cells (Zhang and Kaufman, 2008a). Since we demonstrated that the UPR is induced upon glucose deprivation, we hypothesized that prior to a cell death inducing response, the UPR promotes cytokine secretion. To test that, we performed a secreted protein array using the supernatant of glucose-deprived A549 cells under exclusion of cell death. We detected a broad range of secreted proteins involved in various cell responses (**Figure 12**). We detected for instance VEGF, which is a pro-tumorigenic cytokine associated with angiogenesis. Its release upon glucose deprivation has been reported before in monocytes (Satake et al., 1998) and HepG2 cells mediated by ATF4 (Terashima et al., 2013). We detected other angiogenic cytokines including angiogenin and PDGF-AA. That suggests that glucose deprivation induces an angiogenic response, promoting the revascularisation of the tumor to restore nutrient flux. However, we did not further validate these cytokines by ELISA or qPCR, which should be done, to strengthen this hypothesis.

Adiponectin, a hormone secreted by adipose tissue, was induced in the protein array. Low level of adiponectin have been associated with poor prognosis in leukemia (Aref et al., 2013), in colorectal (Xu et al., 2011) and in breast cancer (Macis et al., 2014). This indicates that release of adiponectin upon glucose deprivation could promote an anti-tumorigenic response. This is further supported by the fact that adiponectin is also associated with AMPK activation and mTOR inactivation (Shibata et al., 2005), suggesting that its release lowers the energetic needs of the cell. On the other hand, adiponectin is involved in immune escape by blunting the activity of dendritic cells (Tan et al., 2014). In conclusion, reports are controversial about the role of adiponectin in cancer (Katira et al., 2016). We did not further confirm adiponectin release by ELISA, however investigating the role of adiponectin upon glucose deprivation may offer an interesting new research field.

We also detected the release of IL-6 and IL-11 in the protein array of starved A549 cells, which are known to promote tumor growth and survival by inducing cell-cell responses. One of the pathways activated by these cytokines is the induction of STAT3 signaling in cancer cells, as well as in other tumor-intrinsic cell populations, which is associated with tumor progression (Huynh et al., 2019). Therefore, the release of IL-6 and IL-11 upon glucose deprivation could transmit stress to neighbouring cells in order to escape or to adapt to nutrient shortage. Secreted IL-8 and CD14 are involved in tumor growth and inflammation. Regarding CD14 it is described, that CD14-high bladder cancer cells are more vascularized and show higher myeloid infiltration (Cheah et al., 2015; Hammond et al., 1995).

114

Interestingly, some cytokines like IGFBP-2 or chemokines like CXCL5 and CCL2 were downregulated upon glucose deprivation, which could be due to impaired posttranslational events such as glycosylation. This assumption is supported by the increased mRNA expression of CCL2 upon glucose deprivation, which does not coherent with its secretion (**Figure 13,33**). IGFBP-2 is associated with chemoresistance in esophageal adenocarcinoma (Myers et al., 2015) and bladder cancer (Zhu et al., 2015). This suggests, that reduced secretion upon glucose deprivation could possibly sensitise cancer cells to chemotherapeutic treatment. However, more in-depth studies and validation of protein level by ELISA or western blot have to be performed to prove this hypothesis.

In summary, we found several up as well as downregulated cytokines with a broad variety of biological functions and impacts on tumor progression. Within this thesis, we did not validate all detected cytokines by ELISA or qPCR. However, to completely understand the interplay between these cytokines, individual analysis has to be performed in order to clarify their regulation and function in tumor settings.

Focusing on chemokines and cytokines involved in inflammation, we validated some of the detected cytokines from the protein array by ELISA. We used several lung cancer cell lines from different origin including A549, H1299, H520, SW900 and H460 cells as well as HeLa cells. We found IL-8, IL-6 and LIF as major secreted proteins in different cell lines (HeLa, A549, H460, SW900), suggesting that this response is conserved between distinct cancer cell lines (**Figure 16,17,20**). IL-8 is described to promote angiogenesis, metastasis and proliferation in lung cancer and it is also described as a chemoattractant for neutrophils. High level of circulating IL-6 are associated with poor prognosis and an a lower overall survival in NSCLC patients (Sunaga et al., 2012). Moreover, IL-6 is well described as an activator of tumor-associated signaling cascades promoting tumor growth and immune cell infiltration (Johnson et al., 2018). In the case of LIF it was just reported, that LIF induces CXCL9 in TAMs and impede CD8^{+} T cell infiltration (Pascual-García et al., 2019) in tumors. Some of the analyzed cells showed high basal level of IL-6 or IL-8 (A549, H460, SW900), which is described to be mediated by KRAS mutations (Sunaga et al., 2012), promoting tumor growth.

Considering the important role of these cytokines in tumor progression and tumor-associated inflammation, our results suggest that the release of IL-8, IL-6 and LIF upon glucose deprivation or upon treatment with anti-metabolic drugs, may worsen patient outcome.

TNFα mRNA was induced in HeLa cells upon glucose deprivation; however, we did not detect its release, neither in HeLa nor in A549 cells. A similar outcome was observed for CXCL1, which was induced at mRNA level but not its release. This indicates that mRNA induction and

Discussion

cytokine release do not correspond for all cytokines upon glucose deprivation, possibly due to impaired posttranslational modifications of some cytokines. Moreover, the peak of mRNA induction is at short time points (3 h) and normalizes for some cytokines, like IL-8, within 24 h to basal level. Surprisingly, cytokines are still steadily released at late time points upon glucose deprivation. This suggests, that cytokines are possibly regulated transcriptionally in a first response, however in a long-term response other mechanism take over, which translationally regulate cytokine release. Another possibility would be, that cytokines accumulate in the cell, as shown for IL-8 but not for LIF (**Figure 21,22**) after being *de novo* synthesized at short time points upon glucose deprivation. When mRNA level decline to basal level, cytokines can still be steadily released. In order to test this hypothesis, *Click-iT Assays* (Thermo Fisher) have to be performed for the time dependent monitoring of *de novo* cytokine synthesis, as well as cytokine secretion. Moreover, sustained glucose deprivation induces cell death receptors such as DR5 and DR4 at late time points (data not shown), which are associated with NF-κB activation. Therefore, other signaling pathway could promote cytokine secretion at later time points.

Recently, it was described that squamous NSCLC cells are more glycolytic and more susceptible to glycolytic inhibitors (Goodwin et al., 2017) compared to adenocarcinomas. This suggests that these cells secreted higher amounts of cytokines. In our study, we could not find a correlation between cytokine release and squamous NSCLC (SW900, H520) or adenocarcinoma (A549, H1299, H460) cell lines. Moreover, all tested cell lines released distinct amounts and types of cytokines. This indicates that cancer cells secrete their own 'cytokine cocktail', which could be based on oncogenic mutations and the induction of distinct downstream (stress) signaling pathways like the UPR or NF-κB. In order to predict the secreted cytokines upon glucose deprivation by a specific cancer cell line, more detailed analysis of cell line specific mutational burden and subsequently induced stress signaling pathways have to be performed. Translating this into a clinical setting, the heterogeneity of patients and systemic responses have to be considered when developing anti-metabolic drugs.

H520 cells are more resistance towards glucose deprivation induced cell death (**Figure 13**). Compared to the other tested cell lines, H520 cells did not release any of the tested cytokines. It is possible that these cells induce alternative metabolic pathways to bypass glucose deprivation, which in turn prevents the induction of stress signaling pathways such as the UPR, which mediate cytokine release. This could also be applied to H1299 cells, which only released LIF upon glucose deprivation among the tested cytokines. Therefore, further investigations have to be performed focusing on the metabolism as well as glucose deprivation induced stress

116

signaling pathways of H520 and H1299 cells compared to A549 cells. This would deepen the knowledge of how glucose deprivation induces cytokines release in a cell type dependant manner. Moreover, it would allow to identify new possible targets for anti-metabolic therapies. Exosomes are small membrane derived vesicles, secreted from many cancer cells. These endocytic membranes are loaded with proteins, micro (mi)RNA or DNA for cell-cell communication. Increased exosome secretion from A549 cells upon cisplatin treatment is associated with resistance and inflammation (Li et al., 2016) and in cardiomyocytes, glucose deprivation promotes the secretion of exosomes (Garcia et al., 2015). Hence, it is likely that A549 cells release exosomes upon glucose deprivation loaded with cytokines. To test this, supernatants from starved A549 cells have to be prior ultra-centrifuged to remove exosomes. Afterwards, supernatants have to be analysed by ELISA in order to test if cytokines are released in soluble form or engulfed in exosomes. Moreover, other cellular molecules like DNA or miRNA engulfed in these vesicles could be secreted as well. Therefore, a future direction of this project could be to test if exosomes are released by glucose deprivation. In case exosomes are released, their content and functions in the TME have to be investigated.

8.3 The impact of nutrient substitution to glucose-deprived media

We added several intermediate substrates of the glucose metabolism to glucose-deprived media to investigate the crucial steps that facilitate cytokine secretion (**Figure 24**). An overview of the results is presented in **Figure 54**. In some cell lines the induction of the UPR can be prevented by the addition of mannose or GlcNAc, which restore glycosylation (Panneerselvam and Freeze, 1996), whereas fructose can be converted to glucose or fuel glycolysis through alternative pathways (Fan et al., 2017). Mannose and partially fructose reversed the release of IL-8 and LIF simultaneously and protected cells from cell death. This suggests that these nutrients can replace glucose and prevent that cells undergo starvation. The addition of GlcNAc, had only minor effects on cytokine release, which suggests that restoring glycosylation by the HBP does not prevent cytokine release. If the UPR is induced due to impaired glycosylation but GlcNAc does not resolve glycosylation and cytokine release, it is possible that ATF4 is induced in a UPR-independent manner. This is suggested by another group who claim that ATF4 is induced in an GCN2-dependent manner due to a secondary loss of amino acids upon glucose deprivation (Chaveroux et al., 2016b). To further validate this observation, ATF4 level need to be tested upon GlcNAc re-addition and knockdown of PERK and GCN2 upon glucose deprivation should be performed.

Discussion

Lactate is described to substitute for glucose by fuelling the TCA cycle in NSCLC cells (Faubert et al., 2017). Substituting lactate to glucose-deprived media did not reverse IL-8 release, whereas LIF release was partially reduced. This suggests that reduced TCA cycle activity could be a cause for LIF release but not for IL-8. However, more experiments should be performed, investigating if lactate fuels the TCA cycle in these cells and/or which other effects lactate has on the cellular signaling events in A549 cells.

Methyl-pyruvate, which serves as a mitochondrial substrate, reversed the mRNA expression of all tested mRNAs, except for LIF, and also the release of IL-8 and partially LIF. Assuming that glucose deprivation promotes ROS production and ATF4 induction, which is suggested by some reports (Graham et al., 2012; Kasai et al., 2018), Methyl-pyruvate could function as an antioxidant, which is described (Ramos-Ibeas et al., 2017; Wang et al., 2007), preventing ATF4 induction and cytokine release. Otherwise, methyl-pyruvate could fuel the TCA cycle independently of glycolysis and prevent a subsequent ATP drop and stress signalling in the cell. Further experiments have to be performed, investigating the energy status and the UPR induction upon treatment with Met-Pyr.

2-DG prevents glycosylation and some reports claim that 2-DG is phosphorylated by the HK and accumulates in form of 2-DG-P in the cell, preventing further glucose utilization. In contrary, another report describes that 2-DG also inhibits the phosphoglucose-isomerase (GPI), which is the enzyme converting G-6-P to be further metabolized by glycolysis. Moreover, this report proved that if GPI is blocked, glucose can still be metabolized by the PPP (Ralser et al., 2008), meaning that the glucose metabolism is still partially functional.

Addition of 2-DG to glucose free media prevented LIF release, whereas IL-8 release remained unchanged. It is possible that upon glucose deprivation some glycosylation remains intact, which is sufficient for the highly glycosylated cytokine LIF to be posttranslational modified and released. This could be mediated by upregulation of alternative metabolic pathways like the HBP, which is described to restore glycosylation in an ATF4 dependent manner in this cell line upon glucose deprivation (Chaveroux et al., 2016c). However, combined treatment of glucose deprivation with 2-DG could entirely inhibit glycosylation, which in turn prevents *de novo* synthesis of LIF. In contrary, IL-8, which is a non-glycosylated cytokine, keeps on being synthesized and released in glucose free media upon 2-DG co-treatment. Another possibility would be that LIF trafficking to the cell membrane is affected by additional treatment with 2-DG, suggesting a distinct secretory pathway for LIF and IL-8 secretion. To further confirm this hypothesis, it is necessary to analyse LIF *de novo* synthesis, trafficking and glycosylation status upon cotreatment with glucose deprivation and 2-DG. Furthermore, a more detailed

118

analysis of how glucose deprivation in combination with 2-DG affects glycosylation of other cellular proteins would give additional important information. Another hypothesis would be that 2-DG and 2-DG-P accumulate in the cell and get detected by glucose level sensors and therefore mimic sufficient glucose level, which prevents LIF induction. This would suggest that LIF is induced upon glucose sensing mechanism, whereas IL-8 is induced upon consequentially upregulated stress signaling pathways upon glucose deprivation.

Regarding cytokine mRNA level, LIF mRNA expression is not reversed by any of the added nutrients, which suggests that LIF mRNA is regulated differently compared to other tested cytokines.

To completely understand how addition of specific nutrients to glucose-deprived culture media influences cytokine release, more detailed analysis has to be performed on how these nutrients affect intracellular stress signaling pathways, with focus on ATF4 and mTOR induction. Furthermore, effects on metabolic outcomes such as ATP levels should be analysed.
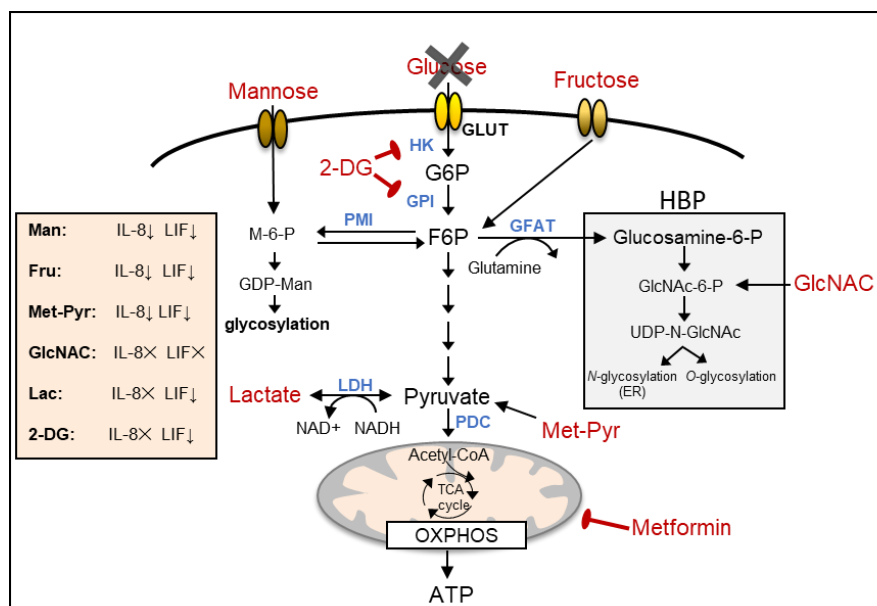
Figure 54 Schematic presentation of glucose metabolism and addition of nutrients in the absence of glucose
Mannose (Man) and fructose (Fru) are uptaken by transporters. Man is converted to F6P, in cells that express the phosphomannose isomerase (PMI) only and fuels glycolysis. Man can also be converted to GDP-Mannose and restore glycosylation. Fructose fuels glycolysis by its conversion to F6P. Methyl-pyruvate (Met-Pyr) fuels the TCA cycle. N-Acetylglucosamine (GlcNAc) fuels the HBP and restores glycosylation. 2-deoxyglucose (2-DG) blocks glycolysis by blocking the hexokinases (HK) or the glucose-6-P isomerase (GPI) resulting in an ATP drop as well as impaired glycosylation mediated by glucose. Metformin blocks complex I of the respiratory chain. IL-8: Interleukin-8; LIF: Leukemia inhibitory factor; ✕: no change in cytokine release; ↓: Less cytokine release. Orange box: Up- and downregulated cytokine release upon substitution of indicated nutrients to glucose-deprived media.

8.4 Glutamine deprivation promotes cytokine release

In our model we found that glutamine deprivation promoted the induction and secretion of IL-6 and IL-8 but not LIF (**Figure 26**). Recently it was shown that glutamine deprivation induces IL-8 release in a mTOR dependent manner (Shanware et al., 2014) as well as due to ROS production (Kim et al., 2014). Moreover, it was reported that glutamine deprivation (Chen et al., 2014) as well as glucose deprivation (Chaveroux et al., 2016c) induces ATF4 in a GCN2-dependent manner. Therefore, IL-8 and IL-6 induction could be mediated by GCN2 and a subsequent induction of ATF4 upon glutamine deprivation. This is supported by our finding that IL-8 and IL-6 secretion is ATF4 dependent. However, to confirm this hypothesis, further analyses have to be done by silencing GCN2 and ATF4 upon glutamine deprivation.

Since LIF release is ATF4 independent it was expected that glutamine deprivation did not induce LIF. This also supports the hypothesis, that LIF release is exclusively glucose dependent, possibly induced by specific glucose sensors in the cell. A possible sensing mechanism could be the ADP/ATP ratio in the cell. Therefore, it would be interesting to see if replenishing ATP to the cell, upon glucose deprivation, reverses LIF release compared to the release of other cytokines. This hypothesis is however contradicted by the fact that glucose deprivation does not induce AMPK in our model, which is the main sensor for the ADP/ATP ratio in our system. Still, there are many other glucose sensors in the cell. Among them is the decrease of the NADH/NAD$^+$ ratio or epigenetic regulatory mechanism. These sensing mechanisms could be involved in LIF induction and have to be investigated more deeply.

In our system total starvation, even in the presence of some glucose, did not induce cytokines possible due to the absence of growth factors and nutrients which could be essential for cytokine synthesis.

8.5 Anti-metabolic drugs promote cytokine release

Importantly, we proved that anti-metabolic drugs induced cytokines such as 2-DG, which induced IL-6, IL-8 and LIF or metformin, which induced IL-6 and IL-8 but not LIF (**Figure 27-28**). Both drugs are associated with ATF4 induction, which could mediate IL-8 and IL-6 release. Since we showed that LIF induction is independent of ATF4, release upon 2-DG treatment needs to be mediated in a different manner, possibly due to impaired glycosylation or reduced ATP level in the cell.

Metformin blocks mitochondrial respiration and it is also described to induce ROS, which in turn could promote ATF4-signaling and cytokine induction (Zeeshan et al., 2016b). An ATF4-

dependent mechanism of cytokine induction by metformin would also explain why metformin did not induce LIF.

To sum it up, these finding are very important since patient treatment with anti-metabolic drugs and subsequent cytokine release and possible inflammatory responses could reverse anti-tumorigenic effects of these drugs in the clinic and promote resistance or even tumor progression.

8.6 The involvement of ATF4 in cytokine induction upon glucose deprivation

Cancer cells are more resistant towards intra- and extracellular perturbations compared to untransformed cells due to the upregulation of adaptive stress responses. Glucose deprivation induces the UPR (Palorini et al., 2013) due to possible impaired glycosylation and a subsequent accumulation of misfolded proteins in the ER. Since the UPR is a pro-survival response in the first place, we hypothesized that ATF4 mediates prior to cell death induction an adaptive response to starvation by release of cytokines. These cytokines in turn could affect the TME in terms of metabolic rewiring, cell death or immune infiltration.

We recently reported that ATF4 mediates cell death upon glucose deprivation in HeLa cells (Iurlaro, Püschel et al., 2017a). In our current model, ATF4 was induced at short time points upon glucose deprivation, which is in accordance with cytokine mRNA induction. Regarding that, ATF4 is linked to IL-6 induction upon metabolic stress in macrophages (Iwasaki et al., 2014) and human tumor cells (Wang et al., 2012) as well as to VEGF release (Malabanan et al., 2008).

We proved that ATF4 mediated the induction and release of IL-6 and IL-8 but not LIF and the mRNA induction of several other cytokines upon glucose deprivation (**Figure 31,32,55**). Surprisingly, we found that ATF4 knockdown in the presence of glucose reduced basal IL-8 release although IL-8 mRNA induction was not altered. This suggests that basal ATF4 level could have functions in protein translation independently of transcription. Since we could not confirm that ATF4 regulates all cytokines to the same extent, ATF4 cannot be considered as an exclusive cytokine regulator. Moreover, we did not evaluate if ATF4 directly induces cytokines transcriptionally by binding to their promotor, or if ATF4 is rather a mediator that promotes cytokine induction and/or synthesis. Further experiments, including Chromatin immunoprecipitation (CHiP), should be performed to strengthen the role of ATF4 in cytokine induction.

Importantly, anti-metabolic drugs including 2-DG and metformin induced ATF4 (Jaime Redondo, 2018) and cytokine release in A549 cells. The most studied mode of action of

Discussion

metformin is blocking complex I of the respiratory chain in the mitochondria, which lowers ATP production (Owen et al., 2000). Other reports show that metformin induces ATF4 in the mouse liver (Kim et al., 2013). Furthermore, metformin induces the PERK arm of the UPR, as described in cardiomyocytes (Quentin et al., 2012). 2-DG is a common UPR stressor and associated with ATF4 induction (León-Annicchiarico et al., 2015b), suggesting that 2-DG promotes IL-8 and IL-6 induction in an ATF4-dependent manner. However, for further confirmation, ATF4 knockdown experiments in combination with 2-DG and metformin treatment need to be performed to strengthen this hypothesis.

CHOP, which is also induced upon glucose deprivation in our model, is described to induce IL-6 (Hattori et al., 2003). In our model we did not study CHOP involvement, which should be done in further experiments.

In summary, we conclude that ATF4 is involved in the induction and release of IL-6 and IL-8 but not LIF, either as a mediator or as a transcription factor in A549 and HeLa cells. However, not all cytokines are regulated by ATF4, suggesting a cytokine dependent regulation by the UPR/ISR, upon glucose deprivation.

An overview of the involvement of the UPR in IL-8 and LIF regulation is shown in **Figure 54**.
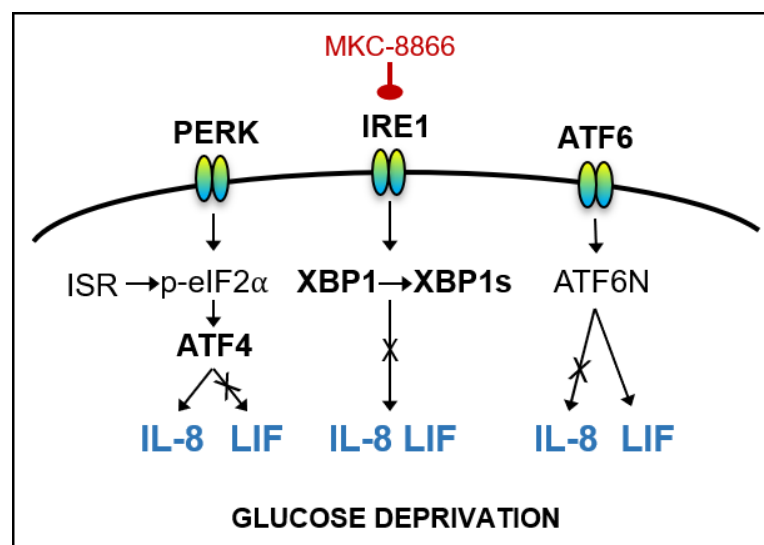
Figure 55 UPR regulation of IL-8 and LIF upon glucose deprivation
Glucose deprivation induces the three UPR stress signaling proteins; inositol requiring kinase 1 (IRE1), the activating transcription factor 6 (ATF6) and the protein kinase RNA-activated (PKR)-like endoplasmic reticulum kinase (PERK). PERK and other ISR kinases phosphorylate eIF2α and facilitate the induction of the transcription factor ATF4, which promoted the induction and release of IL-8 but not LIF. IRE1 promotes the splicing of XBP1. Spliced XBP1 (XBP1s) is a transcription factor, which did not regulate IL-8 or LIF. Cleaved ATF6 (ATF6N) is translocated to the nucleus and functions as a transcription factor. Knockdown of ATF6 partially reduced LIF but not IL-8 release.

122

8.7 The role of PERK in the regulation of IL-8 and LIF

In a nutrient deprived setting, ATF4 is described to be induced by one of the ISR kinases PERK or GCN2. Focusing on PERK, we used the chemical PERK inhibitor GSK2656157 and AMG PERK 44, which both partially reduced ATF4 protein induction upon glucose deprivation. LIF release was strongly reduced by GSK2656157 and minor reduced by AMG PERK 44 upon glucose deprivation (**Figure 37**). Previous results excluded ATF4-dependent regulation of LIF, suggesting an ATF4-independent but PERK-dependent regulation of LIF. UPR-independent functions of PERK include ER-mitochondria tethering at the mitochondria-associated ER membrane (MAMS), regulating among others calcium and ROS signaling as well as ER morphology (Verfaillie et al., 2012). PERK also induces Nuclear Factor Erythroid (NFE) 2-Related Factor 2 (NRF2), which regulates the antioxidant response by transcriptionally inducing antioxidant enzymes by the antioxidant response element (ARE). In cancer, NRF2 has dual roles. On the one hand, it is cytoprotective and prevents tumor initiation through its protective effects against metabolic, xenobiotic and oxidative stresses, however hyperactivation promotes tumor growth, which is associated with drug resistance (Menegon et al., 2016). Moreover, NRF2 is shown to be induced in a PERK dependent manner upon glucose deprivation (Cullinan and Diehl, 2004). LIF could be induced by NRF2 due to its involvement in many biological processes, which could promote LIF induction. Furthermore, recently it was reported that GSK2656157 also inhibits receptor-interacting protein kinase 1 (RIPK1) (Rojas-Rivera et al., 2017), which is a kinase involved in inflammation, cell death (necroptosis and apoptosis) and NF-κB induction downstream of the Tumor necrosis factor receptor (TNFR). Since the GSK2656157 inhibitor had a major effect on LIF release and AMG PERK 44 only a minor, further experiments validating RIPK1 involvement in LIF release upon glucose deprivation have to be performed. An overview of the hypothesis is shown in **Figure 56.**

Regarding IL-8, the two PERK inhibitors had contradictory effects on its release upon glucose deprivation. AMG PERK 44 induced IL-8 release in the presence and absence of glucose, whereas GSK2656157 had no effect on IL-8 release (**Figure 37**).

Possibly PERK alone, independently of ATF4, could negatively regulate IL-8 release upon glucose deprivation. Moreover, RIPK1 is involved in NF-κB signaling, which we proved to mediate IL-8 release. Furthermore, GSK2656157 inhibits RIPK1 which could balance the suppressive effect of PERK on IL-8 release. Therefore, as for LIF, RIPK1 involvement in cytokine release upon glucose deprivation of IL-8 has to be further investigated. Moreover, we showed that LIF induced IL-8. This suggests that reduced secretion of LIF upon GSK2656157 treatment consequently also leads to a reduced IL-8 secretion upon treatment with the

Discussion

GSK2656157 inhibitor, eliminating the inducing effect of PERK inhibition seen upon AMG PERK 44 treatment. An overview of the hypothesis is presented in **Figure 55.**
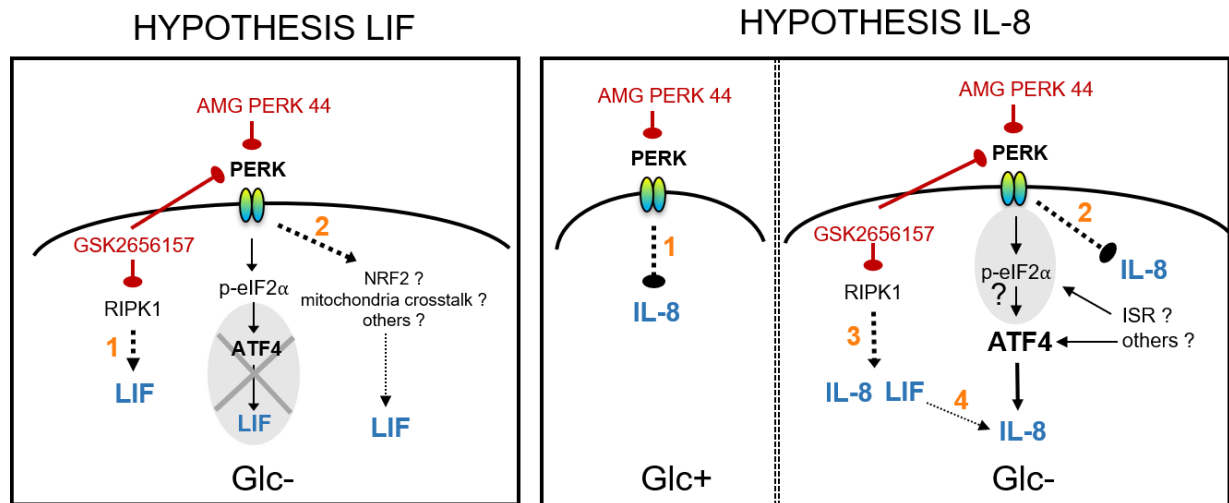
Figure 56 Regulation of IL-8 and LIF by PERK upon treatment with the inhibitor GSK2656157 and AMG PERK 44
Hypothesis LIF: ATF4 was not involved in LIF induction in the absence (Glc-) of glucose. LIF release was reduced by GSK2656157 and minor reduced by AMG PERK 44 treatment upon glucose deprivation. (**1**) GSK2656157 could additionally inhibit RIPK1, which could be an inducer of LIF. (**2**) PERK could ATF4 independently regulate LIF release through induction of NRF2 or through a mitochondrial crosstalk. Hypothesis IL8: (**1**) AMG PERK 44 induced IL-8 release in the presence of glucose (Glc+). Therefore, basal PERK activity, independent of ATF4, could inhibit IL-8 release. In the absence of glucose (Glc-) AMG PERK 44 induced IL-8 release and GSK2656157 had no effect. (**2**) AMG PERK 44 could induce IL-8 due to a negative regulation of PERK on IL-8 release, independent of ATF4. (**3**) IL-8 could be regulated by RIPK1, which is also inhibited by GSK2656157, and would balance the negative regulation of PERK. Hypothesis LIF: (**4**) GSK2656157 reduced LIF release. If LIF induces IL-8 release upon glucose deprivation and LIF release is reduced upon GSK2656157 treatment, IL-8 release would be consequentially reduced as well and balance the negative regulation of PERK on IL-8 release.

124

8.8 The impact of the eIF2α inhibitor ISRIB on cytokine release

To further investigate the ISR involvement in cytokine release, we focused on eIF2α which is phosphorylated by the upstream kinases of the ISR and subsequently leads to the translation of ATF4.

We treated cells with ISRIB, a molecule reversing the phosphorylation of eIF2α upon the activation of the ISR (Sidrauski et al., 2013). Recently, it was reported that treatment with the inhibitor ISRIB results in a reduced secretion of IL-6 and IL-8 upon glutamine deprivation in a breast cancer cell line. This was also supported with a decreased induction of cytokine genes dependent on eIF2α phosphorylation (Gameiro and Struhl, 2018).

Upon treatment with the ISRIB inhibitor in combination with glucose deprivation we found a mild reduction of ATF4 protein level (data not shown). However, we found an induction of IL-8 release, a small reduction of LIF release and no effect on IL-6 release upon 24 h treatment (**Figure 38**). Therefore, we could not confirm that eIF2α-phosphorylation is involved in cytokine induction upon glucose deprivation in our model as reported before by *Gameiro and Struhl*. This result suggests that ATF4 could be induced independently of the upstream ISR kinases PERK or GCN2. Validating eIF2α phosphorylation in A549 cells upon glucose deprivation remained inconclusive, since we already observed basal eIF2α phosphorylation (data not shown). A possible explanation could be that ATF4 is induced partially independent of phosphorylation of eIF2α. Supporting this, a recent publication proved that methionine deficiency induced ATF4 independent of the GCN2/peIF2α pathway (Mazor and Stipanuk, 2016). Moreover, ATF4 can be induced by mTORC1 to induce purine synthesis in cancer cells, independent of the cellular stress response and due to growth factors (Ben-Sahra et al., 2016). Therefore, either ISRIB contains some unknown off target effects independent of ATF4, or ATF4 induction and downstream cytokine release is to some extend induced independent of eIF2α phosphorylation. Furthermore, it would also be possibly, that after ISRIB treatment the remaining ATF4 induction is sufficient to promote cytokine induction.

8.9 IL-8 and LIF regulation by the IRE1 and ATF6 branch of the UPR

Several reports link the IRE1 branch of the UPR to cytokine release and subsequent immune infiltration in cancer (Logue et al., 2018; Rubio-Patiño et al., 2018). In our model we could not confirm a regulation of IL-8 or LIF by IRE1 knockdown or by treatment with the RNase inhibitor MKC-8866 (**Figure 34,35**). However, knockdown efficiency of IRE1 was weak and results of cytokine induction upon treatment with the IRE1 inhibitor MKC–8866 were only measured at mRNA level. Since our results showed that mRNA and protein level are not

regulated simultaneously, the MKC-8866 inhibitor could still prevent cytokine release, which has to be tested in further experiments. However, we investigated if XBP1s, the transcription factor of the IRE1 branch of the UPR, mediates IL-8 and LIF release upon glucose deprivation. We silenced XBP1 with two different siRNA sequences and their efficiency was verified by qPCR. We found reduced mRNA induction for XBP1s, as well as for Erdj4, a known downstream target of XBP1s. The results on IL-8 and LIF release upon silencing of XBP1 in combination with glucose deprivation remained contradicting. However, considering the results of the IRE1 knockdown and the IRE1 RNase Inhibitor MKC-8866, we conclude that the IRE1 arm of the UPR has no regulatory function in cytokine induction upon glucose deprivation in our system.

We found that ATF6 knockdown induced LIF and IL-8 mRNA expression upon glucose deprivation. Though, IL-8 release was not changed, whereas LIF release was slightly reduced. This suggests that ATF6 has contradicting effects on mRNA induction and protein synthesis of cytokines, induced by glucose deprivation. We conclude that ATF6 only minorly regulated IL-8 mRNA induction, however we do not exclude a role for ATF6 in LIF induction upon glucose deprivation. However, we observed ATF6 cleavage at 6 h of glucose deprivation (**Figure 29A**) whereas LIF is induced at earlier time points. Therefore, we suggest that ATF6 is rather involved in the regulation of LIF at later time points, rather than in the initial induction. Therefore, further experiments should be performed by using additional siRNA sequences to finally conclude the role of ATF6 in LIF release upon glucose deprivation. See also overview **Figure 55.**

8.10 mTOR involvement in cytokine release

Protein synthesis is mainly regulated by mTOR signaling and glucose deprivation is known to inactivate mTOR in order to attenuate protein synthesis to restore cell homeostasis. Furthermore, mTOR inactivation is described to be involved in cytokine induction in immune cells (Weichhart et al., 2015).

Glucose deprivation inactivates mTOR in our model. We also found that IL-8 is induced upon glutamine deprivation which, for IL-8, is described to be mediated in an mTOR dependent manner (Shanware et al., 2014). To investigate if mTOR signaling is involved in glucose deprivation induced IL-8 and LIF release, we used the mTOR inhibitor rapamycin, which blocks mTORC1 and Torin1, which blocks mTORC1 and mTORC2.

In our model we proved that Torin1, but not rapamycin, induced slightly IL-8 release in the presence of glucose (**Figure 40**), suggesting that mTORC2 is involved in IL-8 induction.

126

Regarding that it is described, that mTORC2 inhibits PERK in an AKT dependent manner (Tenkerian et al., 2015) and attenuates PERK signaling under oxidative stress (Krishnamoorthy et al., 2018). Therefore, mTORC2 inhibition could induce PERK signaling and possibly ATF4 induction, which could promote IL-8 release. This needs to be further investigated by confirming ATF4 induction upon Torin1 treatment in the presence of glucose. Another suggestion is that possibly both mTOR complexes or at least mTORC2 have to be inactivated to promote IL-8 release in the presence of glucose.

In the absence of glucose, rapamycin as well as Torin1 reduced IL-8 release. Possibly, upon glucose deprivation some mTOR activity remains that is sufficient for IL-8 synthesis. However, using mTOR inhibitors, which block mTOR activity more effective, reduced IL-8 release.

LIF in contrary is not induced by none of the mTOR inhibitors in the presence of glucose, suggesting an mTOR-independent regulation of LIF. In the absence of glucose, LIF release was only minor and not significantly reduced by rapamycin treatment. Therefore, we assume that LIF is regulated independently of mTOR.

8.11 The role of p65 in cytokine release upon glucose deprivation

The function of the NF-κB pathway as major cytokine inducer has been studied in many systems (Liu et al., 2017). NF-κB is reported to be activated downstream of the UPR by the formation of an IRE1-TRAF2 complex, interacting with IKK and resulting in IκB phosphorylation and its subsequent degradation, which results in p65 translocation to the nucleus. Since we could not prove an IRE1 involvement in cytokine release upon glucose deprivation, this is probably not the case in our model. Another UPR-dependent activation of the NF-κB pathway is by phosphorylation of eIF2α, which results in global protein synthesis attenuation. This reduces IκB protein synthesis and could subsequently lead to p65 translocation to the nucleus and cytokine induction. (Schmitz et al., 2018; Zhang and Kaufman, 2008a). Other ways of inducing NF-κB could be mediated by EGFR signaling (Biswas et al., 2002; Jiang et al., 2011; Sun and Carpenter, 1998) which is described to be promoted by glucose deprivation (Graham et al., 2012) and is also associated with cytokine induction (Bald et al., 2014). Another possible way of activating NF-κB is through cell death receptors, including DR5 and DR4 (Yang et al., 2018) as well as though TNFR (Hayden and Ghosh, 2014). Regarding that we found that DR4 and DR5 were induced upon glucose deprivation (Iurlaro et al., 2017a) and therefore could participate in cytokine induction.

We found in HeLa and A549 cells that p65 is involved in the induction and release of IL-8 and IL-6 but not LIF (**Figure 41,42**). Moreover, we also confirmed the regulation of several other

cytokines by p65 upon glucose deprivation. This gives p65 an important role in glucose deprivation induced cytokine regulation.

Within this project we did not investigate how NF-κB signaling is induced upon glucose deprivation. However, NF-κB activation and cytokine release could be mediated by DR5, which is induced after 8 h upon glucose deprivation in A549 cells (Paula De Scheemaeker, Franziska Püschel, Master Thesis, 2017). This could synergistically promote cytokine release at late time points. We observed cytokine mRNA regulation of IL-8 and IL-6 at its highest after 3 h of glucose deprivation, which suggests that NF-kB is activated at short-times in a different manner. Either by the UPR, by EGFR or by toll like receptor (TLR) (Kawai and Akira, 2007) activation. Furthermore, the literature suggests that NF-κB, in cooperation with STAT3, induces IL-6 in starved cells (Yoon et al., 2012). Since it is reported that NF-kB is constitutively active in A549 cells (Zou et al., 2014), it would be possible that p65 is already bound to the cytokine promotor and gets activated by cofactor binding, by the dissociation of repressor proteins or by epigenetic changes upon glucose deprivation. This is supported by our finding that knockdown of p65 also reduced basally IL-8 release in the presence of glucose. Some reports claim LIF induction by NF-kB, however in our model we could not confirm this result concluding that LIF induction is p65-independent upon glucose deprivation in A549 cells.

In this project, we did not perform a more deepened analysis of NF-kB activation upon glucose deprivation, neither in a canonical nor a non-canonical manner. However, our results point out that p65 is to a big extend involved in cytokine induction upon glucose deprivation, however the detailed regulatory mechanism needs to be further investigated.

8.12 Functional analysis of conditioned media of starved A549 cells

We found that nutrient deprivation and metabolic drugs induced cytokines with known functions in immunity, including IL-8, IL-6 and LIF. Translating that into a tumor setting, we suggested that cytokine release upon low glucose or treatment with metabolic drugs, could favour immune cell infiltration. To determine which functions secreted cytokines from starved A549 cells convey, we collected supernatants of glucose-deprived cells and applied them to other A549 cells as well as immune cells and investigated cell death, cytokine secretion and migration.

8.12.1 Cytokine release and its impact on cell death

LIF has been associated with promoting apoptosis in mammary epithelial cells (Schere-Levy et al., 2003) and IL-8 is described to be anti-apoptotic in prostate and ovarian cancer cells (Singh

and Lokeshwar, 2009; Stronach et al., 2015; Wilson et al., 2008) as well as pro-apoptotic by upregulation of Bim in neurons (Thirumangalakudi et al., 2007).

We found that secreted proteins from starved A549 cells slightly increased cell death upon glucose deprivation (**Figure 44**). We also found that silencing of IL-8 but not LIF protected from cell death after 48 h of glucose deprivation.

IL-8 signals through binding to its receptor CXCR1 and CXCR2, which induces several downstream signaling pathways in several cancer cell lines including PI3K, Akt, EGFR and ERK signaling (Chan et al., 2017; Luppi et al., 2007; Waugh and Wilson, 2008). ERK was recently shown to promote glucose deprivation induced cell death (Shin et al., 2015). It would be possible that IL-8 promotes ERK activation through paracrine or autocrine effects. Knockdown of IL-8 also minorly reduced DR5 mRNA level, which we found to be involved in glucose deprivation induced cell death. However, treatment of A549 cells with recombinant IL-8 did not promote cell death induction. This suggests that cell death promoting effects of IL-8 depend on additional factors, which are present in the conditioned media of starved A549 cells. Furthermore, IL-8 signaling could be intracellular and receptor independent, rather than through extracellular receptor activation.

LIF is described to be pro-apoptotic, however in our model we could not confirm this finding. However, knockdown of LIF by siRNA was not very efficient and experiments should be further validated by the generation of LIF knockout cells.

In conclusion, more experiments have to be performed to elucidate how secreted cytokines affect cell death upon glucose deprivation by using cytokine specific neutralising antibodies or by the generation of cytokine and cytokine receptor deficient cells. Nevertheless, these finding are important and worthy to be followed up for the development of new anti-cancer strategies.

8.12.2 The role of LIF in cytokine release

LIF has been reported to induce inflammatory cytokines (MUSSO et al., 1995; Pascual-García et al., 2019; Villiger et al., 1993). We silenced LIF by using siRNA and observed a reduction of IL-8 mRNA expression and release. Using recombinant LIF, we confirmed the induction of IL-8 and slightly IL-6 release in the presence of glucose. The IL-8 release was even higher in the absence of glucose, and cotreatment with LIF, compared to glucose deprivation alone (**Figure 48**). We demonstrated before that IL-8 release upon glucose deprivation is mediated by ATF4 as well as partially by mTOR inactivation. In these cells we could not confirm that recombinant LIF induces ATF4 or inactivates mTOR by western blot (data not shown).

Discussion

Another possible signaling cascades promoting LIF mediated IL-8 release could be STAT3 signaling, which is described to be induced by LIF receptor binding in several cancers (Ohbayashi et al., 2007; Yue et al., 2016) Moreover, NF-κB activation, which was shown to promote IL-6 induction in monocytes (Gruss et al., 1992). Therefore, it has to be investigated if LIF mediates NF-κB activation in our system.

In conclusion, we found that LIF induced IL-8 release in the presence and absence of glucose, however the detailed mechanism remains to be investigated. Therefore, more studies have to be performed investigating intracellular signaling pathways induced by LIF upon glucose deprivation by using LIF deficient cells.

8.12.3 Conditioned media promotes the migration of cancer cells

Chemotaxis is an important feature of cancer cells to metastasize, including the migration and invasion from the primary tumor site to a distant site (Condeelis et al., 2005; McSherry et al., 2007). Metastasis is induced by changes in gene expression, resulting in loss of cell adhesion and matrix remodelling, which are only some mechanisms which promote to the mobilisation of the cell. Cell migration can be favoured by chemotactic factors including cytokines, chemokines or growth factors. Chemical gradients are sensed by the cell and induce several signaling cascades, which promote the migration towards a concentration gradient. Sources of chemotactic factors within the TME are cancer associated fibroblasts (CAFs) and immune cells (Condeelis and Pollard, 2006; Roussos et al., 2011). IL-8 is known to promote metastasis in pancreatic (Shi et al., 1999) and prostate cancer (Inoue et al., 2000) and LIF promotes migration in breast cancer cells (Li et al., 2014)

We found that A549 cells migrate towards the conditioned media of other A549 cells in the presence of glucose, which is independent of metabolites or exhaustion of the media (**Figure 47**). In the absence of glucose this effect was slightly diminished: however, re-addition of glucose reversed the lower migration. This suggests that secreted factors of cancer cells promote migration. However, conditioned media of starved A549 cells did not have a stronger effect on migration which is possibly due to the lack of glucose.

Recombinant IL-8 and LIF alone did not induce migration in these cells, suggesting that either other cytokines or the overall secreted cytokine 'cocktail' is responsible for migration. However, more studies have to be performed by generating IL-8 and LIF knock out cells or by applying neutralizing antibodies to clarify their involvement in the migration of A549 cells.

8.12.4 Conditioned media of cancer cells promotes the migration of immune cells

Neutrophils dominate the immune cell composition in NSCLC (Kargl, Nature Commun. 2017), which is facilitated by secreted chemokines. Moreover, several reports it is described that the induction of the UPR in tumor cells mediates immune infiltration (Obacz et al., 2019).

In our model we identified several released cytokines and chemokines upon glucose deprivation, which potentially could promote immune cell infiltration, including IL-8 and LIF. We therefore validated chemotactic responses of immune cells, isolated from human blood, towards conditioned media of starved A549 cells.

We could not find a major effect of the complete conditioned media of starved A549 cells on the migration of T cells, NKT cells or NK cells (**Figure 49**). This is possibly due to the 'metabolic competition' between cancer and immune cell described in several reports (Chang et al., 2015; Lyssiotis and Kimmelman, 2017). These reports indicate that cancer cells deplete their surrounding tissue of nutrients, which attenuates the activity of several immune cell population. Focusing on glucose, low level decrease anti-tumor T cell and NK cell functions (Ho et al., 2015). Moreover, some reports describe that secreted metabolites from cancer cells, such as lactate, impair T cell and NK cell activation and promote their evasion (Li et al., 2014; Renner et al., 2017). Regarding that, we found that the washed conditioned media, which is free of any secreted metabolites from the cell and only contains secreted proteins had the tendency to promote the migration of T, NKT and NK cells in the presence and absence of glucose. This suggests, that the exhausted media of cancer cells, containing among others metabolites, attenuates the migratory effects of T cells, NKT cells and NK cells towards the conditioned media of starved A549 cells.

In contrary, B cells migrated towards the conditioned media of starved A549 cells and this was amplified towards the washed conditioned media. It is described that B cells infiltrate the tumor to attenuate the anti-tumor immune response mediated by T-cells (Sarvaria et al., 2017). Glucose dependency varies between different stages of B cell differentiation due to metabolic reprogramming. For instance, increased glycolysis is associated with antibody production in plasma cells (Caro-Maldonado et al., 2014). Furthermore, B cells upregulate glycolytic pathways in hypoxic environments to meet their energetic needs (Jellusova et al., 2017). So far, the role of B cells in the tumor environment and their metabolic needs are insufficiently investigated. However, it is suggested that glucose deprivation of B cells favours differentiation with immunosuppressive outcomes (Singer et al., 2018).

Discussion

In our model, B cells seem to be more resistance towards glucose deprivation and therefore migrate towards the conditioned media of starved A549 cells. However, we did not analyse the differentiation status of the migrated B cells and therefore, we cannot predict a pro- or anti-tumorigenic role. Nevertheless, based on the literature it is quite likely that B cell migration towards the media of starved cancer cells to promote tumor progression.

As described before, neutrophils, together with macrophages, are the major immune cell representatives in many tumor types, promoting tumor progression and growth. Performance of chemotactic assays using primary neutrophils purified from human blood and THP-1 cells, which were differentiated towards macrophage-like cells using PMA, confirmed that these cells migrated preferentially towards the conditioned media of starved A549 cells (**Figure 51,52**). Further analysis revealed that migration was due to the secreted cytokines of starved A549 cells, and not due to the exhausted media. Neutrophils were first classified as glycolytic coupled to glucose dependency (Maianski et al., 2004). However, just recently it was reported that a subset of immature neutrophils uses mitochondrial fatty acid oxidation to circumvent low nutrients supply and to generate NADPH in order to maintain ROS secretion, which subsequently attenuates T cell function (Rice et al., 2018). Furthermore, hypoxia was shown to promote the anti-inflammatory effects of TAMs in tumors (LaGory and Giaccia, 2016). This suggests that neutrophils and macrophages are more resistance towards environments low in glucose, which allow them to maintain their cellular functions and migrate towards secreted chemokines from starved cancer cells.

Focusing on IL-8 and LIF as potential chemotactic factors, we observed a tendency of recombinant IL-8 and LIF for attracting THP-1 cells. However, more precise experiments have to be performed by knockout out IL-8 and/or LIF or by using neutralizing antibodies to validate the role of these cytokines in the migration of neutrophils and macrophage-like THP-1 cells.

9. Conclusion and future directions

Within this thesis it was demonstrated that nutrient deprivation as well as the application of anti-metabolic drugs mediated the release of pro-inflammatory cytokines from cancer cells. This finding is very important, since the application of anti-metabolic or anti-angiogenic drugs, could cause inflammatory responses in a tumor setting and worsen patient outcome. Regarding the composition of released cytokines upon glucose deprivation we suggest a cell type dependency, possibly depending on mutational load and metabolic phenotypes. However, the majority of identified cytokines in the tested cell lines were associated with tumor progression and poor patient outcome.

Moreover, we also suggest that this finding could be an evolutionary conserved response and non-cancerous body tissue could also promote the release of cytokines upon glucose deprivation. Physiological conditions in which nutrient limitation occurs in the body tissue include for instance trauma, vessel occlusion followed by stroke and other pathologies, which are associated with transient ischemia. Importantly, these scenarios are associated with inflammation that is up to date related to hypoxia or necrosis, promoting wound healing.

We demonstrated in this project, that nutrient deprivation alone causes cytokine release and the migration of immune cells, which could promote tumor progression as well as wound healing. Regarding the intracellular regulation we found that most of the tested cytokines, with focus on IL-8 and IL-6, are regulated in an UPR-dependent manner, mediated by ATF4. We also confirmed that p65, a transcription factor of the NF-κB pathway, is next to ATF4 the major inducer of the tested cytokines and could be either induced downstream of the UPR or in an independent manner. Within this project we did not demonstrate how glucose deprivation induced the NF-κB pathway. Due to its complexity, the exploration of NF-κB activation upon glucose deprivation is a follow-up project in the group.

Regarding LIF, we could not identify the detailed regulatory mechanism that caused its release upon glucose deprivation. Investigations including the UPR, NF-κB and mTOR pathway only show minor regulatory roles. This suggests that LIF induction is possibly independent of classically induced stress signaling pathways upon glucose deprivation and leads to the temporary conclusion that LIF is induced by glucose sensing mechanisms in a short response rather than by stress signaling pathway. This is supported by the finding that LIF has a major role in inducing cytokines such as IL-8 and IL-6 upon glucose deprivation. This finding is important, since targeting LIF alone could already be sufficient to suppress glucose deprivation induced cytokine release, which could be a new therapeutic target for anti-cancer therapies. Up

Conclusion and future directions

to date, the further investigation of LIF regulation upon glucose deprivation is another follow-up project in the lab.

In general, we conclude that not all cytokines are regulated in the same manner and depending on the cell and cytokine type more investigations have to be performed in order to make predictions for the release of specific cytokines. Moreover, within this project we did not investigate whether the overall impact of these cytokines is pro- or anti-tumorigenic and how this affects tumor progression or patient survival.

The most important finding is that cytokines, released upon glucose deprivation, promoted the migration of primary B cells and neutrophils as well as of macrophage-like THP-1 cells, which are associated with immune suppressive functions and poor patient survival. These finding were not translated in an animal model or in a clinical setting so far. However, it is highly recommended to perform *in vivo* studies, including a mouse model with an inducible knockout of glucose metabolism related genes to mimic glucose deprivation, independent of hypoxia. Moreover, the model should be syngeneic to monitor immune cell infiltration. This would give deeper insights whether cytokines released by glucose deprivation promote a pro- or anti-tumorigenic immune response and how this affects the overall survival of the patient. A schematic overview of the conclusion is presented in **Figure 56.**

A future clinical direction would be to treat patients with anti-metabolic or anti-angiogenic drugs in combination with neutralizing antibodies for specific cytokines, which could increase the efficiency of the anti-metabolic drugs in the clinic through the modulation of the immune response in the tumor.

To sum it up, these finding offer a completely new understanding of how inflammatory responses may be initiated in a tumor and this knowledge opens up new therapeutically targets and therapies for the cure of cancer.
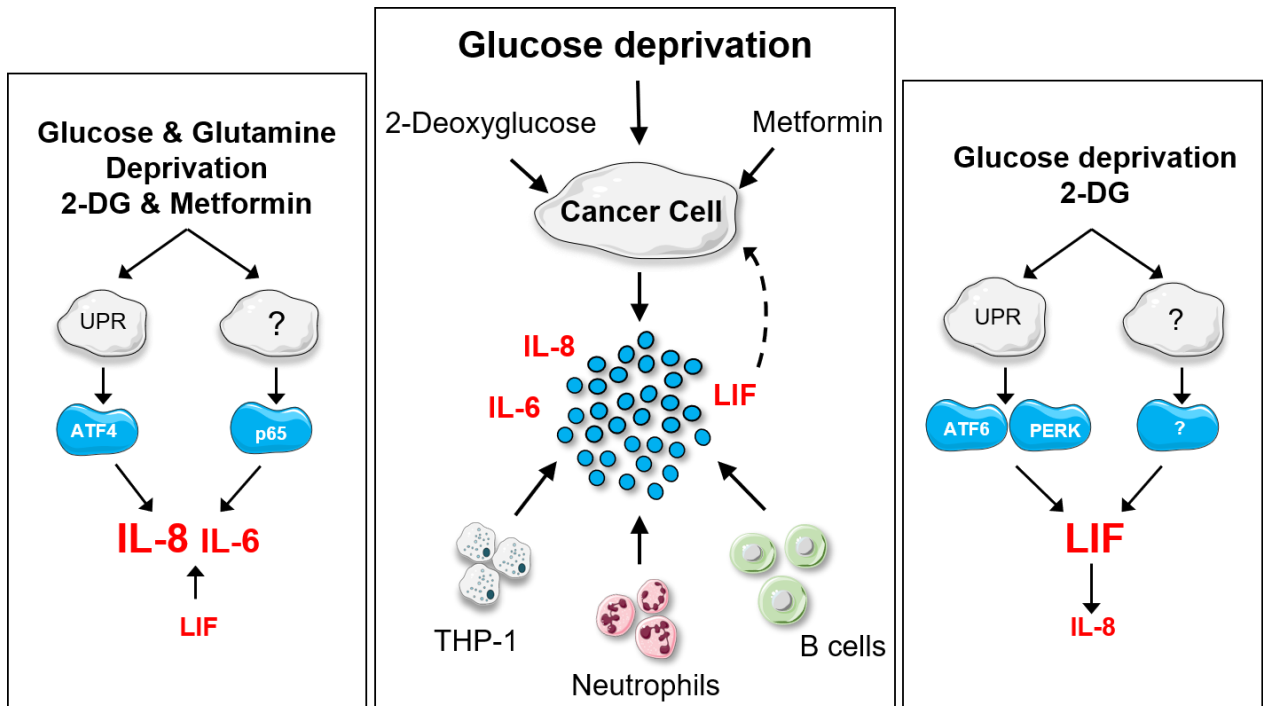
Figure 56 Schematic overview of the conclusion
Middle: We found that glucose deprivation and the application of anti-metabolic drugs promotes the release of inflammatory cytokines from cancer cells. Secreted factors promoted the attraction of macrophage-like THP-1 cells as well as of primary neutrophils and B cells purified from human blood. **Left**: Glucose and glutamine deprivation as well as 2-DG and metformin treatment promoted the release of IL-8 and IL-6 in several cancer cell lines. We found that ATF4, promoted IL-8 and IL-6 release. We also found that the major regulator of IL-8 and IL-6 release was p65. **Right**: Glucose deprivation and 2-DG treatment promoted LIF release from several cancer cell lines. We also found that LIF promoted the release of IL-8 in the presence and absence of glucose. ATF6 and PERK slightly regulated LIF release.

9. References

Albrengues, J., Bourget, I., Pons C., Butet, V., Hofman, P., Tartare-Deckert, S., Feral, C.C., Meneguzzi, G., and Gaggioli, C. (2014). LIF mediates proinvasive activation of stromal fibroblasts in cancer. Cell Rep.

Alfaro, C., Teijeira, A., O~ Nate, C., Erez, G.P., Sanmamed, M.F., Andueza, M.P., Alignani, D., Labiano, S., Azpilikueta, A., Rodriguez-Paulete, A., et al. (2016). Biology of Human Tumors Tumor-Produced Interleukin-8 Attracts Human Myeloid-Derived Suppressor Cells and Elicits Extrusion of Neutrophil Extracellular Traps (NETs). Clin Cancer Res 22.

Almanza, A., Carlesso, A., Chintha, C., Creedican, S., Doultsinos, D., Leuzzi, B., Luís, A., McCarthy, N., Montibeller, L., More, S., et al. (2019). Endoplasmic reticulum stress signalling - from basic mechanisms to clinical applications. FEBS J. 286, 241–278.

Almuhaideb, A., Papathanasiou, N., and Bomanji, J. (2011). 18F-FDG PET/CT imaging in oncology. Ann. Saudi Med.

Altman, B.J., Stine, Z.E., and Dang, C. V (2016). From Krebs to clinic: glutamine metabolism to cancer therapy. Nat. Rev. Cancer.

Amin-Wetzel, N., Saunders, R.A., Kamphuis, M.J., Rato, C., Preissler, S., Harding, H.P., and Ron, D. (2017). A J-Protein Co-chaperone Recruits BiP to Monomerize IRE1 and Repress the Unfolded Protein Response. Cell 171, 1625-1637.e13.

Aref, S., Ibrahim, L., Azmy, E., and Al Ashary, R. (2013). Impact of serum adiponectin and leptin levels in acute leukemia. Hematology.

ArnimJerryMcLaughlin, J.J.Z.S.A. (2011). Cellular Respiration. In Pediatric Critical Care (Fourth Edition), pp. 1058–1072.

Ashkenazi, A., Pai, R.C., Fong, S., Leung, S., Lawrence, D.A., Marsters, S.A., Blackie, C., Chang, L., McMurtrey, A.E., Hebert, A., et al. (1999). Safety and antitumor activity of recombinant soluble Apo2 ligand. J. Clin. Invest.

Atretkhany, K.-S.N., Drutskaya, M.S., Nedospasov, S.A., Grivennikov, S.I., and Kuprash, D. V (2016). Chemokines, cytokines and exosomes help tumors to shape inflammatory microenvironment. Pharmacol. Ther. 168, 98–112.

Badur, M.G., and Metallo, C.M. (2018). Reverse engineering the cancer metabolic network using flux analysis to understand drivers of human disease. Metab. Eng.

Baggiolini, M., Walz, A., and Kunkel, S.L. (1989). Neutrophil-activating peptide-1/interleukin 8, a novel cytokine that activates neutrophils. J. Clin. Invest.

Bald, T., Quast, T., Landsberg, J., Rogava, M., Glodde, N., Lopez-Ramos, D., Kohlmeyer, J., Riesenberg, S., Van Den Boorn-Konijnenberg, D., Hömig-Hölzel, C., et al. (2014). Ultraviolet-radiation-induced inflammation promotes angiotropism and metastasis in melanoma. Nature.

Balkwill, F., and Mantovani, A. (2001). Inflammation and cancer: back to Virchow? Lancet 357, 539–545.

Ballou, L.M., and Lin, R.Z. (2008). Rapamycin and mTOR kinase inhibitors. J. Chem. Biol.

Ben-Sahra, I., Hoxhaj, G., Ricoult, S.J.H., Asara, J.M., and Manning, B.D. (2016). mTORC1 induces purine synthesis through control of the mitochondrial tetrahydrofolate cycle. Science.

Biswas, D.K., Cruz, A.P., Gansberger, E., and Pardee, A.B. (2002). Epidermal growth factor-induced nuclear factor kappa B activation: A major pathway of cell-cycle progression in estrogen-receptor negative breast cancer cells. Proc. Natl. Acad. Sci.

Bollrath, J., Phesse, T.J., von Burstin, V.A., Putoczki, T., Bennecke, M., Bateman, T., Nebelsiek, T., Lundgren-May, T., Canli, Ö., Schwitalla, S., et al. (2009). gp130-Mediated Stat3 Activation in Enterocytes Regulates Cell Survival and Cell-Cycle Progression during Colitis-Associated Tumorigenesis. Cancer Cell.

Brand, A., Singer, K., Koehl, G.E., Kolitzus, M., Schoenhammer, G., Thiel, A., Matos, C., Bruss, C., Klobuch, S., Peter, K., et al. (2016). LDHA-Associated Lactic Acid Production Blunts Tumor Immunosurveillance by T and NK Cells. Cell Metab.

Bremnes, R.M., Busund, L.T., Kilver, T.L., Andersen, S., Richardsen, E., Paulsen, E.E., Hald, S., Khanehkenari, M.R., Cooper, W.A., Kao, S.C., et al. (2016). The role of tumor-infiltrating lymphocytes in development, progression, and prognosis of non-small cell lung cancer. J. Thorac. Oncol.

Busk, M., Walenta, S., Mueller-Klieser, W., Steiniche, T., Jakobsen, S., Horsman, M.R., and Overgaard, J. (2011). Inhibition of tumor lactate oxidation: Consequences for the tumor microenvironment. Radiother. Oncol.

Cairns, R., Harris, I., and Mak, T. (2011a). Regulation of cancer cell metabolism. Nat. Rev. Cancer 11, 85–95.

Carey, A.L., Steinberg, G.R., Macaulay, S.L., Thomas, W.G., Holmes, A.G., Ramm, G., Prelovsek, O., Hohnen-Behrens, C., Watt, M.J., James, D.E., et al. (2006). Interleukin-6 increases insulin-stimulated

References

glucose disposal in humans and glucose uptake and fatty acid oxidation in vitro via AMP-activated protein kinase. Diabetes.

Caro-Maldonado, A., and Muñoz-Pinedo, C. (2011). Dying for Something to Eat: How Cells Respond to Starvation. Open Cell Signal. J. *3*, 42–51.

Caro-Maldonado, A., Wang, R., Nichols, A.G., Kuraoka, M., Milasta, S., Sun, L.D., Gavin, A.L., Abel, E.D., Kelsoe, G., Green, D.R., et al. (2014). Metabolic Reprogramming Is Required for Antibody Production That Is Suppressed in Anergic but Exaggerated in Chronically BAFF-Exposed B Cells. J. Immunol.

Chan, L.-P., Liu, C., Chiang, F.-Y., Wang, L.-F., Lee, K.-W., Chen, W.-T., Kuo, P.-L., and Liang, C.-H. (2017). IL-8 promotes inflammatory mediators and stimulates activation of p38 MAPK/ERK-NF-κB pathway and reduction of JNK in HNSCC. Oncotarget.

Chang, C.H., Hsiao, C.F., Yeh, Y.M., Chang, G.C., Tsai, Y.H., Chen, Y.M., Huang, M.S., Chen, H.L., Li, Y.J., Yang, P.C., et al. (2013). Circulating interleukin-6 level is a prognostic marker for survival in advanced nonsmall cell lung cancer patients treated with chemotherapy. Int. J. Cancer.

Chang, C.H., Qiu, J., O'Sullivan, D., Buck, M.D., Noguchi, T., Curtis, J.D., Chen, Q., Gindin, M., Gubin, M.M., Van Der Windt, G.J.W., et al. (2015). Metabolic Competition in the Tumor Microenvironment Is a Driver of Cancer Progression. Cell *162*, 1229–1241.

Chaveroux, C., Sarcinelli, C., Barbet, V., Belfeki, S., Barthelaix, A., Ferraro-Peyret, C., Lebecque, S., Renno, T., Bruhat, A., Fafournoux, P., et al. (2016a). Nutrient shortage triggers the hexosamine biosynthetic pathway via the GCN2-ATF4 signalling pathway OPEN. Nat. Publ. Gr.

Cheah, M.T., Chen, J.Y., Sahoo, D., Contreras-Trujillo, H., Volkmer, A.K., Scheeren, F.A., Volkmer, J.-P., and Weissman, I.L. (2015). CD14-expressing cancer cells establish the inflammatory and proliferative tumor microenvironment in bladder cancer. Proc. Natl. Acad. Sci. *112*, 4725–4730.

Chen, G.G., and Lai, P.B.S. (2009). Apoptosis in carcinogenesis and chemotherapy: Apoptosis in cancer.

Chen, F., Zhuang, X., Lin, L., Yu, P., Wang, Y., Shi, Y., Hu, G., and Sun, Y. (2015). New horizons in tumor microenvironment biology: Challenges and opportunities. BMC Med.

Chen, L.H., Jiang, C.C., Kiejda, K.A., Wang, Y.F., Thorne, R.F., Zhang, X.D., and Hersey, P. (2007). Thapsigargin sensitizes human melanoma cells to TRAIL-induced apoptosis by up-regulation of

TRAIL-R2 through the unfolded protein response. Carcinogenesis.

Chen, R., Zou, Y., Mao, D., Sun, D., Gao, G., Shi, J., Liu, X., Zhu, C., Yang, M., Ye, W., et al. (2014). The general amino acid control pathway regulates mTOR and autophagy during serum/glutamine starvation. J. Cell Biol.

Chiaradonna, F., Ricciardiello, F., and Palorini, R. (2018). The Nutrient-Sensing Hexosamine Biosynthetic Pathway as the Hub of Cancer Metabolic Rewiring. Cells *7*.

Chockalingam, S., and Ghosh, S.S. (2014). Macrophage colony-stimulating factor and cancer: a review. Tumor Biol.

Cleland, W.W. (1964). Dithiothreitol, a New Protective Reagent for SH Groups. Biochemistry *3*, 480–482.

Clemens, M.J., and ELIA, A. (2009). The Double-Stranded RNA-Dependent Protein Kinase PKR: Structure and Function. J. Interf. Cytokine Res.

Coffelt, S.B., Wellenstein, M.D., and de Visser, K.E. (2016). Neutrophils in cancer: neutral no more. Nat. Publ. Gr. *16*.

Colegio, O.R., Chu, N.Q., Szabo, A.L., Chu, T., Rhebergen, A.M., Jairam, V., Cyrus, N., Brokowski, C.E., Eisenbarth, S.C., Phillips, G.M., et al. (2014). Functional polarization of tumour-associated macrophages by tumour-derived lactic acid. Nature.

Conciatori, F., Ciuffreda, L., Bazzichetto, C., Falcone, I., Pilotto, S., Bria, E., Cognetti, F., and Milella, M. (2018). MTOR cross-talk in cancer and potential for combination therapy. Cancers (Basel).

Condeelis, J., and Pollard, J.W. (2006). Macrophages: Obligate partners for tumor cell migration, invasion, and metastasis. Cell.

Condeelis, J., Singer, R.H., and Segall, J.E. (2005). THE GREAT ESCAPE: When Cancer Cells Hijack the Genes for Chemotaxis and Motility. Annu. Rev. Cell Dev. Biol.

Cubillos-Ruiz, J.R., Bettigole, S.E., and Glimcher, L.H. (2017). Leading Edge Tumorigenic and Immunosuppressive Effects of Endoplasmic Reticulum Stress in Cancer.

Cullinan, S.B., and Diehl, J.A. (2004). PERK-dependent Activation of Nrf2 Contributes to Redox Homeostasis and Cell Survival following Endoplasmic Reticulum Stress. J. Biol. Chem. *279*, 20108–20117.

Dankbar, B., Padró, T., Leo, R., Feldmann, B., Kropff, M., Mesters, R.M., Serve, H., Berdel, W.E., and Kienast, J. (2000). Vascular endothelial growth factor and interleukin-6 in paracrine tumor-stromal

cell interactions in multiple myeloma. Blood.

Deberardinis, R.J., Lum, J.J., Hatzivassiliou, G., and Thompson, C.B. (2008) Cell Metabolism The Biology of Cancer: Metabolic Reprogramming Fuels Cell Growth and Proliferation.

Dejeans, N., Pluquet, O., Lhomond, S., Grise, F., Bouchecareilh, M., Juin, A., Meynard-Cadars, M., Bidaud-Meynard, A., Gentil, C., Moreau, V., et al. (2012). Autocrine control of glioma cells adhesion and migration through IRE1 -mediated cleavage of SPARC mRNA. J. Cell Sci.

Donohoe, D.R., and Bultman, S.J. (2012). Metaboloepigenetics: interrelationships between energy metabolism and epigenetic control of gene expression. J. Cell. Physiol.

Drogat, B., Auguste, P., Nguyen, D.T., Bouchecareilh, M., Pineau, R., Nalbantoglu, J., Kaufman, R.J., Chevet, E., Bikfalvi, A., and Moenner, M. (2007). IRE1 signaling is essential for ischemia-induced vascular endothelial growth factor-A expression and contributes to angiogenesis and tumor growth in vivo. Cancer Res.

Earnshaw, W.C., Martins, L.M., and Kaufmann, S.H. (1999). Mammalian Caspases: Structure, Activation, Substrates, and Functions During Apoptosis. Annu. Rev. Biochem. 68, 383–424.

Elmore, S. (2007). Apoptosis: A Review of Programmed Cell Death. Toxicol. Pathol. 35, 495–516.

Elstrom, R.L., Bauer, D.E., Buzzai, M., Karnauskas, R., Harris, M.H., Plas, D.R., Zhuang, H., Cinalli, R.M., Alavi, A., Rudin, C.M., et al. (2004). Akt stimulates aerobic glycolysis in cancer cells. Cancer Res.

Fan, X., Liu, H., Liu, M., Wang, Y., Qiu, L., and Cui, Y. (2017). Increased utilization of fructose has a positive effect on the development of breast cancer. PeerJ.

Faubert, B., Li, K.Y., Cai, L., Hensley, C.T., Kim, J., Zacharias, L.G., Yang, C., Do, Q.N., Doucette, S., Burguete, D., et al. (2017). Lactate Metabolism in Human Lung Tumors. Cell 171, 358-371.e9.

Favaloro, B., Allocati, N., Graziano, V., Di Ilio, C., and De Laurenzi, V. (2012). Role of apoptosis in disease. Aging (Albany. NY). 4, 330–349.

Fischer, B., Müller, B., Fisch, P., and Kreutz, W. (2000). An acidic microenvironment inhibits antitumoral non-major histocompatibility complex-restricted cytotoxicity: Implications for cancer immunotherapy. J. Immunother.

Fischer, K., Hoffmann, P., Voelkl, S., Meidenbauer, N., Ammer, J., Edinger, M., Gottfried, E., Schwarz, S., Rothe, G., Hoves, S., et al. (2007). Inhibitory effect of tumor cell-derived lactic acid on human T cells. Blood.

Galluzzi, L., Vitale, I., Aaronson, S.A., Abrams, J.M., Adam, D., Agostinis, P., Alnemri, E.S., Altucci, L., Amelio, I., Andrews, D.W., et al. (2018). Molecular mechanisms of cell death: recommendations of the Nomenclature Committee on Cell Death 2018. Cell Death Differ.

Gameiro, P.A., and Struhl, K. (2018). Nutrient Deprivation Elicits a Transcriptional and Translational Inflammatory Response Coupled to Decreased Protein Synthesis. Cell Rep. 24, 1415–1424.

Garcia, N.A., Ontoria-Oviedo, I., González-King, H., Diez-Juan, A., and Sepúlveda, P. (2015). Glucose starvation in cardiomyocytes enhances exosome secretion and promotes angiogenesis in endothelial cells. PLoS One.

Gearing, D.P., Gough, N.M., King, J.A., Hilton, D.J., Nicola, N.A., Simpson, R.J., Nice, E.C., Kelso, A., and Metcalf, D. (1987). Molecular cloning and expression of cDNA encoding a murine myeloid leukaemia inhibitory factor (LIF). EMBO J.

Gentles, A.J., Newman, A.M., Liu, C.L., Bratman, S. V., Feng, W., Kim, D., Nair, V.S., Xu, Y., Khuong, A., Hoang, C.D., et al. (2015). The prognostic landscape of genes and infiltrating immune cells across human cancers. Nat. Med.

Germain, C., Gnjatic, S., Tamzalit, F., Knockaert, S., Remark, R., Goc, J., Lepelley, A., Becht, E., Katsahian, S., Bizouard, G., et al. (2014). Presence of B cells in tertiary lymphoid structures is associated with a protective immunity in patients with lung cancer. Am. J. Respir. Crit. Care Med.

Giammarioli, A.M., Gambardella, L., Barbati, C., Pietraforte, D., Tinari, A., Alberton, M., Gnessi, L., Griffin, R.J., Minetti, M., and Malorni, W. (2012). Differential effects of the glycolysis inhibitor 2-deoxy- D -glucose on the activity of pro-apoptotic agents in metastatic melanoma cells, and induction of a cytoprotective autophagic response. Int. J. Cancer.

Goodwin, J., Neugent, M.L., Lee, S.Y., Choe, J.H., Choi, H., Enkins, D.M.R.J., Ruthenborg, R.J., Robinson, M.W., Jeong, J.Y., Wake, M., et al. (2017). The distinct metabolic phenotype of lung squamous cell carcinoma defines selective vulnerability to glycolytic inhibition. Nat. Commun.

Gottlin, E.B., Bentley, R.C., Campa, M.J., Pisetsky, D.S., Herndon, J.E., and Patz, E.F. (2011). The association of intratumoral germinal centers with early-stage non-small cell lung cancer. J. Thorac. Oncol.

Graham, N.A., Tahmasian, M., Kohli, B.,

References

Komisopoulou, E., Zhu, M., Vivanco, I., Teitell, M.A., Wu, H., Ribas, A., Lo, R.S., et al. (2012). Glucose deprivation activates a metabolic and signaling amplification loop leading to cell death. Mol. Syst. Biol. *8*, 589.

Greenman, C., Stephens, P., Smith, R., Dalgliesh, G.L., Hunter, C., Bignell, G., Davies, H., Teague, J., Butler, A., Stevens, C., et al. (2007). Patterns of somatic mutation in human cancer genomes. Nature.

Grivennikov, S., Karin, E., Terzic, J., Mucida, D., Yu, G.Y., Vallabhapurapu, S., Scheller, J., Rose-John, S., Cheroutre, H., Eckmann, L., et al. (2009). IL-6 and Stat3 Are Required for Survival of Intestinal Epithelial Cells and Development of Colitis-Associated Cancer. Cancer Cell.

Grootjans, J., Kaser, A., Kaufman, R.J., and Blumberg, R.S. (2016). The unfolded protein response in immunity and inflammation. Nat. Rev. Immunol.

Gruss, H.-J., Brach, M.A., and Herrmann, F. (1992). Involvement of Nuclear Factor-KB in Induction of the Interleukin-6 Gene by Leukemia Inhibitory Factor.

Gui, S. liang, Teng, L. chen, Wang, S. qiu, Liu, S., Lin, Y.L., Zhao, X. lian, Liu, L., Sui, H. yu, Yang, Y., Liang, L. chun, et al. (2016). Overexpression of CXCL3 can enhance the oncogenic potential of prostate cancer. Int. Urol. Nephrol.

Gwinn, D.M., Shackelford, D.B., Egan, D.F., Mihaylova, M.M., Mery, A., Vasquez, D.S., Turk, B.E., and Shaw, R.J. (2008). AMPK Phosphorylation of Raptor Mediates a Metabolic Checkpoint. Mol. Cell.

Hammond, M.E., Lapointe, G.R., Feucht, P.H., Hilt, S., Gallegos, C.A., Gordon, C.A., Giedlin, M.A., Mullenbach, G., and Tekamp-Olson, P. (1995). IL-8 induces neutrophil chemotaxis predominantly via type I IL-8 receptors. J. Immunol.

Han, A.P., Yu, C., Lu, L., Fujiwara, Y., Browne, C., Chin, G., Fleming, M., Leboulch, P., Orkin, S.H., and Chen, J.J. (2001). Heme-regulated eIF2α kinase (HRI) is required for translational regulation and survival of erythroid precursors in iron deficiency. EMBO J.

Han, J., Back, S.H., Hur, J., Lin, Y.H., Gildersleeve, R., Shan, J., Yuan, C.L., Krokowski, D., Wang, S., Hatzoglou, M., et al. (2013). ER-stress-induced transcriptional regulation increases protein synthesis leading to cell death. Nat. Cell Biol.

Hanahan, D., and Weinberg, R.A. (2011a). Hallmarks of cancer: The next generation. Cell *144*, 646–674.

Hanahan, D., and Weinberg, R.A. (2011b). Hallmarks of cancer: the next generation. Cell.

Hardie, D.G. (2007). AMPK and SNF1: Snuffing Out Stress. Cell Metab.

Harding, H.P., Novoa, I., Zhang, Y., Zeng, H., Wek, R., Schapira, M., and Ron, D. (2000). Regulated Translation Initiation Controls Stress-Induced Gene Expression in Mammalian Cells. Mol. Cell *6*, 1099–1108.

Hattori, T., Ohoka, N., Hayashi, H., and Onozaki, K. (2003). C/EBP homologous protein (CHOP) up-regulates IL-6 transcription by trapping negative regulating NF-IL6 isoform. FEBS Lett.

Hay, N. (2016). Reprogramming glucose metabolism in cancer: Can it be exploited for cancer therapy? Nat. Rev. Cancer.

Hayden, M.S., and Ghosh, S. (2014). Regulation of NF-κB by TNF family cytokines. Semin. Immunol.

Hecht, S.S. (2002). Cigarette smoking and lung cancer: Chemical mechanisms and approaches to prevention. Lancet Oncol.

Heiden, M.G. Vander, Cantley, L.C., and Thompson, C.B. (2009). Understanding the warburg effect: The metabolic requirements of cell proliferation. Science (80-.).

Vander Heiden, M.G., and DeBerardinis, R.J. (2017). Understanding the Intersections between Metabolism and Cancer Biology. Cell.

Hemming, F.W. (1985). Glycosyl Phosphopolyprenols. In New Comprehensive Biochemistry, p.

Hieshima, K., Imai, T., Opdenakker, G., Van Damme, J., Kusuda, J., Tei, H., Sakaki, Y., Takatsuki, K., Miura, R., Yoshie, O., et al. (1997). Molecular cloning of a novel human CC chemokine liver and activation- regulated chemokine (LARC) expressed in liver. Chemotactic activity for lymphocytes and gene localization on chromosome 2. J. Biol. Chem.

Ho, P.-C., Bihuniak, J.D., Macintyre, A.N., Staron, M., Liu, X., Amezquita, R., Tsui, Y.-C., Cui, G., Micevic, G., Perales, J.C., et al. (2015). Phosphoenolpyruvate Is a Metabolic Checkpoint of Anti-tumor T Cell Responses. Cell *162*, 1217–1228.

Hollien, J., Lin, J.H., Li, H., Stevens, N., Walter, P., and Weissman, J.S. (2009). Regulated Ire1-dependent decay of messenger RNAs in mammalian cells. J. Cell Biol. *186*, 323–331.

Hsu, P.P., and Sabatini, D.M. (2008). Cancer cell metabolism: Warburg and beyond. Cell *134*, 703–707.

Hu, B., Fan, H., Lv, X., Chen, S., and Shao, Z.

(2018). Prognostic significance of CXCL5 expression in cancer patients: A meta-analysis. Cancer Cell Int.

Hunter, C.A., and Jones, S.A. (2015). IL-6 as a keystone cytokine in health and disease. Nat. Immunol.

Huynh, J., Chand, A., Gough, D., and Ernst, M. (2019). Therapeutically exploiting STAT3 activity in cancer — using tissue repair as a road map. Nat. Rev. Cancer.

Inoue, K., Slaton, J.W., Eve, B.Y., Kim, S.J., Perrotte, P., Balbay, M.D., Yano, S., Bar-Eli, M., Radinsky, R., Pettaway, C.A., et al. (2000). Interleukin 8 expression regulates tumorigenicity and metastases in androgen-independent prostate cancer. Clin. Cancer Res.

Iurlaro, R. (2015). Insights into the molecular mechanism of apoptosis induced by glucose deprivation. Doctoral Thesis, Universidat de Barcelona.

Iurlaro, R., and Munoz-Pinedo, C. (2016). Cell death induced by endoplasmic reticulum stress. FEBS J *283*, 2640–2652.

Iurlaro, R., Püschel, F., León-Annicchiarico, C.L., O'Connor, H., Martin, S.J., Palou-Gramón, D., Lucendo, E., and Muñoz-Pinedo, C. (2017a). Glucose Deprivation Induces ATF4-Mediated Apoptosis through TRAIL Death Receptors. Mol. Cell. Biol. *37*, e00479-16.

Iwasaki, Y., Suganami, T., Hachiya, R., Shirakawa, I., Kim-Saijo, M., Tanaka, M., Hamaguchi, M., Takai-Igarashi, T., Nakai, M., Miyamoto, Y., et al. (2014). Activating Transcription Factor 4 Links Metabolic Stress to Interleukin-6 Expression in Macrophages. Diabetes *63*, 152–161.

J.F.K Kerr*, Currie (1972). Apoptosis: A basic biological phenomenon with wide-ranging implications in tissue kinetics.APOPTOSIS: A BASIC BIOLOGICAL PHENO. J. Intern. Med. *258*, 479–517.

Jaime Redondo (2018). Metabolic stressors promote cytokine release in lung cancer cells. Master Thesis, Universitat Autonoma Barcelona

Janssens, K., Van den Haute, C., Baekelandt, V., Lucas, S., van Horssen, J., Somers, V., Van Wijmeersch, B., Stinissen, P., Hendriks, J.J.A., Slaets, H., et al. (2015). Leukemia inhibitory factor tips the immune balance towards regulatory T cells in multiple sclerosis. Brain. Behav. Immun.

Janssens, S., Pulendran, B., and Lambrecht, B.N. (2014). Emerging functions of the unfolded protein response in immunity. Nat. Immunol.

Jellusova, J., Cato, M.H., Apgar, J.R., Ramezani-

Rad, P., Leung, C.R., Chen, C., Richardson, A.D., Conner, E.M., Benschop, R.J., Woodgett, J.R., et al. (2017). Gsk3 is a metabolic checkpoint regulator in B cells. Nat. Immunol.

Jeon, S.M. (2016). Regulation and function of AMPK in physiology and diseases. Exp. Mol. Med.

Ji, H., Ramsey, M.R., Hayes, D.N., Fan, C., McNamara, K., Kozlowski, P., Torrice, C., Wu, M.C., Shimamura, T., Perera, S.A., et al. (2007). LKB1 modulates lung cancer differentiation and metastasis. Nature.

Jiang, T., Grabiner, B., Zhu, Y., Jiang, C., Li, H., You, Y., Lang, J., Hung, M.C., and Lin, X. (2011). CARMA3 is crucial for EGFR-induced activation of NF-κB and tumor progression. Cancer Res.

Johnson, D.E., O'Keefe, R.A., and Grandis, J.R. (2018). Targeting the IL-6/JAK/STAT3 signalling axis in cancer. Nat. Rev. Clin. Oncol. *15*, 234–248.

Kang, H.T., and Hwang, E.S. (2006). 2-Deoxyglucose: An anticancer and antiviral therapeutic, but not any more a low glucose mimetic. Life Sci.

Karczmar, G.S., Arbeit, J.M., Toy, B.J., Speder, A., and Weiner, M.W. (1992). Selective Depletion of Tumor ATP by 2-Deoxyglucose and Insulin, Detected by 31P Magnetic Resonance Spectroscopy. Cancer Res.

Kargl, J., Busch, S.E., Yang, G.H.Y., Kim, K.-H., Hanke, M.L., Metz, H.E., Hubbard, J.J., Lee, S.M., Madtes, D.K., McIntosh, M.W., et al. (2017). Neutrophils dominate the immune cell composition in non-small cell lung cancer. Nat. Commun. *8*, 14381.

Kasai, S., Yamazaki, H., Tanji, K., Engler, M.J., Matsumiya, T., and Itoh, K. (2018). Role of the ISR-ATF4 pathway and its cross talk with Nrf2 in mitochondrial quality control. J. Clin. Biochem. Nutr.

Kataki, A., Scheid, P., Piet, M., Marie, B., Martinet, N., Martinet, Y., and Vignaud, J.M. (2002). Tumor infiltrating lymphocytes and macrophages have a potential dual role in lung cancer by supporting both host-defense and tumor progression. J. Lab. Clin. Med.

Katira, A., H. Tan, P., Katira, A., and H. Tan, P. (2016). Evolving role of adiponectin in cancer-controversies and updateEvolving role of adiponectin in cancer-controversies and update. Cancer Biol. Med.

Kato, H., and Nishitoh, H. (2015). Stress responses from the endoplasmic reticulum in cancer. Front. Oncol. *5*, 93.

Kawada, K., Toda, K., and Sakai, Y. (2017).

References

Targeting metabolic reprogramming in KRAS-driven cancers. Int. J. Clin. Oncol.

Kawai, T., and Akira, S. (2007). Signaling to NF-κB by Toll-like receptors. Trends Mol. Med.

Kellokumpu-Lehtinen, P., Talpaz, M., Harris, D., Van, Q., Kurzrock, R., and Estrov, Z. (1996a). Leukemia-inhibitory factor stimulates breast, kidney and prostate cancer cell proliferation by paracrine and autocrine pathways. Int. J. Cancer.

Kellokumpu-Lehtinen, P., Talpaz, M., Harris, D., Van, Q., Kurzrock, R., and Estrov, Z. (1996b). Leukemia-inhibitory factor stimulates breast, kidney and prostate cancer cell proliferation by paracrine and autocrine pathways. Int. J. Cancer *66*, 515–519.

Kerr, E.M., Gaude, E., Turrell, F.K., Frezza, C., and Martins, C.P. (2016). Mutant Kras copy number defines metabolic reprogramming and therapeutic susceptibilities. Nature.

Kim, K.H., Jeong, Y.T., Kim, S.H., Jung, H.S., Park, K.S., Lee, H.-Y., and Lee, M.-S. (2013). Metformin-induced inhibition of the mitochondrial respiratory chain increases FGF21 expression via ATF4 activation. Biochem. Biophys. Res. Commun. *440*, 76–81.

Kim, M.-H., Kim, A., Yu, J.H., Lim, J.W., and Kim, H. (2014). Glutamine deprivation induces interleukin-8 expression in ataxia telangiectasia fibroblasts. Inflamm. Res. *63*, 347–356.

Kim, S.-H., Turnbull, J., and Guimond, S. (2011). Extracellular matrix and cell signalling: the dynamic cooperation of integrin, proteoglycan and growth factor receptor. J. Endocrinol.

Kim, Y.H., Nakayama, T., and Nayak, J. (2018). Glycolysis and the Hexosamine Biosynthetic Pathway as Novel Targets for Upper and Lower Airway Inflammation. Allergy. Asthma Immunol. Res. *10*, 6–11.

Kishimoto, T. (2003). Factors Affecting B-Cell Growth and Differentiation. Annu. Rev. Immunol.

Kumari, N., Dwarakanath, B.S., Das, A., and Bhatt, A.N. (2016). Role of interleukin-6 in cancer progression and therapeutic resistance. Tumor Biol.

L.J., B., G.L., B., N., J., C.E., C., A.D., R., and B.Z., S. (2012). Tumor-Derived Granulocyte-Macrophage Colony-Stimulating Factor Regulates Myeloid Inflammation and T Cell Immunity in Pancreatic Cancer. Cancer Cell.

LaGory, E.L., and Giaccia, A.J. (2016). The ever-expanding role of HIF in tumour and stromal biology. Nat. Cell Biol.

Landskron, G., De La Fuente, M., Thuwajit, P., Thuwajit, C., and Hermoso, M.A. (2014). Chronic inflammation and cytokines in the tumor microenvironment. J. Immunol. Res.

Laurence Cole, P.R.K. (2016). Sugars, Fatty Acids, and Energy Biochemistry. In Human Physiology, Biochemistry and Basic Medicine, pp. 17–30.

Lee, A.S. Glucose regulated proteins in cancer: molecular mechanisms and therapeutic potential.

Lee, S., and Margolin, K. (2011). Cytokines in cancer immunotherapy. Cancers (Basel).

Lee, H.Y., Itahana, Y., Schuechner, S., Fukuda, M., Je, H.S., Ogris, E., Virshup, D.M., and Itahana, K. (2018). Ca2+-dependent demethylation of phosphatase PP2Ac promotes glucose deprivation-induced cell death independently of inhibiting glycolysis. Sci. Signal. *11*, eaam7893.

León-Annicchiarico, C.L., Ramírez-Peinado, S., Domínguez-Villanueva, D., Gonsberg, A., Lampidis, T.J.T.J.J., Muñoz-Pinedo, C., Leon-Annicchiarico, C.L., Ramirez-Peinado, S., Dominguez-Villanueva, D., Gonsberg, A., et al. (2015a). ATF4 mediates necrosis induced by glucose deprivation and apoptosis induced by 2-deoxyglucose in the same cells. FEBS J. *282*, 3647–3658.

León-Annicchiarico, C.L., Ramírez-Peinado, S., Domínguez-Villanueva, D., Gonsberg, A., Lampidis, T.J., and Muñoz-Pinedo, C. (2015b). ATF4 mediates necrosis induced by glucose deprivation and apoptosis induced by 2-deoxyglucose in the same cells. FEBS J. *282*, 3647–3658.

Levine, A.J., and Puzio-Kuter, A.M. (2010). The control of the metabolic switch in cancers by oncogenes and tumor suppressor genes. Science (80-.).

Levy, A., and Doyen, J. (2018). Metformin for non-small cell lung cancer patients: Opportunities and pitfalls. Crit. Rev. Oncol. Hematol.

Lhomond, S., Avril, T., Dejeans, N., Voutetakis, K., Doultsinos, D., McMahon, M., Pineau, R., Obacz, J., Papadodima, O., Jouan, F., et al. (2018). Dual IRE1 RNase functions dictate glioblastoma development. EMBO Mol. Med. e7929.

Li, X., Yang, Q., Yu, H., Wu, L., Zhao, Y., Zhang, C., Yue, X., Liu, Z., Wu, H., Haffty, B.G., et al. (2014). LIF promotes tumorigenesis and metastasis of breast cancer through the AKT-mTOR pathway. Oncotarget.

Li, X., Wang, S., Zhu, R., Li, H., Han, Q., and Zhao, R.C. (2016). Lung tumor exosomes induce a pro-inflammatory phenotype in mesenchymal stem cells via NFκB-TLR signaling pathway. J. Hematol. Oncol.

Libby, G., Donnelly, L.A., Donnan, P.T., Alessi, D.R., Morris, A.D., and Evans, J.M.M. (2009). New users of metformin are at low risk of incident cancer: A cohort study among people with type 2 diabetes. Diabetes Care.

Lin, S.-C., and Grahame Hardie, D. (2018). AMPK: Sensing Glucose as well as Cellular Energy Status.

Lin, S.C., and Hardie, D.G. (2018). AMPK: Sensing Glucose as well as Cellular Energy Status. Cell Metab.

Lin, B., Podar, K., Gupta, D., Tai, Y.T., Li, S., Weller, E., Hideshima, T., Lentzsch, S., Davies, F., Li, C., et al. (2002). The vascular endothelial growth factor receptor tyrosine kinase inhibitor PTK787/ZK222584 inhibits growth and migration of multiple myeloma cells in the bone marrow microenvironment. Cancer Res.

Liu, E.S., Ou, J.H., and Lee, A.S. (1992). Brefeldin A as a regulator of grp78 gene expression in mammalian cells. J. Biol. Chem. *267*, 7128–7133.

Liu, H., Jiang, C.C., Lavis, C.J., Croft, A., Dong, L., Tseng, H.Y., Yang, F., Tay, K.H., Hersey, P., and Zhang, X.D. (2009). 2-Deoxy-D-glucose enhances TRAIL-induced apoptosis in human melanoma cells through XBP-1-mediated up-regulation of TRAIL-R2. Mol. Cancer.

Liu, T., Zhang, L., Joo, D., and Sun, S.-C. (2017). NF-κB signaling in inflammation. Signal Transduct. Target. Ther.

Logue, S.E., McGrath, E.P., Cleary, P., Greene, S., Mnich, K., Almanza, A., Chevet, E., Dwyer, R.M., Oommen, A., Legembre, P., et al. (2018). Inhibition of IRE1 RNase activity modulates the tumor cell secretome and enhances response to chemotherapy. Nat. Commun. *9*, 3267.

Lohr, M., Edlund, K., Botling, J., Hammad, S., Hellwig, B., Othman, A., Berglund, A., Lambe, M., Holmberg, L., Ekman, S., et al. (2013). The prognostic relevance of tumour-infiltrating plasma cells and immunoglobulin kappa C indicates an important role of the humoral immune response in non-small cell lung cancer. Cancer Lett.

Lu, M., Lawrence, D.A., Marsters, S., Acosta-Alvear, D., Kimmig, P., Mendez, A.S., Paton, A.W., Paton, J.C., Walter, P., and Ashkenazi, A. (2014). Opposing unfolded-protein-response signals converge on death receptor 5 to control apoptosis. Science (80-.). *345*, 98–101.

Luo, J., Solimini, N.L., and Elledge, S.J. (2009). Principles of Cancer Therapy: Oncogene and Non-oncogene Addiction. Cell.

Luppi, F., Longo, A.M., De Boer, W.I., Rabe, K.F., and Hiemstra, P.S. (2007). Interleukin-8 stimulates

cell proliferation in non-small cell lung cancer through epidermal growth factor receptor transactivation. Lung Cancer *56*, 25–33.

Lyssiotis, C.A., and Kimmelman, A.C. (2017). Metabolic Interactions in the Tumor Microenvironment. Trends Cell Biol. *27*, 863–875.

M.D., T., B., N., T., H., and D.J., P. (2014). Cytokines and chemokines: At the crossroads of cell signalling and inflammatory disease. Biochim. Biophys. Acta - Mol. Cell Res.

Macis, D., Guerrieri-Gonzaga, A., and Gandini, S. (2014). Circulating adiponectin and breast cancer risk: A systematic review and meta-analysis. Int. J. Epidemiol.

Maianski, N.A., Geissler, J., Srinivasula, S.M., Alnemri, E.S., Roos, D., and Kuijpers, T.W. (2004). Functional characterization of mitochondria in neutrophils: A role restricted to apoptosis. Cell Death Differ.

Malabanan, K.P., Kanellakis, P., Bobik, A., and Khachigian, L.M. (2008). Activation Transcription Factor-4 Induced by Fibroblast Growth Factor-2 Regulates Vascular Endothelial Growth Factor-A Transcription in Vascular Smooth Muscle Cells and Mediates Intimal Thickening in Rat Arteries Following Balloon Injury. Circ. Res. *103*, 378–387.

Marcus, A., Gowen, B.G., Thompson, T.W., Iannello, A., Ardolino, M., Deng, W., Wang, L., Shifrin, N., and Raulet, D.H. (2014). Recognition of tumors by the innate immune system and natural killer cells. Adv. Immunol.

Marshall, E.A., Ng, K.W., Kung, S.H.Y., Conway, E.M., Martinez, V.D., Halvorsen, E.C., Rowbotham, D.A., Vucic, E.A., Plumb, A.W., Becker-Santos, D.D., et al. (2016). Emerging roles of T helper 17 and regulatory T cells in lung cancer progression and metastasis. Mol. Cancer.

Martín-Pérez, R., Niwa, M., and López-Rivas, A. (2012). ER stress sensitizes cells to TRAIL through down-regulation of FLIP and Mcl-1 and PERK-dependent up-regulation of TRAIL-R2. Apoptosis.

Massagué, J., Hogg, N., Kim, J., Morris, P.G., Oskarsson, T., Acharyya, S., Seshan, V.E., Manova-Todorova, K., Vanharanta, S., Norton, L., et al. (2012). A CXCL1 Paracrine Network Links Cancer Chemoresistance and Metastasis. Cell.

Mazor, K.M., and Stipanuk, M.H. (2016). GCN2- and eIF2α-phosphorylation-independent, but ATF4-dependent, induction of CARE-containing genes in methionine-deficient cells. Amino Acids.

McLean, K., Tan, L., Bolland, D.E., Coffman, L.G., Peterson, L.F., Talpaz, M., Neamati, N., and Buckanovich, R.J. (2018). Leukemia inhibitory

References

factor functions in parallel with interleukin-6 to promote ovarian cancer growth. Oncogene *38*, 1576–1584.

McSherry, E.A., Donatello, S., Hopkins, A.M., and McDonnell, S. (2007). Molecular basis of invasion in breast cancer. Cell. Mol. Life Sci.

Menegon, S., Columbano, A., and Giordano, S. (2016). The Dual Roles of NRF2 in Cancer. Trends Mol. Med.

Metcalfe, S.M. (2011). LIF in the regulation of T-cell fate and as a potential therapeutic. Genes Immun.

Metchnikoff, I. (2015). Mini- review: Macrophage Polarization. Biorad.

Meylan, E., Dooley, A.L., Feldser, D.M., Shen, L., Turk, E., Ouyang, C., and Jacks, T. (2009). Requirement for NF-B signalling in a mouse model of lung adenocarcinoma. Nature.

El Mjiyad, N., Caro-Maldonado, A., Ramírez-Peinado, S., and Muñoz-Pinedo, C. (2011). Sugar-free approaches to cancer cell killing. Oncogene *30*, 253–264.

Mogilenko, D.A., Haas, J.T., L'homme, L., Fleury, S., Quemener, S., Levavasseur, M., Becquart, C., Wartelle, J., Bogomolova, A., Pineau, L., et al. (2019). Metabolic and Innate Immune Cues Merge into a Specific Inflammatory Response via the UPR. Cell.

Mónica Pascual-García, Ester Bonfill-Teixidor, Ester Planas-Rigol, Carlota Rubio-Perez, Raffaella Iurlaro, Alexandra Arias, Isabel Cuartas, Ada Sala-Hojman, Laura Escudero, Francisco Martínez-Ricarte, Isabel Huber-Ruano, Paolo Nuciforo, Leire Pedrosa, Car, J.T.& J.S. (2019). LIF regulates CXCL9 in tumor-associated macrophages and prevents CD8+ T cell tumor-infiltration impairing anti-PD1 therapy. Nat. Commun. *10*.

Motz, G.T., and Coukos, G. (2011). The parallel lives of angiogenesis and immunosuppression: Cancer and other tales. Nat. Rev. Immunol.

Muñoz-Pinedo, C., Ruiz-Ruiz, C., De Almodóvar, C.R., Palacios, C., and López-Rivas, A. (2003). Inhibition of glucose metabolism sensitizes tumor cells to death receptor-triggered apoptosis through enhancement of death-inducing signaling complex formation and apical procaspase-8 processing. J. Biol. Chem.

Muñoz-Pinedo, C., El Mjiyad, N., and Ricci, J.-E. (2012). Cancer metabolism: current perspectives and future directions. Cell Death Dis. *3*, e248–e248.

Murdoch, C., Muthana, M., Coffelt, S.B., and Lewis, C.E. (2008). The role of myeloid cells in the promotion of tumour angiogenesis. Nat. Rev. Cancer.

MUSSO, T., BADOLATO, R., Longo, D.L., Gusella, G.L., and VARESIO, L. (1995). Leukemia Inhibitory Factor Induces Interleukin-8 and Monocyte Chemotactic and Activating Factor in Human Monocytes - Differential Regulation By Interferon-Gamma. Blood *86*, 1961–1967.

Myers, A.L., Lin, L., Nancarrow, D.J., Wang, Z., Ferrer-Torres, D., Thomas, D.G., Orringer, M.B., Lin, J., Reddy, R.M., Beer, D.G., et al. (2015). IGFBP2 modulates the chemoresistant phenotype in esophageal adenocarcinoma. Oncotarget.

Ngo, H., Tortorella, S.M., Ververis, K., and Karagiannis, T.C. (2015). The Warburg effect: molecular aspects and therapeutic possibilities. Mol. Biol. Rep. *42*, 825–834.

Nguyen, D.T., Kebache, S., Fazel, A., Wong, H.N., Jenna, S., Emadali, A., Lee, E.H., Bergeron, J.J., Kaufman, R.J., Larose, L., et al. (2004). Nck-dependent activation of extracellular signal-regulated kinase-1 and regulation of cell survival during endoplasmic reticulum stress. Mol Biol Cell *15*, 4248–4260.

Noy, R., and Pollard, J.W. (2014). Tumor-Associated Macrophages: From Mechanisms to Therapy. Immunity.

O'Neill, H.M., Brandt, N., Schjerling, P., Vernet, E., Kleinert, M., Richter, E.A., Steinberg, G.R., and Jørgensen, S.B. (2015). Leukemia inhibitory factor increases glucose uptake in mouse skeletal muscle. Am. J. Physiol. Metab. *309*, E142–E153.

O'Sullivan, D., Sanin, D.E., Pearce, E.J., and Pearce, E.L. (2019). Metabolic interventions in the immune response to cancer. Nat. Rev. Immunol.

Oakes, S.A. (2017). Endoplasmic reticulum proteostasis: a key checkpoint in cancer. Am. J. Physiol. - Cell Physiol. *312*, C93–C102.

Obacz, J., Archambeau, J., Le Reste, P.J., Pineau, R., Jouan, F., Barroso, K., Fainsod-Levi, T., Obiedat, A., Granot, Z., Tirosh, B., et al. IRE1-UBE2D3 signaling controls the recruitment of myeloid cells to glioblastoma. *7*.

ODEGAARD, A., FLORHOLMEN, G., EID, H., RUSTAN, A., STRAUMANN, N., ANDERSSON, K., CHRISTENSEN, G., DISHINGTON, H., LUNDE, P., and AAS, V. (2005). Leukemia inhibitory factor reduces contractile function and induces alterations in energy metabolism in isolated cardiomyocytes. J. Mol. Cell. Cardiol. *37*, 1183–1193.

Ohbayashi, N., Ikeda, O., Taira, N., Yamamoto, Y., Muromoto, R., Sekine, Y., Sugiyama, K., Honjoh, T., and Matsuda, T. (2007). LIF- and IL-6-Induced

Acetylation of STAT3 at Lys-685 through PI3K/Akt Activation. Biol. Pharm. Bull.

Orimo, A., Gupta, P.B., Sgroi, D.C., Arenzana-Seisdedos, F., Delaunay, T., Naeem, R., Carey, V.J., Richardson, A.L., and Weinberg, R.A. (2005). Stromal fibroblasts present in invasive human breast carcinomas promote tumor growth and angiogenesis through elevated SDF-1/CXCL12 secretion. Cell.

Owen, M.R., Doran, E., and Halestrap, A.P. (2000). Evidence that metformin exerts its anti-diabetic effects through inhibition of complex 1 of the mitochondrial respiratory chain. Biochem. J.

Pakos-Zebrucka, K., Koryga, I., Mnich, K., Ljujic, M., Samali, A., and Gorman, A.M. (2016). The integrated stress response. EMBO Rep. *17*.

Palorini, R., Cammarata, F.P., Balestrieri, C., Monestiroli, A., Vasso, M., Gelfi, C., Alberghina, L., and Chiaradonna, F. (2013). Glucose starvation induces cell death in K-ras-transformed cells by interfering with the hexosamine biosynthesis pathway and activating the unfolded protein response. Cell Death Dis. *4*, e732–e732.

Pan, G., O'Rourke, K., Chinnaiyan, A.M., Gentz, R., Ebner, R., Ni, J., and Dixit, V.M. (1997). The receptor for the cytotoxic ligand TRAIL. Science (80-.).

Panieri, E., and Santoro, M.M. (2016). ROS homeostasis and metabolism: a dangerous liason in cancer cells. Cell Death Dis.

Panneerselvam, K., and Freeze, H.H. (1996). Mannose corrects altered N-glycosylation in carbohydrate-deficient glycoprotein syndrome fibroblasts. J. Clin. Invest.

Pascual-García, M., Bonfill-Teixidor, E., Planas-Rigol, E., Rubio-Perez, C., Iurlaro, R., Arias, A., Cuartas, I., Sala-Hojman, A., Escudero, L., Martínez-Ricarte, F., et al. (2019). LIF regulates CXCL9 in tumor-associated macrophages and prevents CD8 + T cell tumor-infiltration impairing anti-PD1 therapy. Nat. Commun.

Paule De Scheemaeker, Franziska Püschel, C.M.-P. (2017). Apoptosis: the main glucose deprivation induced cell death modality in A549 cell line. University Pompeu Fabara.

Peñuelas, S., Anido, J., Prieto-Sánchez, R.M., Folch, G., Barba, I., Cuartas, I., García-Dorado, D., Poca, M.A., Sahuquillo, J., Baselga, J., et al. (2009). TGF-β Increases Glioma-Initiating Cell Self-Renewal through the Induction of LIF in Human Glioblastoma. Cancer Cell.

Porporato, P.E., Filigheddu, N., Pedro, J.M.B.S., Kroemer, G., and Galluzzi, L. (2018). Mitochondrial metabolism and cancer. Cell Res.

Püschel, F., and Muñoz-Pinedo, C. (2019). Measuring the Activation of Cell Death Pathways upon Inhibition of Metabolism. (Humana Press, New York, NY), pp. 163–172.

Puthalakath, H., O'Reilly, L.A., Gunn, P., Lee, L., Kelly, P.N., Huntington, N.D., Hughes, P.D., Michalak, E.M., McKimm-Breschkin, J., Motoyama, N., et al. (2007). ER Stress Triggers Apoptosis by Activating BH3-Only Protein Bim. Cell.

Pylayeva-Gupta, Y., Grabocka, E., and Bar-Sagi, D. (2011). RAS oncogenes: Weaving a tumorigenic web. Nat. Rev. Cancer.

Qian, B.-Z., and Pollard, J.W. (2010). Macrophage diversity enhances tumor progression and metastasis. Cell.

Quentin, T., Steinmetz, M., Poppe, A., and Thoms, S. (2012). Metformin differentially activates ER stress signaling pathways without inducing apoptosis. Dis. Model. Mech.

Raghuwanshi, S.K., Su, Y., Singh, V., Haynes, K., Richmond, A., and Richardson, R.M. (2012). The Chemokine Receptors CXCR1 and CXCR2 Couple to Distinct G Protein-Coupled Receptor Kinases To Mediate and Regulate Leukocyte Functions. J. Immunol.

Rajalingam, K., Schreck, R., Rapp, U.R., and Albert, Š. (2007). Ras oncogenes and their downstream targets. Biochim. Biophys. Acta - Mol. Cell Res.

Ralser, M., Wamelink, M.M., Struys, E.A., Joppich, C., Krobitsch, S., Jakobs, C., and Lehrach, H. (2008). A catabolic block does not sufficiently explain how 2-deoxy-D-glucose inhibits cell growth. Proc. Natl. Acad. Sci.

Ramírez-Peinado, S., Alcázar-Limones, F., Lagares-Tena, L., El Mjiyad, N., Caro-Maldonado, A., Tirado, O.M.O.M., and Muñoz-Pinedo, C. (2011). 2-deoxyglucose induces Noxa-dependent apoptosis in alveolar rhabdomyosarcoma. Cancer Res *71*, 6796–6806.

Ramos-Ibeas, P., Barandalla, M., Colleoni, S., and Lazzari, G. (2017). Pyruvate antioxidant roles in human fibroblasts and embryonic stem cells. Mol. Cell. Biochem. *429*, 137–150.

Räsänen, K., and Vaheri, A. (2010). Activation of fibroblasts in cancer stroma. Exp. Cell Res.

Rena, G., Hardie, D.G., and Pearson, E.R. (2017). The mechanisms of action of metformin. Diabetologia.

Renner, K., Singer, K., Koehl, G.E., Geissler, E.K., Peter, K., Siska, P.J., and Kreutz, M. (2017). Metabolic Hallmarks of Tumor and Immune Cells in the Tumor Microenvironment. Front. Immunol. *8*,

References

248.

Reznik, E., Luna, A., Aksoy, B.A., Liu, E.M., La, K., Ostrovnaya, I., Creighton, C.J., Hakimi, A.A., and Sander, C. (2018). A Landscape of Metabolic Variation across Tumor Types. Cell Syst.

Rice, C.M., Davies, L.C., Subleski, J.J., Maio, N., Gonzalez-Cotto, M., Andrews, C., Patel, N.L., Palmieri, E.M., Weiss, J.M., Lee, J.-M., et al. (2018). Tumour-elicited neutrophils engage mitochondrial metabolism to circumvent nutrient limitations and maintain immune suppression. Nat. Commun.

Robey, R.B., and Hay, N. (2009). Is Akt the "Warburg kinase"?-Akt-energy metabolism interactions and oncogenesis. Semin. Cancer Biol.

Rojas-Rivera, D., Delvaeye, T., Roelandt, R., Nerinckx, W., Augustyns, K., Vandenabeele, P., and Bertrand, M.J. (2017). When PERK inhibitors turn out to be new potent RIPK1 inhibitors: critical issues on the specificity and use of GSK2606414 and GSK2656157. Nat. Publ. Gr.

Roussos, E.T., Condeelis, J.S., and Patsialou, A. (2011). Chemotaxis in cancer. Nat. Rev. Cancer.

Rubio-Patiño, C., Bossowski, J.P., De Donatis, G.M., Mondragón, L., Villa, E., Aira, L.E., Chiche, J., Mhaidly, R., Lebeaupin, C., Marchetti, S., et al. (2018). Low-Protein Diet Induces IRE1α-Dependent Anticancer Immunosurveillance. Cell Metab. *27*, 828-842.e7.

Ruffell, B., and Coussens, L.M. (2015). Macrophages and therapeutic resistance in cancer. Cancer Cell.

Salt, I.P., Johnson, G., Ashcroft, S.J., and Hardie, D.G. (1998). AMP-activated protein kinase is activated by low glucose in cell lines derived from pancreatic beta cells, and may regulate insulin release. Biochem. J.

Samaniego, R., Gutiérrez-González, A., Gutiérrez-Seijo, A., Sánchez-Gregorio, S., García-Giménez, J., Mercader, E., Márquez-Rodas, I., Avilés, J.A., Relloso, M., and Sánchez-Mateos, P. (2018). CCL20 Expression by Tumor-Associated Macrophages Predicts Progression of Human Primary Cutaneous Melanoma. Cancer Immunol. Res.

Sanmamed, M.F., Perez-Gracia, J.L., Schalper, K.A., Fusco, J.P., Gonzalez, A., Rodriguez-Ruiz, M.E., Oñate, C., Perez, G., Alfaro, C., Martín-Algarra, S., et al. (2017). Changes in serum interleukin-8 (IL-8) levels reflect and predict response to anti-PD-1 treatment in melanoma and non-small-cell lung cancer patients. Ann. Oncol.

Satake, S., Kuzuya, M., Miura, H., Asai, T., Ramos, M.A., Muraguchi, M., Ohmoto, Y., and Iguchi, A. (1998). Up-regulation of vascular endothelial growth factor in response to glucose deprivation. Biol. Cell.

Sawant, K. V., Poluri, K.M., Dutta, A.K., Sepuru, K.M., Troshkina, A., Garofalo, R.P., and Rajarathnam, K. (2016). Chemokine CXCL1 mediated neutrophil recruitment: Role of glycosaminoglycan interactions. Sci. Rep.

Schere-Levy, C., Buggiano, V., Quaglino, A., Gattelli, A., Cirio, M.C., Piazzon, I., Vanzulli, S., and Kordon, E.C. (2003). Leukemia inhibitory factor induces apoptosis of the mammary epithelial cells and participates in mouse mammary gland involution. Exp. Cell Res.

Schmitz, M., Shaban, M., Albert, B., Gökçen, A., and Kracht, M. (2018). The Crosstalk of Endoplasmic Reticulum (ER) Stress Pathways with NF-κB: Complex Mechanisms Relevant for Cancer, Inflammation and Infection. Biomedicines.

Shanware, N.P., Bray, K., Eng, C.H., Wang, F., Follettie, M., Myers, J., Fantin, V.R., and Abraham, R.T. (2014). Glutamine deprivation stimulates mTOR-JNK-dependent chemokine secretion. Nat Commun *5*, 4900.

Shi, Q., Abbruzzese, J.L., Huang, S., Fidler, I.J., Xiong, Q., and Xie, K. (1999). Constitutive and inducible interleukin 8 expression by hypoxia and acidosis renders human pancreatic cancer cells more tumorigenic and metastatic. Clin. Cancer Res.

Shibata, R., Sato, K., Pimentel, D.R., Takemura, Y., Kihara, S., Ohashi, K., Funahashi, T., Ouchi, N., and Walsh, K. (2005). Adiponectin protects against myocardial ischemia-reperfusion injury through AMPK- and COX-2-dependent mechanisms. Nat. Med.

Shin, S., Buel, G.R., Wolgamott, L., Plas, D.R., Asara, J.M., Blenis, J., and Yoon, S.O. (2015). ERK2 Mediates Metabolic Stress Response to Regulate Cell Fate. Mol. Cell.

Sidrauski, C., and Walter, P. (1997). The transmembrane kinase Ire1p is a site-specific endonuclease that initiates mRNA splicing in the unfolded protein response. Cell *90*, 1031–1039.

Sidrauski, C., Acosta-Alvear, D., Khoutorsky, A., Vedantham, P., Hearn, B.R., Li, H., Gamache, K., Gallagher, C.M., Ang, K.K.-H., Wilson, C., et al. (2013). Pharmacological brake-release of mRNA translation enhances cognitive memory. Elife.

Simons, A.L., Mattson, D.M., Dornfeld, K.J., and Spitz, D.R. (2009). Glucose deprivation-induced metabolic oxidative stress and cancer therapy. J. Cancer Res. Ther.

Singer, K., Cheng, W.-C., Kreutz, M., Ho, P.-C., and Siska, P.J. (2018). Immunometabolism in cancer at a glance. Dis. Model. Mech.

Singh, R.K., and Lokeshwar, B.L. (2009). Depletion of intrinsic expression of Interleukin-8 in prostate cancer cells causes cell cycle arrest, spontaneous apoptosis and increases the efficacy of chemotherapeutic drugs. Mol. Cancer.

Stockmann, C., Doedens, A., Weidemann, A., Zhang, N., Takeda, N., Greenberg, J.I., Cheresh, D.A., and Johnson, R.S. (2008). Deletion of vascular endothelial growth factor in myeloid cells accelerates tumorigenesis. Nature.

Stone, T.W., McPherson, M., and Gail Darlington, L. (2018). Obesity and Cancer: Existing and New Hypotheses for a Causal Connection. EBioMedicine.

Stronach, E.A., Cunnea, P., Turner, C., Guney, T., Aiyappa, R., Jeyapalan, S., de Sousa, C.H., Browne, A., Magdy, N., Studd, J.B., et al. (2015). The role of interleukin-8 (IL-8) and IL-8 receptors in platinum response in high grade serous ovarian carcinoma. Oncotarget.

Sullivan, L.B., Gui, D.Y., and Van Der Heiden, M.G. (2016). Altered metabolite levels in cancer: Implications for tumour biology and cancer therapy. Nat. Rev. Cancer.

Sun, L., and Carpenter, G. (1998). Epidermal growth factor activation of NF-κB is mediated through IκBα degradation and intracellular free calcium. Oncogene.

Sun, O.H., and Lee, G.M. (2008). Nutrient deprivation induces autophagy as well as apoptosis in Chinese hamster ovary cell culture. Biotechnol. Bioeng.

Sunaga, N., Imai, H., Shimizu, K., Shames, D.S., Kakegawa, S., Girard, L., Sato, M., Kaira, K., Ishizuka, T., Gazdar, A.F., et al. (2012). Oncogenic KRAS-induced interleukin-8 overexpression promotes cell growth and migration and contributes to aggressive phenotypes of non-small cell lung cancer. Int. J. Cancer 130, 1733–1744.

Taga, T., and Kishimoto, T. (1997). <scp>gp</scp> 130 AND THE INTERLEUKIN-6 FAMILY OF CYTOKINES. Annu. Rev. Immunol.

Tan, P.H., Tyrrell, H.E.J., Gao, L., Xu, D., Quan, J., Gill, D., Rai, L., Ding, Y., Plant, G., Chen, Y., et al. (2014). Adiponectin receptor signaling on dendritic cells blunts antitumor immunity. Cancer Res.

Tanaka, T., Narazaki, M., and Kishimoto, T. (2014). Il-6 in inflammation, Immunity, And disease. Cold Spring Harb. Perspect. Biol.

Templeton, A.J., McNamara, M.G., Šeruga, B., Vera-Badillo, F.E., Aneja, P., Ocaña, A., Leibowitz-Amit, R., Sonpavde, G., Knox, J.J., Tran, B., et al. (2014). Prognostic role of neutrophil-to-lymphocyte ratio in solid tumors: A systematic review and meta-analysis. J. Natl. Cancer Inst.

Tenkerian, C., Krishnamoorthy, J., Mounir, Z., Kazimierczak, U., Khoutorsky, A., Staschke, K.A., Kristof, A.S., Wang, S., Hatzoglou, M., and Koromilas, A.E. (2015). mTORC2 Balances AKT Activation and eIF2 Serine 51 Phosphorylation to Promote Survival under Stress. Mol. Cancer Res. 13, 1377–1388.

Terashima, J., Tachikawa, C., Kudo, K., Habano, W., and Ozawa, S. (2013). An aryl hydrocarbon receptor induces VEGF expression through ATF4 under glucose deprivation in HepG2. BMC Mol. Biol.

Thirumangalakudi, L., Yin, L., Rao, H.V., and Grammas, P. (2007). IL-8 induces expression of matrix metalloproteinases, cell cycle and pro-apoptotic proteins, and cell death in cultured neurons. J. Alzheimer's Dis.

Thoreen, C.C., Kang, S.A., Chang, J.W., Liu, Q., Zhang, J., Gao, Y., Reichling, L.J., Sim, T., Sabatini, D.M., and Gray, N.S. (2009). An ATP-competitive mammalian target of rapamycin inhibitor reveals rapamycin-resistant functions of mTORC1. J. Biol. Chem.

Tokunaga, C., Yoshino, K.I., and Yonezawa, K. (2004). mTOR integrates amino acid- and energy-sensing pathways. In Biochemical and Biophysical Research Communications, p.

Tsou, P., Katayama, H., Ostrin, E.J., and Hanash, S.M. (2016). The emerging role of b cells in tumor immunity. Cancer Res.

Tsuru, A., Imai, Y., Saito, M., and Kohno, K. (2016). Novel mechanism of enhancing IRE1α-XBP1 signalling via the PERK-ATF4 pathway.

Tung, J.-N., Lin, P.-L., Wang, Y.-C., Wu, D.-W., Chen, C.-Y., and Lee, H. (2018). PD-L1 confers resistance to EGFR mutation-independent tyrosine kinase inhibitors in non-small cell lung cancer via upregulation of YAP1 expression. Oncotarget.

Urano, F. (2000). Coupling of Stress in the ER to Activation of JNK Protein Kinases by Transmembrane Protein Kinase IRE1. Science (80-.). 287, 664–666.

Vasconcelos-dos-Santos, A., Oliveira, I.A., Lucena, M.C., Mantuano, N.R., Whelan, S.A., Dias, W.B., and Todeschini, A.R. (2015). Biosynthetic Machinery Involved in Aberrant Glycosylation: Promising Targets for Developing of Drugs Against Cancer. Front. Oncol.

Vaupel, P., Schmidberger, H., and Mayer, A. (2019). The Warburg effect: essential part of metabolic reprogramming and central contributor to cancer progression. Int. J. Radiat. Biol.

References

Vazquez de Aldana, C.R., Wek, R.C., Segundo, P.S., Truesdell, A.G., and Hinnebusch, A.G. (2015). Multicopy tRNA genes functionally suppress mutations in yeast eIF-2 alpha kinase GCN2: evidence for separate pathways coupling GCN4 expression to unchanged tRNA. Mol. Cell. Biol.

Villiger, P.M., Geng, Y., Lotz Sam, M., and Stein, R. (1993). Induction of Cytokine Expression by Leukemia Inhibitory Factor. Clin. Invest 91, 1575–1581.

De Visser, K.E., Korets, L. V., and Coussens, L.M. (2005). De novo carcinogenesis promoted by chronic inflammation is B lymphocyte dependent. Cancer Cell.

Wang, S., and El-Deiry, W.S. (2003). TRAIL and apoptosis induction by TNF-family death receptors. Oncogene.

Wang, S.-S., Liu, W., Ly, D., Xu, H., Qu, L., and Zhang, L. (2018). Tumor-infiltrating B cells: their role and application in anti-tumor immunity in lung cancer. Cell. Mol. Immunol.

Wang, X., Perez, E., Liu, R., Yan, L.-J., Mallet, R.T., and Yang, S.-H. (2007). Pyruvate protects mitochondria from oxidative stress in human neuroblastoma SK-N-SH cells. Brain Res. 1132, 1–9.

Wang, Y., Alam, G.N., Ning, Y., Visioli, F., Dong, Z., Nör, J.E., and Polverini, P.J. The Unfolded Protein Response Induces the Angiogenic Switch in Human Tumor Cells through the PERK/ATF4 Pathway.

Wang, Y., Alam, G.N.N., Ning, Y., Visioli, F., Dong, Z., Nor, J.E., Polverini, P.J.J., Nör, J.E., and Polverini, P.J.J. (2012). The unfolded protein response induces the angiogenic switch in human tumor cells through the PERK/ATF4 pathway. Cancer Res 72, 5396–5406.

Warburg, O. (1956). On the origin of cancer cells. Science (80-.).

Warburg, O., Wind, F., and Negelein, E. (1927). THE METABOLISM OF TUMORS IN THE BODY. J. Gen. Physiol.

Waugh, D.J.J., and Wilson, C. (2008). The interleukin-8 pathway in cancer. Clin. Cancer Res.

Weichhart, T., Hengstschläger, M., and Linke, M. (2015). Regulation of innate immune cell function by mTOR. Nat. Rev. Immunol. 15, 599–614.

Wellen, K.E., Hatzivassiliou, G., Sachdeva, U.M., Bui, T. V., Cross, J.R., and Thompson, C.B. (2009). ATP-citrate lyase links cellular metabolism to histone acetylation. Science (80-.).

Wellenstein, M.D., and De Visser, K.E. (2018). Cancer-Cell-Intrinsic Mechanisms Shaping the Tumor Immune Landscape. Immunity 48, 399–416.

WICK, A.N., DRURY, D.R., NAKADA, H.I., and WOLFE, J.B. (1957). Localization of the primary metabolic block produced by 2-deoxyglucose. J. Biol. Chem.

Wilson, C., Wilson, T., Johnston, P.G., Longley, D.B., and Waugh, D.J.J. (2008). Interleukin-8 signaling attenuates TRAIL- and chemotherapy-induced apoptosis through transcriptional regulation of c-FLIP in prostate cancer cells. Mol. Cancer Ther.

Wolf, J., Rose-John, S., and Garbers, C. (2014). Interleukin-6 and its receptors: a highly regulated and dynamic system. Cytokine.

Won, H., Moreira, D., Gao, C., Duttagupta, P., Zhao, X., Manuel, E., Diamond, D., Yuan, Y.-C., Liu, Z., Jones, J., et al. (2017). TLR9 expression and secretion of LIF by prostate cancer cells stimulates accumulation and activity of polymorphonuclear MDSCs. J. Leukoc. Biol.

Wu, T., and Dai, Y. (2017). Tumor microenvironment and therapeutic response. Cancer Lett.

Wunderlich, F.T., Ströhle, P., Könner, A.C., Gruber, S., Tovar, S., Brönneke, H.S., Juntti-Berggren, L., Li, L.S., Van Rooijen, N., Libert, C., et al. (2010). Interleukin-6 signaling in liver-parenchymal cells suppresses hepatic inflammation and improves systemic insulin action. Cell Metab.

Xu, X.T., Xu, Q., Tong, J.L., Zhu, M.M., Huang, M.L., Ran, Z.H., and Xiao, S.D. (2011). Meta-analysis: Circulating adiponectin levels and risk of colorectal cancer and adenoma. J. Dig. Dis.

Yamaguchi, H., and Wang, H.-G. (2004). CHOP Is Involved in Endoplasmic Reticulum Stress-induced Apoptosis by Enhancing DR5 Expression in Human Carcinoma Cells*.

Yanagitani, K., Imagawa, Y., Iwawaki, T., Hosoda, A., Saito, M., Kimata, Y., and Kohno, K. (2009). Cotranslational Targeting of XBP1 Protein to the Membrane Promotes Cytoplasmic Splicing of Its Own mRNA. Mol. Cell 34, 191–200.

Yang, J., LeBlanc, F.R., Dighe, S.A., Hamele, C.E., Olson, T.L., Feith, D.J., and Loughran, T.P. (2018). TRAIL mediates and sustains constitutive NF-kB activation in LGL leukemia. Blood.

Yaniv, B., Sadraei, N.H., Palackdharry, S., Takiar, V., and Wise-Draper, T. (2018). Metformin Induces Pro-Tumorigenic Cytokines And Natural Killer Cells In Patients With Locally Advanced Head and Neck Squamous Cell Carcinoma. Int. J. Radiat. Oncol. 100, 1369.

Ye, J., Kumanova, M., Hart, L.S., Sloane, K., Zhang,

H., De Panis, D.N., Bobrovnikova-Marjon, E., Diehl, J.A., Ron, D., and Koumenis, C. (2010). The GCN2-ATF4 pathway is critical for tumour cell survival and proliferation in response to nutrient deprivation. EMBO J.

Yoon, S., Woo, S.U., Kang, J.H., Kim, K., Shin, H.J., Gwak, H.S., Park, S., and Chwae, Y.J. (2012). NF-κB and STAT3 cooperatively induce IL6 in starved cancer cells. Oncogene *31*, 3467–3481.

Yoshida, H., Matsui, T., Yamamoto, A., Okada, T., and Mori, K. (2001). XBP1 mRNA is induced by ATF6 and spliced by IRE1 in response to ER stress to produce a highly active transcription factor. Cell *107*, 881–891.

Yoshimura, T. (2018). The chemokine MCP-1 (CCL2) in the host interaction with cancer: A foe or ally? Cell. Mol. Immunol.

Yuan, A., Yang, P.C., Yu, C.J., Chen, W.J., Lin, F.Y., Kuo, S.H., and Luh, K.T. (2000). Interleukin-8 messenger ribonucleic acid expression correlates with tumor progression, tumor angiogenesis, patient survival, and timing of relapse in non-small-cell lung cancer. Am. J. Respir. Crit. Care Med.

Yue, X., Zhao, Y., Zhang, C., Li, J., Liu, Z., Liu, J., and Hu, W. (2016). Leukemia inhibitory factor promotes EMT through STAT3-dependent miR-21 induction. Oncotarget.

Zeeshan, H., Lee, G., Kim, H.-R., and Chae, H.-J. (2016a). Endoplasmic Reticulum Stress and Associated ROS. Int. J. Mol. Sci. *17*, 327.

Zeeshan, H., Lee, G., Kim, H.-R., Chae, H.-J., Zeeshan, H.M.A., Lee, G.H., Kim, H.-R., and Chae, H.-J. (2016b). Endoplasmic Reticulum Stress and Associated ROS. Int. J. Mol. Sci. *17*, 327.

Zeng, H., Qu, J., Jin, N., Xu, J., Lin, C., Chen, Y., Yang, X., He, X., Tang, S., Lan, X., et al. (2016). Feedback Activation of Leukemia Inhibitory Factor Receptor Limits Response to Histone Deacetylase Inhibitors in Breast Cancer. Cancer Cell.

Zhang, K., and Kaufman, R.J. (2008a). From endoplasmic-reticulum stress to the inflammatory response. Nature.

Zhang, K., and Kaufman, R.J. (2008b). From endoplasmic-reticulum stress to the inflammatory response. Nature *454*, 455–462.

Zhang, C., Bai, N., Chang, A., Zhang, Z., Yin, J., Shen, W., Tian, Y., Xiang, R., and Liu, C. (2013a). ATF4 is directly recruited by TLR4 signaling and positively regulates TLR4-trigged cytokine production in human monocytes. Cell. Mol. Immunol. *10*, 84–94.

Zhang, C., Bai, N., Chang, A., Zhang, Z., Yin, J.,

Shen, W., Tian, Y., Xiang, R., and Liu, C. (2013b). ATF4 is directly recruited by TLR4 signaling and positively regulates TLR4-trigged cytokine production in human monocytes. Cell. Mol. Immunol. *10*, 84–94.

Zhang, C.S., Hawley, S.A., Zong, Y., Li, M., Wang, Z., Gray, A., Ma, T., Cui, J., Feng, J.W., Zhu, M., et al. (2017a). Fructose-1,6-bisphosphate and aldolase mediate glucose sensing by AMPK. Nature.

Zhang, J., Lu, Y., and Pienta, K.J. (2010). Multiple roles of chemokine (C-C Motif) ligand 2 in promoting prostate cancer growth. J. Natl. Cancer Inst.

Zhang, X., Wang, Y., Cao, Y., Zhang, X., and Zhao, H. (2017b). Increased CCL19 expression is associated with progression in cervical cancer. Oncotarget.

Zhang, Y., Gallastegui, N., and Rosenblatt, J.D. (2015). Regulatory B cells in anti-tumor immunity. Int. Immunol.

Zhang , Pavicic PG Jr, Datta S, Song Q, Xu X, Wei W, Su F, Rayman PA, Z.C.H.T. (2019). Unfolded Protein Response Differentially Regulates TLR4-Induced Cytokine Expression in Distinct Macrophage Populations. Front. Immunol.

Zhou, G., Myers, R., Li, Y., Chen, Y., Shen, X., Fenyk-Melody, J., Wu, M., Ventre, J., Doebber, T., Fujii, N., et al. (2001). Role of AMP-activated protein kinase in mechanism of metformin action. J. Clin. Invest.

Zhou, P.-T., Li, B., Liu, F.-R., Zhang, M.-C., Wang, Q., Li, Y.-Y., Xu, C., Liu, Y.-H., Yao, Y., and Li, D. (2017). Metformin is associated with survival benefit in pancreatic cancer patients with diabetes: a systematic review and meta-analysis. Oncotarget.

Zhu, H., Yun, F., Shi, X., and Wang, D. (2015). Inhibition of IGFBP-2 improves the sensitivity of bladder cancer cells to cisplatin via upregulating the expression of maspin. Int. J. Mol. Med.

Zhu, S., Liu, H., Sha, H., Qi, L., Gao, D.-S., and Zhang, W. (2017). PERK and XBP1 differentially regulate CXCL10 and CCL2 production HHS Public Access. Exp Eye Res *155*, 1–14.

Zinszner, H., Kuroda, M., Wang, X., Batchvarova, N., Lightfoot, R.T., Remotti, H., Stevens, J.L., and Ron, D. (1998). CHOP is implicated in programmed cell death in response to impaired function of the endoplasmic reticulum. Genes Dev. *12*, 982–995.

Zou, Z., Huang, B., Wu, X., Zhang, H., Qi, J., Bradner, J., Nair, S., and Chen, L.F. (2014). Brd4 maintains constitutively active NF-κB in cancer cells by binding to acetylated RelA. Oncogene.

10. Appendix

Glucose Deprivation Induces ATF4-Mediated Apoptosis through TRAIL Death Receptors

Raffaella Iurlaro,[a] Franziska Püschel,[a] Clara Lucía León-Annicchiarico,[a]
Hazel O'Connor,[b] Seamus J. Martin,[b] Daniel Palou-Gramón,[a] Estefanía Lucendo,[a]
Cristina Muñoz-Pinedo[a]

Cell Death Regulation Group, Molecular Mechanisms and Experimental Therapy in Oncology Program, Bellvitge Biomedical Research Institute (IDIBELL), L'Hospitalet de Llobregat, Barcelona, Spain[a]; Molecular Cell Biology Laboratory, Department of Genetics, The Smurfit Institute, Trinity College, Dublin, Ireland[b]

ABSTRACT Metabolic stress occurs frequently in tumors and in normal tissues undergoing transient ischemia. Nutrient deprivation triggers, among many potential cell death-inducing pathways, an endoplasmic reticulum (ER) stress response with the induction of the integrated stress response transcription factor ATF4. However, how this results in cell death remains unknown. Here we show that glucose deprivation triggered ER stress and induced the unfolded protein response transcription factors ATF4 and CHOP. This was associated with the nontranscriptional accumulation of TRAIL receptor 1 (TRAIL-R1) (DR4) and with the ATF4-mediated, CHOP-independent induction of TRAIL-R2 (DR5), suggesting that cell death in this context may involve death receptor signaling. Consistent with this, the ablation of TRAIL-R1, TRAIL-R2, FADD, Bid, and caspase-8 attenuated cell death, although the downregulation of TRAIL did not, suggesting ligand-independent activation of TRAIL receptors. These data indicate that stress triggered by glucose deprivation promotes the ATF4-dependent upregulation of TRAIL-R2/DR5 and TRAIL receptor-mediated cell death.

KEYWORDS apoptosis, ATF4, cancer metabolism, glucose, TRAIL

Glucose is an essential nutrient for mammalian cells. In particular, cancer cells display glucose avidity and are more sensitive to cell death by starvation than nontransformed cells. This predisposition to cell death has been associated with the hyperactivation of oncogenes and the inactivation of tumor suppressors, most of which regulate glucose uptake and utilization (1–3).

Cell death induced by glucose deprivation is thought to occur in the nutrient-deprived necrotic core and is the desirable outcome of novel anticancer therapies that target glucose metabolism (4). However, the cell death pathways engaged by glucose deprivation remain unclear. Some reports indicate that glucose deprivation leads to energy stress or endoplasmic reticulum (ER) stress that can cause necrosis of mouse embryonic fibroblasts or rhabdomyosarcoma (5, 6). In other cell types, particularly hematopoietic tumor cells, glucose deprivation leads to mitochondrial apoptosis, which is mediated by Bcl-2 family proteins (7–9). In cells that are incapable of undergoing apoptosis through the mitochondrial pathway, such as Bax-Bak-deficient mouse embryonic fibroblasts (MEFs), glucose deprivation stimulates caspase-8-mediated apoptosis instead (10).

The signaling pathways that promote cell death in response to starvation are a subject of debate. It was thought that the loss of ATP and mTOR inactivation were the cause of cell death induced by starvation. However, it was recently shown that cell death caused by the loss of specific nutrients is a highly regulated process that depends on active signaling pathways. In response to glutamine depletion or the inhibition of

glutaminolysis, the transcription factor ATF4 is induced by a mechanism involving its selective translation, and it leads to the induction of proapoptotic Bcl-2 family proteins (11). This transcription factor is part of the integrated stress response (ISR) engaged in the response to viral infection or amino acid depletion and of the unfolded protein response (UPR) activated in response to ER stress. In response to glucose deprivation or inhibition of glucose metabolism with 2-deoxyglucose, ATF4 has also been shown to be induced, and it regulates the mitochondrial apoptotic pathway (12, 13). Here we show that ATF4 is required for apoptosis induced by glucose deprivation in cells in which caspase-8 is the apoptosis-initiating caspase. Glucose deprivation induces the TRAIL receptors DR4 and DR5. TRAIL receptor 2 (TRAIL-R2)/DR5 is regulated by ATF4 in this context, and both receptors mediate cell death, with TRAIL receptor 2 being quantitatively more important.

RESULTS

Glucose deprivation induces apoptosis and endoplasmic reticulum stress in human tumor cells. Human tumor cell lines have been shown to die either by necrosis or by apoptosis upon glucose deprivation. We show here that in HeLa cells, glucose withdrawal resulted in poly(ADP-ribose) polymerase (PARP) and caspase-3 cleavage after 48 and 72 h of treatment that was prevented by cotreatment with the caspase inhibitor Q-VD (Fig. 1A), indicating that cell death is apoptosis. Moreover, HeLa cells were protected by cotreatment with the pancaspase inhibitors Q-VD and Z-VAD but not with Y-VAD, an inhibitor of caspase-1, indicating that cell death is due to apoptotic and not inflammatory caspases (Fig. 1B). To test whether these cells died through mitochondrial apoptosis, we subjected HeLa cells overexpressing Bcl-xL (14) to glucose deprivation and observed that they also died in a caspase-dependent manner, although they were partially protected, and thus, the kinetics were slower (Fig. 1C and D). These cells were completely protected from tumor necrosis factor (TNF), which kills HeLa cells in a mitochondrion-dependent manner. Additionally, we subjected HCT116 cells and their Bax-Bak-deficient counterparts to glucose deprivation and observed that they died with different kinetics, but in both cases, they were significantly protected by cotreatment with Q-VD (Fig. 1E to G). In all cell lines, a necrotic component was observed at later time points. Since HeLa cells do not express RIPK3 (15), this component is probably not necroptotic. However, we employed inhibitors of RIPK1 and RIPK3 in HCT116 cells and their Bax-Bak-deficient counterparts and observed that these inhibitors do not confer protection from cell death when incubated in the presence or absence of the caspase inhibitor Q-VD (Fig. 1F and G). Similarly, HeLa cells were not protected by using necrostatin-1 (Fig. 1H). Indeed, this compound was slightly toxic at high concentrations and longer times, possibly as an inhibitor of the tryptophan-catabolizing enzyme IDO (indoleamine-pyrrole 2,3-dioxygenase) (Fig. 1F to H) (16). All these data suggested that glucose deprivation activates apoptosis partially independently of the mitochondrial apoptotic pathway, together with nonnecroptotic necrosis.

We and others have shown that the transcription factor ATF4 plays a role in cell death induced by the deprivation of glucose or glutamine (6, 11, 17) or by treatment with the nonmetabolizable glucose analog 2-deoxyglucose (12). ATF4 is central to the integrated stress response and the unfolded protein response induced, among other stimuli, upon ER stress. Glucose is required to provide glycosylation precursors, and its absence disturbs the ER and Golgi apparatus (18). Additionally, glucose deprivation may cause a secondary loss of amino acids, which is known to activate the ISR, which is mediated by the uncharged tRNA-activated kinase GCN2. As shown in Fig. 2A and B, glucose deprivation induces ATF4, its downstream effector CHOP, and ER stress, as measured by the induction of the chaperone GRP78/Bip and splicing of the mRNA of XBP1, a target of the ER stress sensor IRE1. This suggests that the ISR/UPR may participate in cell death, as previously observed for other cell lines (19).

Glucose deprivation regulates levels of TRAIL receptors. Stimuli that promote endoplasmic reticulum stress, such as tunicamycin and thapsigargin, can induce apoptotic cell death through the mitochondrial pathway. However, they have also been
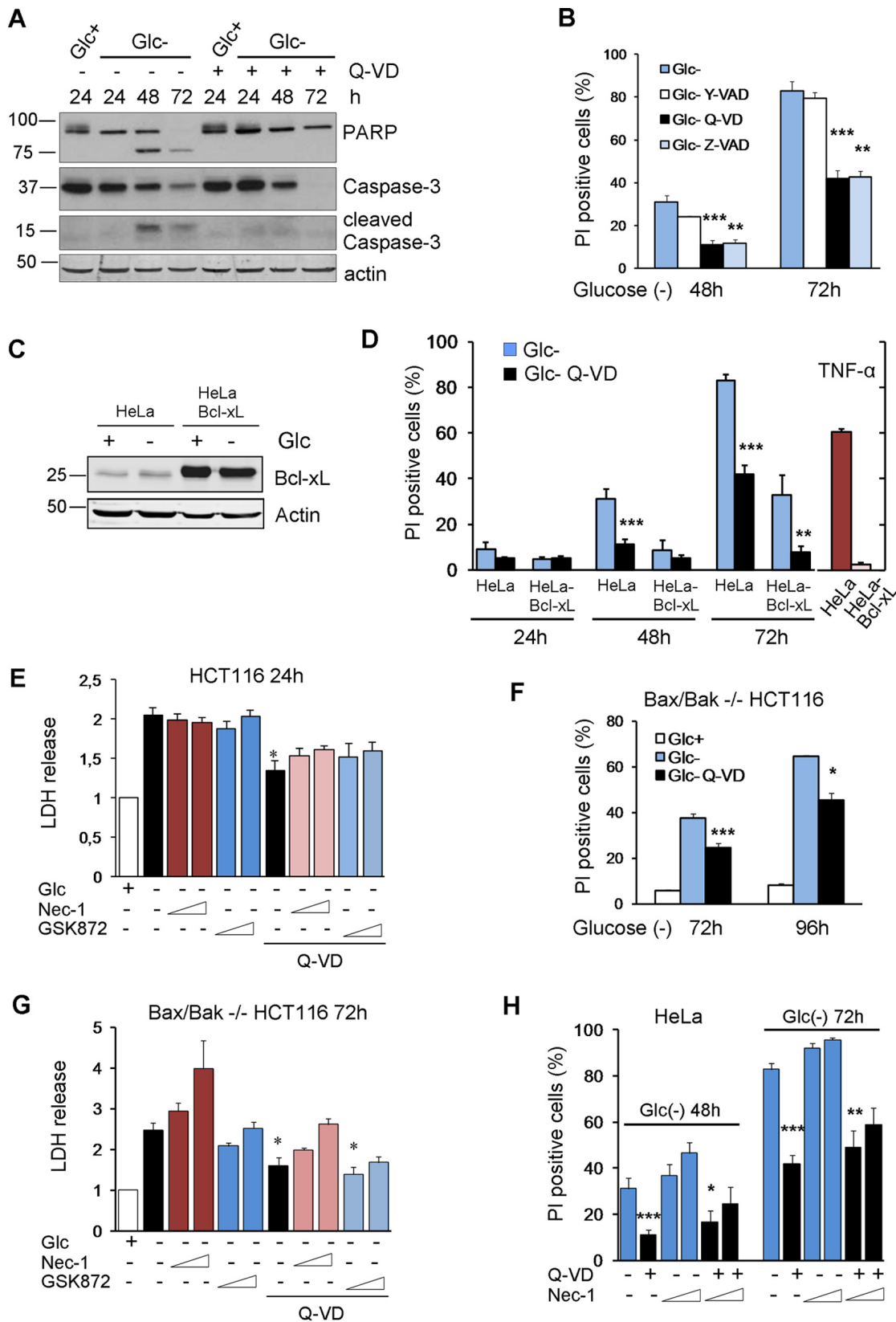
FIG 1 Glucose deprivation induces apoptosis and necrosis in human tumor cell lines. (A) HeLa cells were plated at 20% confluence in 60-mm dishes, and 24 h later, they were incubated with (Glc+) or without (Glc−) glucose for the indicated times in the presence of DMSO (Q-VD−) or Q-VD (Q-VD+). Western blotting of caspase-3 and PARP is shown. (B) HeLa cells were incubated in the presence or absence of glucose plus DMSO, Y-VAD, Q-VD, or Z-VAD and collected to determine PI incorporation by FACS analysis at the indicated time points. The averages and SEM of data from at least three experiments are shown. (C and D) HeLa and HeLa-Bcl-xL cells were plated at 20% confluence in 12-well plates, and 24 h later, they were incubated without glucose for 24, 48,

shown to induce TRAIL receptors and to be sensitized to TRAIL (20). Intriguingly, some TRAIL receptors can mediate ER stress-induced cell death in a manner independent of death receptor-death ligand interactions (21–23). Since glucose deprivation induced ATF4 and CHOP, the latter of which has been linked to TRAIL receptor transcription (24), we examined the levels of TRAIL receptors upon treatment without glucose. Figure 2C shows that glucose deprivation strongly induced the accumulation of the TRAIL receptors DR4/TRAIL-R1 and DR5/TRAIL-R2. Next, we analyzed their mRNA levels. Quantitative PCR (qPCR) analysis indicated that mRNA levels of *DR4* did not change upon glucose withdrawal at any time examined, with the exception of later time points at which *DR4* mRNA levels are reduced (Fig. 2D). In contrast, the accumulation of DR5 may involve its transcriptional upregulation at short times (Fig. 2E), although by 24 h of glucose deprivation, *DR5* mRNA levels returned to control levels, while the protein levels continued to increase. DR5 was previously shown to be localized mainly in intracellular membranes upon treatment with ER-stressing drugs (22), although an increase in plasma membrane translocation was also detected (25). We analyzed DR5 localization in cells grown without glucose and observed that the majority of DR5 detected after treatment accumulated in the Golgi apparatus and did not colocalize with mitochondria or the endoplasmic reticulum protein calnexin (see Fig. 6F and G and data not shown). However, we also observed some accumulation in the plasma membrane (see Fig. 6F and G).

Altogether, these data indicated that glucose deprivation regulates the expression of TRAIL receptors, possibly via ER stress-dependent pathways and most likely in a posttranscriptional manner.

Caspase-8, FADD, and Bid mediate apoptosis induced by glucose deprivation. Caspase-8 is the apical caspase in the death receptor pathway, which cleaves and activates executioner caspases directly or indirectly upon death receptor ligation. Death receptors activate caspase-8 through the recruitment of adapter molecules to a death-inducing signaling complex (DISC) to which this protease is recruited. Previously, we showed that Bax-Bak-deficient MEFs subjected to glucose deprivation die in a caspase-8-dependent manner that could bypass the mitochondrial pathway (10). To test whether caspase-8 was involved in the apoptosis of HeLa cells, we silenced caspase-8 using small interfering RNA (siRNA), and we detected a significant reduction of cell death under glucose deprivation (10) (Fig. 3A and B). siRNA against this protease revealed that caspase-8 also participated in the apoptosis of Bcl-xL-overexpressing HeLa cells (Fig. 3C). Moreover, the apoptosis of Bax-Bak-deficient HCT116 cells was also dependent on caspase-8, although the amount of protection conferred by the siRNA was small, consistent with the small amount of protection conferred by caspase inhibitors (Fig. 1D and 3D and E). All these data suggest that glucose deprivation induces caspase-8-dependent apoptosis in diverse human tumor lines with either an intact or a deficient mitochondrial pathway.

The fact that HeLa cells overexpressing Bcl-xL died slower suggested that the mitochondria could participate in apoptosis in these cells through the cleavage of Bid by caspase-8. Indeed, silencing of Bid in HeLa cells partially prevented cell death (Fig. 3F and G). In contrast, levels of BH3-only proteins such as Bim and Noxa, previously

FIG 1 Legend (Continued)
and 72 h or with TNF plus cycloheximide for 24 h and subjected to Western blotting (C) or collected to determine PI incorporation by FACS (D). The averages and SEM of data from at least three experiments are shown. (E) HCT116 cells were incubated in the presence or absence of glucose plus DMSO, Q-VD, necrostatin-1 (40 or 100 μM), and/or a RIPK3 inhibitor (1 or 3 μM) as indicated and collected for an LDH test at 24 h. The averages and SEM of data from three experiments are shown. (F) Bax/Bak$^{-/-}$ HCT116 cells were plated at 20% confluence in 60-mm dishes, and 24 h later, they were incubated without glucose in the presence or absence of Q-VD and collected to determine PI incorporation by FACS analysis at the indicated time points. The averages and SEM of data from three experiments are shown. (G) Bax/Bak$^{-/-}$ HCT116 cells were incubated in the presence or absence of glucose plus DMSO, Q-VD, necrostatin-1 (40 or 100 μM), and/or a RIPK3 inhibitor (1 or 3 μM) as indicated and collected for an LDH test at 72 h. The averages and SEM of data from at least three experiments are shown. (H) HeLa cells were incubated in the absence of glucose plus DMSO, Q-VD, or necrostatin-1 or a combination of Q-VD and necrostatin-1 (1 or 3 μM) and collected for PI analysis by FACS analysis at the indicated time points. The averages and SEM of data from at least three experiments are shown. *, $P <$ 0.05; **, $P <$ 0.01; ***, $P <$ 0.001.
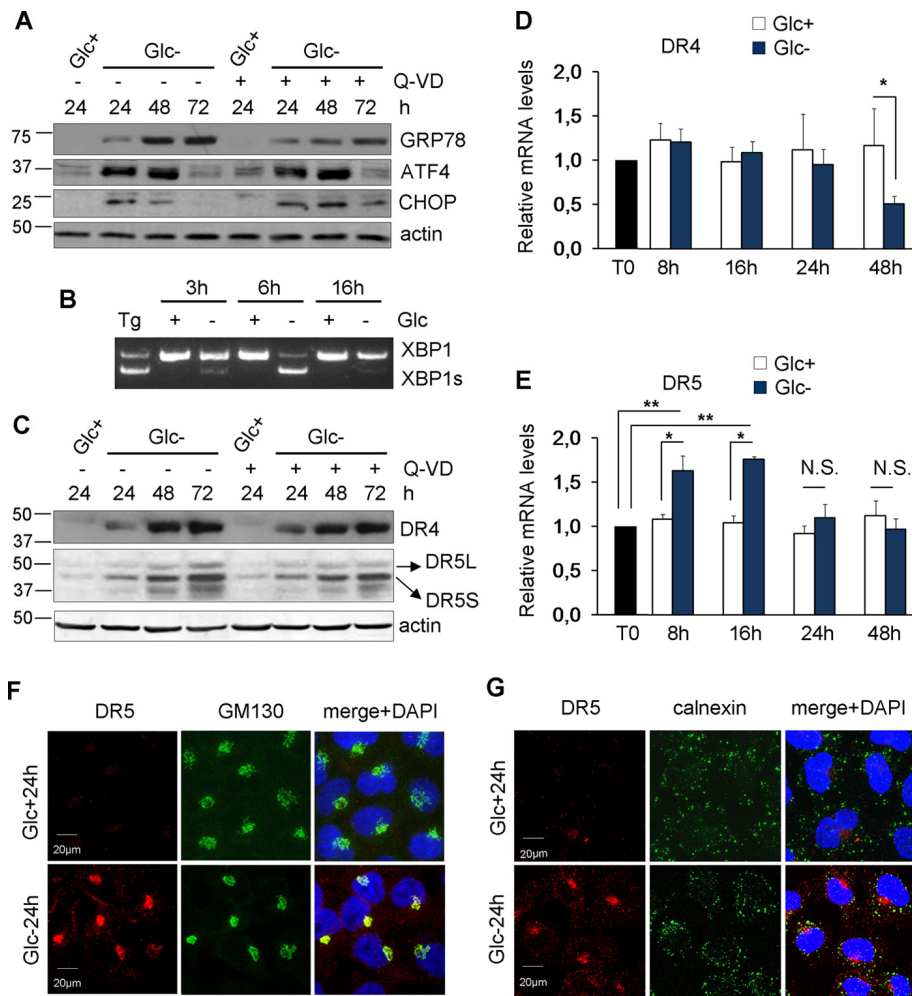
FIG 2 Glucose deprivation induces ER stress and TRAIL receptors. (A) HeLa cells were incubated with glucose and/or Q-VD (Q-VD+) or DMSO (Q-VD−) as indicated for 24, 48, and 72 h and collected for Western blotting of GRP78, ATF4, and CHOP. (B) HeLa cells were treated with thapsigargin (Tg) for 24 h or incubated in the presence (+) or absence (−) of glucose for the indicated times and collected for reverse transcription-PCR analysis of unspliced and spliced XBP1. (C) HeLa cells were incubated with glucose and/or Q-VD (Q-VD+) or DMSO (Q-VD−) as shown for the indicated times and then collected for Western blotting of DR4 (TRAIL-R1) and DR5 (TRAIL-R2). (D and E) HeLa cells were incubated with or without glucose for the times shown and collected for qPCR analysis. DR4 mRNA levels relative to the values for the housekeeping gene and time zero (T0) are reported in panel B. DR5 mRNA levels relative to the values for the housekeeping gene and time zero (T0) are reported in panel C. The averages and SEM of data from at least three experiments are shown. (F and G) HeLa cells were plated for immunofluorescence, and 24 h later, they were incubated with or without glucose for 24 h before performing confocal analysis of DR5 and GM130 (F) or calnexin (G) localization. *, $P < 0.05$; **, $P < 0.01$; N.S., not significant.

linked to apoptosis induced by ER stress or by starvation (reviewed in reference 21), were increased with treatment (Fig. 4A and B), but they did not participate in cell death, as revealed by siRNA (Fig. 4C to F).

Caspase-8 is usually activated upon its dimerization in intracellular or membrane DISCs through recruitment by the adapter molecule FADD in response to the interaction of death ligands with death receptors. We previously analyzed the role of these interactions in cell death induced by glucose deprivation in Bax-Bak-deficient MEFs and could not detect any role of death ligand-receptor interactions (10). For this reason, we analyzed two unconventional platforms to activate caspase-8: the ripoptosome and p62. The ripoptosome is nucleated by the kinase RIPK1 and is formed upon the inhibition and degradation of cellular inhibitor of apoptosis proteins (cIAP) (26, 27). We observed that glucose deprivation promoted the disappearance of cIAP1, cIAP2, and X-linked inhibitor of apoptosis protein (XIAP) (Fig. 5A). This, however, did not lead to a
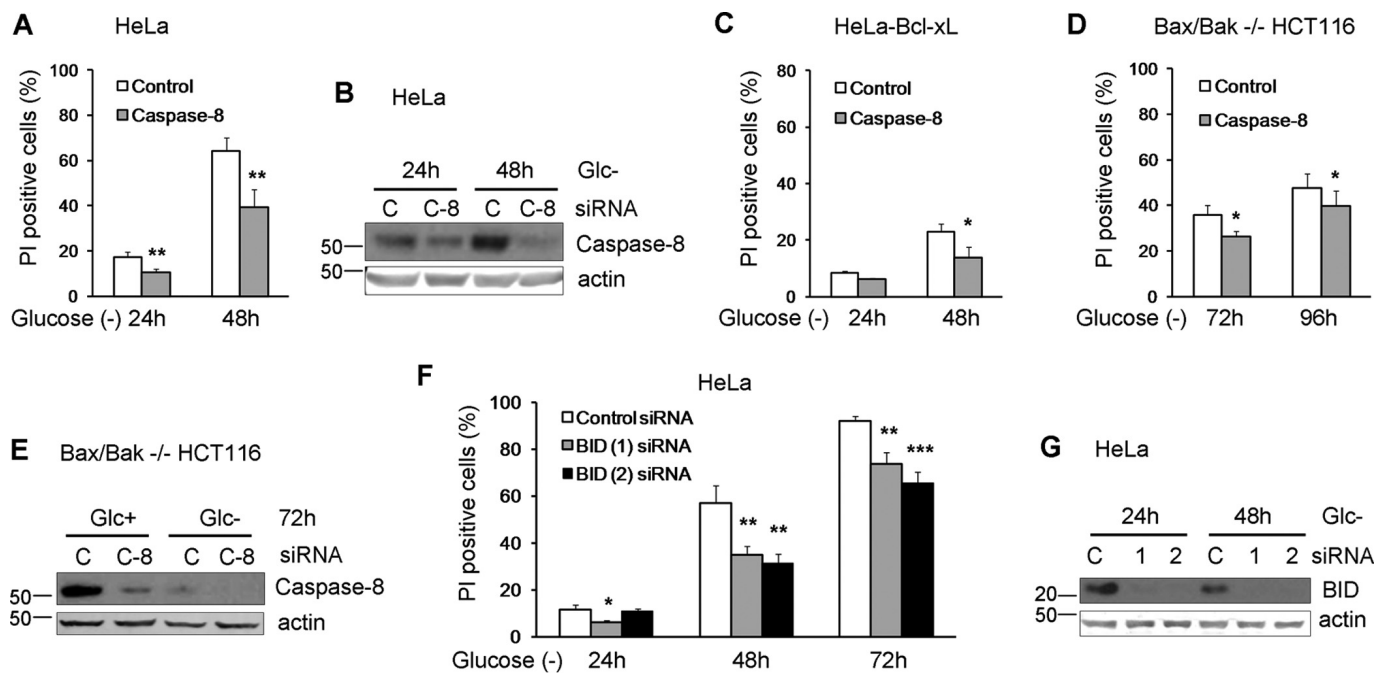
FIG 3 Human cell lines die in a caspase-8- and Bid-dependent manner under glucose deprivation. (A to C) HeLa cells (A and B) and HeLa-Bcl-xL cells (C) were plated at 50% confluence in 6-well plates, and 5 h later, they were transfected with caspase-8 or control siRNA. At 24 h posttransfection, cells were treated without glucose for 24 and 48 h and collected to determine PI incorporation by FACS analysis. The averages and SEM of data from three experiments are shown. Western blotting of control and caspase-8 siRNA-transfected HeLa cells treated without glucose for the indicated times is shown in panel B. (D and E) Bax/Bak$^{-/-}$ HCT116 cells were plated at 50% confluence in 6-well plates, and 5 h later, they were transfected with caspase-8 siRNA or control siRNA. At 24 h posttransfection, cells were incubated without glucose for 72 and 96 h and collected to determine PI incorporation by FACS analysis. The averages and SEM of data from three experiments are shown. Western blotting of cells transfected with control or caspase-8 siRNAs is shown in panel E. (F and G) HeLa cells were plated at 50% confluence in 6-well plates, and 5 h later, they were transfected with Bid (1) and Bid (2) siRNAs or the control siRNA. At 24 h posttransfection, cells were treated without glucose for 24, 48, and 72 h and collected to determine PI incorporation by FACS analysis. The averages and SEM of data from three experiments are shown. Western blotting of cells transfected with control, Bid (1), or Bid (2) siRNAs and treated without glucose for the indicated times is shown in panel G. *, $P < 0.05$; **, $P < 0.01$; ***, $P < 0.001$.

detectable interaction of RIPK1 and caspase-8 in the absence (Fig. 5B) or presence (data not shown) of caspase inhibitors. Moreover, the downregulation of RIPK1 did not prevent cell death induced by glucose deprivation (Fig. 5C and D). Caspase-8 has been shown to interact with the autophagosomal proteins LC3 and p62 upon several stimuli, with p62 contributing to its aggregation and activation (21, 28, 29). We previously described the accumulation of p62 upon glucose deprivation due to an inactivation of autophagic flux (30) (Fig. 5E and F, input). We observed that caspase-8 coimmunoprecipitated with p62 upon glucose deprivation (Fig. 5E and F), However, there was no measurable translocation of caspase-8 to p62 spots (aggresomes) (Fig. 5G and H), and similar to what we previously observed in Bax-Bak-deficient MEFs (30), p62 knockdown did not prevent glucose deprivation-induced cell death (Fig. 5I and J).

In order to examine the role of FADD, we performed colocalization analysis of caspase-8 and FADD by immunostaining under normal and glucose-deprived conditions (Fig. 6A and B). We detected a basal interaction of the two proteins, but no changes were observed after glucose removal. In order to clarify the role of FADD in cell death induced by glucose deprivation, we employed siRNA to target this protein (Fig. 6C) and observed that its downregulation protected from glucose deprivation to the same extent that it protected from cross-linking the Fas receptor with an antibody (Fig. 6D). Moreover, the elimination of FADD by using clustered regularly interspaced short palindromic repeats (CRISPR) prevented cell death by glucose deprivation (Fig. 6E and F).

ATF4 and TRAIL receptors mediate apoptosis upon glucose deprivation. It has been reported that ER stressors induce DR4 and DR5 through the transcription factor CHOP, which is itself a transcriptional target of ATF4 (24, 31). We thus investigated a role for the ATF4/CHOP axis in apoptosis induced by glucose deprivation and in the
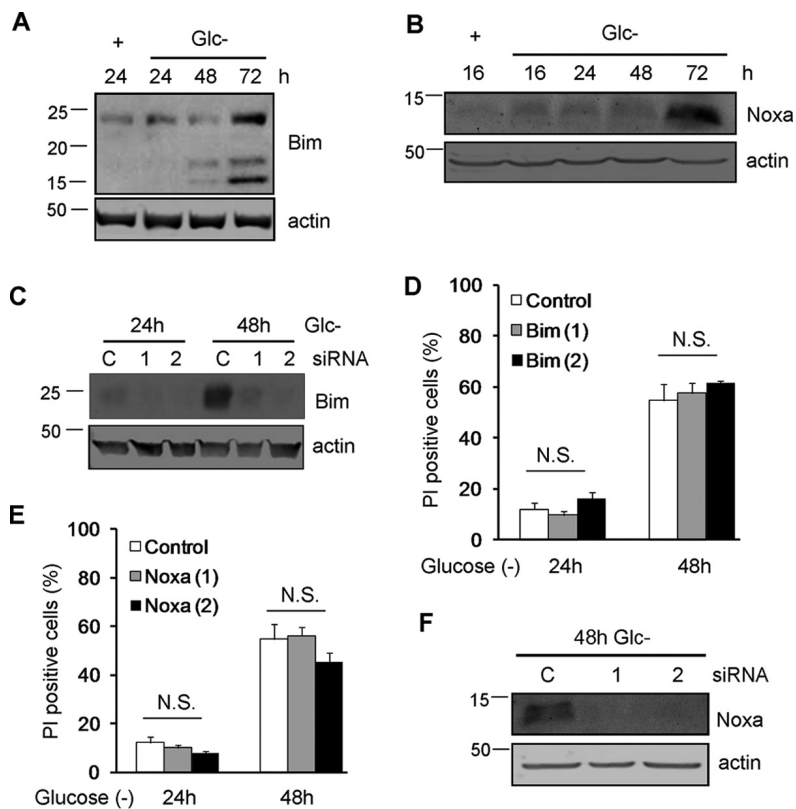
FIG 4 Noxa and Bim are dispensable for glucose deprivation-induced cell death of HeLa cells. (A and B) HeLa cells were incubated in the presence (+) or absence (Glc−) of glucose for the indicated times and collected for Western blotting of Bim (A) and Noxa (B). (C and D) HeLa cells were transfected with control siRNA or siRNAs against Bim, incubated for 24 and 48 h without glucose, and collected for Western blotting of Bim (C) or FACS analysis (D). (E and F) HeLa cells were transfected with siRNA against Noxa, incubated for the indicated times without glucose, and collected for FACS analysis (E) and Western blot analysis (F). N.S., not significant.

accumulation of death receptors. ATF4 downregulation with siRNA strongly reduced cell death, as described by other models of starvation (Fig. 7A and B). Its downregulation also prevented DR5 accumulation although not DR4 expression (Fig. 7C). We analyzed the role of CHOP and observed that different siRNAs partially protected from cell death (Fig. 7D and E). Different from a number of studies that reported the induction of DR5 mediated by CHOP in response to other stimuli, siRNA against CHOP did not prevent DR5 induction induced by glucose deprivation (Fig. 7F). However, a modest reduction of the accumulation of DR4 was observed. Because the amount of protection from cell death conferred by siRNA was very small, we generated cells lacking CHOP via CRISPR knockout (Fig. 7G and H). These cells showed no protection from cell death, which indicates that cell death is mediated by ATF4 but is independent of CHOP.

We subsequently analyzed the role of TRAIL death receptors in apoptosis induced by glucose deprivation. siRNAs against DR5 protected from cell death, although protection was not uniform, and their strength depended on the sequence employed (Fig. 8A and B). Up to five bands corresponding to different isoforms of DR5 (long and short) and possibly their unglycosylated counterparts were detected upon glucose deprivation (Fig. 8B). It was previously shown that DR5-mediated cell death in response to thapsigargin is dependent on the long isoform of DR5 (22). We observed that siRNA against the short isoform (DR5S) did not prevent the death of HeLa cells subjected to glucose deprivation (Fig. 6A and B). In contrast, sequences that downregulated the long isoform (DR5L) were effective in protecting HeLa and HeLa-Bcl-xL cells from apoptosis, correlating with their efficiency in suppressing DR5L expression (Fig. 8A to C). In order to
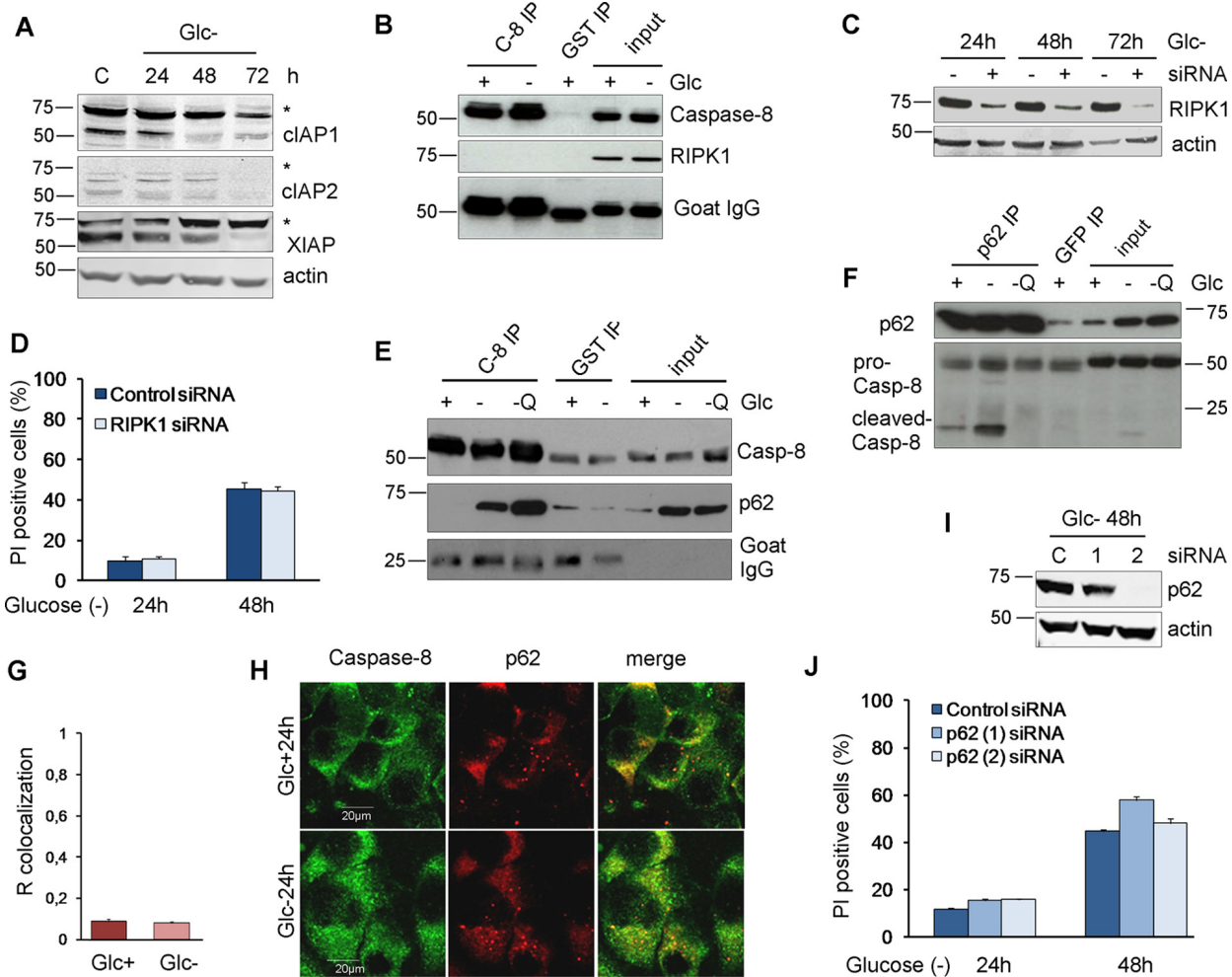
FIG 5 RIPK1 and p62 are not involved in cell death under glucose deprivation. (A) HeLa cells were plated at 20% confluence in 60-mm dishes, and 24 h later, they were incubated without glucose for 24, 48, and 72 h and collected for Western blot analysis of cIAPs and XIAP. (B) HeLa cells were plated at 20% confluence in 100-mm dishes, and 24 h later, they were incubated with or without glucose for 24 h before performing immunoprecipitation of caspase-8 or GST as a control. Western blots of caspase-8 and RIPK1 are shown. (C) Western blot analysis of glucose-deprived cells transfected with control (−) or RIPK1 (+) siRNA and incubated without glucose for the times shown. (D) HeLa cells were plated at 50% confluence in 6-well plates, and 5 h later, they were transfected with 50 nM RIPK1 siRNAs or the control siRNA. Twenty-four hours after transfection, cells were incubated without glucose for 24 and 48 h and collected for PI analysis by FACS analysis. The averages and SEM of data from three experiments are shown. (E and F) HeLa cells were plated at 20% confluence in 100-mm dishes, and 24 h later, they were incubated with glucose (+), without glucose or Q-VD (−), or without glucose but with 10 μM Q-VD (-Q) for 24 h before immunoprecipitation of caspase-8 (E) or p62 (F) was performed. Western blot analyses of caspase-8 and p62 are shown. (G and H) HeLa cells were plated for immunofluorescence analysis, and they were treated with or without glucose for 24 h. Representative confocal microscopy images of caspase-8 and p62 (H) and data from colocalization analysis using ImageJ software (G) are shown. The graph shows the averages and the standard deviations of data from four independent experiments. (I and J) HeLa cells were transfected with 50 nM p62 (1) and p62 (2) siRNAs and the control siRNA. At 24 h posttransfection, cells were incubated without glucose for 24 and 48 h and collected to determine PI incorporation by FACS analysis. Western blotting of p62 is shown in panel I. The averages and SEM of data from three experiments are shown in panel J. Differences between siRNAs were not statistically significant.

verify the results obtained by using siRNA, we generated cells deficient in DR5, and we observed protection from cell death (Fig. 8D). DR5 downregulation also prevented the death of HCT116 and Bax-Bak-deficient HCT116 cells, and in these cells, the downregulation of the short isoform of DR5 was also effective (Fig. 8E to H).

Since we also observed an upregulation of DR4, we employed siRNAs against this TRAIL receptor and observed that they produced a small but significant reduction of cell death in HeLa cells (Fig. 9A and B). The deletion of *DR4* via CRISPR significantly protected HeLa cells from glucose deprivation (Fig. 9C). We also observed that the combination of DR4 and DR5 siRNAs conferred better protection from glucose deprivation than did the single siRNAs ($P = 0.04$ for DR4 versus the combination; $P = 0.01$ for DR5 versus the combination) (Fig. 9D and E). However, the double combination of
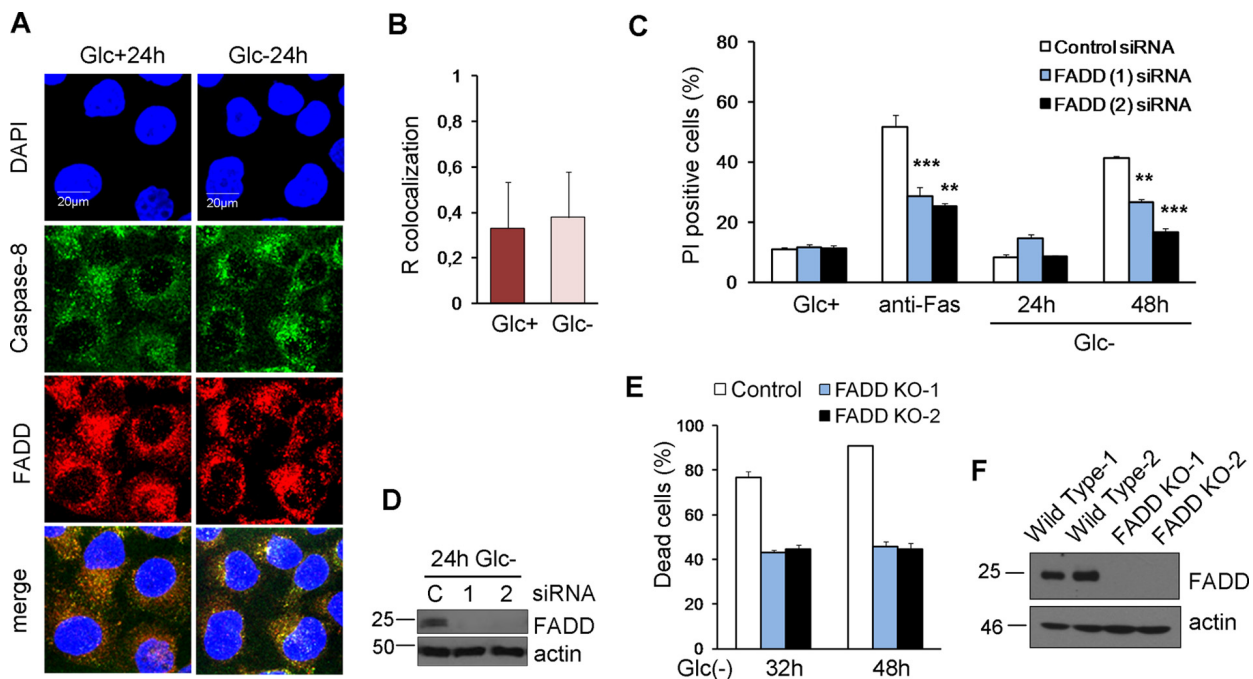
FIG 6 FADD is involved in cell death under glucose deprivation. (A and B) HeLa cells were plated for immunofluorescence, and 24 h later, they were incubated with (Glc+) or without (Glc−) glucose for 24 h. Confocal microscope pictures of colocalization of caspase-8 with FADD (A) and quantification by using ImageJ software (B) are reported. The graph shows the averages and the standard deviations of data from four independent experiments. (C and D) HeLa cells were transfected with control, FADD (1), or FADD (2) siRNA. At 48 h posttransfection, cells were incubated without glucose for 24 and 48 h or with an anti-Fas antibody for 48 h and collected for Western blotting (D) and for determining PI incorporation by FACS analysis (C). The averages and SEM of data from at least three experiments are shown. (E and F) HeLa cells knocked out for FADD (clones 1 and 2) and their controls were subjected to glucose deprivation for the indicated times and subjected to Western blot analysis (F) or determination of the number of dead cells under a microscope (E). Data show the averages and SEM of results from three independent experiments. **, $P < 0.01$; ***, $P < 0.001$.

CRISPR-deleted DR4 and DR5 did not provide significantly better protection than did DR5 alone (Fig. 9F and G).

DR5 has been shown to play a role in cell death induced by other stimuli that induce ER stress: thapsigargin and the GRP78-depleting bacterial agent subtilase cytotoxin AB (22, 23). Moreover, the authors of that study reported that TRAIL receptor-mediated cell death occurred in a manner independent of the ligand TRAIL upon treatment with ER inducers. We tested whether TRAIL participated in cell death induced by glucose deprivation in these cells. In agreement with our previous results in which a blockade of death receptor-ligand interactions did not prevent cell death by glucose deprivation in MEFs (10), the downregulation of TRAIL using two different siRNA oligonucleotides did not prevent cell death (Fig. 10A and B).

DISCUSSION

This study places the integrated stress response and ER stress-associated factor ATF4 as a central player in apoptosis induced by glucose deprivation. ATF4 is one of the small subsets of proteins induced under conditions of general translational repression upon the phosphorylation of the translation initiation factor eIF2α. At least two kinases are responsible for eIF2α phosphorylation upon glucose deprivation: PERK and GCN2 (19, 32). PERK participates in the unfolded protein response and is activated by endoplasmic reticulum stress, an event that occurs when the glucose level is low, probably due to the accumulation of misfolded, unglycosylated proteins. GCN2 is activated in the ISR by amino acid loss (11). The role of these responses and the subsequent translational arrest is to restore homeostasis; however, eIF2α phosphorylation and ATF4 induction also induce cell death if damage is not repaired. The role of ATF4 in apoptosis induced by "classical" ER stressors has been widely documented, although it is unclear which proteins mediate cell death in this context, and it may depend on the cell type or the
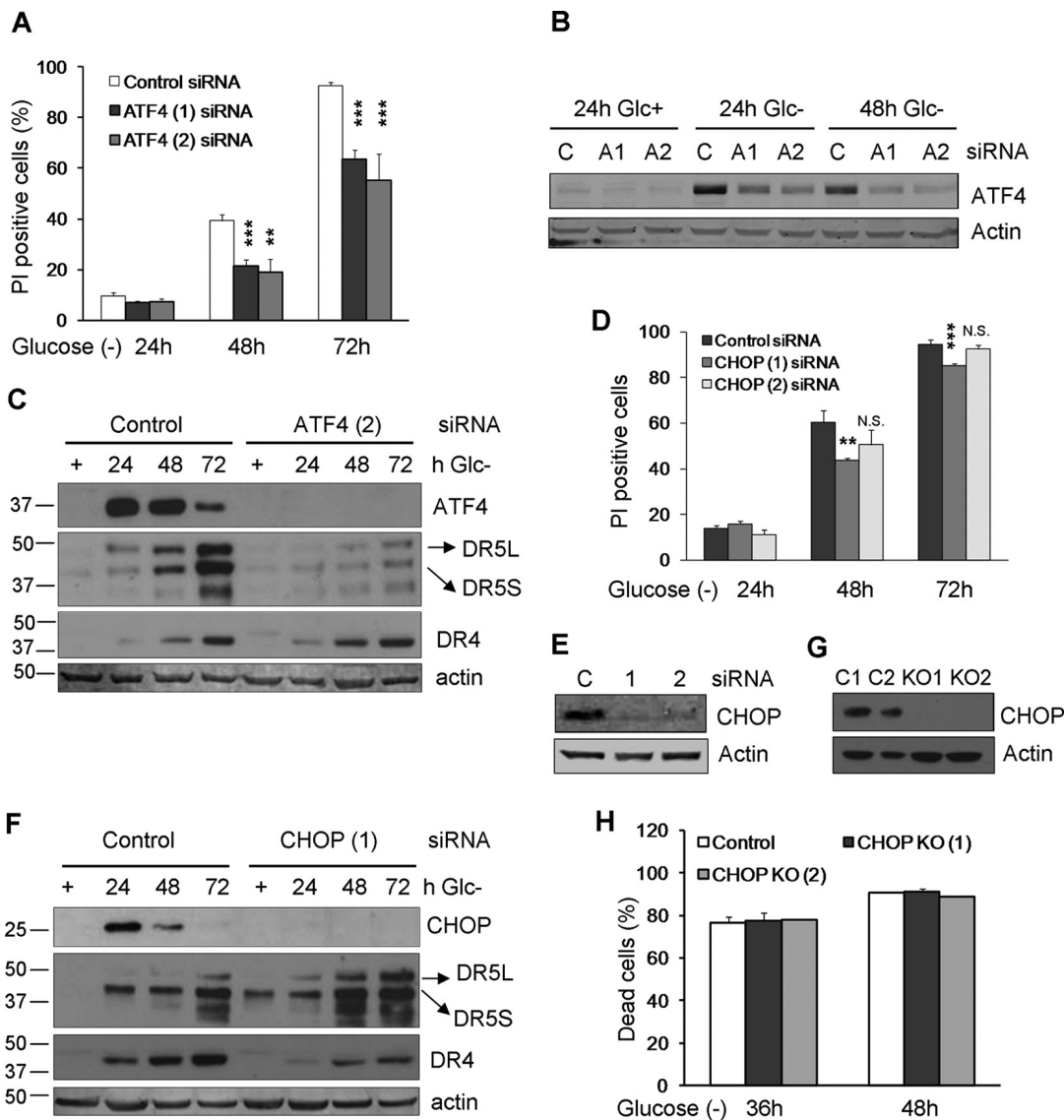
FIG 7 ATF4 and CHOP. (A to C) HeLa cells were transfected with ATF4 siRNAs or the control siRNA. At 24 h posttransfection, cells were incubated without glucose for 24, 48, and 72 h and collected to determine PI incorporation by FACS analysis (C). The averages and SEM of data from four to seven experiments under each condition are shown. Western blots of ATF4, DR5, and DR4 in cells transfected with control, ATF4 (1), and ATF (2) siRNAs are shown in panels B and C. (D to F) HeLa cells were transfected with CHOP siRNAs and the control siRNA. At 24 h posttransfection, cells were incubated without glucose for 24, 48, and 72 h and collected to determine PI incorporation by FACS analysis (D). The averages and SEM of data from at least three experiments are shown. Western blots of CHOP, DR5, and DR4 in cells transfected with control or CHOP siRNAs are shown in panels E and F. (G and H) HeLa cells knocked out for CHOP (clones 1 and 2) and their controls were subjected to glucose deprivation for the indicated times and subjected to Western blot analysis after treatment with 10 μg/ml brefeldin A or determination of the number dead cells under a microscope. Data show averages and SEM of results from three independent experiments. **, $P < 0.01$; ***, $P < 0.001$; N.S., not significant.

coactivation of other pathways (21). Only recently has this protein emerged as a crucial regulator of metabolic sensing and also as a cell death effector upon amino acid depletion (11, 17).

We previously reported that ATF4 participates in mitochondrial apoptosis induced by the glucose analog 2-deoxyglucose, which works as an ER stressor (12). In addition, it was recently shown that ATF4 participates in the induction of apoptosis in response to glucose deprivation in HEK293 cells (13) and in the necrosis of rhabdomyosarcoma cells deprived of glucose (6). However, in these studies, the mechanism of cell death was not elucidated. Shin et al. reported a role for the BH3-only protein Bid downstream of ATF4 (13). Our data indicate that Bid, Bax, and Bak participate in the transduction of
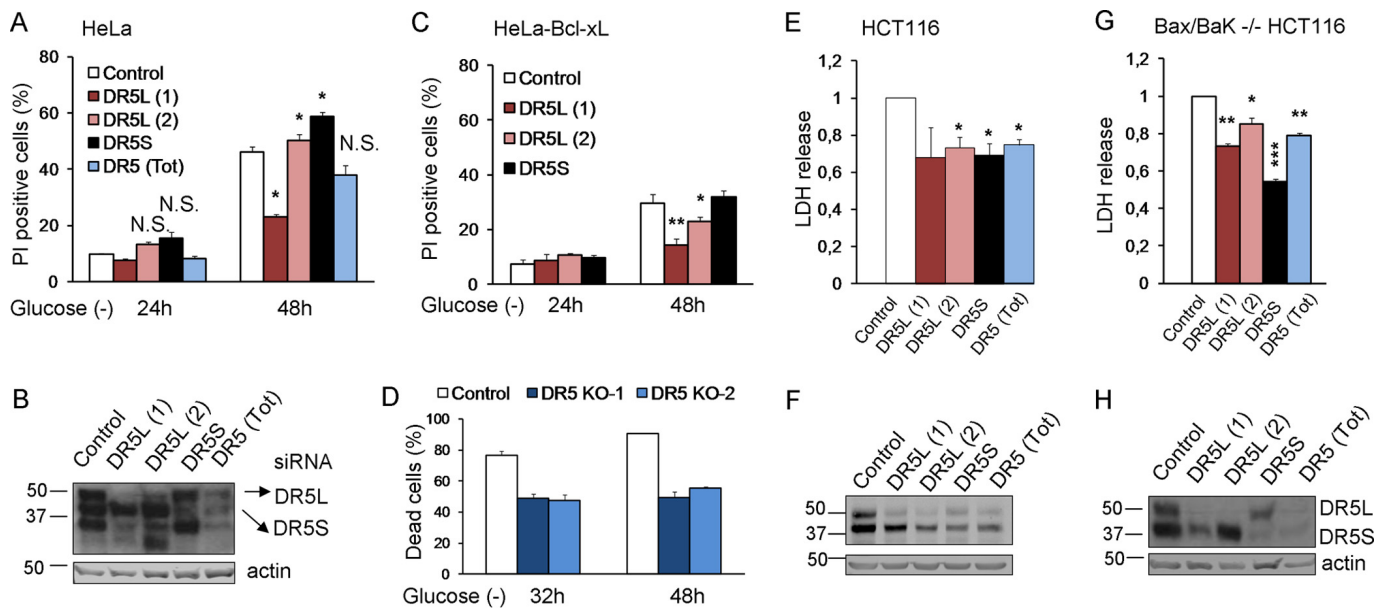
FIG 8 DR5 siRNAs protect from death induced by glucose deprivation. (A and B) HeLa cells were transfected with DR5L (1), DR5L (2), DR5S, DR5 (Tot), or the control siRNA. At 24 h posttransfection, cells were incubated without glucose for 24 and 48 and collected to determine PI incorporation by FACS analysis (A) or Western blot analysis of DR5 48 h after treatment (B). The averages and SEM of data from at least three experiments are shown. (C) HeLa-Bcl-xL cells were transfected with DR5L (1), DR5L (2), DR5S, or the control siRNA. At 24 h posttransfection, cells were incubated without glucose for 24 and 48 h and collected to determine PI incorporation by FACS analysis. The averages and SEM of data from at least three experiments are shown. (D) Control HeLa cells and cells deficient in *DR5* (KO1 and KO2) were incubated without glucose for the indicated times, and the number of dead cells was determined with a microscope. Shown are averages and SEM of data from three independent experiments. Western blotting for the expression of DR5 is shown in Fig. 9F. (E and F) HCT116 cells were transfected with DR5L (1), DR5L (2), DR5S, DR5 (Tot), or the control siRNA. At 24 h posttransfection, the cells were incubated without glucose for 24 h and collected for an LDH test. The averages and SEM of data from four experiments are shown. Western blotting of DR5 after 24 h of treatment is shown in panel F. (G and H) Bax/Bak$^{-/-}$ HCT116 cells were transfected with DR5L (1), DR5L (2), DR5S, DR5 (Tot), or the control siRNA. At 24 h posttransfection, cells were incubated without glucose for 72 h and collected for an LDH test. The averages and SEM of data from four experiments are shown. Western blotting of DR5 in Bax/Bak$^{-/-}$ HCT116 cells 72 h after treatment is shown in panel H. *, $P < 0.05$; **, $P < 0.01$; ***, $P < 0.001$; N.S., not significant.

cell death signals from caspase-8 to mitochondria, although apoptosis also occurred in Bcl-xL-overexpressing or Bax-Bak-deficient cells. Cell death in response to ER stressors, including glucose deprivation and inhibitors of glycolysis, is generally thought to be mediated through the transcriptional activation of the mitochondrial pathway of apoptosis by CHOP downstream of ATF4. Indeed, CHOP induces Bim in response to the glycolytic inhibitor 2-deoxyglucose (33). CHOP is not only important for the activation of the mitochondrial pathway but is also the ER stress-associated transcription factor that mediates TRAIL receptor induction in several cell lines upon ER stress (22–24, 31). However, ER stress-dependent, CHOP-independent upregulation of DR5 has also been documented (20). In the present study, and in contrast to other reports, CHOP did not play a role in the induction of DR5, although participation in DR4 accumulation upon glucose deprivation was observed. However, the mRNA levels of *DR4* do not change after the treatment, which suggests that the regulation of this receptor is achieved mostly at the posttranscriptional level. In contrast, we observed the transcriptional induction of DR5 at early time points of glucose removal and a strong accumulation of the protein at later time points, which could be prevented by ATF4 but not CHOP silencing. These data suggest that ATF4 might directly regulate the expression of DR5, independently of CHOP, possibly at both the transcriptional and posttranscriptional levels (Fig. 10).

Downstream of death receptors, glucose deprivation has been described to reduce FLIP levels, thus leading to sensitization to TRAIL, although FLIP downregulation does not occur in all cell types (34, 35). We describe here an unequivocal role of FADD as a mediator of apoptosis induced by glucose deprivation, while the FADD- and caspase-8-interacting protein RIPK1 did not play any role in cell death, nor did p62, which we have previously shown accumulates upon glucose deprivation in these cells and can regulate caspase-8 activation downstream of TRAIL receptors (28, 30). A possible role of TRADD and other adapter molecules remains to be tested.
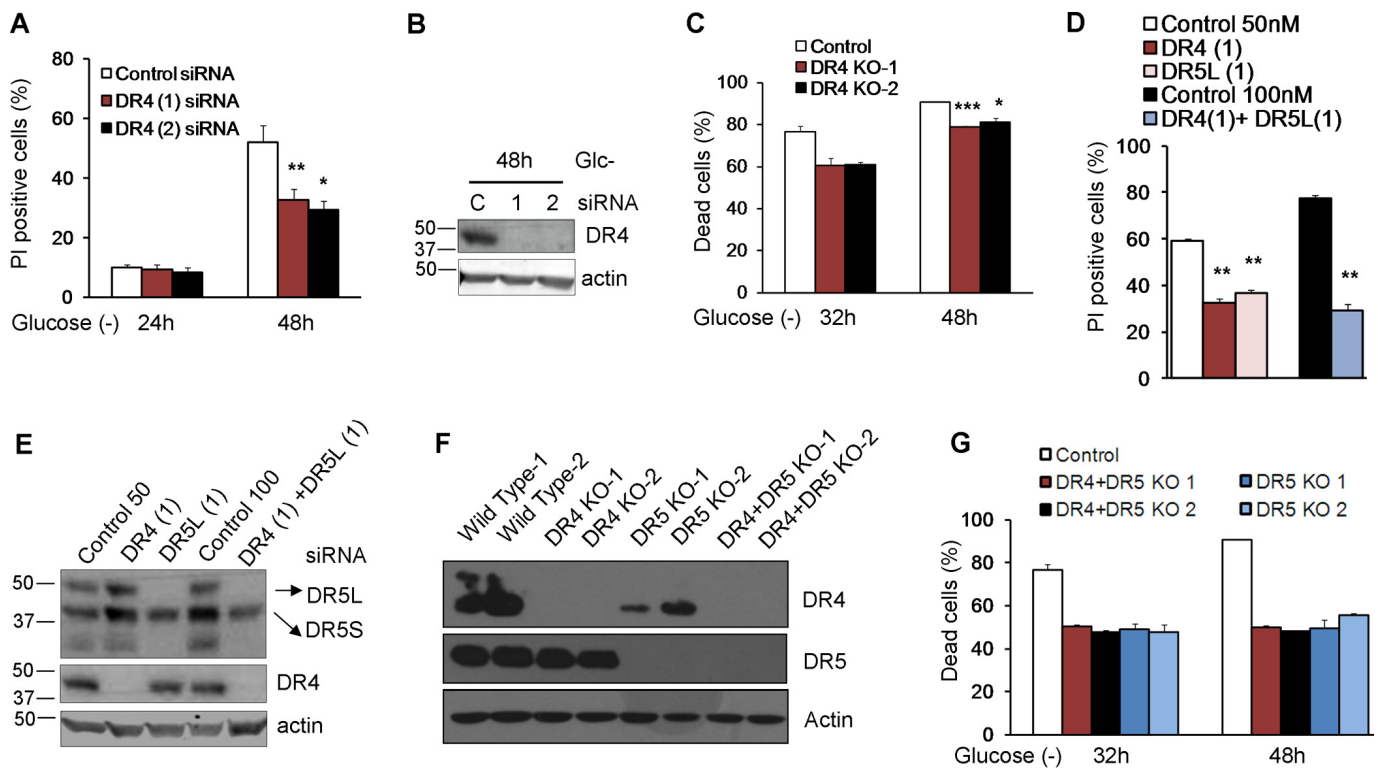
FIG 9 DR4 is involved in cell death under glucose deprivation. (A and B) HeLa cells were transfected with DR4 (1), DR4 (2), or the control siRNA. At 24 h posttransfection, cells were incubated without glucose for 24 and 48 h and collected to determine PI incorporation by FACS analysis. The averages and SEM of data from at least three experiments are shown in panel A. Western blotting of cells treated for 48 h without glucose and transfected with control, DR4 (1), or DR4 (2) siRNA is shown in panel B. (C) Control HeLa cells and cells deficient in *DR4* (KO1 and KO2) were incubated without glucose for the indicated times, and the dead cells were counted under a microscope. Shown are averages and SEM of data from three independent experiments. Western blotting is shown in panel F. (D) HeLa cells were transfected with DR4 (1), DR5L (1), or control siRNA (50 nM) or the combination of DR4 (1) plus DR5L (1) siRNAs at 100 nM as a control. At 24 h posttransfection, cells were incubated without glucose for 24 and 48 h and collected to determine PI incorporation by FACS analysis. The averages and SEM of data from at least three experiments are shown. Numbers indicate the average protection (percent) conferred by each siRNA or siRNA combination versus its control. (E) Western blotting of DR5 and DR4 in HeLa cells 48 h after treatment. (F) Western blotting of knockout cells (*DR4*, *DR5*, and *DR4-DR5* double knockout) generated as described in Materials and Methods. (G) Control HeLa cells and cells doubly deficient in *DR4* and *DR5* (KO1 and KO2) were incubated without glucose for the indicated times, and the dead cells were counted under a microscope. Shown are averages and SEM of data from three independent experiments and include *DR5* data from Fig. 8D for comparison. Western blotting is shown in panel F. *, $P < 0.05$; **, $P < 0.01$; ***, $P < 0.001$.

DR5 has been shown in several reports to play a role in cell death induced by other stimuli that induce ER stress, most notably thapsigargin (22–24). The role of DR4 is less established, although it has also been documented (31). The precise mechanism that activates these receptors upon glucose deprivation remains to be determined. In the case of "classical" ER stressors such as tunicamycin and thapsigargin, death mediated by DR5 could not be blocked by using siRNA against TRAIL or incubating cells in the presence of an extracellular, soluble form of TRAIL receptors (22, 23). Here we show that the downregulation of TRAIL to undetectable levels did not prevent cell death by glucose deprivation. This suggests that these receptors are activated through ligand-independent, intracellular aggregation. In fact, it is known that the overexpression of death receptors can induce their activation (36). This aggregation could possibly occur in membranes of the secretory pathway, such as those of the Golgi apparatus, although this remains to be proven, and the mechanism remains to be identified. Glucose is required not only for energy production but also as a substrate for the posttranscriptional modification of proteins. It is possible that the lack of glucose modifies trafficking through secretory pathways, which, together with the modification of glycosylation patterns of the receptors themselves, may promote ligand-independent associations.

MATERIALS AND METHODS

Cell culture and treatments. HeLa cells from the ATCC and Bax/Bak$^{-/-}$ simian virus 40 (SV40)-transformed MEFs (37) were cultured in pyruvate-free high-glucose (25 mM) DMEM (Dulbecco's modified Eagle's medium; Gibco Life Technologies, Waltham, MA). HCT116 cells and Bax/Bak$^{-/-}$ HCT116 cells
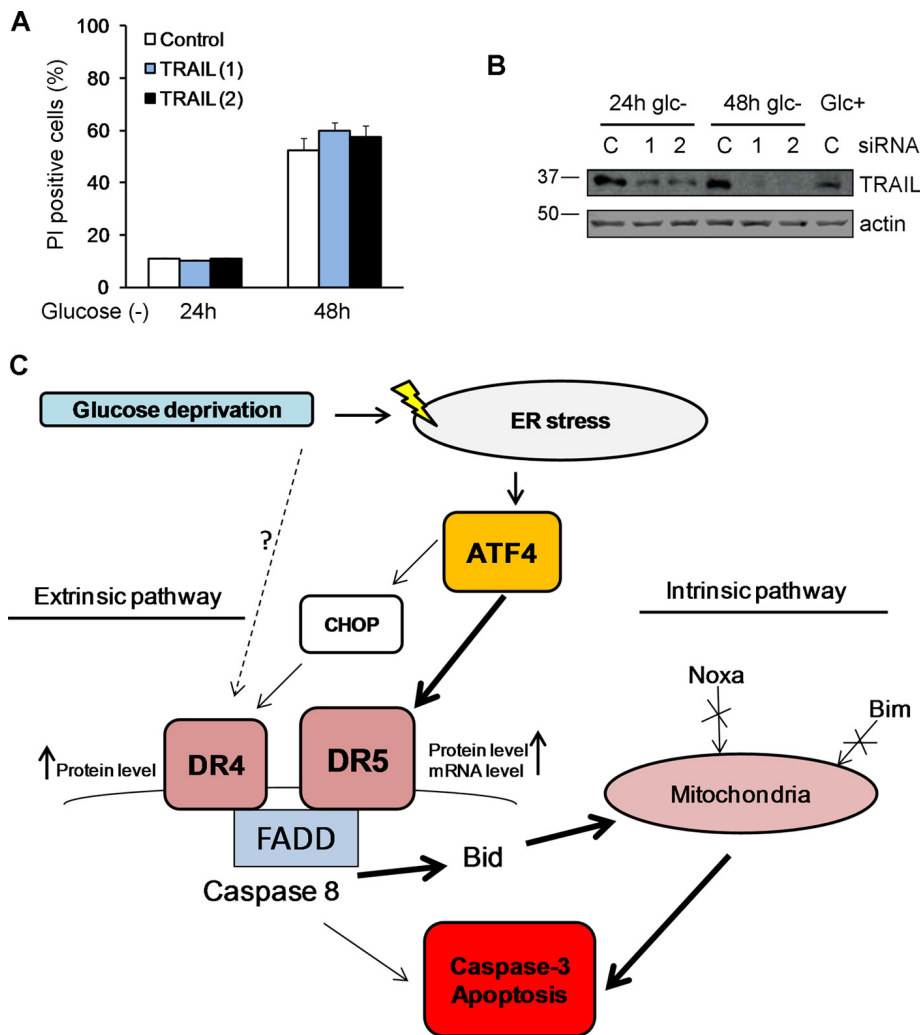
FIG 10 TRAIL does not participate in cell death. HeLa cells were transfected with 50 nM TRAIL siRNAs or the control siRNA. At 24 h posttransfection, cells were incubated with or without glucose for 24 and 48 h. (A) Averages and SEM of data from three experiments to determine PI incorporation by FACS analysis. (B) Western blotting of cells incubated for 24 h or 48 h without glucose or for 24 h with glucose and transfected with control, TRAIL (1), or TRAIL (2) siRNA. (C) Summary of pathways leading to cell death of glucose-deprived HeLa cells.

(provided by M. Rehm, Royal College of Surgeons Ireland) were cultured in RPMI medium supplemented with 10% FBS (fetal bovine serum; Invitrogen, Carlsbad, CA), 200 mg/ml of penicillin (Invitrogen), 100 mg/ml of streptomycin (Invitrogen), and 2 mM glutamine (Invitrogen). Cells were maintained at 37°C in a 5% CO_2 atmosphere and split 3 times per week by using a 0.05% trypsin–EDTA solution (Invitrogen). For glucose deprivation treatment, cells were plated at a concentration of 150,000 cells/ml in 6-well plates or 60-mm dishes (BD) and treated 24 h later, when they reached a concentration of 500,000 cells/ml, corresponding to 80% confluence. Cells were washed twice with FBS-free, pyruvate-free, glucose-free DMEM (Gibco Life Technologies) and then treated with this medium supplemented with 200 mg/ml penicillin, 100 mg/ml streptomycin, freshly added 2 mM glutamine, and 10% dialyzed FBS. The same procedure was used for treating Bax/Bak$^{-/-}$ HCT116 cells by using glucose-free RPMI medium (Gibco Life Technologies). Q-VD-OPH (apeXbio, Houston, TX) and Ac-Y-VAD-cmk (Sigma-Aldrich, St. Louis, MO) were used at 10 μM, Z-VAD-fmk (apeXbio) was used at 20 μM, and all components were added at the moment of treatment. The same amount of dimethyl sulfoxide (DMSO) was added to control wells. TNF-α (Peprotech, Le-Perray-en-Yvelines, France) was used at 10 ng/ml in combination with 10 μM cycloheximide. Necrostatin-1 (catalog number BML-AP309-0020; Enzo, Farmingdale, NY) was used at 40 and 100 μM, while a RIPK3 inhibitor (GSK'872; Calbiochem, Darmstadt, Germany) was used at 1 and 3 μM. Fas human-activating CH11 antibody (Millipore, Darmstadt, Germany) was used at 50 ng/ml. Thapsigargin (Sigma-Aldrich) was used at 300 ng/ml.

siRNA transfection. HeLa and Bax/Bak$^{-/-}$ HCT116 cells were plated into 6-well plates at a confluence of 50% and transfected 5 h later. A transfecting solution containing 50 nM each siRNA and 1 μl/ml Dharmafect1 (Fisher-Thermo Scientific, Waltham, MA) was incubated for 30 min in DMEM without serum and antibiotics and then added to the cells that had previously been incubated in DMEM without

antibiotics. Cells were maintained in transfection medium for 24 h or 48 h in the case of FADD siRNAs before treatments were performed. Control sequences were a nontargeting sequence (5'-UAAGGCUAU GAGAGAUAC-3') and an On-Target control (Dharmacon, Lafayette, CO). siRNA sequences were 5'-GCC UAGGUCUCUUAGAUGA-3' for ATF4 (1), 5'-CCAGAUCAAUCCUUUAGUUUA-3' for ATF4 (2), 5'-GAAGACAUCAUCCGGAAUA-3' for Bid (1), 5'-CAGGGAUGAGUGCAUCACAAA-3' for Bid (2), 5'-GCACCCAU GAGUUGUGACA-3' for Bim (1), 5'-GACCGAGAAGGUAGACAAUUG-3' for Bim (2), Dharmacon On-Target Plus siRNA pools of 4 oligonucleotides for caspase-8 in HCT116 cells, 5'-GGAGCUGCUCUUCCGAAUU-3' for caspase-8 in HeLa cells, 5'-AAGAACCAGCAGAGGUCACAA-3' for CHOP (1), 5'-GCCUGGUAUGAGGAC CUGC for CHOP(2), 5'-CACCAAUGCUUCCAACAAU-3' for DR4 (1), 5'-AACGAGAUUCUGAGCAACGCA-3' for DR4 (2), 5'-GACCCUUGUGCUCGUUGUC-3' for DR5 (Tot), 5'-CCUGUUCUCUCUCAGGCAUUU-3' for DR5L (1), 5'-UGUGCUUUGUACCUGAUUCUU-3' for DR5L (2), 5'-UAUGAUGCCUGAUUCUUUGUG-3' for DR5S, 5'-GAUUGGAGAAGGCUGGCUC-3' for FADD (1), 5'-GAACUCAAGCUGCGUUUAU-3' for FADD (2), 5'-GGU GCACGUUUCAUCAAUU-3' for Noxa (1), 5'-GCUACUCAACUCAGGAGAUTT-3' for Noxa (2), 5'-GAUCUGCG AUGGCUGCAAUUU-3' for p62 (1), 5'-GCAUUGAAGUUGAUAUCGAU-3' for p62 (2), an On-Target Plus siRNA pool of 4 oligonucleotides for RIPK1, 5'-AACGAGCUGAAGCAGAUGCAG-3' for TRAIL (1), and 5'-UUGUUUGUCGUUCUUUGUGUU-3' for TRAIL (2).

Generation of knockout cell lines via CRISPR-Cas9. HeLa cells (10^5 cells/well in 6-well plates) were transfected with 1 μg plasmid plentiCas9-BLAST (Addgene plasmid 52962) by using GenJet, followed 24 h later by selection with blasticidin (6 mg/ml) for 7 days. Blasticidin-resistant cells were then seeded as single cells into 96-well plates. After 3 to 4 weeks, colonies derived from single clones were screened for Cas9 expression by immunoblotting. Targeted single guide RNAs (sgRNAs) were designed with the help of the Broad Institute sgRNA design tool (http://portals.broadinstitute.org/gpp/public/analysis-tools/ sgrna-design) and cloned into pLentiguidePuro (Addgene plasmid 52963). HeLa cells stably expressing Cas9, generated as described above, were transfected with plasmids containing sgRNAs of interest by using GenJet and selected with 250 ng/ml puromycin for 7 days. Puromycin-resistant cells were seeded as single colonies into 96-well plates. After 3 to 4 weeks, colonies derived from single clones were screened for the expression of proteins of interest by immunoblotting. Sequences are GCGGGGAGGAT TGAACCACG for DR4 sgRNA 1, AAGTGTGGGGCTCTTCCGCG for DR4 sgRNA 2, CCAGGACCCAGGGAGG CGCG for DR5 sgRNA 1, CCTAGCTCCCAGCAGAGAG for DR5 sgRNA 2, GAGGCATAGGAACTTGAGCT for FADD sgRNA 1, GCTCCAGCAGCATGGAGAAG for FADD sgRNA 2, CCAGCTGGACAGTGTCCCGA for CHOP sgRNA 1, and AGCACATCTGCAGGATAATG for CHOP sgRNA 2. Controls used for experiments were cells transfected with the empty vector and subjected to the same procedures.

Cell death analysis. Cell death analysis was performed quantifying propidium iodide (PI) incorporation by fluorescence-activated cell sorter (FACS) analysis. After treatment, adherent cells and dead cells in suspension were collected by trypsinization and centrifuged at $450 \times g$ for 7 min. The cells were then resuspended in a final volume of 300 μl of phosphate-buffered saline (PBS) plus 0.5 μg/ml of PI and analyzed by using a Gallios flow cytometer (Beckman Coulter). Quantification was done by using FlowJo software version 7.6.4. A lactate dehydrogenase (LDH) test (Promega, Fitchburg, WI) was also used to measure cell death. After treatment, 50 μl of conditioned medium was resuspended in reactive solution and incubated for 30 min at 37°C in a 96-well plate. The absorbance at 490 nm was acquired by using a BioTek PowerWave XS microplate spectrophotometer. Cell death of knockout (CRISPR) cell lines was analyzed by counting dead cells under an inverted microscope. A total of 150 cells per well and 3 wells per condition were counted.

Immunoprecipitation. After treatment, cells were collected by using immunoprecipitation (IP) buffer (20 mM Tris-HCl [pH 7.5], 137 mM NaCl, 1% Triton X-100, 2 mM EDTA [pH 8]) containing protease inhibitors (Roche, Basel, Switzerland), lysed on ice for 20 min, sonicated, and quantified by using a bicinchoninic acid (BCA) colorimetric kit (Pierce-Thermo Scientific, Waltham, MA) according to the manufacturer's instructions. The Pure Proteome protein G magnetic bead system (Millipore) was used for immunoprecipitation. Twenty-five microliters of magnetic beads under each condition was blocked by incubation with IP buffer including 1% bovine serum albumin (BSA) for 1 h at 4°C under rotation. The beads were then incubated with 1 μg of primary antibodies for 3 to 4 h at 4°C under rotation. This solution was replaced with 1,200 μg of lysates in 1 ml of IP buffer supplemented with protease inhibitors (Roche), and the mixture was incubated overnight at 4°C under rotation. Beads were then washed 3 to 4 times with IP buffer, and proteins were eluted with IP buffer plus 2% SDS and then incubated with Laemmli buffer (with freshly added 2-mercaptoethanol) and warmed at 95°C for 10 min before being loaded onto an SDS-PAGE gel. Inputs were total lysates and represent 5% of the immunoprecipitated fraction. Primary antibodies used for IP were anti-human caspase-8 p18 (C-20; Santa Cruz, Dallas, TX) and anti-p62 (catalog number BML-PW9860; Enzo, Farmingdale, NY). Anti-glutathione S-transferase (anti-GST) (rabbit IgG) and anti-green fluorescent protein (anti-GFP) (mouse IgG), used as isotype controls, were obtained from Rockland (Limerick, PA). Horseradish peroxidase (HRP)-conjugated Clean-Blot IP detection reagent (Thermo Scientific) was used as a secondary antibody for Western blotting of p62.

Western blotting. After treatments, cells were collected by trypsinization, mixed with floating cells, washed with PBS, and centrifuged at $500 \times g$. The pellet was resuspended in radioimmunoprecipitation assay (RIPA) buffer (Thermo Scientific) supplemented with protease inhibitors (Roche) and phosphatase inhibitors (Roche). The lysates were then sonicated and quantified by using BCA. Forty micrograms of proteins under each condition was prepared in a 40-μl final volume of 4× Laemmli buffer (63 mM Tris-HCl, 10% glycerol, 2% SDS, 0.01% bromophenol blue, 5% 2-mercaptoethanol) and warmed at 95°C for 10 min. The proteins were loaded onto an SDS-PAGE gel (Mini-protean; Bio-Rad, Hercules, CA) and run at 120 V for 1 h 30 min. The proteins were then transferred to an Immobilon-FL polyvinylidene difluoride (PVDF) membrane (Merck Chemicals, Darmstadt, Germany) using the Trans-Blot SD (Bio-Rad) semidry

system for 1 h at 200 mA. The transfer of the proteins was checked by Ponceau S staining (Sigma-Aldrich). Membranes were blocked with 5% nonfat dry milk in Tween–Tris-buffered saline (TBS) (TTBS) or in Odyssey blocking solution (Li-Cor Biosciences, Lincoln, NE) for 1 h at room temperature. The membranes were then incubated with primary antibodies generally diluted 1:1,000 in blocking solution for 1 to 2 h at room temperature or overnight at 4°C with agitation. The next day, the membranes were incubated with HRP-conjugated secondary antibodies diluted 1:5,000 in blocking buffer or with fluorescent secondary antibodies diluted 1:15,000 in a 1:1 solution of TBS-Odyssey blocking buffer for 1 h at room temperature. After 3 washes in TTBS, the membranes were developed with an enhanced chemiluminescence (ECL) reaction using a freshly prepared ECL reagent (Promega) or with the Odyssey infrared imaging system. Primary antibodies were antibodies to actin (C-4; ICN), ATF4 (C-20; Santa Cruz), Bid (catalog number 2002; Cell Signaling, Beverly, MA), cIAP1 (catalog number B75-1; Pharmingen, San Diego, CA), cIAP2 (catalog number AF8171; R&D, Minneapolis, MN), caspase-3 (catalog number 9662S; Cell Signaling), caspase-8 p18 (C-20; Santa Cruz), CHOP (catalog number F-168; Santa Cruz), DR4 (catalog number B-N28 [Diaclone, Besançon, France] or D9S1R [Cell Signaling]) for the data shown in Fig. 9F, DR5 (catalog number D4E9; Cell Signaling), FADD (catalog number H-10 [Santa Cruz] or 610400 [BD Transduction Laboratories]) for the data shown in Fig. 6F, GRP78 (N-20; Santa Cruz), PARP (catalog number 9542S; Cell Signaling), p62 (catalog number BML-PW9860; Enzo), RIPK1 (catalog number C38; Pharmingen), and TRAIL/TNFSF10 (catalog number 55B709.3; Novus Bio). HRP-conjugated secondary antibodies were anti-rabbit and anti-mouse antibodies from Zymax and anti-goat antibody from Rockland. Secondary anti-mouse, anti-rabbit, or anti-goat antibodies (IRDye 800CW donkey anti-rabbit, IRDye 680LT donkey anti-mouse, and IRDye 680CW donkey anti-goat antibodies) were obtained from Li-Cor Biosciences.

Immunocytochemistry. Cells were plated in 12-well plates (BD) on 12-mm round sterile coverslips precoated with a 0.1% poly-L-lysine solution (Sigma) at 37°C. Twenty-four hours later, cells were treated at a confluence of 70 to 80% without glucose for 24 h. Cells were then fixed with a PBS–4% paraformaldehyde solution (Merck) for 20 min at room temperature. Cells were washed 3 times with PBS for 5 min each and then incubated with blocking buffer (0.05% Triton, 3% BSA in PBS) for 1 h, with shaking, at room temperature. The cells were then incubated with primary antibodies diluted 1:200 in blocking buffer at 4°C overnight in a humid covered dish. The coverslips were washed 3 times with PBS for 5 min each and incubated for 1 h with secondary antibodies diluted 1:400 in blocking buffer at room temperature. Cells were then washed 3 times with PBS and once with 4′,6-diamidino-2-phenylindole (DAPI) diluted 1:10,000 in PBS for 10 min at room temperature. The coverslips were then mounted by using 3 μl of Vectashield solution (Vector Laboratories, Burlingame, CA) and allowed to dry for at least 1 day. Photographs at different zooms were acquired by using the Suite Advanced Fluorescence software application (2.6.0.7266; LAS AF) using a Leica TSC SP5 spectral confocal microscope with an HCX PLAPO lambda blue 63×, 1.4-numerical-aperture objective. Colocalization analysis was done by using the colocalization plug-in of Fiji/Image J software, measuring three images per experiment (~80 cells). The graphs show the averages and the standard deviations of data from at least three independent experiments. Primary antibodies used for immunocytochemistry were anticalnexin (catalog number AF18; Abcam), anti-human caspase-8 (C-20; Santa Cruz), anti-DR5 (catalog number D4E9; Cell Signaling), anti-FADD (catalog number H-181; Santa Cruz), anti-GM130 (catalog number 35; BD Pharmingen), and anti-p62 (catalog number BML-PW9860; Enzo). Secondary antibodies were rabbit Alexa Fluor 568 (Life Technologies, Waltham, MA)-conjugated, mouse Alexa Fluor 647 (Life Technologies)-conjugated, and goat Alexa Fluor 488 (Life Technologies)-conjugated antibodies.

qPCR analysis. Cells were collected at room temperature by trypsinization, washed once with PBS, and centrifuged for 5 min at 300 × g. RNA was extracted from the pellets by using the RNeasy minikit (Qiagen, Valencia, CA) according to the manufacturer's instructions. One microgram of RNA under each condition was retrotranscribed to cDNA by using the High-Capacity cDNA reverse transcription kit from Applied Biosystems (Waltham, MA). qPCR analysis was performed by using LightCycler 480 SYBR green I Master solution (Roche) starting with 10 ng of cDNA per reaction mixture. Amplification was performed with a LightCycler 96-well plate (Roche) by using the following protocol: a preincubation step of 1 cycle at 95°C, amplification for 45 cycles at 95°C (primer-dependent temperature) and 72°C, a melting curve of 1 cycle at 95°C, 65°C, and 97°C; and cooling for 1 cycle at 40°C. The primers used for analyses were hTRAIL-R1 (DR4) (forward primer GCTGTGCTGATTGTCTGTTG and reverse primer TCGTTGTGAGCATTGTC CTC) and hTRAIL-R2 (DR5) (forward primer TGAGACCTTTCAGCTTCTGC and reverse primer ATCGTGAGT ATCTTGCAGCC). The housekeeping gene used for analysis was the RPL32 gene (forward primer AACG TCAAGGAGCTGGAAG and reverse primer GGGTTGGTGACTCTGATGG). Results were further normalized to the values for control treatment.

RT-PCR analysis of spliced XBP1. Total RNA was isolated by using the RNeasy minikit (Qiagen) according to the manufacturer's instructions. One microgram of RNA under each condition was retro-transcribed at cDNA by using the High-Capacity cDNA reverse transcription (RT) kit from Applied Biosystems. Amplification was performed with a 2720 thermal cycler (Applied Biosystems, Waltham, MA) by using the following protocol: 95°C for 5 min, 95°C for 1 min, 55°C for 1 min, and 72°C for 1 min for 34 cycles and 72°C for 1 min, 72°C for 5 min, and 16°C to the end. The primers used for analysis were forward primer TTACGAGAGAAAACTCATGGCC and reverse primer GGGTCCAAGTTGTCCAGAATGC. PCR products were analyzed on an 8% acrylamide gel.

Statistics. Error bars represent the standard errors of the means (SEM). The significance of data was measured by using two-tailed, paired Student's t test. Significant differences are marked as indicated in the figure legends.

REFERENCES

1. Choo AY, Kim SG, Vander Heiden MG, Mahoney SJ, Vu H, Yoon S-O, Cantley LC, Blenis J. 2010. Glucose addiction of TSC null cells is caused by failed mTORC1-dependent balancing of metabolic demand with supply. Mol Cell 38:487–499. https://doi.org/10.1016/j.molcel.2010.05.007.
2. DeBerardinis RJ, Sayed N, Ditsworth D, Thompson CB. 2008. Brick by brick: metabolism and tumor cell growth. Curr Opin Genet Dev 18:54–61. https://doi.org/10.1016/j.gde.2008.02.003.
3. Iurlaro R, León-Annicchiarico CL, Munoz-Pinedo C. 2014. Regulation of cancer metabolism by oncogenes and tumor suppressors. Methods Enzymol 542:59–80. https://doi.org/10.1016/B978-0-12-416618-9.00003-0.
4. El Mjiyad N, Caro-Maldonado A, Ramirez-Peinado S, Munoz-Pinedo C. 2011. Sugar-free approaches to cancer cell killing. Oncogene 30:253–264. https://doi.org/10.1038/onc.2010.466.
5. Degenhardt K, Mathew R, Beaudoin B, Bray K, Anderson D, Chen G, Mukherjee C, Shi Y, Gélinas C, Fan Y, Nelson DA, Jin S, White E. 2006. Autophagy promotes tumor cell survival and restricts necrosis, inflammation, and tumorigenesis. Cancer Cell 10:51–64. https://doi.org/10.1016/j.ccr.2006.06.001.
6. Leon-Annicchiarico CL, Ramirez-Peinado S, Dominguez-Villanueva D, Gonsberg A, Lampidis TJ, Munoz-Pinedo C. 2015. ATF4 mediates necrosis induced by glucose deprivation and apoptosis induced by 2-deoxyglucose in the same cells. FEBS J 282:3647–3658. https://doi.org/10.1111/febs.13369.
7. Caro-Maldonado A, Munoz-Pinedo C. 2011. Dying for something to eat: how cells respond to starvation. Open Cell Signal J 3:42–51. https://doi.org/10.2174/1876390101103010042.
8. Lowman XH, McDonnell MA, Kosloske A, Odumade OA, Jenness C, Karim CB, Jemmerson R, Kelekar A. 2010. The proapoptotic function of Noxa in human leukemia cells is regulated by the kinase Cdk5 and by glucose. Mol Cell 40:823–833. https://doi.org/10.1016/j.molcel.2010.11.035.
9. Zhao Y, Coloff JL, Ferguson EC, Jacobs SR, Cui K, Rathmell JC. 2008. Glucose metabolism attenuates p53 and puma-dependent cell death upon growth factor deprivation. J Biol Chem 283:36344–36353. https://doi.org/10.1074/jbc.M803580200.
10. Caro-Maldonado A, Tait SWG, Ramirez-Peinado S, Ricci JE, Fabregat I, Green DR, Munoz-Pinedo C. 2010. Glucose deprivation induces an atypical form of apoptosis mediated by caspase-8 in Bax-, Bak-deficient cells. Cell Death Differ 17:1335–1344. https://doi.org/10.1038/cdd.2010.21.
11. Qing G, Li B, Vu A, Skuli N, Walton ZE, Liu X, Mayes PA, Wise DR, Thompson CB, Maris JM, Hogarty MD, Simon MC. 2012. ATF4 regulates MYC-mediated neuroblastoma cell death upon glutamine deprivation. Cancer Cell 22:631–644. https://doi.org/10.1016/j.ccr.2012.09.021.
12. Ramírez-Peinado S, Alcázar-Limones F, Lagares-Tena L, El Mjiyad N, Caro-Maldonado A, Tirado OM, Muñoz-Pinedo C. 2011. 2-Deoxyglucose induces noxa-dependent apoptosis in alveolar rhabdomyosarcoma. Cancer Res 71:6796–6806. https://doi.org/10.1158/0008-5472.CAN-11-0759.
13. Shin S, Buel GR, Wolgamott L, Plas DR, Asara JM, Blenis J, Yoon SO. 2015. ERK2 mediates metabolic stress response to regulate cell fate. Mol Cell 59:382–398. https://doi.org/10.1016/j.molcel.2015.06.020.
14. Llambi F, Moldoveanu T, Tait SW, Bouchier-Hayes L, Temirov J, McCormick LL, Dillon CP, Green DR. 2011. A unified model of mammalian BCL-2 protein family interactions at the mitochondria. Mol Cell 44:517–531. https://doi.org/10.1016/j.molcel.2011.10.001.
15. He S, Wang L, Miao L, Wang T, Du F, Zhao L, Wang X. 2009. Receptor interacting protein kinase-3 determines cellular necrotic response to TNF-alpha. Cell 137:1100–1111. https://doi.org/10.1016/j.cell.2009.05.021.
16. Vandenabeele P, Grootjans S, Callewaert N, Takahashi N. 2013. Necrostatin-1 blocks both RIPK1 and IDO: consequences for the study of cell death in experimental disease models. Cell Death Differ 20:185–187. https://doi.org/10.1038/cdd.2012.151.
17. Zhang J, Fan J, Venneti S, Cross JR, Takagi T, Bhinder B, Djaballah H, Kanai M, Cheng EH, Judkins AR, Pawel B, Baggs J, Cherry S, Rabinowitz JD, Thompson CB. 2014. Asparagine plays a critical role in regulating cellular adaptation to glutamine depletion. Mol Cell 56:205–218. https://doi.org/10.1016/j.molcel.2014.08.018.
18. Palorini R, Cammarata FP, Balestrieri C, Monestiroli A, Vasso M, Gelfi C, Alberghina L, Chiaradonna F. 2013. Glucose starvation induces cell death in K-ras-transformed cells by interfering with the hexosamine biosynthesis pathway and activating the unfolded protein response. Cell Death Dis 4:e732. https://doi.org/10.1038/cddis.2013.257.
19. Muaddi H, Majumder M, Peidis P, Papadakis AI, Holcik M, Scheuner D, Kaufman RJ, Hatzoglou M, Koromilas AE. 2010. Phosphorylation of eIF2alpha at serine 51 is an important determinant of cell survival and adaptation to glucose deficiency. Mol Biol Cell 21:3220–3231. https://doi.org/10.1091/mbc.E10-01-0023.
20. Martin-Perez R, Niwa M, Lopez-Rivas A. 2012. ER stress sensitizes cells to TRAIL through down-regulation of FLIP and Mcl-1 and PERK-dependent up-regulation of TRAIL-R2. Apoptosis 17:349–363. https://doi.org/10.1007/s10495-011-0673-2.
21. Iurlaro R, Munoz-Pinedo C. 2016. Cell death induced by endoplasmic reticulum stress. FEBS J 283:2640–2652. https://doi.org/10.1111/febs.13598.
22. Lu M, Lawrence DA, Marsters S, Acosta-Alvear D, Kimmig P, Mendez AS, Paton AW, Paton JC, Walter P, Ashkenazi A. 2014. Opposing unfolded-protein-response signals converge on death receptor 5 to control apoptosis. Science 345:98–101. https://doi.org/10.1126/science.1254312.
23. Martin-Perez R, Palacios C, Yerbes R, Cano-Gonzalez A, Iglesias-Serret D, Gil J, Reginato MJ, Lopez-Rivas A. 2014. Activated ERBB2/HER2 licenses sensitivity to apoptosis upon endoplasmic reticulum stress through a PERK-dependent pathway. Cancer Res 74:1766–1777. https://doi.org/10.1158/0008-5472.CAN-13-1747.
24. Yamaguchi H, Wang HG. 2004. CHOP is involved in endoplasmic reticulum stress-induced apoptosis by enhancing DR5 expression in human carcinoma cells. J Biol Chem 279:45495–45502. https://doi.org/10.1074/jbc.M406933200.
25. Jiang CC, Chen LH, Gillespie S, Kiejda KA, Mhaidat N, Wang YF, Thorne R, Zhang XD, Hersey P. 2007. Tunicamycin sensitizes human melanoma cells to tumor necrosis factor-related apoptosis-inducing ligand-induced apoptosis by up-regulation of TRAIL-R2 via the unfolded protein response. Cancer Res 67:5880–5888. https://doi.org/10.1158/0008-5472.CAN-07-0213.
26. Feoktistova M, Geserick P, Kellert B, Dimitrova DP, Langlais C, Hupe M, Cain K, MacFarlane M, Hacker G, Leverkus M. 2011. cIAPs block ripoptosome formation, a RIP1/caspase-8 containing intracellular cell death complex differentially regulated by cFLIP isoforms. Mol Cell 43:449–463. https://doi.org/10.1016/j.molcel.2011.06.011.
27. Tenev T, Bianchi K, Darding M, Broemer M, Langlais C, Wallberg F, Zachariou A, Lopez J, MacFarlane M, Cain K, Meier P. 2011. The ripop-

tosome, a signaling platform that assembles in response to genotoxic stress and loss of IAPs. Mol Cell 43:432–448. https://doi.org/10.1016/j.molcel.2011.06.006.

28. Jin Z, Li Y, Pitti R, Lawrence D, Pham VC, Lill JR, Ashkenazi A. 2009. Cullin3-based polyubiquitination and p62-dependent aggregation of caspase-8 mediate extrinsic apoptosis signaling. Cell 137:721–735. https://doi.org/10.1016/j.cell.2009.03.015.

29. Pan JA, Ullman E, Dou Z, Zong WX. 2011. Inhibition of protein degradation induces apoptosis through a microtubule-associated protein 1 light chain 3-mediated activation of caspase-8 at intracellular membranes. Mol Cell Biol 31:3158–3170. https://doi.org/10.1128/MCB.05460-11.

30. Ramírez-Peinado S, León-Annicchiarico CL, Galindo-Moreno J, Iurlaro R, Caro-Maldonado A, Prehn JHM, Ryan KM, Muñoz-Pinedo C. 2013. Glucose starved cells do not engage in pro-survival autophagy. J Biol Chem 288:30387–30398. https://doi.org/10.1074/jbc.M113.490581.

31. Li T, Su L, Lei Y, Liu X, Zhang Y, Liu X. 2015. DDIT3 and KAT2A proteins regulate TNFRSF10A and TNFRSF10B expression in endoplasmic reticulum stress-mediated apoptosis in human lung cancer cells. J Biol Chem 290:11108–11118. https://doi.org/10.1074/jbc.M115.645333.

32. Ye J, Kumanova M, Hart LS, Sloane K, Zhang H, De Panis DN, Bobrovnikova-Marjon E, Diehl JA, Ron D, Koumenis C. 2010. The GCN2-ATF4 pathway is critical for tumour cell survival and proliferation in response to nutrient deprivation. EMBO J 29:2082–2096. https://doi.org/10.1038/emboj.2010.81.

33. Zagorodna O, Martin SM, Rutkowski DT, Kuwana T, Spitz DR, Knudson CM. 2012. 2-Deoxyglucose-induced toxicity is regulated by Bcl-2 family members and is enhanced by antagonizing Bcl-2 in lymphoma cell lines. Oncogene 31:2738–2749. https://doi.org/10.1038/onc.2011.454.

34. Munoz-Pinedo C, Ruiz-Ruiz C, Ruiz de Almodovar C, Palacios C, Lopez-Rivas A. 2003. Inhibition of glucose metabolism sensitizes tumor cells to death receptor-triggered apoptosis through enhancement of death-inducing signaling complex formation and apical procaspase-8 processing. J Biol Chem 278:12759–12768. https://doi.org/10.1074/jbc.M212392200.

35. Nam SY, Amoscato AA, Lee YJ. 2002. Low glucose-enhanced TRAIL cytotoxicity is mediated through the ceramide-Akt-FLIP pathway. Oncogene 21:337–346. https://doi.org/10.1038/sj.onc.1205068.

36. Chan FK, Chun HJ, Zheng L, Siegel RM, Bui KL, Lenardo MJ. 2000. A domain in TNF receptors that mediates ligand-independent receptor assembly and signaling. Science 288:2351–2354. https://doi.org/10.1126/science.288.5475.2351.

37. Wei MC, Zong W-X, Cheng EHY, Lindsten T, Panoutsakopoulou V, Ross AJ, Roth KA, MacGregor GR, Thompson CB, Korsmeyer SJ. 2001. Proapoptotic BAX and BAK: a requisite gateway to mitochondrial dysfunction and death. Science 292:727–730. https://doi.org/10.1126/science.1059108.

REVIEW ARTICLE

Endoplasmic reticulum stress signalling – from basic mechanisms to clinical applications

Aitor Almanza[1], Antonio Carlesso[2], Chetan Chintha[1], Stuart Creedican[3], Dimitrios Doultsinos[4,5], Brian Leuzzi[1], Andreia Luís[6], Nicole McCarthy[7], Luigi Montibeller[8], Sanket More[9], Alexandra Papaioannou[4,5], Franziska Püschel[10], Maria Livia Sassano[9], Josip Skoko[11], Patrizia Agostinis[9], Jackie de Belleroche[8], Leif A. Eriksson[2], Simone Fulda[7], Adrienne M. Gorman[1] (iD), Sandra Healy[1], Andrey Kozlov[6], Cristina Muñoz-Pinedo[10] (iD), Markus Rehm[11], Eric Chevet[4,5] (iD) and Afshin Samali[1]

1 Apoptosis Research Centre, National University of Ireland, Galway, Ireland
2 Department of Chemistry and Molecular Biology, University of Gothenburg, Göteborg, Sweden
3 Randox Teoranta, Dungloe, County Donegal, Ireland
4 INSERM U1242, University of Rennes, France
5 Centre de Lutte Contre le Cancer Eugène Marquis, Rennes, France
6 Ludwig Boltzmann Institute for Experimental and Clinical Traumatology, AUVA Research Centre, Vienna, Austria
7 Institute for Experimental Cancer Research in Paediatrics, Goethe-University, Frankfurt, Germany
8 Neurogenetics Group, Division of Brain Sciences, Faculty of Medicine, Imperial College London, UK
9 Department Cellular and Molecular Medicine, Laboratory of Cell Death and Therapy, KU Leuven, Belgium
10 Cell Death Regulation Group, Oncobell Program, Bellvitge Biomedical Research Institute (IDIBELL), Barcelona, Spain
11 Institute of Cell Biology and Immunology, University of Stuttgart, Germany

The endoplasmic reticulum (ER) is a membranous intracellular organelle and the first compartment of the secretory pathway. As such, the ER contributes to the production and folding of approximately one-third of cellular proteins, and is thus inextricably linked to the maintenance of cellular homeostasis and the fine balance between health and disease. Specific ER stress signalling pathways, collectively known as the unfolded protein response (UPR), are required for maintaining ER homeostasis. The UPR is triggered when ER protein folding capacity is overwhelmed by cellular

Abbreviations

4-PBA, 4-phenylbutyric acid; ALS, amyotrophic lateral sclerosis; ATF4, activating transcription factor 4; ATF6f, cytosolic domain of ATF6; ATF6α, activating transcription factor 6 α; ATF6β, activating transcription factor 6 β; BBF2H7, cAMP responsive element-binding protein 3 like 2; BiP, binding immunoglobulin protein (gene *GRP78*); bZIP, basic-leucine zipper; CHOP, CAAT/enhancer-binding protein (C/EBP) homologous protein; CRCL, chaperone-rich cell lysate; CREB3L3, cAMP responsive element-binding protein 3 like 3; CREB, cAMP response element-binding protein; eIF2B, eukaryotic translation initiation factor 2B; eIF2α, eukaryotic translation initiation factor 2α; ERAD, ER-associated protein degradation; ER, endoplasmic reticulum; ERN1, endoplasmic reticulum to nucleus signalling 1; ERN2, endoplasmic reticulum to nucleus signalling 2; ERO-1, ER oxidoreductin 1; ERα, oestrogen receptor α; GADD34, growth arrest and DNA-damage-inducible 34; GRP78, glucose-regulated protein 78; GSH, glutathione; IBD, inflammatory bowel disease; IRE1α, inositol-requiring enzyme 1 α; IRE1β, inositol-requiring enzyme 1 β; LUMAN, cAMP responsive element-binding protein 3 or CREB3; MAM, mitochondria-associated membrane; MBTPS1, membrane bound transcription factor peptidase, site 1; MBTPS2, membrane bound transcription factor peptidase, site 2; MDM1/SNX13, mitochondrial distribution and morphology 1/sorting nexin 13; mTOR, mammalian target of rapamycin; N-ATF6, N-terminal portion of ATF6 or ATF6f; NF-Y, nuclear transcription factor Y; NGLY1, *N*-glycanase; NPR, NADPH-P450 reductase; OASIS, cAMP responsive element-binding protein 3 like 1; ORAI1, calcium release-activated calcium channel protein 1; PDI, protein disulfide isomerase; p-eIF2α, phospho-eIF2α; PERK, protein kinase RNA-like (PKR-like) endoplasmic reticulum kinase; PKR, protein kinase RNA-activated; PM, plasma membrane; PP1, protein phosphatase type 1; qPCR, quantitative polymerase chain reaction; RER, rough endoplasmic reticulum; RIDD, regulated IRE1-dependent decay; ROS, reactive oxygen species; SEC22b, vesicle-trafficking protein SEC22b; SERCA, sarco/endoplasmic reticulum ATPase Ca^{2+}-ATPase; SER, smooth endoplasmic reticulum; TAD, transcriptional activation domain; TRAF2, tumour necrosis factor receptor-associated factor 2; TUDCA, tauroursodeoxycholic acid; UDCA, ursodeoxycholic acid; UPR, unfolded protein response; WT, wild-type; XBP1s, spliced isoform of XBP1; XBP1u, unspliced isoform of XBP1; XBP1, X-box binding protein 1.

Fax: +33 (0)299253164
Tel: +33 (0)223237258
E-mail: eric.chevet@inserm.fr
A. Samali, Apoptosis Research Centre,
Biomedical Sciences, NUI Galway, Dangan,
Galway, Ireland
Fax: +353 91 494596
Tel: +353 91 492440
E-mail: afshin.samali@nuigalway.ie

Aitor Almanza, Antonio Carlesso, Chetan
Chintha, Stuart Creedican, Dimitrios
Doultsinos, Brian Leuzzi, Andreia Luís,
Nicole McCarthy, Luigi Montibeller, Sanket
More, Alexandra Papaioannou, Franziska
Püschel, Maria Livia Sassano and Josip
Skoko contributed equally to this work and
are listed in alphabetical order.

demand and the UPR initially aims to restore ER homeostasis and normal cellular functions. However, if this fails, then the UPR triggers cell death. In this review, we provide a UPR signalling-centric view of ER functions, from the ER's discovery to the latest advancements in the understanding of ER and UPR biology. Our review provides a synthesis of intracellular ER signalling revolving around proteostasis and the UPR, its impact on other organelles and cellular behaviour, its multifaceted and dynamic response to stress and its role in physiology, before finally exploring the potential exploitation of this knowledge to tackle unresolved biological questions and address unmet biomedical needs. Thus, we provide an integrated and global view of existing literature on ER signalling pathways and their use for therapeutic purposes.

Introduction

The endoplasmic reticulum (ER) is a cellular organelle that was first visualized in chicken fibroblast-like cells using electron microscopy and was described as a 'delicate lace-work extending throughout the cytoplasm' [1]. Its current name was coined almost 10 years later by Porter in 1954 [2]. The ER appears as a membranous network of elongated tubules and flattened discs that span a great area of the cytoplasm [3]. This membrane encloses the ER lumen and allows for the transfer of molecules to and from the cytoplasm.

ER structure

The ER is classically divided into the rough ER (RER) and smooth ER (SER), depending on the presence or absence of ribosomes on the cytosolic face of the membrane respectively. The SER and RER can exist either as interconnected or spatially separated compartments [4]. More recently, a novel classification was proposed based on membrane structure rather than appearance. According to this classification, the ER comprises the nuclear envelope, sheet-like cisternae and a polygonal array of tubules connected by three-way junctions [5]. A striking difference between these ER structures is the curvature of the membrane, whereby ER tubules possess a high membrane curvature compared to the sheets of the nuclear envelope and cisternae. The ER occupies an extensive cell-type-specific footprint within the cell and is in contact with many other intracellular organelles. It forms physical contact sites with mitochondria named mitochondria-associated membranes (MAMs), which play a crucial role in Ca^{2+} homeostasis [6]. It also comes in contact with the plasma membrane (PM), an interaction regulated by proteins like stromal interaction molecule 1 in the ER and calcium release-activated calcium channel protein 1 in the PM which are controlled by Ca^{2+} levels [7]. Vesicle-trafficking protein SEC22b (SEC22b) and vesicle-associated membrane protein 7 are also involved in the stabilization of ER-PM contacts and PM expansion [8]. The ER also interacts with endosomes [9] and is tethered by StAR-related lipid transfer protein 3 and StAR-related lipid transfer protein 3 [10], which also contribute to cholesterol maintenance in endosomes [11]. Interestingly, an ER interaction with the endolysosomal system, mediated by the mitochondrial distribution and morphology 1/sorting nexin 13 (MDM1/SNX13) complex [12], suggests ER involvement in autophagy. Indeed, a specialized ER structure called the omegasome forms contact sites with the phagophore, which elongates and becomes a mature autophagosome [13,14] (Fig. 1). In this way, the ER on its own or in coordination with other cell
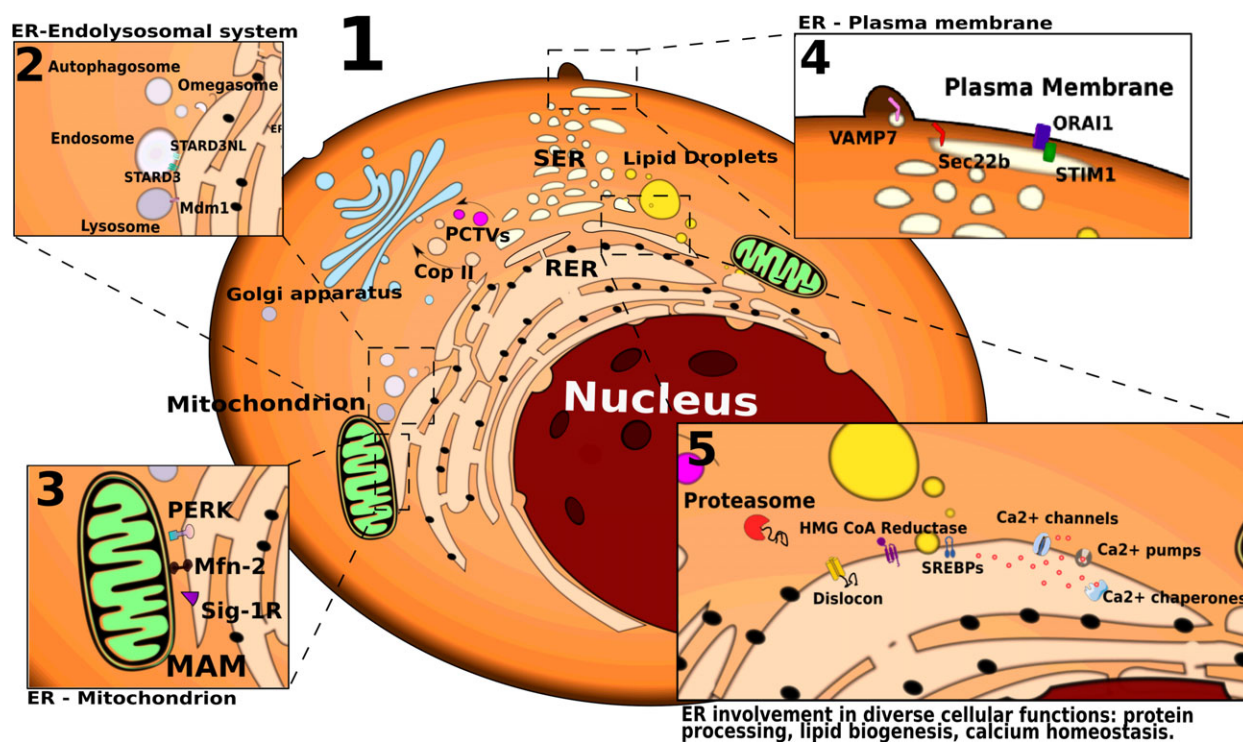
Fig. 1. ER molecular machines and contact sites with other organelles. The ER is primarily subdivided into the SER and RER, with the latter characterized by the presence of ribosomes at its cytosolic surface. Alternatively, the ER has been recently classified into the nuclear envelope, ER sheet-like cisternae and tubular ER (panel 1). The ER forms multiple membrane contact sites with other organelles, including the endosomes and lysosomes (through STARD3, STARD3NL, Mdm1; panel 2), the mitochondria (through Mfn-2, Sig-1R, PERK; panel 3), and the PM (through ORAI1, STIM1, Sec22b, VAMP7; panel 4) with various functional implications. The ER plays instrumental roles in secretory and transmembrane protein folding and quality control, protein and lipid trafficking, lipid metabolism, and Ca^{2+} homeostasis, all of these processes being mediated by a diverse series of ER resident proteins (schematically depicted in panels 1 and 5).

organelles exerts its multifaceted roles in the functionality of the cell as it is discussed in the next sections.

ER functions

The ER is involved in many different cellular functions. It acts as a protein synthesis factory, contributes to the storage and regulation of calcium, to the synthesis and storage of lipids, and to glucose metabolism [3]. These diverse functions indicate a pivotal role for the ER as a dynamic 'nutrient sensing' organelle that coordinates energetic fluctuations with metabolic reprogramming responses, regulating metabolism and cell fate decisions (Fig. 1).

Protein folding and quality control

The ER is involved in secretory and transmembrane protein synthesis, folding, maturation, quality control and degradation, and ensures that only properly folded proteins are delivered to their site of action [15]. About 30% of all proteins are cotranslationally targeted to the

ER [16] where they are exposed to an environment abundant in chaperones and foldases that facilitate their folding, assembly and post-translational modification before they are exported from the ER [16]. Protein processing within the ER includes signal sequence cleavage, N-linked glycosylation, formation, isomerization or reduction of disulfide bonds [catalysed by protein disulfide isomerases (PDIs), oxidoreductases], isomerization of proline or lipid conjugation, all of which ultimately result in a properly folded conformation [16–19]. Misfolded proteins are potentially detrimental to cell function and are therefore tightly controlled. Although protein misfolding takes place continually, it can be exacerbated during adverse intrinsic and environmental conditions. The ER has developed quality control systems to ensure that there are additional opportunities to correct misfolded proteins or, if terminally misfolded, to be disposed of by the cell. Terminally misfolded secretory proteins are eliminated by a process called ER-associated degradation (ERAD) [20]. Proteins are first recognized by an ER resident luminal and transmembrane protein machinery, then retrotranslocated into

the cytosol by a channel named dislocon [21] and the cytosolic AAA+ ATPase p97 [22], deglycosylated by N-glycanase (NGLY1; [23]) and targeted for degradation via the ubiquitin–proteasome pathway [20,24,25] (Fig. 1).

Lipid synthesis

The ER also plays essential roles in membrane production, lipid droplet/vesicle formation and fat accumulation for energy storage. Lipid synthesis is localized at membrane interfaces and organelle contact sites, and the lipid droplets/vesicles are exported in a regulated fashion. The ER dynamically changes its membrane structure to adapt to the changing cellular lipid concentrations. The ER contains the sterol regulatory element-binding protein family of cholesterol sensors ensuring cholesterol homeostasis [26]. This compartment also hosts enzymes catalysing the synthesis of cell membrane lipid components, namely sterols, sphingolipids and phospholipids [27]. The synthesis of those lipids from fatty acyl-CoA and diacylglycerols takes place at the ER membrane [28], which also hosts 3-hydroxy-3-methyl-glutaryl-coenzyme A reductase, the rate-limiting enzyme of the mevalonate/isoprenoid pathway that produces sterol and isoprenoid precursors [29]. Precursors made by ER membrane-localized enzymes are subsequently converted into structural lipids, sterols, steroid hormones, bile acids, dolichols, prenyl donors and a myriad of isoprenoid species with key functions for cell metabolism. Interestingly, MAMs have been identified as a privileged site of sphingolipid synthesis [30] (Fig. 1).

ER export

Most of the proteins and lipids synthesized in the ER must be transported to other cellular structures, which occurs mostly through the secretory pathway. To maintain the constant anabolic flux, export needs to be tightly regulated, and defects in secretion can lead to serious structural and functional consequences for the ER. Central to this export process is the generation of ER COPII transport vesicles, named after the family of proteins that shapes and coats them [31]. In addition to COPII vesicle transport, several other mechanisms of lipid export have been described. A variety of lipids can be transported by nonvesicular mechanisms; for example, large lipoprotein cargo has been shown to be exported out of the ER in another type of vesicle termed prechylomicron transport vesicles [32] or to accumulate in lipid droplets (Fig. 1).

Ca^{2+} homeostasis

Ca^{2+} is involved as a secondary messenger in many intracellular and extracellular signalling networks, playing an essential role in gene expression, protein synthesis and trafficking, cell proliferation, differentiation, metabolism or apoptosis [33]. ER, as the main cellular compartment for Ca^{2+} storage, plays a pivotal role in the regulation of Ca^{2+} levels and reciprocally many ER functions are controlled in a Ca^{2+}-dependent way, thereby regulating the calcium homeostasis of the whole cell [34]. Consequently, both ER and cytosolic Ca^{2+} concentrations need to be highly spatiotemporally regulated in order for the ER to maintain a much increased physiological intraluminal Ca^{2+} concentration and oxidizing redox potential than the cytoplasm. To modulate these levels, the ER employs a number of mechanisms that control Ca^{2+} concentration on both sides of the membrane: (a) ER membrane ATP-dependent Ca^{2+} pumps for cytosol-to-lumen transport; (b) ER luminal Ca^{2+}-binding chaperones for sequestering free Ca^{2+}; and (c) ER membrane channels for the regulated release of Ca^{2+} into the cytosol. These mechanisms are facilitated by a tight communication between the ER and other organelles, such as the PM and the mitochondria, thereby supporting the cell needs.

Traditionally thought as a site of protein synthesis, recent evidence has established the involvement of the ER in many different cellular functions: from novel roles in lipid metabolism to connections with cytoskeletal structures or roles in cytoplasmic streaming, our view of the ER keeps rapidly expanding, placing it increasingly as a key organelle governing the whole cellular metabolism.

Perturbing ER functions

Conditions that disrupt ER homeostasis create a cellular state commonly referred to as 'ER stress'. The cellular response to ER stress involves the activation of adaptive mechanisms to overcome stress and restore ER homeostasis. This response is dependent on the perturbing agent/condition and the intensity/duration of the stress [35].

Intrinsic ER perturbations

Cell autonomous mechanisms can lead to ER perturbation and examples of this can be seen in several diseases, including cancer, neurodegenerative diseases and diabetes. The hallmarks of cancer such as genetic instability and mutations [36] can result in constitutive

activation of ER stress response pathways leading to cell growth, proliferation, differentiation and migration. In addition, the uncontrolled, rapid growth of cancer cells requires high protein production rates with a consequent impact on ER systems [37]. Many cancers have a high mutation load which results in an intrinsically higher level of ER stress. For example, melanoma has the highest mutation burden of any cancer and the sheer numbers of mutated proteins are a source of intrinsically higher ER stress levels. In chronic myeloid leukaemia, the fusion protein produced the Philadelphia chromosome, BCR-ABL1, is a constitutively active oncoprotein that enhances cell proliferation and interferes with Ca^{2+}-dependent apoptotic response [38]. In addition, mutation-driven ER stress can also induce senescence that contributes to chemoresistance [39]. ER stress has also been linked to several neurodegenerative diseases. For example, mutations in the ER resident vesicle-associated membrane protein-associated protein B in familial amyotrophic lateral sclerosis (ALS) are linked to induction of motor neuron death mediated by the alteration of ER stress signalling [40,41]. On the other hand, secretory cells such as pancreatic β cells have a highly developed ER to manage insulin production and release in response to increases in blood glucose. The C96Y insulin variant leads to its impaired biogenesis and ER accumulation in the Akita mouse. As the ER cannot cope with the mutation induced stress, beta cells die and type 1 diabetes develops [42,43]. Insulin mutation-related ER stress was also reported in neonatal diabetes [44,45].

Extrinsic perturbations

Microenvironmental stress

In tumours, the ER stress observed in rapidly proliferating cells is compounded by the fact that increased proliferation eventually depletes the microenvironment of nutrients and oxygen, causing local microenvironmental stress and resulting in hypoxia, starvation and acidosis, all of which cause ER stress and perturb protein, and possibly lipid synthesis [46]. Nutrient deprivation, and particularly glucose starvation, at least in part, promotes ER stress by impairing glycosylation.

Exposure to ER stressors

Several small molecules that induce ER stress through a variety of mechanisms have been identified [47,48]. Stressors such as tunicamycin [49,50], or 2-deoxyglucose [51] target the N-linked glycosylation of proteins,

whereas dithiothreitol inhibits protein disulfide bond formation[52]. Alternatively, Brefeldin A impairs ER-to-Golgi trafficking, thus causing a rapid and reversible inhibition of protein secretion [53]. Targeting the Sarco/ER Ca^{2+}-ATPase (SERCA) with compounds, such as thapsigargin and cyclopiazonic acid [54,55], induces ER stress by reducing ER Ca^{2+} concentration and impairing protein folding capacity.

Exposure to enhancers of ER homeostasis

Conversely, other molecules have been found that can alleviate ER stress. These include small molecules, peptides and proteostasis regulators. The frequently used 4-phenylbutyric acid (4-PBA) reduces the accumulation of misfolded proteins in the ER [56]. Tauroursodeoxycholic acid (TUDCA) is an endogenous bile acid able to resolve ER stress in islet cells [57]. TUDCA is the taurine conjugate of ursodeoxycholic acid (UDCA), an FDA-approved drug for primary biliary cirrhosis that is also able to alleviate ER stress [58]. The precise mode of action of such proteostasis modulators still remains elusive.

Temperature

Body temperature is crucial for the viability of metazoans; normal mammalian physiological temperatures are 36–37 °C. Deviations from this range can disrupt cellular homeostasis causing protein denaturation and/or aggregation [59]. Moreover, an acute increase in temperature, known as heat shock, causes the fragmentation of both ER and Golgi [59]. Heat preconditioning at mildly elevated temperatures (up to 40 °C) in mammalian cellular and animal models has been shown to lead to the development of thermotolerance, which is associated with an increase in the expression of several heat shock proteins and ER stress markers [60,61]. In addition, moderate hypothermia (28 °C) induces mild ER stress in human pluripotent stem cells, the activation of which may be sufficient to protect against severe stress through an effect known as ER hormesis [62,63].

Reactive oxygen species production and other perturbations

Several external agents can induce intracellular reactive oxygen species (ROS) production, and when ROS production exceeds the antioxidant capacity oxidative stress negatively affects protein synthesis and ER homeostasis [64]. ROS, including free radicals, are generated by the UPR-regulated oxidative folding

machinery in the ER [65] and in the mitochondria [66]. In this context, increased mitochondrial respiration and biogenesis promotes survival during ER stress through a reduction of ROS [67]. The ER provides an oxidizing environment to facilitate disulfide bond formation and this process is believed to contribute to as much as 25% of the overall ROS generated [68,69]. The interconnection between the ER and ROS is mediated by signalling pathways which involve glutathione (GSH)/glutathione disulfide, NADPH oxidase 4, NADPH-P450 reductase, Ca^{2+}, ER oxidoreductin 1 (ERO1) and PDI [70]. The latter, in particular, has been found upregulated in the central nervous system of Alzheimer's disease patients thus highlighting the relevance of these pathways in neurodegenerative disease [71]. Overall, from the sections above it is apparent that directly or indirectly impaired ER function contributes to disease development and treatment resistance.

ER stress consequences

In response to ER stress, cells trigger an adaptive signalling pathway called the unfolded protein response (UPR), which acts to help cells to cope with the stress by attenuating protein synthesis, clearing the unfolded/misfolded proteins and increasing the capacity of the ER to fold proteins.

The UPR

The UPR is a cellular stress response originating in the ER and is predominantly controlled by three major sensors: inositol requiring enzyme 1 (IRE1), protein kinase RNA-activated (PKR)-like ER kinase (PERK) and activating transcription factor 6 (ATF6). The ER luminal domains of all three ER stress sensors are normally bound by the ER resident chaperone, heat shock protein A5 [heat shock protein family A (Hsp70) member 5, also known as glucose-regulated protein 78 (GRP78) and binding immunoglobulin protein (gene *GRP78*) (BiP)], keeping them in an inactive state [72,73]. Accumulating misfolded proteins in the ER lumen engage BiP thus releasing the three sensors. A FRET UPR induction assay, developed to quantify the association and dissociation of the IRE1 luminal domain from BiP upon ER stress [74], demonstrated that the ER luminal co-chaperone ERdj4/DNAJB9 represses IRE1 by promoting a complex between BiP and the luminal stress-sensing domain of IRE1α [75]. Moreover, it has recently been reported that another ER luminal chaperone, Hsp47, displaces BiP from the IRE1 UPRosome to promote its oligomerization [76]. Once released from

BiP, IRE1 and PERK homodimerize or oligomerize and trans-autophosphorylate to activate their downstream pathways [72]. In contrast, BiP dissociation from AFT6 reveals an ER export motif [73] which facilitates its translocation to the Golgi apparatus [77]. This 'competition model' of UPR activation assumes that BiP acts as a negative regulator of UPR signalling. However, other BiP-dependent or independent models have been proposed (reviewed in [78]; Fig. 2).

IRE1 signalling

In humans, there are two paralogues of IRE1 (IRE1α and β), encoded by endoplasmic reticulum to nucleus signalling 1 and 2 (*ERN1* and *ERN2*), respectively [79–81]. Both human IRE1 isoforms share significant sequence homology (39%) [20]. IRE1α (referred to IRE1 hereafter) is ubiquitously expressed; however, inositol-requiring enzyme 1 β (IRE1β) expression is restricted mainly to the gastrointestinal tract and the pulmonary mucosal epithelium [82,83]. *Ern1* knockout (KO) in mice is embryonic lethal due to growth retardation and defects in liver organogenesis and placental development [84] while *Ern2* KO mice develop colitis of increased severity and shorter latency [82] but are otherwise histologically indistinguishable from the *Ern2*WT mice. BiP dissociation, caused by accumulating unfolded proteins, triggers IRE1 oligomerization and activation of its cytosolic kinase domain. The oligomers position in close proximity, in a face-to-face orientation, enabling trans-autophosphorylation. This face-to-face configuration is adopted by both human and murine IRE1 [85,86]. Phosphorylation in the activation loop of the kinase domain, specifically at Ser724, Ser726 and Ser729, is not only necessary to activate its cytosolic RNase domain [87] but is also required to initiate recruitment of tumour necrosis factor receptor-associated factor 2 (TRAF2) and JNK pathway signalling [88]. The IRE1 cytosolic domain, which is highly homologous with RNase L [89], induces a selective cleavage of dual stem loops within the X-box binding protein 1 (XBP1) mRNA [79,90,91]. Therefore, IRE1, in a spliceosome independent-manner, but together with the tRNA ligase RNA 2′,3′-cyclic phosphate and 5′-OH ligase [92–97], catalyses the splicing of a 26 nucleotide intron from human XBP1 mRNA to produce spliced isoform of XBP1 (XBP1s) [90,91]. XBP1s is a basic leucine zipper (bZIP) transcription factor [98–100] and the unspliced isoform of XBP1 (XBP1u) is unable to activate gene expression due to lack of a transactivation domain [91]. The N-terminal region of XBP1u contains a basic region and a leucine zipper domain
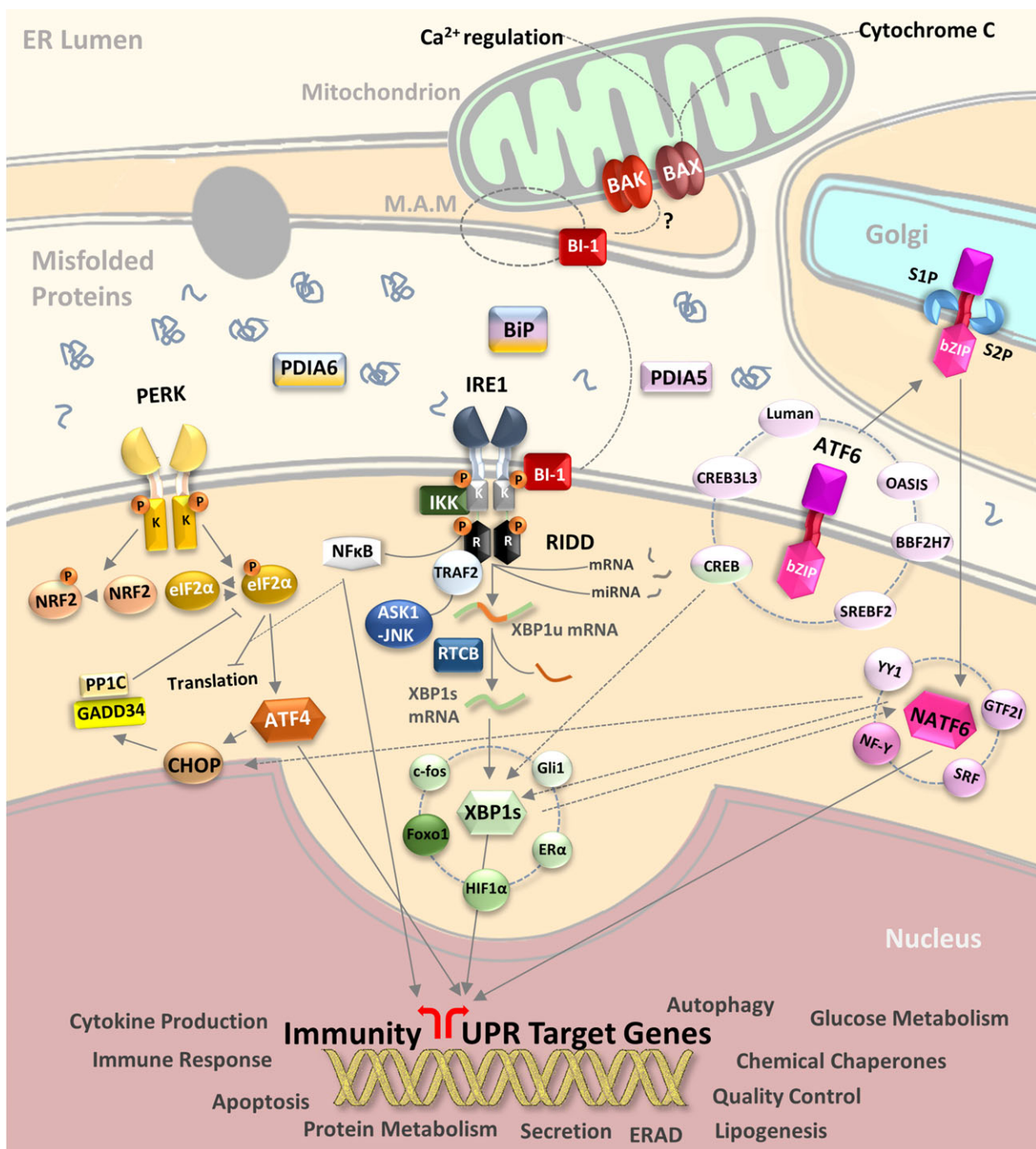
Fig. 2. Signalling the UPR and downstream pathways. The 3ER stress sensors (PERK, IRE1, ATF6) upon release from BiP, PDIA5, 6 initiate signalling cascades through transcription factor production (ATF4, XBP1s, ATF6f) and associated processes such as RIDD, NFκB activation and ERAD to address the misfolded protein load on the ER. By modulating transcriptional output and translational demand the UPR attempts to re-establish ER protein folding homeostasis and promote cell survival. If ER stress cannot be resolved then mechanisms are triggered to promote cell death.

involved in dimerization and DNA binding [91,98,100,101]. The XBP1u C-terminal region contains a P (proline), E (glutamic acid), S (serine) and

T (threonine) motif which destabilizes proteins (ubiquitin-dependent proteolysis) and contributes to its short half-life [98,101–103]. The N-terminal region

also contains two other domains: a hydrophobic region that targets XBP1u to the ER membrane and a domain that promotes efficient XBP1 splicing [104–106] and cleavage [103] by pausing XBP1 translation. IRE1-mediated splicing of XBP1 mRNA results in an open reading frame-shift inducing the expression of a transcriptionally active and BP1s [90,91,101]. XBP1u has been reported to negatively regulate XBP1s transcriptional activity as well as to promote the recruitment of its own mRNA to the ER membrane through the partial translation of its N-terminal region [107,108]. XBP1s directs the transcription of a wide range of targets including the expression of chaperones, foldases and components of the ERAD pathway, in order to relieve ER stress and restore homeostasis [109,110]. However, XBP1s can also participate in the regulation of numerous metabolic pathways such as lipid biosynthesis [111–113], glucose metabolism [114–118], insulin signalling [117,119,120], redox metabolism [121], DNA repair [122] and it influences cell fate including cell survival [123], cell differentiation [124–128] and development [126,129–131]. Although there is strong evidence pointing to a key role for XBP1 in multiple cellular functions, the exact mechanisms by which XBP1 mediates gene transactivation are still elusive. Indeed, in addition to the known interaction of the XBP1s transactivation domain with RNA polymerase II, other mechanisms could exist. For example, XBP1 can physically interact with many other transcription factors such as AP-1 transcription factor subunit [132], oestrogen receptor α (ERα) [133], GLI-family zinc finger 1 [134], SSX family member 4 [134], forkhead box O1 [114], ATF6 [135], cAMP response element-binding protein (CREB)/ATF [135] and hypoxia inducible factor 1 alpha subunit [136] (Fig. 2).

The RNase activity of IRE1 can also efficiently target other transcripts through a mechanism called regulated IRE1-dependent decay (RIDD) [137]. Analysis of the *in vitro* RNase activity of wild-type (WT) vs mutant IRE1 led to the discovery of a broad range of other IRE1 substrates [138,139] and, interestingly, it was noted that IRE1 can also degrade its own mRNA [140]. RIDD is a conserved mechanism in eukaryotes [137,141–145] by which IRE1 cleaves transcripts containing the consensus sequence (CUGCAG) accompanied by a stem-loop structure [142,146]. The cleaved RNA fragments are subsequently rapidly degraded by cellular exoribonucleases [141,147]. RIDD is required for the maintenance of ER homeostasis by reducing ER client protein load through mRNA degradation [137,141,142]. Recently, it has been proposed that there is basal activity of RIDD [138] which increases

progressively with the severity of ER stress. However, this hypothesis needs further experimental validation. Interestingly, IRE1β was found to selectively induce translational repression through the 28S ribosomal RNA cleavage [81] demonstrating that IRE1α and IRE1β display differential activities [148]. Characterizing RIDD activity, particularly *in vivo*, has proven difficult due to the complex challenge of separating the RIDD activity from the XBP1 splicing activity of IRE1. In addition, basal RIDD can only target specific mRNA substrates, as full activation and subsequent targeting of further transcripts requires strong ER stress stimuli (Fig. 2).

PERK signalling

PERK was identified in rat pancreatic islets as a serine/threonine kinase and, similar to PKR, heme regulated initiation factor 2 alpha kinase and general control nonderepressible 2, can phosphorylate eIF2α [149,150]. PERK is ubiquitously expressed in the body [149] and has an ER luminal domain as well as a cytoplasmic kinase domain [150]. BiP detachment from the ER luminal domain leads to oligomerization [72], trans-autophosphorylation and activation of PERK [151]. Active PERK phosphorylates eIF2α on serine 51 [150]. eIF2α is a subunit of the eIF2 heterotrimer [152,153] which regulates the first step of protein synthesis initiation by promoting the binding of the initiator tRNA to 40S ribosomal subunits [154]. However, eIF2α phosphorylation by PERK inhibits eukaryotic translation initiation factor 2B (eIF2B) activity and thereby downregulates protein synthesis [155]. Blocking translation during ER stress consequently reduces the protein load on the ER folding machinery [156].

Remarkably, some transcripts are translated more efficiently during PERK-dependent global repression of translation initiation. The ubiquitously expressed activating transcription factor 4 (ATF4) [157], whose transcript contains short upstream open reading frames (uORFs) [158], is normally inefficiently translated from the protein-coding AUG [159]. However, attenuation of translation from uORFs shifts translation initiation towards the protein coding AUG, resulting in more efficient synthesis of ATF4 [158]. ATF4 can then bind to the C/EBP-ATF site in the promoter of CAAT/enhancer-binding protein (C/EBP) homologous protein (CHOP)/GADD153 [160] and induce its expression [158]. ATF4 and CHOP directly induce genes involved in protein synthesis and the UPR [161], but conditions under which ATF4 and CHOP increase protein synthesis can result in ATP depletion, oxidative stress and cell death [162]. eIF2α

phosphorylation (p-eIF2α) can also directly enhance the translation of CHOP [163,164] and other proteins involved in the ER stress response, as reviewed in [165]. For example, growth arrest and DNA-damage-inducible 34 (GADD34) [166,167] is positively regulated by eIF2α phosphorylation [168] and likewise transcriptionally induced by ATF4 [169] and CHOP [170]. Interestingly, GADD34 interacts with the catalytic subunit of type 1 protein serine/threonine phosphatase (PP1) [171], which dephosphorylates eIF2α thereby creating a negative feedback loop that antagonizes p-eIF2α-dependent translation inhibition and restores protein synthesis [169,170,172]. The translational arrest induced by p-eIF2α reduces protein load in ER lumen and conserves nutrients, while ATF4 driven expression of adaptive genes involved in amino acid transport and metabolism, protection from oxidative stress, protein homeostasis and autophagy together help the cell to cope with ER stress [173,174]. However, sustained stress changes the adaptive response to a prodeath response and ultimately, the phosphorylation status of eIF2α appears to codetermine the balance between prosurvival or prodeath signalling [175,176]. This is accomplished by the above mentioned delayed feedback through which the interplay of GADD34, ATF4 and CHOP results in the activation of genes involved in cell death, cell-cycle arrest and senescence [177–180] (Fig. 2).

ATF6 signalling

The transcription factor ATF6, which belongs to an extensive family of leucine zipper proteins [8], is encoded in humans by two different genes: *ATF6A* for ATF6α [181] and *ATF6B* for ATF6β [153]. After its activation in the ER and export to the Golgi, it is cleaved by the two Golgi-resident proteases membrane bound transcription factor peptidase, site 1 (MBTPS1) and MBTPS1, releasing a fragment of ∼ 400 amino acids corresponding to ATF6 cytosolic N-terminal portion (ATF6f). ATF6f comprises a transcriptional activation domain (TAD), a bZIP domain, a DNA-binding domain and nuclear localization signals. In the nucleus, ATF6f induces UPR gene expression [73,182]. Although the two ATF6 paralogs share high homology [153], ATF6β is a very poor activator of UPR genes due to the absence of eight important amino acids in the TAD domain [157]. Indeed, it rather seems to function as an inhibitor by forming heterodimers with ATF6α [10,158]. Interestingly, ATF6 can modulate gene expression by interacting with other bZIPs, such as CREB [159], cAMP responsive element-binding protein 3 like 3 (CREB3L3) [160], sterol regulatory element-binding

transcription factor 2 [161] and XBP1 [71], and various other transcription factors such as serum response factor [181], components of the nuclear transcription factor Y (NF-Y) complex [159,162,163], yin yang 1 [163,164] and general transcription factor I [165]. Converging with IRE1 and PERK signalling cascades, ATF6 can also induce the expression of XBP1 and CHOP to enhance UPR signalling [30,166,167]. However, ATF6 is not the only ER-resident bZIP transcription factor. At least five other tissue-specific bZIPs, named Luman, cAMP responsive element-binding protein 3 like 1 (OASIS), cAMP responsive element-binding protein 3 like 2 (BBF2H7), CREB3L3 and CREB, reviewed in [183], are involved in ER stress signalling (Fig. 2), highlighting the regulatory complexity this branch of the ER stress response is subjected to at the organismal level.

Noncoding RNAs

Noncoding RNAs are connected to the three UPR sensors with effects on both physiological and pathological conditions [184]. These RNA species mostly include microRNAs (miRNAs) and also long noncoding RNAs (lncRNAs). This additional level of regulation works in fact in a bidirectional manner. This means that either the UPR sensors themselves or their downstream components can also modulate their expression levels. A certain number of miRNAs have been so far recognized to regulate IRE1, which in turn regulates miRNAs through XBP1s at a transcriptional level and through RIDD activity via degradation. One miRNA regulates PERK expression, while this in turn regulates miRNAs through its downstream targets. ATF6 is also modulated by miRNAs, but only one miRNA has been found under its direct effect. Upstream of IRE1, PERK and ATF6, the BiP chaperone is also regulated by miRNAs but does not control any. In addition to miRNAs, lncRNAs exhibit a similar role regarding the regulation of UPR factors and vice versa. Their levels change in accordance to the cell stress status and depending on the pathophysiological context lead to distinct cell fates. This interconnection between noncoding RNAs and the UPR may contribute to a more complex network but at the same time reveals the existence of fine-tuning mechanisms governing ER stress responses and their effects in cell homeostasis (described in [184]).

Proximal impact of UPR activation

Transcriptional programmes

Each branch of the UPR pathway culminates in transcriptional regulation and, together the UPR's major

transcription factors, ATF6f, XBP1s and ATF4, stimulate many adaptive responses to restore ER function and maintain cell survival [35]. They regulate genes encoding ER chaperones, ERAD factors, amino acid transport and metabolism proteins, phospholipid biosynthesis enzymes, and numerous others [185]. In particular, the IRE1–XBP1 pathway is involved in the induction of ER chaperones and capacity control of ERAD [186] as well as promoting cytoprotection [187] and cleaving miRNAs that regulate the cell death-inducing caspases [188]. ATF6f translocates to the nucleus where it activate genes involved in protein folding, processing, and degradation [185]. ATF4, activated downstream of PERK and p-eIF2α, increases the transcription of many genes that promote survival under ER stress. Some of these prosurvival genes include genes that are involved in redox balance, amino acid metabolism, protein folding and autophagy [189].

Translational programmes

Translation is directly impacted by UPR activation under ER stress conditions, particularly by PERK as described above. It also affects the expression of several miRNAs, which may further contribute to translation attenuation or protein synthesis [35]. It has been shown that ER stress can regulate the execution phase of apoptosis by causing the transient induction of inhibitor of apoptosis proteins (IAPs). Several papers have reported that cIAP1, cIAP2 and XIAP are induced by ER stress, and that this induction is important for cell survival, as it delays the onset of caspase activation and apoptosis. PERK induction of cIAPs and the transient activity of PI3K–AKT signalling suggest that PERK not only allows adaptation to ER stress, but it also actively inhibits the ER stress-induced apoptotic programme [190].

Protein degradation

There are two main protein degradation pathways activated by components of the UPR following ER stress: ubiquitin–proteasome-mediated degradation via ERAD and lysosome-mediated protein degradation via autophagy. ERAD is responsible for removing misfolded proteins from the ER and several genes involved in ERAD are upregulated by ATF6f and XBP1s [185]. ERAD involves the retrotranslocation of misfolded proteins from the ER into the cytosol where they are degraded by the proteasome (see above) [187]. When accumulation of misfolded proteins overwhelms ERAD, autophagy is induced as a secondary response

to limit protein build-up [187,191]. Autophagy is a pathway involved in the degradation of bulk components such as cellular macromolecules and organelles. It involves target recognition and selectivity, sequestering targets within autophagosomes, followed by the fusion of the autophagosome with the lysosome, where targets are then degraded by lysosomal hydrolases [187,192]. The direct link between ER stress and autophagy has been established in both *Saccharomyces cerevisiae* and mammalian cells, where autophagy plays a solely cytoprotective role. The PERK (eIF2α) and IRE1 (TRAF2/JNK) branches of the UPR have been implicated in ER stress-induced autophagy in mammalian systems to avoid accumulation of lethal disease-associated protein variants [192]. IRE1–JNK signalling activates Beclin 1, a key player and regulator of autophagy, via the phosphorylation of Bcl-2 and the subsequent dissociation from Beclin 1. This then leads to the activation of ATG proteins required for the formation of the autophagolysosome [193]. Overall, these mechanisms decrease the build-up of improperly folded proteins in the ER thus allowing adaptive and repair mechanisms to re-establish homeostasis. As the amounts of improperly folded proteins decrease, the UPR switches off. However, the molecular details of UPR attenuation still remain to be further elucidated.

Overall, the three mechanisms describe above decrease the build-up of proteins in the ER which allows adaptive and repair mechanisms to re-establish homeostasis. As the amounts of improperly folded proteins decrease, the UPR switches off. However, the molecular details of UPR attenuation remain to be further elucidated.

Regulation of MAMs

Mitochondria-associated membranes (MAMs), which are mainly responsible for Ca^{2+} homeostasis maintenance as well as lipid transport, mediate the interaction between the ER and mitochondria thereby controlling mitochondrial metabolism and apoptosis [194]. MAMs contain many proteins and transporters which mediate mitochondrial clustering and fusion, such as the dynamin-like GTPase mitofusin-2 (MFN2) [195]. MFN2 interacts with PERK, serving as an upstream modulator and thereby regulating mitochondrial morphology and function as well as the induction of apoptosis [196]. Furthermore, the cytosolic domain of PERK serves as an ER-mitochondria tether, thus facilitating ROS-induced cell death [197].The sigma 1 receptor (Sig-1R) is located in the MAMs and forms a complex with BiP. Recent studies show that S1R stabilizes IRE1

at the MAMs upon ER stress, promoting its dimerization and conformational change, and prolonging the activation of the IRE1–XBP1 signalling pathway through its long-lasting endoribonuclease activity. Furthermore, mitochondria-derived ROS stimulates IRE1 activation at MAMs [198]. Another MAM component is Bax-inhibitor-1 (BI-1), regulating mitochondrial Ca^{2+} uptake and apoptosis. BI-1 is a negative regulator of IRE1-XBP1 signalling and in BI-1 deficient cells there is IRE1 hyperactivation and increased levels of its downstream targets [199]. Apoptosis activation by the UPR results in mitochondrial membrane permeabilization, with the resulting Ca^{2+} transfer potentially triggering mitochondrial cytochrome c release [200]. Less well understood are the interactions of the mitochondria with the ER during sublethal ER stress. The latter results in more ER-mitochondria contacts than lethal levels of ER stress, allowing for transfer of Ca^{2+} and enhancement of ATP production through increased mitochondrial metabolism [201] (Fig. 1). These evidences demonstrate the importance of the ER-mitochondria communication in regulating the ER homeostasis and in coordinating the cellular response to ER stress, thereby restoring cellular homeostatic condition or leading towards cell death.

Redox homeostasis

Oxidative stress can be induced through several mechanisms and is critically controlled by the UPR. PERK activity helps to maintain redox homeostasis through phosphorylation of NRF2 which functions as a transcription factor for the antioxidant response [202]. ATF4 also regulates redox control and has been shown to protect fibroblasts and hepatocytes from oxidative stress [173], as well as ensuring that there is an adequate supply of amino acids for protein and GSH biosynthesis [203]. However, in neurons and HEK293 cells ATF4 was shown to induce cell death in response to oxidative stress while CHOP was reported to induce ERO1-α, resulting in ER Ca^{2+} release and apoptosis in macrophages [204]. Direct interactions of PDIs with ER stress sensors, protein S-nitrosylation and ER Ca^{2+} efflux that is promoted by ROS contribute to redox homeostasis and by extension to the balance between prosurvival and prodeath UPR signalling [205]. As such, these signalling loops are paramount to normal cellular function.

Global metabolic impact of the UPR

It was recently shown that the UPR and mitochondrial proteotoxic stress signalling pathways converge on ATF4 to induce the expression of cytoprotective genes [174]. Another pathway regulating energy metabolism is the nutrient-sensing mammalian target of rapamycin (mTOR) signalling hub. mTOR is associated with the UPR through crosstalk with regulatory pathways (reviewed in [206]), and mTOR inhibitors such as rapamycin lead to the activation of PERK signalling, thus favouring cell viability [207]. PERK can also regulate the PI3K–AKT–mTORC1 axis through the activation of AKT. Furthermore, it was observed that mTORC2 plays a role in the inhibition of PERK through AKT activation [208]. Altogether these data suggest that crosstalk between mTOR and the UPR is complex and occurs through multiple pathways.

Lipid metabolism

The UPR can also be activated by deregulated lipid metabolism. In this regard, the UPR has been shown to be activated in cholesterol-loaded macrophages resulting in increased CHOP signalling and apoptosis [209]. Notably, chronic ER stress leads to insulin resistance and diabetes in obesity. This is caused by alterations in lipid composition which lead to inhibition of SERCA activity and hence ER stress [210]. On the other hand, the UPR is involved in systemic metabolic regulation. Disturbance of ER homeostasis in the liver is involved in hepatic inflammation, steatosis and nonalcoholic fatty liver disease [211]. The PERK–eIF2α pathway has been reported to regulate lipogenesis and hepatic steatosis. Compromising eIF2a phosphorylation in mice by overexpression of GADD34 results in reduced hepatosteatosis upon high-fat diet [212]. ATF4 the downstream effector of PERK–eIF2α pathway has also been suggested to regulate lipid metabolism in hepatocytes in response to nutritional stimuli by regulating expression of genes involved in fatty acid and lipid production [213,214]. Furthermore, it has been demonstrated that the IRE1–XBP1–PDI axis links ER homeostasis with VLDL production which plays an important role in dyslipidaemia [215]. In addition, XBP1 is required for the normal hepatic fatty acid synthesis and it was shown that selective XBP1 deletion in mice resulted in marked hypocholesterolaemia and hypotriglyceridaemia [216]. These studies suggest that ER stress and the UPR are involved in lipid metabolism. Relieving ER stress ameliorates the disease state associated with lipid metabolism alterations, suggesting that targeting ER stress might serve as a therapeutic strategy for treating diseases associated with lipid accumulation.

Glucose metabolism

It has been suggested that in the liver the PERK–eIF2α pathway is responsible for disruption of insulin signalling caused by intermittent hypoxia, though IRE1–JNK pathways may still play a role [217]. Adiponectin is widely regarded as a marker of functional glucose metabolism and as a suppressor of metabolic dysfunctions. In hypoxic and ER-stressed adipocytes, reduced adiponectin mRNA levels are observed due to negative regulation by CHOP [218,219]. In β-cells, it was shown that IRE1 is involved in insulin biosynthesis after transient high glucose levels. However, chronic exposure to high glucose leads to full UPR induction and insulin downregulation[220]. IRE1 signalling was shown to be involved in insulin resistance and obesity through JNK activation. In hepatocytes, IRE1-dependent JNK activation leads (a) to insulin receptor substrate 1 (IRS1) tyrosine phosphorylation (pY896) decrease and (b) to AKT activation leading to an increase of IRS1 phosphorylation (pS307), consequently blocking insulin signalling. A role for XBP1 in the pancreas was demonstrated by the fact that β-cell-specific XBP1 mutant mice show hyperglycaemia and glucose intolerance due to decreased insulin release of β-cells [221]. ER stress-induced activation of ATF6 in rat pancreatic beta cells exposed to high glucose, impairs insulin gene expression and glucose-stimulated insulin secretion. Interestingly, knocking down expression of orphan nuclear receptor short heterodimer partner (SHP) previously reported to be involved in beta cell dysfunction by downregulating expression of PDX-1 and RIPE3b1/MafA partly mitigated this effect. However, it remains unclear how ATF6 induces expression of SHP and whether ATF6 alone can directly regulate the expression of insulin, PDX-1 and RIPE3b1/MafA [222]. It has been suggested that physiological impact of ER stress with respect to glucose metabolism depends upon the availability of glucose. Indeed acute glucose availability in beta cells leads to concerted efforts of each branch of UPR to supply insulin, while chronic glucose stimulation leads to depletion of insulin production and beta cell mass due to apoptosis. Moreover, chronic fasting conditions in mice have shown that XBP1s directly activates the promoter of the master regulator of starvation response, PPARα demonstrating a further link between the UPR and glucose and lipid metabolism [223]. Acquiring further knowledge on link between UPR and metabolic sensor mechanisms will significantly expand the possibility of gaining beneficial metabolic output. Taken together this indicates that the UPR arms are critical for the cell to regulate metabolism through regulating mTOR signalling, lipid homeostasis as well as insulin signalling.

Downstream impact of UPR activation

The activation of UPR leads to the modulation of many cellular pathways, thereby influencing prosurvival mechanisms as well as processes such as proliferation, differentiation, metabolism and cell death.

UPR-associated cell death

Following prolonged activation of the UPR, the cellular response switches from prosurvival to prodeath. Several types of cell death, including apoptosis, necrosis/necroptosis and autophagic cell death, can be induced following ER stress.

Apoptosis

Unresolved ER stress can lead to the activation of either the intrinsic (mitochondrial) or extrinsic [death receptor (DR)] pathways of apoptosis. Both pathways trigger activation of caspase proteases that dismantle the cell, and all of the three branches of the UPR are involved in apoptosis. In the extrinsic pathway, the activation of DRs on the PM leads to the recruitment of caspases to the DRs and their proximity-induced trans-autoactivation. Intrinsic apoptosis involves the release of cytochrome *c* (along with other proapoptotic factors) from the mitochondria, which promotes the formation of a cytosolic protein complex to activate a caspase cascade. This release is controlled by pro- and antiapoptotic members of the BCL-2 protein family. In particular, the BH3-only members of the family including PUMA, NOXA and BIM are pivotal components of ER stress-induced apoptosis [224], and cells deficient in BH3-only proteins are protected against ER stress-induced cell death [190]. ER stress leads to transcriptional upregulation of these proapoptotic molecules resulting in cytochrome *c* release. Both the IRE1 and PERK arms of the UPR have been linked to induction of apoptosis during ER stress. In particular, CHOP, a transcription factor that is downstream of PERK, and a direct target of ATF4, has been implicated in the regulation of apoptosis during ER stress. As discussed in section PERK signalling CHOP-induced expression of GADD34 promotes dephosphorylation of p-eIF2α reversing translational inhibition and allowing transcription of genes including apoptosis-related genes [172]. CHOP activates

transcription of BIM and PUMA, while it represses transcription of certain antiapoptotic BCL-2 family members such as MCL-1 [225]. In addition, the ATF4/CHOP pathway can increase the expression of other proapoptotic genes, such as TRAIL-R1/DR4 and TRAIL-R2/DR5 which promote extrinsic apoptosis [180]. Apart from CHOP, p53 is also involved in the direct transcriptional upregulation of BH3- only proteins during ER stress. However, the link between p53 activation and ER stress is unclear [226].

Although IRE1–XBP1s signalling is mainly prosurvival, IRE1 can promote apoptosis. Activated IRE1 can interact directly with TRAF2, leading to the activation of apoptosis signal-regulating kinase 1 (ASK1) and its downstream targets c-Jun NH2-terminal kinase (JNK) and p38 MAPK [227,228]. Phosphorylation by JNK has been reported to regulate several BCL-2 family members, including the activation of proapoptotic BID and BIM, and inhibition of antiapoptotic BCL-2, BCL-XL and MCL-1 [229,230]. In addition, p38 MAPK phosphorylates and activates CHOP, which increases expression of BIM and DR5, thereby promoting apoptosis [231,232]. In fact, cell death induction in HeLa cells overexpressing CHOP is dependent on its phosphorylation by p38 MAPK [233]. Interestingly, it was proposed that ER stress and MAPK signalling act in a positive feed-forward relationship, as ER stress induces MAPK signalling which in turn increases ER stress [234]. IRE1 signalling may also contribute to apoptosis induction through prolonged RIDD activity which degrades the mRNA of protein folding mediators [142].

Interestingly, recent studies indicate a role for miRNAs in the induction of apoptosis following prolonged ER stress. For example, miRNA29a which is induced during ER stress via ATF4 results in the downregulation of antiapoptotic Bcl-2 family protein Mcl-1, and thus promotes apoptosis [235]. miRNA7 has also been linked with ER stress-induced apoptosis, where IRE1 reduces miRNA7 levels which results in the stability of a membrane-spanning RING finger protein, RNF183. RNF183 has an E3 ligase domain that then causes the ubiquitination and subsequent degradation of the antiapoptotic member of the BCL-2 family BCL-XL. Following prolonged ER stress, increased expression of RNF183 via IRE1 leads to increased apoptosis [236].

In the last decade, it also became clear that ER stress can profoundly modify the immunological consequences of apoptotic cell death. Accumulating *in vitro* and *in vivo* evidence have highlighted that the activation of the PERK arm of ER stress evoked in response to selected of anticancer therapies (including anthracyclines, oxaliplatin, radiation and

photodynamic therapy (reviewed in [237]), drives a danger signalling module resulting in the surface exposure of the ER luminal chaperone calreticulin and the exodus of other danger-associated molecular patterns, eliciting immunogenic cell death (reviewed in [238]).

Necroptosis

Necroptosis, a programmed form of cell death, is dependent on the activation of receptor-interacting protein kinase 1 (RIPK1), RIPK3 and mixed lineage kinase domain-like (MLKL) protein and has been linked to ER stress. In an *in vivo* mouse model of spinal cord injury, there is induction of necroptosis and ER stress, with localization of MLKL and RIPK3 on the ER in necroptotic microglia/macrophages suggesting a link between necroptosis and ER stress in these cells [239]. Necroptosis is frequently activated downstream of TNFR1 when apoptosis is blocked [240]. This has been linked to ER stress-induced necroptosis whereby tunicamycin kills L929 murine fibrosarcoma cells by caspase-independent, death ligand-independent, TNFR1-mediated necroptosis [241].

Autophagic cell death

Endoplasmic reticulum stress has also been connected to autophagic cell death. Autophagy not only promotes cell survival, but can also mediate nonapoptotic cell death under experimental conditions when apoptosis is blocked, or in response to treatments that specifically trigger caspase-independent autophagic cell death [192]. IRE1α mediated TRAF2 and ASK1 recruitment, and subsequent JNK activation mediates autophagy. JNK-mediated phosphorylation of BCL-2 releases Beclin-1 (while XBP1s also transcriptionally upregulates its expression), which interacts with the ULK1 complex to promote vesicle nucleation that leads to the formation of the autophagosome [242]. Activated PERK can induce autophagy through ATF4 by inducing vesicle elongation while Ca^{2+} release from the ER lumen through the IP3R can relieve mTOR inhibition on the ULK1 complex [187].

UPR-associated morphological changes

Endoplasmic reticulum stress causes morphological changes in cellular models. Experiments to date have largely focused on the morphologies associated with apoptotic and autophagic cell death resulting from UPR activation. UPR-regulated flattening and rounding of cells, indicative of cell death, has been observed in many model systems, with traditional caspase-

dependent apoptosis being responsible [200,243–248]. These morphological changes can be reversed by physiological and pharmacological ER stress relief [247,249]. Both IRE1 and PERK arms of the UPR have been implicated in the observed changes [193,243,244,247,249–251]. As described above, programmed cell death and its associated morphological changes have become a focal and much researched outcome of the use of UPR-inducing cytotoxic agents.

An intensively studied consequence of ER stress is the epithelial to mesenchymal transition (EMT) and its role in cancer invasion and metastasis. EMT is an essential component of tissue repair following wounding, allowing for the migration of new healthy cells into any lesions that have occurred. Morphological changes indicative of EMT have been observed in multiple cell models under physiologically relevant stress (e.g. hypoxia) and pharmacological induction of ER stress [252–255]. The IRE1–XBP1 pathway has been reported to negatively regulate the traditional epithelial marker E-cadherin, while positively regulating the mesenchymal marker *N*-cadherin in models of colorectal, breast and pulmonary fibrosis [254,256,257]. Breast cancer and pulmonary fibrosis models showed an IRE1–XBP1-dependent regulation of mesenchymal promoting transcription factor SNAIL that is responsible for EMT [254,256]. Human mammary epithelial cells undergo EMT in response to PERK activation, and PERK-mediated phosphorylation of eIF2α is required for invasion and metastasis [258]. Other ER stress-regulated pathways have been proposed to act in the EMT in cellular models, including autophagy and activation of c-SRC kinase in tubular epithelial cells [259] and the compensatory activation of the NRF-2/HO-1 antioxidative stress response pathway in HT-29 and DLD-1 colon cancer cells [252]. Therefore, UPR signalling pathways appear to induce morphological changes indicative of EMT. These data have generated interest in the field of cancer research where the pharmacological inhibition of UPR components might be used to reduce tumour invasiveness and metastasis.

Hormone production

The tissues and cells of the endocrine system responsible for hormone production and extracellular signalling often have a high protein load, resulting in ER stress and activation of the UPR. OASIS (CREB3L1) and ATF6α have been shown to regulate arginine vasopressin (AVP), a potent vasoconstrictor, in murine and rat models [260,261]. Upon dehydration or salt loading in rat models, cleaved active OASIS is observed binding the AVP promoter region, directly

upregulating protein expression [260]. In ATF6$^{-/-}$ murine models subjected to intermittent water deprivation, similar downstream effects were observed, but signalling pathways were not investigated [261]. ER stress-inducing agents palmitate and oxysterol 27-hydroxycholesterol both result in a reduction in leptin (a long-term mediator of energy balance) expression and extracellular concentrations. This has been attributed, by using ChIP analysis and siRNA knockdowns, to the fact that the PERK downstream target CHOP negatively regulates C/EBPα, transcriptionally downregulating its translation and release [262,263]. UPR activation has been implicated in the hypothalamic and brown adipose tissue response to thyroid hormone triiodothyronine (T3). Elevated T3 levels induce the UPR downstream of AMPK in the ventromedial nucleus of the hypothalamus, resulting in decreased ceramide levels. JNK1 KO revealed that it acts downstream of this AMPK-dependent activation, possibly as a target of IRE1 but to our knowledge no studies have yet confirmed this [264]. In response to ER stress in hepatocytes, CREBH is exported from the ER and cleaved in the Golgi apparatus. The CREBH cytosolic fragment binds to the promoter region of hepcidin and transcriptionally upregulates its production [265]. These examples of UPR-regulated hormone production and release give scope for further investigation into the longer term, system wide effects of UPR signalling outside of the current focuses on cytotoxicity and acute diseases.

Physiological ER stress signalling

It has been established that ER stress signalling is important in interorganelle and intercellular interactions. It therefore comes as no surprise that it forms a significant network of interactions upon which normal physiology is based. This is not only the case in humans, but is also conserved throughout species and has been an important fact in the design of experimental model organisms to further study ER stress signalling and it role in physiology and disease.

Embryology and development

The UPR as the major conduit of ER stress regulation has been extensively studied in developmental biology in the majority of organisms commonly used in translational research. The use of multiple models has been important in discerning the variable ER stress signalling between species, as demonstrated by the discovery that protein quality control in mammals is critically dependent on ATF6 while the major player in

Caenorhabditis elegans and Drosophila melanogaster is IRE1 [182,266]. Mammalian and other embryos implanted *in vitro* or naturally, undergo a multitude of physical, biochemical and cellular stresses involving epigenetic changes as well as a disproportional increase in protein synthesis load that affect cell differentiation, proliferation and growth.[267]. In zebrafish, transgenic models have been generated to monitor XBP1 splicing during development and implantation, showing that maternal XBP1s is active in oocytes, fertilized eggs and early stage embryos, presenting a potential model for study of the impact of water pollutants on embryogenesis [268]. It was recently shown that in medaka fish the JNK and RIDD pathways are dispensable for growth, with development solely dependent on the XBP1 arm of IRE1 signalling, thereby supporting the hypothesis that XBP1 and RIDD may be differentially utilized in development and homeostasis [269]. In *C. elegans* it has been postulated that the IRE1-XBP1 axis as well as the PERK pathway are responsible for the maintenance of cellular homeostasis during larval development [270]. Pronephros formation was shown to be BiP dependent in *Xenopus* embryos, where BiP morpholino knockdown not only blocked pronephros formation but also attenuated retinoic acid signalling, impacting markers such as the Lim homeobox protein [271]. In early mouse development, it was shown that the BiP promoter is activated in both the trophoectoderm and inner cell mass at embryonic day 3.5 and that absence of BiP leads to proliferative defects and inner cell mass apoptosis, suggesting it is necessary for embryonic cell growth and pluripotent cell survival [272]. Furthermore, mouse studies revealed that ER stress proteins such as BiP, GRP94, calreticulin and PDIA3 were downregulated in adult neural tissues compared to embryonic ones, suggesting a pivotal role for ER stress signalling in the development of neural tissues such as the brain and retina [273]. Beyond the nervous system, ER stress signalling impairment has repeatedly shown mouse embryonic lethality and, in particular in the hepatocellular system, multiple studies have demonstrated that IRE1 and XBP1 signalling defects lead to fetal liver hypoplasia, intrauterine anaemia and early antenatal pancreatic dysfunction [274]. The UPR is intrinsically linked to the mouse embryonic morula–blastocyst transition [275] and this, in combination with evidence that there is an immediate postnatal downregulation of BiP, shows that there is an important role for the UPR both in early and late gestation [276]. Taking all this evidence into consideration, it is apparent that the correct integration of signals both intracellularly and between the developing oocyte, follicular environment and supporting cumulus cells is absolutely essential for embryonic development, making ER stress signalling a key regulator in the earliest stages of life in all organisms [277].

Growth and differentiation

Many cell types experience a high protein load during various stages of differentiation and maturation, resulting in ER stress. In several cases, morphological changes required for the final function of the cell would not be possible without transient activation of the UPR's cytoprotective mechanisms. Deletion of PERK in murine models results in loss of pancreatic β cell architecture but not in cell death, and was accompanied by an increase in β cell proliferation. This morphological change results in a diabetes mellitus-like pathology and is not a result of increased cell death as previously proposed [278]. Various haematopoietic lineages require the activation of the UPR in order to survive ER stress resulting from production of immunoglobulins and lysosomal compartments in order to reach maturity [279–281]. One physiological function that is indispensable for survival is the innate immune response, and cell differentiation is at its epicentre. The conversion of B lymphocytes to highly secretory plasma cells is accompanied by a huge expansion of the ER compartment, and genetic alterations to induce immunoglobulin production are good examples of the necessity of ER signalling in normal physiology [123]. This is supported by a study that suggests the UPR, and the PERK pathway in particular, govern the integrity of the haematopoietic stem-cell pool during stress to prevent loss of function [282]. The ability of skin fibroblasts to produce collagens and matrix metalloproteinases (proteins increased at wound sites), along with their ability to differentiate into myofibroblasts, provides another example where physiological ER stress may drive morphological cellular transition [283]. Although not yet fully characterized, the RIDD pathway has been linked to a multitude of physiological processes including lysosomal degradation and xenobiotic metabolism through cytochrome P450 regulation [284]. At the same time, substrates of regulated intramembrane proteolysis such as CREBH are involved in normal physiological processes such as gluconeogenesis [284]. Another substrate of regulated intramembrane proteolysis, OASIS, is involved in multiple stages of bone homeostasis and development. Mice lacking OASIS present with severe osteopenia, which is compounded by the fact that the gene for type 1 collagen is an OASIS target [285]. Moreover, osteoblast OASIS expression is controlled by factors essential to osteogenesis (BMP2), pointing to a PERK-eIF2α-ATF4 pathway upregulation during osteoblast

differentiation, where ATF4 restores deficiencies of PERK null osteoblasts all the while impacting apoptosis for bone remodelling [251,286]. Furthermore, a link between osteoblast differentiation and hypoxia has been established, with decreased vascularization shown in OASIS null mice pointing towards a potential role of ER stress in angiogenesis during bone development [287]. This signalling cascade does not only restrict itself to the normal physiology of bone but also modulates UPR signalling in astrocytes and is responsible for the terminal, early to mature, goblet cell differentiation in the large intestine [288–290].

Metabolism

The ER is a site of significant metabolic regulation. The UPR plays a major role in the regulation of glycolysis and it was recently shown that IRE1 mediates a metabolic decrease upon glucose shortage in neurons, suggesting an important role for the UPR as an adaptive response mechanism in relation to energy metabolism [291]. Moreover, mTOR signalling adjusts global protein synthesis, which is a highly energy consuming process, and thereby regulates energy metabolism (reviewed in [292]).

Lipid homeostasis

The ER is heavily involved in lipid homeostasis. Characteristically, hepatocytes are enriched in SER, because in addition to protein synthesis, these cells also synthesize bile acids, cholesterol and phospholipids. XBP1 ablation in murine liver results in hypolipidaemia due to feedback activation of IRE1 caused by the lack of XBP1. Activated IRE1 induces the degradation of mRNAs of a cohort of lipid metabolism genes via RIDD, demonstrating the critical role of IRE1–XBP1 signalling in lipid metabolism and suggesting that targeting XBP1 may be a viable approach to the treatment of dyslipidaemias [113]. It was also reported that in hepatocyte-specific IRE1-null mice, XBP1 is involved in very low-density lipoprotein synthesis and secretion [215]. Interestingly, ATF6 has also been shown to have a role in adipogenesis by inducing adipogenic genes and lipid accumulation [293].

Glucose metabolism

The UPR is also involved in regulating glucose metabolism. Initial murine studies suggested the PERK–eIF2α arm was responsible for impaired insulin signalling due to knock out effects on beta cells during development. Further studies have since shown that

IRE1 RIDD activity is responsible for a reduction in the mRNA of proinsulin processing proteins, including *INS1*, *PC1* and *SYP*. These effects can be observed in cases of XBP1 deficiency and in cases of extensive UPR activation, highlighting the divergent effects of IRE1 RNase activity [119,221,294].

Amino acid metabolism

The UPR is also described to be involved in amino acid metabolism. It was recently described that ATF4 mediates increased amino acid uptake upon glutamine deprivation [295]. Furthermore, a low protein diet leads to the upregulation of cytokines mediated by IRE1 and RIG1 which results in an anticancer immune response in tumours [296]. In summary, these findings show the importance of the various UPR arms in cell metabolism and energy homeostasis with effects not only on the cell itself but also on the whole cellular environment.

Pharmacological targeting of the UPR

Several small molecules have been reported to modulate (activate or inhibit) one or more arms of the UPR. Importantly, these molecules have shown promising beneficial effects in diverse human diseases (Table 1). X-ray cocrystal structures are now available for IRE1 and PERK with several endogenous or exogenous ligands. The understanding of how small molecules bind to the active sites and modulate the function of IRE1 and PERK will have a profound impact on the structure-based drug discovery of novel UPR modulators. Available X-ray structures, in addition to mutagenesis analysis of critical amino acids [297], have revealed a variety of unexpected allosteric binding sites on IRE1 [297–299].

Pharmacological modulators of IRE1

IRE1 signalling information along with CHOP/Gal4-Luc cells and UPRE-Luc engineered cells were used to screen large chemical libraries in high throughput screening assays for discovery of pathway-selective modulators of IRE1 [300].

IRE1 ATP-binding site

IRE1 modulators have been discovered primarily by traditional drug discovery methods, identifying inhibitors specific to the kinase or RNase domain (Table 1). The IRE1 kinase modulators were used as tools to understand the allosteric relationship between the

Table 1. Different modulators that target the UPR-transducer protein pathways. Molecule name, respective molecular target and brief description with the associated reference are provided (ND: not determined).

UPR Arm	Name	Target	Brief description	Reference
PERK	GSK2656157	PERK Kinase	In preclinical stage for multiple myeloma and pancreatic cancer	[314,364]
	Salubrinal	GADD34/PP1c	Inhibition of eIF2α dephosphorylation In ALS, it increases lifespan of mutant superoxide dismutase 1 transgenic mice In Parkinson's disease, it increases neuronal survival of α-synuclein transgenic mice	[365–367]
	ISRIB	eIF2β	Decreased ATF4 expression	[322]
	Guanabenz	GADD34/PP1c	Inhibitor of eIF2α phosphatase,	[368]
	Sephin1	GADD34 (PP1c)	Inhibitor of eIF2α phosphatase	[369]
IRE1	Salicylaldimines	IRE1 RNase	IRE1αRNase active-site inhibitor	[305]
	STF-083010	IRE1 RNase	IRE1α RNase active-site inhibitor In preclinical stage for multiple myeloma treatment	[308]
	MKC-3946	IRE1 RNase	IRE1α RNase active-site inhibitor In preclinical stage for multiple myeloma treatment	[307,370]
	4μ8c	IRE1 RNase	IRE1α RNase active-site inhibitor In preclinical stage for multiple myeloma treatment	[306]
	APY29	IRE1 Kinase	IRE1α kinase active-site inhibitor	[303]
	Sunitinib	IRE1 Kinase	IRE1α kinase active-site inhibitor FDA approved for renal cell carcinoma It acts on multiple kinases	[85,304]
	KIRA	IRE1 Kinase	IRE1α kinase active-site inhibitor	[371]
	Toyocamycin	IRE1 RNase	IRE1α RNase active-site inhibitor In preclinical stage for various cancers treatment	[309,372]
	3-ethoxy-5,6-dibromosalicylaldehyde	IRE1 RNase	IRE1α RNase active site inhibitor	[305]
	Apigenin	Proteasome	Increase of IRE1a nuclease activity in model	[373]
	FIRE peptide	IRE1 Kinase	Modulation IRE1 oligomerization *in vitro*, Xbp1 mRNA cleavage *in vitro*, in cell culture and *in vivo* (*Caenorhabditis elegans*)	[85]
ATF6	Apigenin	ATF6	Upregulation of ATF6 expression	[373]
	Baicalein	ATF6	Upregulation of ATF6 expression	[374]
	Ceapin	ND	Inhibitor of ATF6	[323]
	Kaempferol	ATF6	Downregulation of ATF6 expression	[375]
	Melatonin	ATF6	Inhibitor of ATF6	[325]
	Compound 147	ATF6	Activator of ATF6	[376]
	Compound 263	ATF6	Activator of ATF6	[376]
	16F16	PDI	Inhibitor of PDI	[377]

kinase and RNase domains [301,302]. Kinase inhibitors can be broadly classed as (a) ATP-competitive inhibitors that inhibit the kinase domain and activate the RNase domain and (b) ATP-competitive inhibitors that inhibit the kinase domain and inactivate RNase (kinase inhibiting RNase attenuators – KIRAs). Available IRE1 crystal structures reveal a possible mechanism of RNase activation by conformational changes that occur in the kinase domain when transitioning from a monomeric to an active dimeric state. Type I IRE1 kinase inhibitors include APY29 [303] and sunitinib [304], which target the ATP-binding site and inhibit the phosphorylation but stabilize the active form of the kinase domain. An active kinase conformation is seen in human *apo* dP-IRE1* (PDB 5HGI), as a back-to-back dimer. Notably, the DFG motif (Asp711-Phe712-Gly713) faces into the active site (DFG-in), with helix-αC-in conformation. In contrast, human IRE1 bound to KIRA compound 33 (PDB: 4U6R) shows an inactive kinase conformation, with DFG-in and helix-αC-out conformation. The inactive conformation is incompatible with back-to-back dimer formation due to the displaced helix-αC [301]. Imidazopyrazine-based inhibitors and other KIRAs

allosterically inhibit the RNase activity of phosphory-lated IRE1 by possibly displacing helix-αC from an active conformation to an inactive conformation [301].

IRE1 RNase-binding site

IRE1 RNase inhibitors include salicylaldehydes [305] 4μ8C [306], MKC-946 [307], STF-83010 [308], toyocamycin [309] and hydroxyl-aryl-aldehydes [86]. The reported cocrystal structures of murine IRE1α with salicylaldehyde-based inhibitor show that Lys 907 is involved in Schiff base arrangement (PDB code: 4PL3 [86]). Lys 907 is a crucial residue present within the hydrophobic pocket of the IRE1 RNase catalytic site [310]. Quercetin is reported to activate IRE1 through a site distinct from the nucleotide-binding site (crystal structure PDB 3LJ0), increasing the population of IRE1 dimers *in vitro* [299]. A recent *in silico* study identified the anthracycline antibiotic doxorubicin as an inhibitor of the IRE1-XBP1 axis [311]. Covalent binders are very efficient in the sense that they completely block the proteins to which they bind, but this can also have several drawbacks [312]. Noncovalent kinase and allosteric modulators in general inhibit competitively and are thus less efficient, but can at the same time be extremely useful in obtaining new insights for developing selective and potent modulators of IRE1α-XBP1 signalling (Table 1).

Other IRE1 modulators

Peptides derived from the kinase domain of human IRE1 promote oligomerization *in vitro*, enhancing XBP1 mRNA cleavage activity *in vitro* and *in vivo* [85]. However, although peptide-based modulators have limited clinical application [313] (Table 1) peptide mimetics may prove more useful. These are different aspects that can be exploited to develop selective IRE1 modulators. Despite significant progress in understanding IRE1 signalling and in the development of modulators of IRE1 activity, several questions still remain to be answered to fully control IRE1 activity and signalling outcomes, including how to selectively target the XBP1 and RIDD arms of IRE1 signalling.

Pharmacological modulators of PERK

Through biochemical screening of exclusive library collections and structure-based lead optimization, GSK discovered PERK inhibitors GSK2606414 and GSK2656157 [314]. These potent PERK inhibitors can be orally administered [314], reducing tumour growth in mouse xenograft models [314,315]. GSK2606414

was also the first oral small molecule to prevent neurodegeneration *in vivo* in prion-diseased mice, with GSK2606414 reducing the levels of p-PERK and p-eIF2α and restoring protein synthesis rates [316]. Despite the promising selectivity profile, pharmacological inhibition of PERK in mice caused damage to exocrine cells and pancreatic beta cells, a similar phenotype to that observed in PERK$^{-/-}$ mice [317]. Furthermore, GSK2606414 and GSK2656157 were found recently to inhibit RIPK1 at nanomolar concentrations [318]. To overcome the β-cell toxicity, small molecules modulating the eIF2α pathway without directly inhibiting PERK were examined. Integrated stress response inhibitor (ISRIB) is the first small molecule described to bind and activate guanine nucleotide exchange factor eIF2B [319,320]. Unlike GSK inhibitors, ISRIB did not show any pancreatic toxicity [321]. Interestingly, ISRIB increased learning and memory in WT mice [322] (Table 1).

ATF6 modulators

The identification of small molecules that modulate ATF6 has been challenging due to lack of potentially druggable binding sites and unavailability of the protein crystal structure. Recently, Walter and colleagues identified selective inhibitors of ATF6 signalling, the small molecules Ceapins, using a high throughput cell-based screen [323]. Ceapins do not affect the IRE1 and PERK arms of the UPR. Ceapins are chemically classed as pyrazole amides and extensive biochemical and cell biology evidence show that they trap ATF6 in the ER and thus prevent its translocation to the Golgi upon stress [324]. Ceapins sensitize cells to ER stress without affecting unstressed cells and hence have potential to be developed within the framework of a therapeutic strategy to induce cell death in cancer cells. A recent study identified melatonin as an ATF6 inhibitor, leading to enhanced liver cancer cell apoptosis through decreased COX-2 expression [325]. The activation of ATF6 depends on a redox process involving PDIs suggesting that PDI inhibitors such as PACMA31 [326], RB-11-ca [327], P1 [327] and 16F16 [328] may be able to modulate ATF6 activation. Additionally, the serine protease inhibitor 4-(2-aminoethyl) benzenesulfonyl fluoride is reported to prevent ER stress-induced cleavage of ATF6 [329] (Table 1). Albeit the above developments hold strong promise for the future, very little is known to date about specific binding sites, which together with the lack of a crystal structure and insufficient templates to enable homology modelling, rational drug design targeting ATF6 remains a

challenge. Availability of an ATF6 crystal structure is in this sense the key aspect, as this will provide atomistic level understanding of interactions and mechanism of action, and enable *in silico* based rational design of ATF6 modulators.

The UPR in the clinic

In this section, we review recent preclinical and clinical studies in which UPR components were used as disease biomarkers or as therapeutic targets (Fig. 3). As already described in section Perturbing ER functions molecules have been designed to modulate ER stress by inducing the UPR (Brefeldin A, DTT), inhibiting SERCA Ca^{2+} ATPases (thapsigargin) or preventing the generation of glycoproteins, and hence, the induction of ER stress through calcium imbalance or misfolded protein accumulation. They were touted as potential antitumour therapies as they could potentially induce tumour cell death through ER stress overactivation. However, none of these compounds were used in the clinic due to their lack of specificity and high toxicity. It has been reported though that a prodrug analogue of thapsigargin, mipsagargin, did display acceptable tolerability and favourable pharmacokinetic profiles in patients with solid tumours [330]. On the other hand, section 6 describes molecules that inhibit the various arms of the UPR.

UPR biomarkers

Changes in UPR and ER stress markers in blood or tissue biopsy samples can be indicative of disease state and could be/are utilized as valuable biomarkers for different human pathologies. For instance, BiP has strong immunological reactivity when released into the extracellular environment [331], and in 1993, it was the first ER stress protein associated with the pathogenesis of osteogenesis imperfecta [332]. Since then, further evidence suggests overexpression of BiP in several human diseases (reviewed in [333]). The UPR transcription factors can also be seen as potential biomarkers of various diseases. ATF4 is upregulated and contributes to progression and metastasis in patients with oesophageal squamous cell carcinoma [334]. Similarly, XBP1 overexpression is linked to progressive clinical stages and degree of tumour malignancy in osteosarcoma [335]. In contrast, IRE1–XBP1 downregulation can differentiate germinal centre B cell-like lymphoma from other diffuse large B-cell lymphoma subtypes and contributes to tumour growth [336]. Moreover, XBP1 is genetically linked to inflammatory bowel disease (IBD) [337]. Using cohorts of IBD

patients to test the association of 20 SNPs across the XBP1 gene region, it was found that three SNPs rs5997391, rs5762795 and rs35873774 are associated with disease, thus linking cell-specific ER stress changes with the induction of organ-specific inflammation. Quantitative changes in ER stress chaperones in the CSF have been proposed as possible biomarkers to monitor the progression of neurodegenerative diseases such as ALS [338,339]. Finally, the mesencephalic astrocyte-derived neurotrophic factor (MANF) can be used as a urine biomarker for ER stress-related kidney diseases [340]. MANF localizes in the ER lumen and is secreted in response to ER stress in several cell types. Similarly, angiogenin was identified as an ER stress responsive biomarker found in the urine of patients with kidney damage [341]. Thus, noninvasive ER stress-related biomarkers can be used to stratify disease risk and disease development (Fig. 3).

ER stress and UPR-based therapies

Beyond their use as biomarkers, ER stress signalling components also represent relevant therapeutic targets. BiP was recently recognized as a universal therapeutic target for human diseases such as cancer and bacterial/viral infections [333]. Antibodies targeting BiP exhibited antitumoural activity and enhanced radiation efficacy in non-small-cell lung cancer and glioblastoma multiforme in mouse xenograft models [342]. It was also shown that short-term systemic treatment with a monoclonal antibody against BiP suppressed AKT activation and increased apoptosis in mice with endometrial adenocarcinoma [343]. Moreover, the ER-resident GRP94 is being evaluated as a therapeutic target because of its ability to associate with cellular peptides irrespective of size or sequence [344]. Preclinical studies have linked GRP94 expression to cancer progression in multiple myeloma, hepatocellular carcinoma, breast cancer and colon cancer. Finally, this protein has been identified as a strong modulator of the immune system that could be used in anticancer immunotherapy [345].

ER stress-induced transcription factors can also represent relevant targets. Thus, XBP1s has been one of the main targets for drug discovery and gene therapy [346]. Elimination of XBP1 improves hepatosteatosis, liver damage and hypercholesterolaemia in animal models. As such direct targeting of IRE1 or XBP1 can be a possible strategy to treat dyslipidaemias [113]. In cancer, toyocamycin was shown to inhibit the constitutive activation of XBP1s expression in multiple myeloma cells as well as in patient primary samples [309]. Despite being the least studied UPR arm, there are
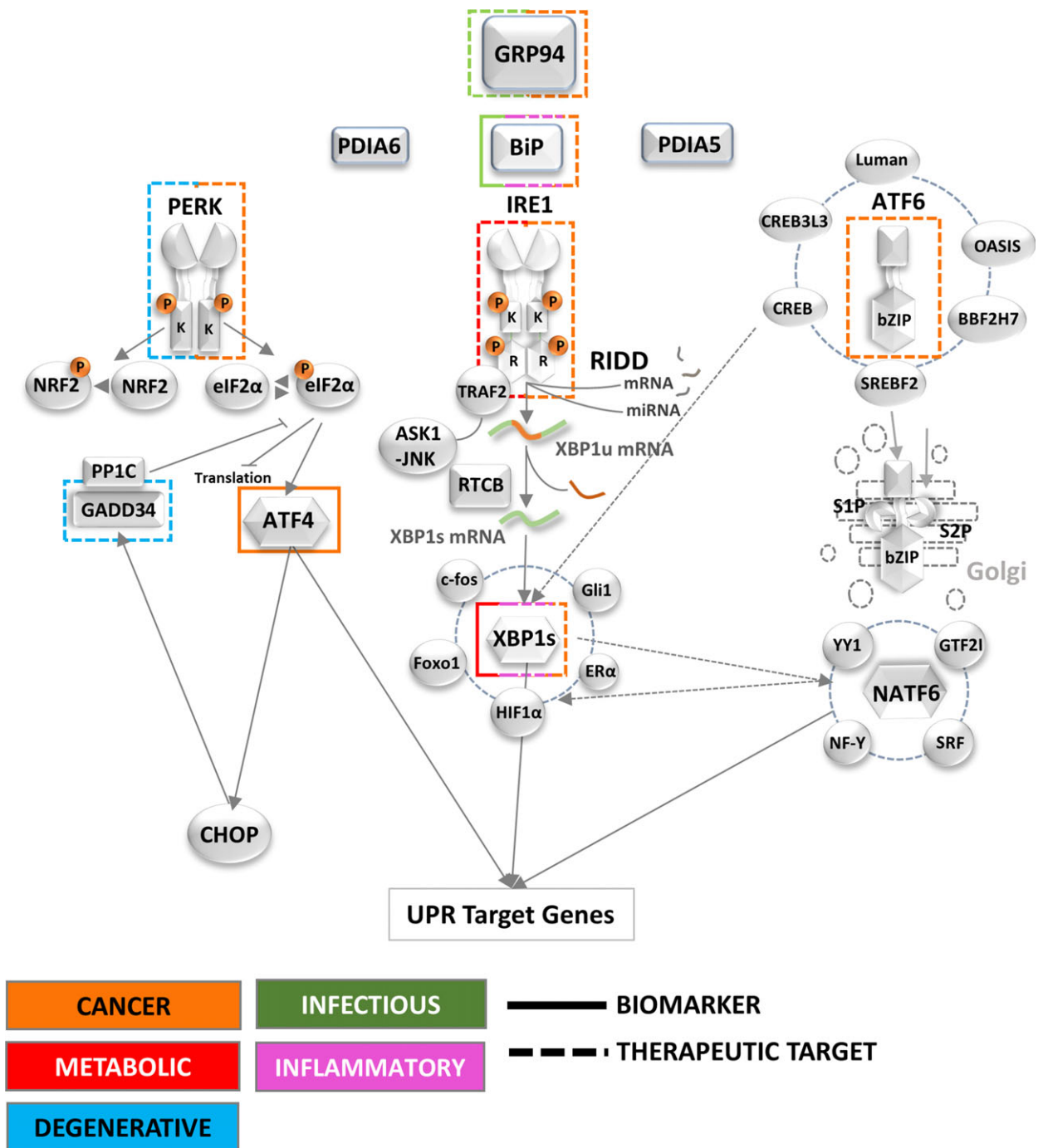
Fig. 3. UPR disease biomarkers and therapeutic targets. Schematic representation of the UPR signalling pathway as defined in Fig. 2 and annotated with the relevance to disease of each component. The colour code indicates the type of disease (cancer: orange; metabolic disease: red; degenerative disease: blue; infectious disease: green; inflammatory disease: pink) and the lines indicate the role as biomarker (continuous line) or therapeutic target (dashed line).

instances that ATF6 can be a specific clinical target. The activation of ATF6 but not IRE1 or PERK has been linked with airway remodelling in a mouse model of asthma [347]. Additionally, these studies showed that expression of orosomucoid-like 3 (ORMDL3) regulates ATF6 expression and airway remodelling through ATF6 target genes such as SERCA2b, TGFβ1, ADAM8 and MMP9 (Fig. 3, Table 2).

ER stress targets are also strong candidates for immunotherapy and vaccines development, a good example of which is the production of chaperone protein-based cancer vaccines termed chaperone-rich cell lysate (CRCL) [348]. The CRCL are purified from tumour tissue or recombinantly produced and applied as vaccines against murine and canine cancers or infectious diseases. Advantages of CRCL vaccines include small quantities and easily obtained starting materials [349]. Furthermore, DNA vaccination with gp96-peptide fusion proteins showed increased resistance against the intracellular bacterial pathogen *Listeria monocytogenes* in a mouse model [350]. To improve the efficacy of gp96 vaccines, gp96 was pooled with CpG in combination with anti-B7H1 or anti–interleukin-10 monoclonal antibodies to treat mice with large tumours [351]. The heterogeneous or allogeneic gp96 vaccines protected mice from tumour challenge and re-challenge. In addition to its role as a molecular chaperone, GRP94 was likewise identified as a peptide carrier for T-cell immunization [352]. However, the immunological application of GRP94 derived from its peptide binding capacity was not further investigated (Fig. 3, Table 2). The activation of ER stress has been

reported as well in different critical care diseases models, such as sepsis [331,332], liver, heart, brain and kidney ischaemia [353–359] and haemorrhagic shock [334,335]. But, the pathophysiological impact of ER stress activation in these conditions severely lacks characterization. Multiple factors such as inflammation, hypoxia present in sepsis and shock can induce ER stress but its effects are ambivalent. It has been shown that induction of ER stress is cytoprotective [353,354], and that proteostasis promotors/disruptors such as 4-PBA [336] or TUDCA [337] can be used to improve disease outcome. The increase of CHOP in renal tissue was reported to inhibit inflammatory response in and provide protection against kidney injury [336]. Moreover, the activation of PERK seems to facilitate survival of lipopolysaccharide-treated cardiomyocytes by promoting autophagy [338]. Additionally, the activation of ATF6 before ischaemia reduced myocardial tissue damage during ischaemia/reperfusion (I/R) injury [339]. Furthermore, induction of BiP in cardiomyocytes stimulated AKT signalling and protected against oxidative stress, conferring cellular I/R damage protection [340]. In contrast, inhibition of ER stress was indicated to limit cellular damage in

Table 2. ER stress-centred clinical trials. A range of clinical entities in endocrinology, oncology and paediatrics have been targeted through clinical trials. This table presents such trials detailing the trial targeted, interventional agent investigated and national authority carrying out the investigation.

Trial	Disease	Intervention	Country
Role of ER stress in the pathophysiology of type 2 diabetes	• Diabetes mellitus, type 2	No intervention	France
ER stress and resistance to treatments in Ph-negative myeloproliferative neoplasms	• Polycythemia vera • Essential thrombocythemia	Biological: RNA sample of total leucocytes before start of treatment	France
Effect of ER stress on metabolic function	• Insulin resistance • Diabetes • Obesity	Drug: TUDCA Other: placebo Drug: sodium phenylbutyrate	United States
ER stress in chronic respiratory diseases	• Chronic airway disorders • Lung cancer	Observational	South Korea
TUDCA for protease-inhibitor associated insulin resistance	• HIV-related insulin resistance • Protease inhibitor-related Insulin resistance	Drug: TUDCA Other: placebo tablet	United States
ER stress in NAFLD	• Obesity • NAFLD	Drug: methyl-D9-choline	United States
TUDCA in new-onset type 1 diabetes	• Type 1 diabetes	Drug: TUDCA Drug: Sugar Pill (placebo)	United States
Effects of Liraglutide on ER stress in obese patients with type 2 diabetes	• Type 2 diabetes	Drug: liraglutide	United States
A clinical trial of dantrolene sodium in paediatric and adult patients with wolfram syndrome	• Wolfram syndrome • Diabetes mellitus • optic nerve atrophy • Ataxia	Drug: dantrolene sodium	United States

Box 1. First-in-human trial

Intravenous infusion of GRP78/BiP is safe in patients
In 2006, Brownlie *et al.* [362] reported that the prophylactic or therapeutic parenteral delivery of BiP ameliorates clinical and histological signs of inflammatory arthritis in mice. Ten years later, the first human clinical trial using intravenous BiP demonstrated that GRP78/BiP is safe in patients with active rheumatoid arthritis and some patients had clinical and biological improvements [363]. In phase I/IIA RAGULA trial, 42 patients were screened, and 24 were randomized to receive either BiP or placebo. The study showed that after a single intravenous infusion, BiP may induce remission lasting up to 3 months in rheumatoid arthritis patients.

pathologies such as hepatic I/R [341]. This contradiction may be due to interference between UPR and inflammatory pathways. CHOP-/- mice were reported to have more prominent increase in NF-kB activation and further upregulation of proinflammatory genes (CXCL-1, MIP-2, IL-6) [342]. Interestingly, inhibition of IRE1-NF-kB by resveratrol protected against sepsis-induced kidney failure [343]. In this light, the modulation of specific UPR branches is promising approach for therapy of critical care diseases.

As discussed above, understanding and characterizing the UPR has provided several potential targets to develop new therapeutics for various diseases, with an encouraging increase in the number of clinical trials based on ER stress pathway targets or associated drugs. Several of these trials [ClinicalTrials.gov, European Clinical Trials Database and the ISRCTN registry] have focused on diabetes mellitus. A trial testing TUDCA and 4-PBA for the treatment of high lipid levels or insulin resistance was conducted by the Washington University School of Medicine; however, although this study was completed in 2014, the findings are not available yet. The results from the first completed human trial using BiP for rheumatoid arthritis are described in Box 1. We can anticipate that clinical trials to test ER stress targeting drugs in several other diseases will shortly ensue.

Concluding remarks

The ER has evolved in our knowledge from a key player in proteostasis and the secretory pathway to a cornerstone of metabolic functions. Such wealth of information has allowed the identification of numerous mechanisms for fine-tuning ER signalling, as well as motivated the need for their better characterization towards relevant health-related applications. This drive to further ER knowledge has also led to the identification of emerging roles for the ER in physiology and disease. In particular, it appears an indispensable tool for cellular communication that reaches beyond the intracellular space. The concept of transmissible ER stress illustrates the far-reaching control that ER signalling exerts in interorgan communication affecting disease pathogenesis and normal physiology [360,361].

Our increasing knowledge of ER signalling mechanisms presents opportunities to exploit the resulting applications on multiple fronts, including bioengineering and health, concepts that may routinely overlap. For example, boosting ER protein production capacity may be applied to cell engineering to increase biologic therapy production. This will drive down costs of biologics, helping demand to be met and leading to more widely available medications, thus having a significant effect on public health. Population-wide consequences of ER modulation may not be restricted to the production of biologic therapies as its applications could also contribute to bioengineering approaches for crop or livestock improvement.

A thorough understanding of the ER stress response and its role in physiology and pathophysiology can be applied to develop new ER stress targeted therapies and stratifying patients into cohorts suitable for ER-targeted therapies. Considering the enormity of attrition rates of novel therapeutic discovery in an ever-tightening financial climate, there is an urgent need for new therapeutic targets as well as precision tools that target and guide innovation to specific patient pools. ER stress signalling may provide such tools. Not only is it central to life itself but it is involved in a wide array of clinical presentations. Moreover, its effect on heterogeneous presentations within the same diseases makes it an attractive target for translational precision medicine. Of course, when undertaking medical research or trying to solve a biomolecular functional mystery one cannot look past the logistical aspect of the task ahead. The conserved metazoan nature of ER stress signalling combined with the emergence of high throughput and *in silico* strategies supplies researchers with a wealth of tools to study pathophysiology, from structure to function in multiple *in vivo* and *in vitro* models, producing robust results to be put forward for clinical scrutiny while all the while observing both the safeguards of the declaration of Helsinki and ethics on animal experimentation. Our deeper understanding of the ER and its major homeostatic regulator, the UPR response, is introducing an individualized molecular

approach to health management at a preventative, diagnostic and therapeutic level and, uncovering the genetic architecture underlying the ER stress response could significantly influence future therapeutic strategies in patients.

Acknowledgements

References

1 Porter KR, Claude A & Fullam EF (1945) A study of tissue culture cells by electron microscopy: methods and preliminary observations. *J Exp Med* **81**, 233–246.

2 Palade GE & Porter KR (1954) Studies on the endoplasmic reticulum. I. Its identification in cells *in situ*. *J Exp Med* **100**, 641–656.

3 Alberts B, Johnson A, Lewis J, Raff M, Roberts K & Walter P (2002) Molecular Biology of the Cell, 4th edn. Garland Science, New York, NY.

4 Borgese N, Francolini M & Snapp E (2006) Endoplasmic reticulum architecture: structures in flux. *Curr Opin Cell Biol* **18**, 358–364.

5 Shibata Y, Voeltz GK & Rapoport TA (2006) Rough sheets and smooth tubules. *Cell* **126**, 435–439.

6 Hayashi T, Rizzuto R, Hajnoczky G & Su TP (2009) MAM: more than just a housekeeper. *Trends Cell Biol* **19**, 81–88.

7 Toulmay A & Prinz WA (2011) Lipid transfer and signaling at organelle contact sites: the tip of the iceberg. *Curr Opin Cell Biol* **23**, 458–463.

8 Daste F, Galli T & Tareste D (2015) Structure and function of longin SNAREs. *J Cell Sci* **128**, 4263–4272.

9 Rowland AA, Chitwood PJ, Phillips MJ & Voeltz GK (2014) ER contact sites define the position and timing of endosome fission. *Cell* **159**, 1027–1041.

10 Wilhelm LP, Tomasetto C & Alpy F (2016) Touché! STARD3 and STARD3NL tether the ER to endosomes. *Biochem Soc Trans* **44**, 493–498.

11 Wilhelm LP, Wendling C, Védie B, Kobayashi T, Chenard M, Tomasetto C, Drin G & Alpy F (2017) STARD3 mediates endoplasmic reticulum-to-endosome cholesterol transport at membrane contact sites. *EMBO J* **36**, 1412–1433.

12 Henne WM, Zhu L, Balogi Z, Stefan C, Pleiss JA & Emr SD (2015) Mdm1/Snx13 is a novel ER–endolysosomal interorganelle tethering protein. *J Cell Biol* **210**, 541–551.

13 Hayashi-Nishino M, Fujita N, Noda T, Yamaguchi A, Yoshimori T & Yamamoto A (2010) Electron tomography reveals the endoplasmic reticulum as a membrane source for autophagosome formation. *Autophagy* **6**, 301–303.

14 Uemura T, Yamamoto M, Kametaka A, Sou Y, Yabashi A, Yamada A, Annoh H, Kametaka S, Komatsu M & Waguri S (2014) A cluster of thin tubular structures mediates transformation of the endoplasmic reticulum to autophagic isolation membrane. *Mol Cell Biol* **34**, 1695–1706.

15 Stefan CJ, Manford AG, Baird D, Yamada-Hanff J, Mao Y & Emr SD (2011) Osh proteins regulate phosphoinositide metabolism at ER-plasma membrane contact sites. *Cell* **144**, 389–401.

16 Braakman I & Bulleid NJ (2011) Protein folding and modification in the mammalian endoplasmic reticulum. *Annu Rev Biochem* **80**, 71–99.

17 Hebert DN & Molinari M (2007) In and out of the ER: protein folding, quality control, degradation, and related human diseases. *Physiol Rev* **87**, 1377–1408.

18 Wallis AK & Freedman RB (2013) Assisting oxidative protein folding: how do protein disulphide-isomerases couple conformational and chemical processes in protein folding? *Top Curr Chem* **328**, 1–34.

19 Aebi M, Bernasconi R, Clerc S & Molinari M (2010) N-glycan structures: recognition and processing in the ER. *Trends Biochem Sci* **35**, 74–82.

20 Meusser B, Hirsch C, Jarosch E & Sommer T (2005) ERAD: the long road to destruction. *Nat Cell Biol* **7**, 766–772.

21 Hebert DN, Bernasconi R & Molinari M (2010) ERAD substrates: which way out? *Semin Cell Dev Biol* **21**, 526–532.

22 Kobayashi T, Tanaka K, Inoue K & Kakizuka A (2002) Functional ATPase activity of p97/valosin-containing protein (VCP) is required for the quality control of endoplasmic reticulum in neuronally differentiated mammalian PC12 cells. *J Biol Chem* **277**, 47358–47365.

23 Enns GM, Shashi V, Bainbridge M, Gambello MJ, Zahir FR, Bast T, Crimian R, Schoch K, Platt J, Cox R *et al.* (2014) Mutations in NGLY1 cause an inherited disorder of the endoplasmic reticulum-associated degradation (ERAD) pathway. *Genet Med* **16**, 751–758.

24 Kamhi-Nesher S, Shenkman M, Tolchinsky S, Fromm SV, Ehrlich R & Lederkremer GZ (2001) A novel quality control compartment derived from the endoplasmic reticulum. *Mol Biol Cell* **12**, 1711–1723.

25 Huyer G, Longsworth GL, Mason DL, Mallampalli MP, McCaffery JM, Wright RL & Michaelis S (2004)

A striking quality control subcompartment in *Saccharomyces cerevisiae*: the endoplasmic reticulum-associated compartment. *Mol Biol Cell* **15**, 908–921.

26 Brown MS & Goldstein JL (1999) A proteolytic pathway that controls the cholesterol content of membranes, cells, and blood. *Proc Natl Acad Sci USA* **96**, 11041–11048.

27 Fagone P & Jackowski S (2009) Membrane phospholipid synthesis and endoplasmic reticulum function. *J Lipid Res* **50**, S311–S316.

28 Yen C-LE, Stone SJ, Koliwad S, Harris C & Farese RV (2008) Thematic review series: glycerolipids. DGAT enzymes and triacylglycerol biosynthesis. *J Lipid Res* **49**, 2283–2301.

29 Jo Y & DeBose-Boyd RA (2010) Control of cholesterol synthesis through regulated ER-associated degradation of HMG CoA reductase. *Crit Rev Biochem Mol Biol* **45**, 185–198.

30 Patwardhan GA, Beverly LJ & Siskind LJ (2016) Sphingolipids and mitochondrial apoptosis. *J Bioenerg Biomembr* **48**, 153–168.

31 Barlowe C, Orci L, Yeung T, Hosobuchi M, Hamamoto S, Salama N, Rexach MF, Ravazzola M, Amherdt M & Schekman R (1994) COPII: a membrane coat formed by Sec proteins that drive vesicle budding from the endoplasmic reticulum. *Cell* **77**, 895–907.

32 Siddiqi S, Saleem U, Abumrad NA, Davidson NO, Storch J, Siddiqi SA & Mansbach CM (2010) A novel multiprotein complex is required to generate the prechylomicron transport vesicle from intestinal ER. *J Lipid Res* **51**, 1918–1928.

33 Clapham DE (2007) Calcium signaling. *Cell* **131**, 1047–1058.

34 Meldolesi J & Pozzan T (1998) The endoplasmic reticulum Ca2 + store: a view from the lumen. *Trends Biochem Sci* **23**, 10–14.

35 Hetz C (2012) The unfolded protein response: controlling cell fate decisions under ER stress and beyond. *Nat Rev Mol Cell Biol* **13**, 89–102.

36 Hanahan D & Weinberg RA (2011) Hallmarks of cancer: the next generation. *Cell* **144**, 646–674.

37 Holderfield M, Deuker MM, McCormick F & McMahon M (2014) Targeting RAF kinases for cancer therapy: BRAF mutated melanoma and beyond. *Nat Rev Cancer* **14**, 455–467.

38 Piwocka K, Vejda S, Cotter TG, O'Sullivan GC & McKenna SL (2006) Bcr-Abl reduces endoplasmic reticulum releasable calcium levels by a Bcl-2-independent mechanism and inhibits calcium-dependent apoptotic signaling. *Blood* **107**, 4003–4010.

39 Pluquet O, Pourtier A & Abbadie C (2015) The unfolded protein response and cellular senescence. A review in the theme: cellular mechanisms of endoplasmic reticulum stress signaling in health and disease. *Am J Physiol Cell Physiol* **308**, C415–C425.

40 Chen H-J, Anagnostou G, Chai A, Withers J, Morris A, Adhikaree J, Pennetta G & de Belleroche JS (2010) Characterization of the properties of a novel mutation in VAPB in familial amyotrophic lateral sclerosis. *J Biol Chem* **285**, 40266–40281.

41 Nishimura AL, Mitne-Neto M, Silva HCA, Richieri-Costa A, Middleton S, Cascio D, Kok F, Oliveira JRM, Gillingwater T, Webb J *et al.* (2004) A Mutation in the vesicle-trafficking protein VAPB causes late-onset spinal muscular atrophy and amyotrophic lateral sclerosis. *Am J Hum Genet* **75**, 822–831.

42 Harding HP & Ron D (2002) Endoplasmic reticulum stress and the development of diabetes: a review. *Diabetes* **51**, S455–S461.

43 Oyadomari S, Koizumi A, Takeda K, Gotoh T, Akira S, Araki E & Mori M (2002) Targeted disruption of the Chop gene delays endoplasmic reticulum stress-mediated diabetes. *J Clin Invest* **109**, 525–532.

44 Colombo C, Porzio O, Liu M, Massa O, Vasta M, Salardi S, Beccaria L, Monciotti C, Toni S, Pedersen O *et al.* (2008) Seven mutations in the human insulin gene linked to permanent neonatal/infancy-onset diabetes mellitus. *J Clin Invest* **118**, 2148–2156.

45 Støy J, Edghill EL, Flanagan SE, Ye H, Paz VP, Pluzhnikov A, Below JE, Hayes MG, Cox NJ, Lipkind GM *et al.* (2007) Insulin gene mutations as a cause of permanent neonatal diabetes. *Proc Natl Acad Sci USA* **104**, 15040–15044.

46 Giampietri C, Petrungaro S, Conti S, Facchiano A, Filippini A & Ziparo E (2015) Cancer microenvironment and endoplasmic reticulum stress response. *Mediators Inflamm* **2015**, 417281.

47 Jin ML, Park SY, Kim YH, Oh J-I, Lee SJ & Park G (2014) The neuroprotective effects of cordycepin inhibit glutamate-induced oxidative and ER stress-associated apoptosis in hippocampal HT22 cells. *Neurotoxicology* **41**, 102–111.

48 Stechmann B, Bai S-K, Gobbo E, Lopez R, Merer G, Pinchard S, Panigai L, Tenza D, Raposo G, Beaumelle B *et al.* (2010) Inhibition of retrograde transport protects mice from lethal ricin challenge. *Cell* **141**, 231–242.

49 Olden K, Pratt RM, Jaworski C & Yamada KM (1979) Evidence for role of glycoprotein carbohydrates in membrane transport: specific inhibition by tunicamycin. *Proc Natl Acad Sci USA* **76**, 791–795.

50 Schultz AM & Oroszlan S (1979) Tunicamycin inhibits glycosylation of precursor polyprotein encoded by env gene of Rauscher murine leukemia virus. *Biochem Biophys Res Commun* **86**, 1206–1213.

51 Datema R & Schwarz RT (1979) Interference with glycosylation of glycoproteins. Inhibition of formation

of lipid-linked oligosaccharides *in vivo*. *Biochem J* **184**, 113–123.

52　Cleland WW (1964) Dithiothreitol, a new protective reagent for SH groups. *Biochemistry* **3**, 480–482.

53　Liu ES, Ou JH & Lee AS (1992) Brefeldin A as a regulator of grp78 gene expression in mammalian cells. *J Biol Chem* **267**, 7128–7133.

54　Thastrup O, Cullen PJ, Drøbak BK, Hanley MR & Dawson AP (1990) Thapsigargin, a tumor promoter, discharges intracellular Ca2 + stores by specific inhibition of the endoplasmic reticulum Ca2(+)-ATPase. *Proc Natl Acad Sci USA* **87**, 2466–2470.

55　Pirot P, Naamane N, Libert F, Magnusson NE, Ørntoft TF, Cardozo AK & Eizirik DL (2007) Global profiling of genes modified by endoplasmic reticulum stress in pancreatic beta cells reveals the early degradation of insulin mRNAs. *Diabetologia* **50**, 1006–1014.

56　Malo A, Krüger B, Göke B & Kubisch CH (2013) 4-phenylbutyric acid reduces endoplasmic reticulum stress, trypsin activation, and acinar cell apoptosis while increasing secretion in rat pancreatic acini. *Pancreas* **42**, 92–101.

57　Lee YY, Hong SH, Lee YJ, Chung SS, Jung HS, Park SG & Park KS (2010) Tauroursodeoxycholate (TUDCA), chemical chaperone, enhances function of islets by reducing ER stress. *Biochem Biophys Res Commun* **397**, 735–739.

58　Ozcan U, Yilmaz E, Ozcan L, Furuhashi M, Vaillancourt E, Smith RO, Görgün CZ & Hotamisligil GS (2006) Chemical chaperones reduce ER stress and restore glucose homeostasis in a mouse model of type 2 diabetes. *Science* **313**, 1137–1140.

59　Lepock JR (2005) How do cells respond to their thermal environment? *Int J Hyperthermia* **21**, 681–687.

60　Bettaieb A & Averill-Bates DA (2005) Thermotolerance induced at a mild temperature of 40°C protects cells against heat shock-induced apoptosis. *J Cell Physiol* **205**, 47–57.

61　Liu Y, Sakamoto H, Adachi M, Zhao S, Ukai W, Hashimoto E, Hareyama M, Ishida T, Imai K & Shinomura Y (2012) Heat stress activates ER stress signals which suppress the heat shock response, an effect occurring preferentially in the cortex in rats. *Mol Biol Rep* **39**, 3987–3993.

62　Liu X, Wang M, Chen H, Guo Y, Ma F, Shi F, Bi Y & Li Y (2013) Hypothermia protects the brain from transient global ischemia/reperfusion by attenuating endoplasmic reticulum response-induced apoptosis through CHOP. *PLoS ONE* **8**, e53431.

63　Mollereau B (2015) Cooling-induced ER stress is good for your brain. *EBioMedicine* **2**, 482–483.

64　Zeeshan H, Lee G, Kim H-R & Chae H-J (2016) Endoplasmic reticulum stress and associated ROS. *Int J Mol Sci* **17**, 327.

65　Bhandary B, Marahatta A, Kim H-R & Chae H-J (2012) An involvement of oxidative stress in endoplasmic reticulum stress and its associated diseases. *Int J Mol Sci* **14**, 434–456.

66　Cadenas E & Davies KJ (2000) Mitochondrial free radical generation, oxidative stress, and aging. *Free Radic Biol Med* **29**, 222–230.

67　Knupp J, Arvan P & Chang A (2018) Increased mitochondrial respiration promotes survival from endoplasmic reticulum stress. *Cell Death Differ*. https://doi.org/10.1038/s41418-018-0133-4

68　Tu BP & Weissman JS (2004) Oxidative protein folding in eukaryotes: mechanisms and consequences. *J Cell Biol* **164**, 341–346.

69　Malhotra JD & Kaufman RJ (2007) Endoplasmic reticulum stress and oxidative stress: a vicious cycle or a double-edged sword? *Antioxid Redox Signal* **9**, 2277–2293.

70　Cao SS & Kaufman RJ (2014) Endoplasmic reticulum stress and oxidative stress in cell fate decision and human disease. *Antioxid Redox Signal* **21**, 396–413.

71　Montibeller L & de Belleroche J (2018) Amyotrophic lateral sclerosis (ALS) and Alzheimer's disease (AD) are characterised by differential activation of ER stress pathways: focus on UPR target genes. *Cell Stress Chaperones*. https://doi.org/10.1007/s12192-018-0897-y

72　Bertolotti A, Zhang Y, Hendershot LM, Harding HP & Ron D (2000) Dynamic interaction of BiP and ER stress transducers in the unfolded-protein response. *Nat Cell Biol* **2**, 326–332.

73　Shen J, Chen X, Hendershot L & Prywes R (2002) ER stress regulation of ATF6 localization by dissociation of BiP/GRP78 binding and unmasking of Golgi localization signals. *Dev Cell* **3**, 99–111.

74　Kopp MC, Nowak PR, Larburu N, Adams CJ & Ali MMU (2018) *In vitro* FRET analysis of IRE1 and BiP association and dissociation upon endoplasmic reticulum stress. *Elife* **7**, e30257.

75　Amin-Wetzel N, Saunders RA, Kamphuis MJ, Rato C, Preissler S, Harding HP & Ron D (2017) A J-Protein co-chaperone recruits BiP to monomerize IRE1 and repress the unfolded protein response. *Cell* **171**, 1625–1637.e13.

76　Sepulveda D, Rojas-Rivera D, Rodríguez DA, Groenendyk J, Köhler A, Lebeaupin C, Ito S, Urra H, Carreras-Sureda A, Hazari Y *et al.* (2018) Interactome screening identifies the ER luminal chaperone Hsp47 as a regulator of the unfolded protein response transducer IRE1α. *Mol Cell* **69**, 238–252.e7.

77　Ye J, Rawson RB, Komuro R, Chen X, Davé UP, Prywes R, Brown MS & Goldstein JL (2000) ER stress induces cleavage of membrane-bound ATF6 by the same proteases that process SREBPs. *Mol Cell* **6**, 1355–1364.

78 Carrara M, Prischi F & Ali MMU (2013) UPR signal activation by luminal sensor domains. *Int J Mol Sci* **14**, 6454–6466.

79 Tirasophon W, Welihinda AA & Kaufman RJ (1998) A stress response pathway from the endoplasmic reticulum to the nucleus requires a novel bifunctional protein kinase/endoribonuclease (Ire1p) in mammalian cells. *Genes Dev* **12**, 1812–1824.

80 Wang XZ, Harding HP, Zhang Y, Jolicoeur EM, Kuroda M & Ron D (1998) Cloning of mammalian Ire1 reveals diversity in the ER stress responses. *EMBO J* **17**, 5708–5717.

81 Iwawaki T, Hosoda A, Okuda T, Kamigori Y, Nomura-Furuwatari C, Kimata Y, Tsuru A & Kohno K (2001) Translational control by the ER transmembrane kinase/ribonuclease IRE1 under ER stress. *Nat Cell Biol* **3**, 158–165.

82 Bertolotti A, Wang X, Novoa I, Jungreis R, Schlessinger K, Cho JH, West AB & Ron D (2001) Increased sensitivity to dextran sodium sulfate colitis in IRE1β-deficient mice. *J Clin Invest* **107**, 585–593.

83 Martino MB, Jones L, Brighton B, Ehre C, Abdulah L, Davis CW, Ron D, O'Neal WK & Ribeiro CMP (2013) The ER stress transducer IRE1β is required for airway epithelial mucin production. *Mucosal Immunol* **6**, 639–654.

84 Iwawaki T, Akai R, Yamanaka S & Kohno K (2009) Function of IRE1 alpha in the placenta is essential for placental development and embryonic viability. *Proc Natl Acad Sci USA* **106**, 16657–16662.

85 Bouchecareilh M, Higa A, Fribourg S, Moenner M & Chevet E (2011) Structure of the Ire1 autophosphorylation complex and implications for the unfolded protein response. *FASEB J* **25**, 3115–3129.

86 Sanches M, Duffy NM, Talukdar M, Thevakumaran N, Chiovitti D, Canny MD, Lee K, Kurinov I, Uehling D, Al-awar R *et al.* (2014) Structure and mechanism of action of the hydroxy-aryl-aldehyde class of IRE1 endoribonuclease inhibitors. *Nat Commun* **5**, 4202.

87 Prischi F, Nowak PR, Carrara M & Ali MMU (2014) Phosphoregulation of Ire1 RNase splicing activity. *Nat Commun* **5**, 3554.

88 Urano F, Wang X-Z, Bertolotti A, Zhang Y, Chung P, Harding HP & Ron D (2000) Coupling of stress in the endoplasmic reticulum to activation of JNK protein kinases by transmembrane protein kinase IRE1. *Science* **287**, 664–666.

89 Bork P & Sander C (1993) A hybrid protein kinase-RNase in an interferon-induced pathway? *FEBS Lett* **334**, 149–152.

90 Sidrauski C & Walter P (1997) The transmembrane kinase Ire1p is a site-specific endonuclease that initiates mRNA splicing in the unfolded protein response. *Cell* **90**, 1031–1039.

91 Yoshida H, Matsui T, Yamamoto A, Okada T & Mori K (2001) XBP1 mRNA is induced by ATF6 and spliced by IRE1 in response to ER stress to produce a highly active transcription factor. *Cell* **107**, 881–891.

92 Greer CL, Peebles CL, Gegenheimer P & Abelson J (1983) Mechanism of action of a yeast RNA ligase in tRNA splicing. *Cell* **32**, 537–546.

93 Sidrauski C, Cox JS & Walter P (1996) tRNA ligase is required for regulated mRNA splicing in the unfolded protein response. *Cell* **87**, 405–413.

94 Schwer B, Sawaya R, Ho CK & Shuman S (2004) Portability and fidelity of RNA-repair systems. *Proc Natl Acad Sci USA* **101**, 2788–2793.

95 Tanaka N, Meineke B & Shuman S (2011) RtcB, a novel RNA ligase, can catalyze tRNA splicing and HAC1 mRNA splicing *in vivo*. *J Biol Chem* **286**, 30253–30257.

96 Baltz AG, Munschauer M, Schwanhäusser B, Vasile A, Murakawa Y, Schueler M, Youngs N, Penfold-Brown D, Drew K, Milek M *et al.* (2012) The mRNA-bound proteome and its global occupancy profile on protein-coding transcripts. *Mol Cell* **46**, 674–690.

97 Lu Y, Liang FX & Wang X (2014) A synthetic biology approach identifies the mammalian UPR RNA ligase RtcB. *Mol Cell* **55**, 758–770.

98 Liou HC, Boothby MR, Finn PW, Davidon R, Nabavi N, Zeleznik-Le NJ, Ting JP & Glimcher LH (1990) A new member of the leucine zipper class of proteins that binds to the HLA DR alpha promoter. *Science* **247**, 1581–1584.

99 Yoshimura T, Fujisawa J & Yoshida M (1990) Multiple cDNA clones encoding nuclear proteins that bind to the tax-dependent enhancer of HTLV-1: all contain a leucine zipper structure and basic amino acid domain. *EMBO J* **9**, 2537–2542.

100 Nojima H, Leem Sh, Araki H, Sakai A, Nakashima N, Kanaoka Y & Ono Y (1994) Hac1: a novel yeast bZIP protein binding to the CRE motif is a multicopy suppressor for cdcW mutant of *Schizosaccharomyces pombe*. *Nucleic Acids Res* **22**, 5279–5288.

101 Cox JS & Walter P (1996) A novel mechanism for regulating activity of a transcription factor that controls the unfolded protein response. *Cell* **87**, 391–404.

102 Calfon M, Zeng H, Urano F, Till JH, Hubbard SR, Harding HP, Clark SG & Ron D (2002) IRE1 couples endoplasmic reticulum load to secretory capacity by processing the XBP-1 mRNA. *Nature* **415**, 92–96.

103 Chen CY, Malchus NS, Hehn B, Stelzer W, Avci D, Langosch D & Lemberg MK (2014) Signal peptide peptidase functions in ERAD to cleave the unfolded

protein response regulator XBP1u. *EMBO J* 33, 2492–2506.

104 Yanagitani K, Imagawa Y, Iwawaki T, Hosoda A, Saito M, Kimata Y & Kohno K (2009) Cotranslational Targeting of XBP1 protein to the membrane promotes cytoplasmic splicing of its own mRNA. *Mol Cell* 34, 191–200.

105 Yanagitani K, Kimata Y, Kadokura H & Kohno K (2011) Translational pausing ensures membrane targeting and cytoplasmic splicing of XBP1u mRNA. *Science* 331, 586–589.

106 Kanda S, Yanagitani K, Yokota Y, Esaki Y & Kohno K (2016) Autonomous translational pausing is required for XBP1u mRNA recruitment to the ER via the SRP pathway. *Proc Natl Acad Sci* 113, E5886–E5895.

107 Chalmers F, Sweeney B, Cain K & Bulleid NJ (2017) Inhibition of IRE1α-mediated XBP1 mRNA cleavage by XBP1 reveals a novel regulatory process during the unfolded protein response. *Wellcome Open Res* 2, 36.

108 He Y, Sun S, Sha H, Liu Z, Yang L, Xue Z, Chen H & Qi L (2010) Emerging roles for XBP1, a sUPeR transcription factor. *Gene Expr* 15, 13–25.

109 Travers KJ, Patil CK, Wodicka L, Lockhart DJ, Weissman JS & Walter P (2000) Functional and genomic analyses reveal an essential coordination between the unfolded protein response and ER-associated degradation. *Cell* 101, 249–258.

110 Iwakoshi NN, Lee A-H & Glimcher LH (2003) The X-box binding protein-1 transcription factor is required for plasma cell differentiation and the unfolded protein response. *Immunol Rev* 194, 29–38.

111 Sriburi R, Jackowski S, Mori K & Brewer JW (2004) XBP1: a link between the unfolded protein response, lipid biosynthesis, and biogenesis of the endoplasmic reticulum. *J Cell Biol* 167, 35–41.

112 Korchak HM (2008) Regulation of hepatic lipogenesis. *Tufts Folia Med* 8, 134–143.

113 So JS, Hur KY, Tarrio M, Ruda V, Frank-Kamenetsky M, Fitzgerald K, Koteliansky V, Lichtman AH, Iwawaki T, Glimcher LH *et al.* (2012) Silencing of lipid metabolism genes through IRE1α-mediated mRNA decay lowers plasma lipids in mice. *Cell Metab* 16, 487–499.

114 Zhou Y, Lee J, Reno CM, Sun C, Park SW, Chung J, Lee J, Fisher SJ, White MF, Biddinger SB *et al.* (2011) Regulation of glucose homeostasis through a XBP-1–FoxO1 interaction. *Nat Med* 17, 356–365.

115 Park SW, Herrema H, Salazar M, Cakir I, Cabi S, Basibuyuk Sahin F, Chiu YH, Cantley LC & Ozcan U (2014) BRD7 regulates XBP1s' activity and glucose homeostasis through its interaction with the regulatory subunits of PI3K. *Cell Metab* 20, 73–84.

116 Liu J, Ibi D, Taniguchi K, Lee J, Herrema H, Akosman B, Mucka P, Salazar Hernandez MA, Uyar

MF, Park SW *et al.* (2016) Inflammation improves glucose homeostasis through IKKβ-XBP1s interaction. *Cell* 167, 1052–1066.e18.

117 Lee J, Sun C, Zhou Y, Lee J, Gokalp D, Herrema H, Park SW, Davis RJ & Ozcan U (2011) p38 MAPK–mediated regulation of Xbp1s is crucial for glucose homeostasis. *Nat Med* 17, 1251–1260.

118 Yingfeng D, Zhao WV, Caroline T, Ningguo G, William HL, Anwarul F, Joyce RJ, Guosheng L, Jin Y, Mark LA *et al.* (2013) The Xbp1s/GalE axis links ER stress to postprandial hepatic metabolism. *J Clin Invest* 123, 455–468.

119 Özcan U, Cao Q, Yilmaz E, Lee A-H, Iwakoshi NN, Özdelen E, Tuncman G, Görgün C, Glimcher Laurie H & Hotamisligil GS (2004) Endoplasmic reticulum stress links obesity, insulin action, and type 2 diabetes. *Science* 306, 457–461.

120 Akiyama M, Liew CW, Lu S, Hu J, Martinez R, Hambro B, Kennedy RT & Kulkarni RN (2013) X-box binding protein 1 is essential for insulin regulation of pancreatic a-cell function. *Diabetes* 62, 2439–2449.

121 Liu Y, Adachi M, Zhao S, Hareyama M, Koong AC, Luo D & Rando TA (2010) Preventing oxidative stress a new role for XBP1. *Cell* 16, 847–857.

122 Tao R, Chen H, Gao C, Xue P, Yang F, Han J-DJ, Zhou B & Chen Y-G (2011) Xbp1-mediated histone H4 deacetylation contributes to DNA double-strand break repair in yeast. *Cell Res* 21, 1619–1633.

123 Wu J & Kaufman RJ (2006) From acute ER stress to physiological roles of the Unfolded Protein Response. *Cell Death Differ* 13, 374–384.

124 Blais A, Tsikitis M, Acosta-Alvear D, Sharan R, Kluger Y & Dynlacht BD (2005) An initial blueprint for myogenic differentiation. *Genes Dev* 19, 553–569.

125 Reimold AM, Iwakoshi NN, Manis J, Vallabhajosyula P, Szomolanyi-Tsuda E, Gravallese EM, Friend D, Grusby MJ, Alt F & Glimcher LH (2001) Plasma cell differentiation requires the transcription factor XBP-1. *Nature* 412, 300–307.

126 Lee A-H, Chu GC, Iwakoshi NN & Glimcher LH (2005) XBP-1 is required for biogenesis of cellular secretory machinery of exocrine glands. *EMBO J* 24, 4368–4380.

127 Huh WJ, Esen E, Geahlen JH, Bredemeyer AJ, Lee A, Shi G, Konieczny SF, Glimcher LH & Mills JC (2010) XBP1 controls maturation of gastric zymogenic cells by induction of MIST1 and expansion of the rough endoplasmic reticulum. *Gastroenterology* 139, 2038–2049.

128 Sha H, He Y, Chen H, Wang C, Zenno A, Shi H, Yang X & Zhang X (2009) The IRE1α-XBP1 pathway of the unfolded protein response is required for adipogenesis. *Cell Metab* 9, 556–564.

129 Masaki T, Yoshida M & Noguchi S (1999) Targeted disruption of CRE-Binding factor TREB5 gene leads

to cellular necrosis in cardiac myocytes at the embryonic stage. *Biochem Biophys Res Commun* **261**, 350–356.

130 Reimold AM, Etkin A, Clauss I, Perkins A, Friend DS, Zhang J, Horton HF, Scott A, Orkin SH, Byrne MC *et al.* (2000) An essential role in liver development for transcription factor XBP-1. *Genes Dev* **14**, 152–157.

131 Sone M, Zeng X, Larese J & Ryoo HD (2013) A modified UPR stress sensing system reveals a novel tissue distribution of IRE1/XBP1 activity during normal Drosophila development. *Cell Stress Chaperones* **18**, 307–319.

132 Ono SJ, Liout H, Davidont R, Strominger JL & Glimchert LH (1991) Human X-box-binding protein 1 is required for the transcription of a subset of human class II major histocompatibility genes and forms a heterodimer with c-fos. *Proc Natl Acad Sci USA* **88**, 4309–4312.

133 Ding L, Yan J, Zhu J, Zhong H, Lu Q, Wang Z, Huang C & Ye Q (2003) Ligand-independent activation of estrogen receptor α by XBP-1. *Nucleic Acids Res* **31**, 5266–5274.

134 Ravasi T, Suzuki H, Cannistraci CV, Katayama S, Bajic VB, Tan K, Akalin A, Schmeier S, Kanamori-Katayama M, Bertin N *et al.* (2010) An atlas of combinatorial transcriptional regulation in mouse and man. *Cell* **140**, 744–752.

135 Reinke AW, Baek J, Ashenberg O & Keating AE (2013) Networks of bZIP protein-protein interactions diversified over a billion years of evolution. *Science* **340**, 730–734.

136 Chen X, Iliopoulos D, Zhang Q, Tang Q, Greenblatt MB, Hatziapostolou M, Lim E, Tam WL, Ni M, Chen Y *et al.* (2014) XBP1 promotes triple-negative breast cancer by controlling the HIF1α pathway. *Nature* **508**, 103–107.

137 Hollien J, Lin JH, Li H, Stevens N, Walter P & Weissman JS (2009) Regulated Ire1-dependent decay of messenger RNAs in mammalian cells. *J Cell Biol* **186**, 323–331.

138 Maurel M, Chevet E, Tavernier J & Gerlo S (2014) Getting RIDD of RNA: IRE1 in cell fate regulation. *Trends Biochem Sci* **39**, 245–254.

139 Lhomond S, Avril T, Dejeans N, Voutetakis K, Doultsinos D, McMahon M, Pineau R, Obacz J, Papadodima O, Jouan F *et al.* (2018) Dual IRE1 RNase functions dictate glioblastoma development. *EMBO Mol Med* **10**, e7929. https://doi.org/10.15252/emmm.201707929

140 Tirasophon W, Lee K, Callaghan B, Welihinda A & Kaufman RJ (2000) The endoribonuclease activity of mammalian IRE1 autoregulates its mRNA and is required for the unfolded protein response. *Genes Dev* **14**, 2725–2736.

141 Hollien J & Weissman JS (2006) Decay of endoplasmic reticulum-localized mRNAs during the unfolded protein response. *Science* **313**, 104–107.

142 Han D, Lerner AG, Vande WL, Upton J-P, Xu W, Hagen A, Backes BJ, Oakes SA & Papa FR (2009) IRE1α kinase activation modes control alternate endoribonuclease outputs to determine divergent cell fates. *Cell* **138**, 562–575.

143 Kimmig P, Diaz M, Zheng J, Williams CC, Lang A, Aragón T, Li H & Walter P (2012) The unfolded protein response in fission yeast modulates stability of select mRNAs to maintain protein homeostasis. *Elife* **2012**, 1–20.

144 Mishiba K-0049, Nagashima Y, Suzuki E, Hayashi N, Ogata Y, Shimada Y & Koizumi N (2013) Defects in IRE1 enhance cell death and fail to degrade mRNAs encoding secretory pathway proteins in the Arabidopsis unfolded protein response. *Proc Natl Acad Sci* **110**, 5713–5718.

145 Hayashi S, Wakasa Y, Ozawa K & Takaiwa F (2016) Characterization of IRE1 ribonuclease-mediated mRNA decay in plants using transient expression analyses in rice protoplasts. *New Phytol* **210**, 1259–1268.

146 Oikawa D, Tokuda M, Hosoda A & Iwawaki T (2010) Identification of a consensus element recognized and cleaved by IRE1α. *Nucleic Acids Res* **38**, 6265–6273.

147 Iqbal J, Dai K, Seimon T, Jungreis R, Oyadomari M, Kuriakose G, Ron D, Tabas I & Hussain MM (2008) IRE1β Inhibits chylomicron production by selectively degrading MTP mRNA. *Cell Metab* **7**, 445–455.

148 Imagawa Y, Hosoda A, Sasaka S, Tsuru A & Kohno K (2008) RNase domains determine the functional difference between IRE1α and IRE1β. *FEBS Lett* **582**, 656–660.

149 Shi Y, Vattem KM, Sood R, An J, Liang J, Stramm L & Wek RC (1998) Identification and characterization of pancreatic eukaryotic initiation factor 2 alpha-subunit kinase, PEK, involved in translational control. *Mol Cell Biol* **18**, 7499–7509.

150 Harding HP, Zhang Y & Ron D (1999) Protein translation and folding are coupled by an endoplasmic-reticulum-resident kinase. *Nature* **397**, 271–274.

151 McQuiston A & Diehl JA (2017) Recent insights into PERK-dependent signaling from the stressed endoplasmic reticulum. *F1000Research* **6**, 1897.

152 Lloyd MA, Osborne JC, Safer B, Powell GM & Merrick WC (1980) Characteristics of eukaryotic initiation factor 2 and its subunits. *J Biol Chem* **255**, 1189–1193.

153 Ernst H, Duncan RF & Hershey JWB (1987) Cloning and sequencing of complementary DNAs encoding the

alpha-subunit of translational initiation factor-Eif-2 - characterization of the protein and its messenger RNA. *J Biol Chem* **262**, 1206–1212.

154 Adams SL, Safer B & Anderson WFMW (1975) Eukaryotic initiation complex formation. Evidence for two distinct pathways. *J Biol Chem* **250**, 9083–9089.

155 Rowlands AG, Panniers R & Henshaw EC (1988) The catalytic mechanism of guanine nucleotide exchange factor action and competitive inhibition by phosphorylated eukaryotic initiation factor 2. *J Biol Chem* **263**, 5526–5533.

156 Harding HP, Zhang Y, Bertolotti A, Zeng H & Ron D (2000) Perk is essential for translational regulation and cell survival during the unfolded protein response. *Mol Cell* **5**, 897–904.

157 Hai T, Liu F, Coukos WJ & Green MR (1989) Transcription factor ATF cDNA clones: an extensive family of leucine zipper proteins able to selectively form DNA-binding heterodimers. *Genes Dev* **3**, 2083–2090.

158 Harding HP, Novoa I, Zhang Y, Zeng H, Wek R, Schapira M & Ron D (2000) Regulated translation initiation controls stress-induced gene expression in mammalian cells. *Mol Cell* **6**, 1099–1108.

159 Vallejo M, Ron D, Miller CP & Habener JF (1993) C/ATF, a member of the activating transcription factor family of DNA-binding proteins, dimerizes with CAAT/enhancer-binding proteins and directs their binding to cAMP response elements. *Proc Natl Acad Sci USA* **90**, 4679–4683.

160 Fawcett TW, Martindale JL, Guyton KZ, Hai T & Holbrook NJ (1999) Complexes containing activating transcription factor (ATF)/cAMP-responsive-element-binding protein (CREB) interact with the CCAAT/enhancer-binding protein (C/EBP)–ATF composite site to regulate Gadd153 expression during the stress response. *Biochem J* **339**, 135–141.

161 Han J, Back SH, Hur J, Lin Y, Gildersleeve R, Shan J, Yuan CL, Krokowski D, Wang S, Hatzoglou M *et al.* (2013) ER-stress-induced transcriptional regulation increases protein synthesis leading to cell death. *Nat Cell Biol* **15**, 481–490.

162 Hiramatsu N, Messah C, Han J, LaVail MM, Kaufman RJ & Lin JH (2014) Translational and posttranslational regulation of XIAP by eIF2α and ATF4 promotes ER stress-induced cell death during the unfolded protein response. *Mol Biol Cell* **25**, 1411–1420.

163 Chen YJ, Tan BCM, Cheng YY, Chen JS & Lee SC (2009) Differential regulation of CHOP translation by phosphorylated eIF4E under stress conditions. *Nucleic Acids Res* **38**, 764–777.

164 Palam LR, Baird TD & Wek RC (2011) Phosphorylation of eIF2 facilitates ribosomal bypass of an inhibitory upstream ORF to enhance CHOP translation. *J Biol Chem* **286**, 10939–10949.

165 Barbosa C, Peixeiro I & Romão L (2013) Gene expression regulation by upstream open reading frames and human disease. *PLoS Genet* **9**, 1–12.

166 Fornace AJ, Alamo I & Hollander MC (1988) DNA damage-inducible transcripts in mammalian cells. *Proc Natl Acad Sci USA* **85**, 8800–8804.

167 Fornace AJ, Nebert DW, Hollander MC, Luethy JD, Papathanasiou M, Fargnoli J & Holbrook NJ (1989) Mammalian genes coordinately regulated by growth arrest signals and DNA-damaging agents. *Mol Cell Biol* **9**, 4196–4203.

168 Lee YY, Cevallos RC & Jan E (2009) An upstream open reading frame regulates translation of GADD34 during cellular stresses that induce eIF2 phosphorylation. *J Biol Chem* **284**, 6661–6673.

169 Ma Y & Hendershot LM (2003) Delineation of a negative feedback regulatory loop that controls protein translation during endoplasmic reticulum stress. *J Biol Chem* **278**, 34864–34873.

170 Marciniak SJ, Yun CY, Oyadomari S, Novoa I, Zhang Y, Jungreis R, Nagata K, Harding HP & Ron D (2004) CHOP induces death by promoting protein synthesis and oxidation in the stressed endoplasmic reticulum. *Genes Dev* **18**, 3066–3077.

171 Connor JH, Weiser DC, Li S, John M, Li SHI & Hallenbeck JM (2001) Growth arrest and DNA damage-inducible protein GADD34 assembles a novel signaling complex containing Protein Phosphatase 1 and inhibitor 1. *Mol Cell Biol* **21**, 6841–6850.

172 Novoa I, Zeng H, Harding HP & Ron D (2001) Feedback inhibition of the unfolded protein response by GADD34-mediated dephosphorylation of eIF2alpha. *J Cell Biol* **153**, 1011–1022.

173 Harding HP, Zhang Y, Zeng H, Novoa I, Lu PD, Calfon M, Sadri N, Yun C, Popko B, Paules R *et al.* (2003) An integrated stress response regulates amino acid metabolism and resistance to oxidative stress. *Mol Cell* **11**, 619–633.

174 Quirós PM, Prado MA, Zamboni N, D'Amico D, Williams RW, Finley D, Gygi SP & Auwerx J (2017) Multi-omics analysis identifies ATF4 as a key regulator of the mitochondrial stress response in mammals. *J Cell Biol* **216**, 2027–2045.

175 Rajesh K, Krishnamoorthy J, Kazimierczak U, Tenkerian C, Papadakis AI, Wang S, Huang S & Koromilas AE (2015) Phosphorylation of the translation initiation factor eIF2α at serine 51 determines the cell fate decisions of Akt in response to oxidative stress. *Cell Death Dis* **6**, e1591.

176 Lee IC, Ho XY, George SE, Goh CW, Sundaram JR, Pang KKL, Luo W, Yusoff P, Sze NSK & Shenolikar S (2017) Oxidative stress promotes SIRT1 recruitment to the GADD34/PP1α complex to activate its deacetylase function. *Cell Death Differ* **25**, 255–267.

177 Chen D, Fan Z, Rauh M, Buchfelder M, Eyupoglu IY & Savaskan N (2017) ATF4 promotes angiogenesis and neuronal cell death and confers ferroptosis in a xCT-dependent manner. *Oncogene* **36**, 5593–5608.

178 Wu Z, Li M, Zheng W, Hu Q, Cheng Z & Guo F (2017) Silencing of both ATF4 and PERK inhibits cell cycle progression and promotes the apoptosis of differentiating chondrocytes. *Int J Mol Med* **40**, 101–111.

179 Ishizawa J, Kojima K, Chachad D, Ruvolo P, Ruvolo V, Jacamo RO, Borthakur G, Mu H, Zeng Z, Tabe Y *et al.* (2016) ATF4 induction through an atypical integrated stress response to ONC201 triggers p53-independent apoptosis in hematological malignancies. *Sci Signal* **9**, ra17.

180 Iurlaro R, Püschel F, León-Annicchiarico CL, O'Connor H, Martin SJ, Palou-Gramón D, Lucendo E & Muñoz-Pinedo C (2017) Glucose deprivation induces ATF4-mediated apoptosis through TRAIL death receptors. *Mol Cell Biol* **37**, e00479–16. https://doi.org/10.1128/MCB.00479-16

181 Zhu C, Johansen FE & Prywes R (1997) Interaction of ATF6 and serum response factor. *Mol Cell Biol* **17**, 4957–4966.

182 Yamamoto K, Sato T, Matsui T, Sato M, Okada T, Yoshida H, Harada A & Mori K (2007) Transcriptional induction of mammalian ER quality control proteins is mediated by single or combined action of ATF6alpha and XBP1. *Dev Cell* **13**, 365–376.

183 Asada R, Kanemoto S, Kondo S, Saito A & Imaizumi K (2011) The signalling from endoplasmic reticulum-resident bZIP transcription factors involved in diverse cellular physiology. *J Biochem* **149**, 507–518.

184 McMahon M, Samali A & Chevet E (2017) Regulation of the unfolded protein response by noncoding RNA. *Am J Physiol Cell Physiol* **313**, C243–C254.

185 Oslowski CM & Urano F (2011) Measuring ER stress and the unfolded protein response using mammalian tissue culture system. *Methods Enzymol* **490**, 71–92.

186 Yoshida H, Matsui T, Hosokawa N, Kaufman RJ, Nagata K & Mori K (2003) A time-dependent phase shift in the mammalian unfolded protein response. *Dev Cell* **4**, 265–271.

187 Sano R & Reed JC (2013) ER stress-induced cell death mechanisms. *Biochim Biophys Acta* **1833**, 3460–3470.

188 Bartoszewska S, Kochan K, Madanecki P, Piotrowski A, Ochocka R, Collawn JF & Bartoszewski R (2013) Regulation of the unfolded protein response by microRNAs. *Cell Mol Biol Lett* **18**, 555–578.

189 Wortel IMN, van der Meer LT, Kilberg MS & van Leeuwen FN (2017) Surviving stress: modulation of ATF4-mediated stress responses in normal and malignant cells. *Trends Endocrinol Metab* **28**, 794–806.

190 Gorman AM, Healy SJ, Jager R & Samali A (2012) Stress management at the ER: regulators of ER stress-induced apoptosis. *Pharmacol Ther* **134**, 306–316.

191 Ron D & Walter P (2007) Signal integration in the endoplasmic reticulum unfolded protein response. *Nat Rev Mol Cell Biol* **8**, 519–529.

192 Hoyer-Hansen M & Jaattela M (2007) Connecting endoplasmic reticulum stress to autophagy by unfolded protein response and calcium. *Cell Death Differ* **14**, 1576–1582.

193 Cheng X, Liu H, Jiang CC, Fang L, Chen C, Zhang XD & Jiang ZW (2014) Connecting endoplasmic reticulum stress to autophagy through IRE1/JNK/beclin-1 in breast cancer cells. *Int J Mol Med* **34**, 772–781.

194 Giorgi C, Missiroli S, Patergnani S, Duszynski J, Wieckowski MR & Pinton P (2015) Mitochondria-associated membranes: composition, molecular mechanisms, and physiopathological implications. *Antioxid Redox Signal* **22**, 995–1019.

195 Santel A & Fuller MT (2001) Control of mitochondrial morphology by a human mitofusin. *J Cell Sci* **114**, 867–874.

196 Muñoz JP, Ivanova S, Sánchez-Wandelmer J, Martínez-Cristóbal P, Noguera E, Sancho A, Díaz-Ramos A, Hernández-Alvarez MI, Sebastián D, Mauvezin C *et al.* (2014) Erratum: Mfn2 modulates the UPR and mitochondrial function via repression of PERK (EMBO Journal 32 (2348-2361) https://doi.org/10.1038/emboj.2013.168). *EMBO J* **33**, 171.

197 Verfaillie T, Rubio N, Garg AD, Bultynck G, Rizzuto R, Decuypere JP, Piette J, Linehan C, Gupta S, Samali A *et al.* (2012) PERK is required at the ER-mitochondrial contact sites to convey apoptosis after ROS-based ER stress. *Cell Death Differ* **19**, 1880–1891.

198 Mori T, Hayashi T, Hayashi E & Su TP (2013) Sigma-1 receptor chaperone at the er-mitochondrion interface mediates the mitochondrion-er-nucleus signaling for cellular survival. *PLoS ONE* **8**, e76941.

199 Lisbona F, Rojas-Rivera D, Thielen P, Zamorano S, Todd D, Martinon F, Glavic A, Kress C, Lin JH, Walter P *et al.* (2009) BAX inhibitor-1 is a negative regulator of the ER stress sensor IRE1alpha. *Mol Cell* **33**, 679–691.

200 Vannuvel K, Renard P, Raes M & Arnould T (2013) Functional and morphological impact of ER stress on mitochondria. *J Cell Physiol* **228**, 1802–1818.

201 Bravo R, Vicencio JM, Parra V, Troncoso R, Munoz JP, Bui M, Quiroga C, Rodriguez AE, Verdejo HE, Ferreira J *et al.* (2011) Increased ER-mitochondrial coupling promotes mitochondrial respiration and bioenergetics during early phases of ER stress. *J Cell Sci* **124**, 2511.

202 Cullinan SB & Diehl JA (2004) PERK-dependent activation of Nrf2 contributes to redox homeostasis

and cell survival following endoplasmic reticulum stress. *J Biol Chem* **279**, 20108–20117.

203 Wang C, Li H, Meng Q, Du Y, Xiao F, Zhang Q, Yu J, Li K, Chen S, Huang Z *et al.* (2014) ATF4 deficiency protects hepatocytes from oxidative stress via inhibiting CYP2E1 expression. *J Cell Mol Med* **18**, 80–90.

204 Li G, Mongillo M, Chin KT, Harding H, Ron D, Marks AR & Tabas I (2009) Role of ERO1-α-mediated stimulation of inositol 1,4,5-triphosphate receptor activity in endoplasmic reticulum stress-induced apoptosis. *J Cell Biol* **186**, 783–792.

205 Eletto D, Chevet E, Argon Y & Appenzeller-Herzog C (2014) Redox controls UPR to control redox. *J Cell Sci* **127**, 3649–3658.

206 Appenzeller-Herzog C & Hall MN (2012) Bidirectional crosstalk between endoplasmic reticulum stress and mTOR signaling. *Trends Cell Biol* **22**, 274–282.

207 Patricia F, Julien B, Justine L, Patrick M, Joëlle F, Cécile V, Thomas W, Serge M, Colette R, Jean-Yves S *et al.* (2017) mTOR inhibitors activate PERK signaling and favor viability of gastrointestinal neuroendocrine cell lines. *Oncotarget* **8**, 20974–20987.

208 Tenkerian C, Krishnamoorthy J, Mounir Z, Kazimierczak U, Khoutorsky A, Staschke KA, Kristof AS, Wang S, Hatzoglou M & Koromilas AE (2015) mTORC2 balances AKT activation and eIF2α serine 51 phosphorylation to promote survival under stress. *Mol Cancer Res* **13**, 1377–1388.

209 Feng B, Yao PM, Li Y, Devlin CM, Zhang D, Harding HP, Sweeney M, Rong JX, Kuriakose G, Fisher EA *et al.* (2003) The endoplasmic reticulum is the site of cholesterol-induced cytotoxicity in macrophages. *Nat Cell Biol* **5**, 781–792.

210 Fu S, Yang L, Li P, Hofmann O, Dicker L, Hide W, Lin X, Watkins SM, Ivanov AR & Hotamisligil GS (2011) Aberrant lipid metabolism disrupts calcium homeostasis causing liver endoplasmic reticulum stress in obesity. *Nature* **473**, 528–531.

211 Kaplowitz N, Than TA, Ph D, Shinohara M & Ji C (2007) Endoplasmic reticulum stress and liver injury. *Semin Liver Dis* **27**, 367–377.

212 Oyadomari S, Harding HP, Zhang Y, Oyadomari M & Ron D (2008) De-phosphorylation of translation initiation factor 2α (eIF2α) enhances glucose tolerance and attenuates hepato-steatosis in mice. *Cell Metab* **7**, 520–532.

213 Li H, Meng Q, Xiao F, Chen S, Du Y, Yu J, Wang C & Guo F (2011) ATF4 deficiency protects mice from high-carbohydrate-diet-induced liver steatosis. *Biochem J* **438**, 283–289.

214 Xiao G, Zhang T, Yu S, Lee S, Calabuig-Navarro V, Yamauchi J, Ringquist S & Dong HH (2013) ATF4 protein deficiency protects against high fructose-induced hypertriglyceridemia in mice. *J Biol Chem* **288**, 25350–25361.

215 Wang S, Chen Z, Lam V, Han J, Hassler J, Finck BN, Davidson NO & Kaufman RJ (2012) IRE1α-XBP1s induces PDI expression to increase MTP activity for hepatic VLDL assembly and lipid homeostasis. *Cell Metab* **16**, 473–486.

216 Lee AH, Scapa EF, Cohen DE & Glimcher LH (2008) Regulation of hepatic lipogenesis by the transcription factor XBP1. *Science (80-)* **320**, 1492–1496.

217 Yi H, Gu C, Li M, Zhang Z, Li Q, Feng J, Zhou J & Du J (2017) PERK/eIF2α contributes to changes of insulin signaling in HepG2 cell induced by intermittent hypoxia. *Life Sci* **181**, 17–22.

218 Hosogai N, Fukuhara A, Oshima K, Miyata Y, Tanaka S, Segawa K, Furukawa S, Tochino Y, Komuro R, Matsuda M *et al.* (2007) Adipose tissue hypoxia in obesity and its impact on adipocytokine dysregulation. *Diabetes* **56**, 901–911.

219 Kim B, Kim MS & Hyun CK (2017) Syringin attenuates insulin resistance via adiponectin-mediated suppression of low-grade chronic inflammation and ER stress in high-fat diet-fed mice. *Biochem Biophys Res Commun* **488**, 40–45.

220 Lipson KL, Fonseca SG, Ishigaki S, Nguyen LX, Foss E, Bortell R, Rossini AA & Urano F (2006) Regulation of insulin biosynthesis in pancreatic beta cells by an endoplasmic reticulum-resident protein kinase IRE1. *Cell Metab* **4**, 245–254.

221 Lee A-H, Heidtman K, Hotamisligil GS & Glimcher LH (2011) Dual and opposing roles of the unfolded protein response regulated by IRE1alpha and XBP1 in proinsulin processing and insulin secretion. *Proc Natl Acad Sci* **108**, 8885–8890.

222 Seo H-Y, Kim YD, Lee K-M, Min A-K, Kim M-K, Kim H-S, Won K-C, Park J-Y, Lee K-U, Choi H-S *et al.* (2008) Endoplasmic reticulum stress-induced activation of activating transcription factor 6 decreases insulin gene expression via up-regulation of orphan nuclear receptor small heterodimer partner. *Endocrinology* **149**, 3832–3841.

223 Shao M, Shan B, Liu Y, Deng Y, Yan C, Wu Y, Mao T, Qiu Y, Zhou Y, Jiang S *et al.* (2014) Hepatic IRE1α regulates fasting-induced metabolic adaptive programs through the XBP1s–PPARα axis signalling. *Nat Commun* **5**, 3528.

224 Kim H, Tu HC, Ren D, Takeuchi O, Jeffers JR, Zambetti GP, Hsieh JJ & Cheng EH (2009) Stepwise activation of BAX and BAK by tBID, BIM, and PUMA initiates mitochondrial apoptosis. *Mol Cell* **36**, 487–499.

225 Gomez-Bougie P, Halliez M, Moreau P, Pellat-Deceunynck C & Amiot M (2016) Repression of Mcl-1 and disruption of the Mcl-1/Bak interaction in

myeloma cells couple ER stress to mitochondrial apoptosis. *Cancer Lett* **383**, 204–211.

226 Li J, Lee B & Lee AS (2006) Endoplasmic reticulum stress-induced apoptosis: multiple pathways and activation of p53-up-regulated modulator of apoptosis (PUMA) and NOXA by p53. *J Biol Chem* **281**, 7260–7270.

227 Ogata M, Hino S, Saito A, Morikawa K, Kondo S, Kanemoto S, Murakami T, Taniguchi M, Tanii I, Yoshinaga K *et al.* (2006) Autophagy is activated for cell survival after endoplasmic reticulum stress. *Mol Cell Biol* **26**, 9220–9231.

228 Yu L, Alva A, Su H, Dutt P, Freundt E, Welsh S, Baehrecke EH & Lenardo MJ (2004) Regulation of an ATG7-beclin 1 program of autophagic cell death by caspase-8. *Science (80-.)* **304**, 1500–1502.

229 Kim I, Shu CW, Xu W, Shiau CW, Grant D, Vasile S, Cosford ND & Reed JC (2009) Chemical biology investigation of cell death pathways activated by endoplasmic reticulum stress reveals cytoprotective modulators of ASK1. *J Biol Chem* **284**, 1593–1603.

230 Deng X, Xiao L, Lang W, Gao F, Ruvolo P & May WS (2001) Novel Role for JNK as a Stress-activated Bcl2 Kinase. *J Biol Chem* **276**, 23681–23688.

231 Puthalakath H, O'Reilly LA, Gunn P, Lee L, Kelly PN, Huntington ND, Hughes PD, Michalak EM, McKimm-Breschkin J, Motoyama N *et al.* (2007) ER stress triggers apoptosis by activating BH3-only protein Bim. *Cell* **129**, 1337–1349.

232 Yamaguchi H & Wang H-G (2004) CHOP is involved in endoplasmic reticulum stress-induced apoptosis by enhancing DR5 expression in human carcinoma cells. *J Biol Chem* **279**, 45495–45502.

233 Maytin EV, Ubeda M, Lin JC & Habener JF (2001) Stress-Inducible Transcription Factor CHOP/gadd153 Induces Apoptosis in Mammalian Cells via p38 Kinase-Dependent and -Independent Mechanisms. *Exp Cell Res* **267**, 193–204.

234 Wei S-G, Yu Y, Weiss RM & Felder RB (2016) Endoplasmic reticulum stress increases brain MAPK signaling, inflammation and renin-angiotensin system activity and sympathetic nerve activity in heart failure. *Am J Physiol Heart Circ Physiol* **311**, H871–H880.

235 Nolan K, Walter F, Tuffy LP, Poeschel S, Gallagher R, Haunsberger S, Bray I, Stallings RL, Concannon CG & Prehn JH (2016) Endoplasmic reticulum stress-mediated upregulation of miR-29a enhances sensitivity to neuronal apoptosis. *Eur J Neurosci* **43**, 640–652.

236 Wu Y, Li X, Jia J, Zhang Y, Li J, Zhu Z, Wang H, Tang J & Hu J (2018) Transmembrane E3 ligase RNF183 mediates ER stress-induced apoptosis by degrading Bcl-xL. *Proc Natl Acad Sci USA* **115**, E2762–E2771.

237 Galluzzi L, Buqué A, Kepp O, Zitvogel L & Kroemer G (2016) Immunogenic cell death in cancer and infectious disease. *Nat Rev Immunol* **17**, 97.

238 Garg AD & Agostinis P (2017) Cell death and immunity in cancer: from danger signals to mimicry of pathogen defense responses. *Immunol Rev* **280**, 126–148.

239 Fan H, Tang HB, Kang J, Shan L, Song H, Zhu K, Wang J, Ju G & Wang YZ (2015) Involvement of endoplasmic reticulum stress in the necroptosis of microglia/macrophages after spinal cord injury. *Neuroscience* **311**, 362–373.

240 Linkermann A & Green DR (2014) Necroptosis. *N Engl J Med* **370**, 455–465.

241 Saveljeva S, Mc Laughlin SL, Vandenabeele P, Samali A & Bertrand MJ (2015) Endoplasmic reticulum stress induces ligand-independent TNFR1-mediated necroptosis in L929 cells. *Cell Death Dis* **6**, e1587.

242 Pattingre S, Tassa A, Qu X, Garuti R, Liang XH, Mizushima N, Packer M, Schneider MD & Levine B (2005) Bcl-2 antiapoptotic proteins inhibit Beclin 1-dependent autophagy. *Cell* **122**, 927–939.

243 Gandin V, Pellei M, Tisato F, Porchia M, Santini C & Marzano C (2012) A novel copper complex induces paraptosis in colon cancer cells via the activation of ER stress signalling. *J Cell Mol Med* **16**, 142–151.

244 Fan J, Long H, Li Y, Liu Y, Zhou W, Li Q, Yin G, Zhang N & Cai W (2013) Edaravone protects against glutamate-induced PERK/EIF2α/ATF4 integrated stress response and activation of caspase-12. *Brain Res* **1519**, 1–8.

245 Akamatsu K, Shibata M-A, Ito Y, Sohma Y, Azuma H & Otsuki Y (2009) Riluzole induces apoptotic cell death in human prostate cancer cells via endoplasmic reticulum stress. *Anticancer Res* **29**, 2195–2204.

246 Cao J, Dai DL, Yao L, Yu HH, Ning B, Zhang Q, Chen J, Cheng WH, Shen W & Yang ZX (2012) Saturated fatty acid induction of endoplasmic reticulum stress and apoptosis in human liver cells via the PERK/ATF4/CHOP signaling pathway. *Mol Cell Biochem* **364**, 115–129.

247 Du S, Zhou J, Jia Y & Huang K (2010) SelK is a novel ER stress-regulated protein and protects HepG2 cells from ER stress agent-induced apoptosis. *Arch Biochem Biophys* **502**, 137–143.

248 Li S, Zhao F, Cheng S, Wang X & Hao Y (2013) Uric acid-induced endoplasmic reticulum stress triggers phenotypic change in rat glomerular mesangial cells. *Nephrology* **18**, 682–689.

249 Apostolou A, Shen Y, Liang Y, Luo J & Fang S (2008) Armet, a UPR-upregulated protein, inhibits cell proliferation and ER stress-induced cell death. *Exp Cell Res* **314**, 2454–2467.

250 Morishima N, Nakanishi K, Takenouchi H, Shibata T & Yasuhiko Y (2002) An endoplasmic reticulum stress-specific caspase cascade in apoptosis. Cytochrome c-independent activation of caspase-9 by caspase-12. *J Biol Chem* **277**, 34287–34294.

251 Saito A, Ochiai K, Kondo S, Tsumagari K, Murakami T, Cavener DR & Imaizumi K (2011) Endoplasmic reticulum stress response mediated by the PERK-eIF2(alpha)-ATF4 pathway is involved in osteoblast differentiation induced by BMP2. *J Biol Chem* **286**, 4809–4818.

252 Chang YJ, Chen WY, Huang CY, Liu HH & Wei PL (2015) Glucose-regulated protein 78 (GRP78) regulates colon cancer metastasis through EMT biomarkers and the NRF-2/HO-1 pathway. *Tumor Biol* **36**, 1859–1869.

253 Tanjore H, Cheng D-S, Degryse AL, Zoz DF, Abdolrasulnia R, Lawson WE & Blackwell TS (2011) Alveolar epithelial cells undergo epithelial-to-mesenchymal transition in response to endoplasmic reticulum stress. *J Biol Chem* **286**, 30972–30980.

254 Mo XT, Zhou WC, Cui WH, Li DL, Li LC, Xu L, Zhao P & Gao J (2015) Inositol-requiring protein 1 - X-box-binding protein 1 pathway promotes epithelial-mesenchymal transition via mediating snail expression in pulmonary fibrosis. *Int J Biochem Cell Biol* **65**, 230–238.

255 Minchenko DO, Kharkova AP, Halkin OV, Karbovskyi LL & Minchenko OH (2016) Effect of hypoxia on the expression of genes encoding insulin-like growth factors and some related proteins in u87 glioma cells without IRE1 function. *Endocr Regul* **50**, 43–54.

256 Li H, Chen X, Gao Y, Wu J, Zeng F & Song F (2015) XBP1 induces snail expression to promote epithelial- to-mesenchymal transition and invasion of breast cancer cells. *Cell Signal* **27**, 82–89.

257 Jin C, Jin Z, Chen N-Z, Lu M, Liu C-B, Hu W-L & Zheng C-G (2016) Activation of IRE1α-XBP1 pathway induces cell proliferation and invasion in colorectal carcinoma. *Biochem Biophys Res Commun* **470**, 75–81.

258 Feng YX, Sokol ES, Del Vecchio CA, Sanduja S, Claessen JHL, Proia TA, Jin DX, Reinhardt F, Ploegh HL, Wang Q *et al.* (2014) Epithelial-to-mesenchymal transition activates PERK-eIF2α and sensitizes cells to endoplasmic reticulum stress. *Cancer Discov* **4**, 702–715.

259 Moon SY, Kim HS, Nho KW, Jang YJ & Lee SK (2014) Endoplasmic reticulum stress induces epithelial-mesenchymal transition through autophagy via activation of c-Src kinase. *Nephron Exp Nephrol* **126**, 127–140.

260 Greenwood M, Bordieri L, Greenwood MP, Rosso Melo M, Colombari DS, Colombari E, Paton JFR & Murphy D (2014) Transcription factor CREB3L1 regulates vasopressin gene expression in the rat hypothalamus. *J Neurosci* **34**, 3810–3820.

261 Azuma Y, Hagiwara D, Lu W, Morishita Y, Suga H, Goto M, Banno R, Sugimura Y, Oyadomari S, Mori K *et al.* (2014) Activating transcription factor 6α is required for the vasopressin neuron system to maintain water balance under dehydration in male mice. *Endocrinology* **155**, 4905–4914.

262 Marwarha G, Claycombe K, Schommer J, Collins D & Ghribi O (2016) Palmitate-induced endoplasmic reticulum stress and subsequent C/EBPα homologous protein activation attenuates leptin and Insulin-like growth factor 1 expression in the brain. *Cell Signal* **28**, 1789–1805.

263 Marwarha G, Dasari B & Ghribi O (2012) Endoplasmic reticulum stress-induced CHOP activation mediates the down-regulation of leptin in human neuroblastoma SH-SY5Y cells treated with the oysterol 27-hydroxycholesterol. *Cell Signal* **24**, 484–492.

264 Martínez-Sánchez N, Seoane-Collazo P, Contreras C, Varela L, Villarroya J, Rial-Pensado E, Buqué X, Aurrekoetxea I, Delgado TC, Vázquez-Martínez R *et al.* (2017) Hypothalamic AMPK-ER Stress-JNK1 axis mediates the central actions of thyroid hormones on energy balance. *Cell Metab* **26**, 212–229.e12.

265 Zughaier SM, Stauffer BB & McCarty NA (2014) Inflammation and ER stress downregulate BDH2 expression and dysregulate intracellular iron in macrophages. *J Immunol Res* **2014**, 140728.

266 Mori K (2009) Signalling pathways in the unfolded protein response: development from yeast to mammals. *J Biochem* **146**, 743–750.

267 Michalak M & Gye MC (2015) Endoplasmic reticulum stress in periimplantation embryos. *Clin Exp Reprod Med* **42**, 1–7.

268 Li J, Chen Z, Gao LY, Colorni A, Ucko M, Fang S & Du SJ (2015) A transgenic zebrafish model for monitoring xbp1 splicing and endoplasmic reticulum stress *in vivo*. *Mech Dev* **137**, 33–44.

269 Ishikawa T, Kashima M, Nagano AJ, Ishikawa-Fujiwara T, Kamei Y, Todo T & Mori K (2017) Unfolded protein response transducer IRE1-mediated signaling independent of XBP1 mRNA splicing is not required for growth and development of medaka fish. *Elife* **6**, 1–29.

270 Richardson CE, Kinkel S & Kim DH (2011) Physiological IRE-1-XBP-1 and PEK-1 signaling in *Caenorhabditis elegans* larval development and immunity. *PLoS Genet* **7**, 1–10.

271 Shi W, Xu G, Wang C, Sperber SM, Chen Y, Zhou Q, Deng Y & Zhao H (2015) Heat shock 70-kDa protein 5 (Hspa5) is essential for pronephros

formation by mediating retinoic acid signaling. *J Biol Chem* **290**, 577–589.

272 Luo S, Mao C, Lee B & Lee AS (2006) GRP78/BiP Is required for cell proliferation and protecting the inner cell mass from apoptosis during early mouse embryonic development. *Mol Cell Biol* **26**, 5688–5697.

273 Zhang X, Szabo E, Michalak M & Opas M (2007) Endoplasmic reticulum stress during the embryonic development of the central nervous system in the mouse. *Int J Dev Neurosci* **25**, 455–463.

274 Kratochvílová K, Moráň L, Paďourová S, Stejskal S, Tesařová L, Šimara P, Hampl A, Koutná I & Vaňhara P (2016) The role of the endoplasmic reticulum stress in stemness, pluripotency and development. *Eur J Cell Biol* **95**, 115–123.

275 Hao L, Vassena R, Wu G, Han Z, Cheng Y, Latham KE & Sapienza C (2009) The unfolded protein response contributes to preimplantation mouse embryo death in the DDK syndrome. *Biol Reprod* **80**, 944–953.

276 Yang Y, Cheung HH, Tu J, Miu KK & Chan WY (2016) New insights into the unfolded protein response in stem cells. *Oncotarget* **7**, 54010–54027.

277 Latham KE (2015) Endoplasmic reticulum stress signaling in mammalian oocytes and embryos: life in balance. *Int Rev Cell Mol Biol* **316**, 227–265.

278 Gao Y, Sartori DJ, Li C, Yu Q-C, Kushner JA, Simon MC & Diehl JA (2012) PERK is required in the adult pancreas and is essential for maintenance of glucose homeostasis. *Mol Cell Biol* **32**, 5129–5139.

279 Bettigole SE, Lis R, Adoro S, Lee AH, Spencer LA & Weller PFGL (2015) The transcription factor XBP1 is selectively required for eosinophil differentiation. *Nat Immunol* **16**, 829–837.

280 Leung A, Gregory NS, Allen L-AH & Sluka KA (2017) Regular physical activity prevents chronic pain by altering muscle macrophage phenotype and increasing IL-10 in mice. *Pain* **157**, 70–79.

281 Todd DJ, McHeyzer-Williams LJ, Kowal C, Lee AH, Volpe BT, Diamond B, McHeyzer-Williams MG & Glimcher LH (2009) XBP1 governs late events in plasma cell differentiation and is not required for antigen-specific memory B cell development. *J Exp Med* **206**, 2151–2159.

282 van Galen P, Kreso A, Mbong N, Kent DG, Fitzmaurice T, Chambers JE, Xie S, Laurenti E, Hermans K, Eppert K *et al.* (2014) The unfolded protein response governs integrity of the haematopoietic stem-cell pool during stress. *Nature* **510**, 268–272.

283 Matsuzaki S, Hiratsuka T, Taniguchi M, Shingaki K, Kubo T, Kiya K, Fujiwara T, Kanazawa S, Kanematsu R, Maeda T *et al.* (2015) Physiological ER stress mediates the differentiation of fibroblasts. *PLoS ONE* **10**, 1–11.

284 Arensdorf AM, Diedrichs D & Rutkowski DT (2013) Regulation of the transcriptome by ER stress: non-canonical mechanisms and physiological consequences. *Front Genet* **4**, 1–16.

285 Murakami T, Saito A, Hino S, Kondo S, Kanemoto S, Chihara K, Sekiya H, Tsumagari K, Ochiai K, Yoshinaga K *et al.* (2009) Signalling mediated by the endoplasmic reticulum stress transducer OASIS is involved in bone formation. *Nat Cell Biol* **11**, 1205–1211.

286 Hamamura K & Yokota H (2007) Stress to endoplasmic reticulum of mouse osteoblasts induces apoptosis and transcriptional activation for bone remodeling. *FEBS Lett* **581**, 1769–1774.

287 Cui M, Kanemoto S, Cui X, Kaneko M, Asada R, Matsuhisa K, Tanimoto K, Yoshimoto Y, Shukunami C & Imaizumi K (2015) OASIS modulates hypoxia pathway activity to regulate bone angiogenesis. *Sci Rep* **5**, 16455.

288 Kondo S, Murakami T, Tatsumi K, Ogata M, Kanemoto S, Otori K, Iseki K, Wanaka A & Imaizumi K (2005) OASIS, a CREB/ATF-family member, modulates UPR signalling in astrocytes. *Nat Cell Biol* **7**, 186–194.

289 Asada R, Saito A, Kawasaki N, Kanemoto S, Iwamoto H, Oki M, Miyagi H, Izumi S & Imaizumi K (2012) The endoplasmic reticulum stress transducer OASIS is involved in the terminal differentiation of goblet cells in the large intestine. *J Biol Chem* **287**, 8144–8153.

290 Saito A (2014) Physiological functions of endoplasmic reticulum stress transducer OASIS in central nervous system. *Anat Sci Int* **89**, 11–20.

291 van der Harg JM, van Heest JC, Bangel FN, Patiwael S, van Weering JRT & Scheper W (2017) The UPR reduces glucose metabolism via IRE1 signaling. *Biochim Biophys Acta* **1864**, 655–665.

292 Topisirovic I & Sonenberg N (2011) mRNA translation and energy metabolism in cancer: the role of the MAPK and mTORC1 Pathways. *Cold Spring Harb Symp Quant Biol* **76**, 355–367.

293 Lowe CE, Dennis RJ, Obi U, O'Rahilly S & Rochford JJ (2012) Investigating the involvement of the ATF6α pathway of the unfolded protein response in adipogenesis. *Int J Obes (Lond)* **36**, 1248–1251.

294 Lipson KL, Ghosh R & Urano F (2008) The role of IRE1α in the degradation of insulin mRNA in pancreatic β-cells. *PLoS ONE* **3**, 1–7.

295 Zhang N, Yang X, Yuan F, Zhang L, Wang Y, Wang L, Mao Z, Luo J, Zhang H, Zhu WG *et al.* (2018) Increased amino acid uptake supports autophagy-deficient cell survival upon glutamine deprivation. *Cell Rep* **10**, 3006–3020.

296 Rubio-Patiño C, Bossowski JP, De Donatis GM, Mondragón L, Villa E, Aira LE, Chiche J, Mhaidly R, Lebeaupin C, Marchetti S *et al.* (2018) Low-protein diet induces IRE1α-dependent anticancer immunosurveillance. *Cell Metab* **27**, 828–842.

297 Xue Z, He Y, Ye K, Gu Z, Mao Y & Qi L (2011) A conserved structural determinant located at the interdomain region of mammalian inositol-requiring enzyme 1α. *J Biol Chem* **286**, 30859–30866.

298 Waller DD, Jansen G, Golizeh M, Martel-Lorion C, Dejgaard K, Shiao TC, Mancuso J, Tsantrizos YS, Roy R, Sebag M *et al.* (2016) A covalent cysteine-targeting kinase inhibitor of Ire1 permits allosteric control of endoribonuclease activity. *ChemBioChem* **17**, 843–851.

299 Wiseman RL, Zhang Y, Lee KPK, Harding HP, Haynes CM, Price J, Sicheri F & Ron D (2010) Flavonol activation defines an unanticipated ligand-binding site in the kinase-RNase domain of IRE1. *Mol Cell* **38**, 291–304.

300 Rong J, Pass I, Diaz PW, Ngo TA, Sauer M, Magnuson G, Zeng F-Y, Hassig CA, Jackson MR, Cosford NDP *et al.* (2015) Cell-based high-throughput luciferase reporter gene assays for identifying and profiling chemical modulators of endoplasmic reticulum signaling protein, IRE1. *J Biomol Screen* **20**, 1232–1245.

301 Feldman HC, Tong M, Wang L, Meza-Acevedo R, Gobillot TA, Lebedev I, Gliedt MJ, Hari SB, Mitra AK, Backes BJ *et al.* (2016) Structural and functional analysis of the allosteric inhibition of IRE1α with ATP-competitive ligands. *ACS Chem Biol* **11**, 2195–2205.

302 Harrington PE, Biswas K, Malwitz D, Tasker AS, Mohr C, Andrews KL, Dellamaggiore K, Kendall R, Beckmann H, Jaeckel P *et al.* (2015) Unfolded protein response in cancer: IRE1α inhibition by selective kinase ligands does not impair tumor cell viability. *ACS Med Chem Lett* **6**, 68–72.

303 Wang L, Perera BGK, Hari SB, Bhhatarai B, Backes BJ, Seeliger MA, Schürer SC, Oakes SA, Papa FR & Maly DJ (2012) Divergent allosteric control of the IRE1α endoribonuclease using kinase inhibitors. *Nat Chem Biol* **8**, 982–989.

304 Jha BK, Polyakova I, Kessler P, Dong B, Dickerman B, Sen GC & Silverman RH (2011) Inhibition of RNase L and RNA-dependent protein kinase (PKR) by sunitinib impairs antiviral innate immunity. *J Biol Chem* **286**, 26319–26326.

305 Volkmann K, Lucas JL, Vuga D, Wang X, Brumm D, Stiles C, Kriebel D, Der-Sarkissian A, Krishnan K, Schweitzer C *et al.* (2011) Potent and selective inhibitors of the inositol-requiring enzyme 1 endoribonuclease. *J Biol Chem* **286**, 12743–12755.

306 Cross BC, Bond PJ, Sadowski PG, Jha BK, Zak J, Goodman JM, Silverman RH, Neubert TA, Baxendale IR, Ron D *et al.* (2012) The molecular basis for selective inhibition of unconventional mRNA splicing by an IRE1-binding small molecule. *Proc Natl Acad Sci USA* **109**, E869–E878.

307 Mimura N, Fulciniti M, Gorgun G, Tai Y-T, Cirstea D, Santo L, Hu Y, Fabre C, Minami J, Ohguchi H *et al.* (2012) Blockade of XBP1 splicing by inhibition of IRE1 is a promising therapeutic option in multiple myeloma. *Blood* **119**, 5772–5781.

308 Papandreou I, Denko NC, Olson M, Van Melckebeke H, Lust S, Tam A, Solow-Cordero DE, Bouley DM, Offner F, Niwa M *et al.* (2011) Identification of an Ire1alpha endonuclease specific inhibitor with cytotoxic activity against human multiple myeloma. *Blood* **117**, 1311–1314.

309 Ri M, Tashiro E, Oikawa D, Shinjo S, Tokuda M, Yokouchi Y, Narita T, Masaki A, Ito A, Ding J *et al.* (2012) Identification of Toyocamycin, an agent cytotoxic for multiple myeloma cells, as a potent inhibitor of ER stress-induced XBP1 mRNA splicing. *Blood Cancer J* **2**, e79.

310 Tomasio SM, Harding HP, Ron D, Cross BCS & Bond PJ (2013) Selective inhibition of the unfolded protein response: targeting catalytic sites for Schiff base modification. *Mol BioSyst* **9**, 2408–2416.

311 Jiang D, Lynch C, Medeiros BC, Liedtke M, Bam R, Tam AB, Yang Z, Alagappan M, Abidi P, Le Q-T *et al.* (2016) Identification of Doxorubicin as an Inhibitor of the IRE1α-XBP1 Axis of the Unfolded Protein Response. *Sci Rep* **6**, 33353.

312 Park BK, Boobis A, Clarke S, Goldring CEP, Jones D, Kenna JG, Lambert C, Laverty HG, Naisbitt DJ, Nelson S *et al.* (2011) Managing the challenge of chemically reactive metabolites in drug development. *Nat Rev Drug Discov* **10**, 292–306.

313 Wilson AJ (2009) Inhibition of protein–protein interactions using designed molecules. *Chem Soc Rev* **38**, 3289.

314 Atkins C, Liu Q, Minthorn E, Zhang S-Y, Figueroa DJ, Moss K, Stanley TB, Sanders B, Goetz A, Gaul N *et al.* (2013) Characterization of a novel PERK kinase inhibitor with antitumor and antiangiogenic activity. *Cancer Res* **73**, 1993–2002.

315 Axten JM, Medina JR, Feng Y, Shu A, Romeril SP, Grant SW, Li WH, Heerding DA, Minthorn E, Mencken T *et al.* (2012) Discovery of 7-methyl-5-(1-{[3-(trifluoromethyl)phenyl]acetyl}-2,3-dihydro-1H-indol-5-yl)-7H-pyrrolo[2,3-d]pyrimidin-4-amine (GSK2606414), a potent and selective first-in-class inhibitor of protein kinase R (PKR)-like endoplasmic reticulum kinase (PERK). *J Med Chem* **55**, 7193–7207.

316 Moreno JA, Halliday M, Molloy C, Radford H, Verity N, Axten JM, Ortori CA, Willis AE, Fischer PM, Barrett DA *et al.* (2013) Oral treatment targeting the unfolded protein response prevents neurodegeneration and clinical disease in prion-infected mice. *Sci Transl Med* **138**, 206ra138.

317 Harding HP, Zeng H, Zhang Y, Jungries R, Chung P, Plesken H, Sabatini DD & Ron D (2001) Diabetes mellitus and exocrine pancreatic dysfunction in perk-/- mice reveals a role for translational control in secretory cell survival. *Mol Cell* **7**, 1153–1163.

318 Rojas-Rivera D, Delvaeye T, Roelandt R, Nerinckx W, Augustyns K, Vandenabeele P & Bertrand MJ (2017) When PERK inhibitors turn out to be new potent RIPK1 inhibitors: critical issues on the specificity and use of GSK2606414 and GSK2656157. *Cell Death Differ* **24**, 1100–1110.

319 Sidrauski C, Tsai JC, Kampmann M, Hearn BR, Vedantham P, Jaishankar P, Sokabe M, Mendez AS, Newton BW, Tang EL *et al.* (2015) Pharmacological dimerization and activation of the exchange factor eIF2B antagonizes the integrated stress response. *Elife* **2015**, e07314.

320 Sekine Y, Zyryanova A, Crespillo-Casado A, Fischer PM, Harding HP & Ron D (2015) Stress responses. Mutations in a translation initiation factor identify the target of a memory-enhancing compound. *Science* **348**, 1027–1030.

321 Halliday M, Radford H, Sekine Y, Moreno J, Verity N, Le Quesne J, Ortori CA, Barrett DA, Fromont C, Fischer PM *et al.* (2015) Partial restoration of protein synthesis rates by the small molecule ISRIB prevents neurodegeneration without pancreatic toxicity. *Cell Death Dis* **6**, e1672.

322 Sidrauski C, McGeachy AM, Ingolia NT & Walter P (2015) The small molecule ISRIB reverses the effects of eIF2α phosphorylation on translation and stress granule assembly. *Elife* **2015**, 1–16.

323 Gallagher CM, Garri C, Cain EL, Ang KKH, Wilson CG, Chen S, Hearn BR, Jaishankar P, Aranda-Diaz A, Arkin MR *et al.* (2016) Ceapins are a new class of unfolded protein response inhibitors, selectively targeting the ATF6α branch. *Elife* **5**, 1–33.

324 Gallagher CM & Walter P (2016) Ceapins inhibit ATF6α signaling by selectively preventing transport of ATF6α to the Golgi apparatus during ER stress. *Elife* **5**, e11880.

325 Bu L, Yu H, Fan L, Li X, Wang F, Liu J, Zhong F, Zhang C, Wei W, Wang H *et al.* (2017) Melatonin, a novel selective ATF-6 inhibitor, induces human hepatoma cell apoptosis through COX-2 downregulation. *World J Gastroenterol* **23**, 986–998.

326 Xu S, Butkevich AN, Yamada R, Zhou Y, Debnath B, Duncan R, Zandi E, Petasis NA & Neamati N (2012) Discovery of an orally active small-molecule irreversible inhibitor of protein disulfide isomerase for ovarian cancer treatment. *Proc Natl Acad Sci* **109**, 16348–16353.

327 Banerjee R, Pace NJ, Brown DR & Weerapana E (2013) 1,3,5-Triazine as a modular scaffold for covalent inhibitors with streamlined target identification. *J Am Chem Soc* **135**, 2497–2500.

328 Chevet E, Hetz C & Samali A (2015) Endoplasmic reticulum stress-activated cell reprogramming in oncogenesis. *Cancer Discov* **5**, 586–597.

329 Okada T, Haze K, Nadanaka S, Yoshida H, Seidah NG, Hirano Y, Sato R, Negishi M & Mori K (2003) A serine protease inhibitor prevents endoplasmic reticulum stress-induced cleavage but not transport of the membrane-bound transcription factor ATF6. *J Biol Chem* **278**, 31024–31032.

330 Doultsinos D, Avril T, Lhomond S, Dejeans N, Guédat P & Chevet E (2017) Control of the unfolded protein response in health and disease. *SLAS Discov* **22**, 787–800.

331 Delpino A & Castelli M (2002) The 78 kDa glucose-regulated protein (GRP78/BIP) is expressed on the cell membrane, is released into cell culture medium and is also present in human peripheral circulation. *Biosci Rep* **22**, 407–420.

332 Chessler SD & Byers PH (1993) BiP binds type I procollagen pro alpha chains with mutations in the carboxyl-terminal propeptide synthesized by cells from patients with osteogenesis imperfecta. *J Biol Chem* **268**, 18226–18233.

333 Booth L, Roberts JL, Cash DR, Tavallai S, Jean S, Fidanza A, Cruz-Luna T, Siembiba P, Cycon KA, Cornelissen CN *et al.* (2015) GRP78/BiP/HSPA5/ DNA K is a universal therapeutic target for human disease. *J Cell Physiol* **230**, 1661–1676.

334 Zhu H, Chen X, Chen B, Chen B, Song W, Sun D & Zhao Y (2014) Activating transcription factor 4 promotes esophageal squamous cell carcinoma invasion and metastasis in mice and is associated with poor prognosis in human patients. *PLoS ONE* **9**, 1–11.

335 Yang J, Cheng D, Zhou S, Zhu B, Hu T & Yang Q (2015) Overexpression of X-Box binding protein 1 (XBP1) correlates to poor prognosis and up-regulation of PI3K/mTOR in human osteosarcoma. *Int J Mol Sci* **16**, 28635–28646.

336 Bujisic B, De Gassart A, Tallant R, Demaria O, Zaffalon L, Chelbi S, Gilliet M, Bertoni F & Martinon F (2017) Impairment of both IRE1 expression and XBP1 activation is a hallmark of GCB DLBCL and contributes to tumor growth. *Blood* **129**, 2420–2428.

337 Kaser A, Lee A-H, Franke A, Glickman JN, Zeissig S, Tilg H, Nieuwenhuis EES, Higgins DE, Schreiber S,

Glimcher LH *et al.* (2008) XBP1 links ER stress to intestinal inflammation and confers genetic risk for human inflammatory bowel disease. *Cell* **134**, 743–756.

338 Atkin JD, Farg MA, Walker AK, McLean C, Tomas D & Horne MK (2008) Endoplasmic reticulum stress and induction of the unfolded protein response in human sporadic amyotrophic lateral sclerosis. *Neurobiol Dis* **30**, 400–407.

339 Nardo G, Pozzi S, Pignataro M, Lauranzano E, Spano G, Garbelli S, Mantovani S, Marinou K, Papetti L, Monteforte M *et al.* (2011) Amyotrophic lateral sclerosis multiprotein biomarkers in peripheral blood mononuclear cells. *PLoS ONE* **6**, e25545.

340 Kim Y, Lee H, Manson SR, Lindahl M, Evans B, Miner JH, Urano F & Chen YM (2016) Mesencephalic astrocyte-derived neurotrophic factor as a urine biomarker for endoplasmic reticulum stress-related kidney diseases. *J Am Soc Nephrol* **27**, 2974–2982.

341 Mami I, Bouvier N, El Karoui K, Gallazzini M, Rabant M, Laurent-Puig P, Li S, Tharaux PL, Beaune P, Thervet E *et al.* (2016) Angiogenin mediates cell-autonomous translational control under endoplasmic reticulum stress and attenuates kidney injury. *J Am Soc Nephrol* **27**, 863–876.

342 Dadey DYA, Kapoor V, Hoye K, Khudanyan A, Collins A, Thotala D & Hallahan DE (2016) Antibody targeting GRP78 enhances the efficacy of radiation therapy in human glioblastoma and non-small-cell lung cancer cell lines and tumor models. *Clin Cancer Res* **23**, 2556–2564.

343 Lin YG, Shen J, Yoo E, Liu R, Yen HY, Mehta A, Rajaei A, Yang W, Mhawech-Fauceglia P, DeMayo FJ *et al.* (2015) Targeting the glucose-regulated protein-78 abrogates Pten-null driven AKT activation and endometrioid tumorigenesis. *Oncogene* **34**, 5418–5426.

344 Chen YG, Ashok BT, Liu X, Garikapaty VPS, Mittelman A & Tiwari RK (2003) Induction of heat shock protein gp96 by immune cytokines. *Cell Stress Chaperones* **8**, 242–248.

345 Zhang K, Peng Z, Huang X, Qiao Z, Wang X, Wang N, Xi H, Cui J, Gao Y, Huang X *et al.* (2017) Phase II trial of adjuvant immunotherapy with autologous tumor-derived Gp96 vaccination in patients with gastric cancer. *J Cancer* **8**, 1826–1832.

346 Tian S, Liu Z, Donahue C, Falo LD Jr & You Z (2012) Genetic targeting of the active transcription factor XBP1s to dendritic cells potentiates vaccine-induced prophylactic and therapeutic antitumor immunity. *Mol Ther* **20**, 432–442.

347 Miller M, Rosenthal P, Beppu A, James L, Hoffman HM, Tam AB, Taylor A, Mcgeough MD, Pena CA, Niwa M *et al.* (2014) ORMDL3 transgenic mice have increased airway remodeling and airway

responsiveness characteristic of asthma. *J Immunol* **192**, 3475–3487.

348 Graner MW, Lillehei KO & Katsanis E (2015) Endoplasmic reticulum chaperones and their roles in the immunogenicity of cancer vaccines. *Front Oncol* **4**, 1–12.

349 Graner MW, Zeng Y, Feng H & Katsanis E (2003) Tumor-derived chaperone-rich cell lysates are effective therapeutic vaccines against a variety of cancers. *Cancer Immunol Immunother* **52**, 226–234.

350 Rapp UK & Kaufmann SH (2004) DNA vaccination with gp96-peptide fusion proteins induces protection against an intracellular bacterial pathogen. *Int Immunol* **16**, 597–605.

351 Qian J, Hong S, Wang S, Zhang L, Sun L, Wang M, Yang J & Kwak LW (2009) Myeloma cell line – derived, pooled heat shock proteins as a universal vaccine for immunotherapy of multiple myeloma. *Blood* **114**, 3880–3890.

352 Argon Y & Simen BB (1999) GRP94, an ER chaperone with protein and peptide binding properties. *Semin Cell Dev Biol* **10**, 495–505.

353 Liu D, Liu X, Zhou T, Yao W, Zhao J, Zheng Z, Jiang W, Wang F, Aikhionbare FO, Hill DL *et al.* (2015) IRE1-RACK1 axis orchestrates ER stress preconditioning-elicited cytoprotection from ischemia/reperfusion injury in liver. *J Mol Cell Biol* **8**, 144–156.

354 Bailly-Maitre B, Fondevila C, Kaldas F, Droin N, Luciano F, Ricci J-E, Croxton R, Krajewska M, Zapata JM, Kupiec-Weglinski JW *et al.* (2006) Cytoprotective gene bi-1 is required for intrinsic protection from endoplasmic reticulum stress and ischemia-reperfusion injury. *Proc Natl Acad Sci USA* **103**, 2809–2814.

355 Bi X, Zhang G, Wang X, Nguyen C, May HI, Li X, Al-Hashimi AA, Austin RC, Gillette TG, Fu G *et al.* (2018) Endoplasmic reticulum chaperone GRP78 protects heart from ischemia/reperfusion injury through Akt activation. *Circ Res* **122**, 1545–1554.

356 Martindale JJ, Fernandez R, Thuerauf D, Whittaker R, Gude N, Sussman MA & Glembotski CC (2006) Endoplasmic reticulum stress gene induction and protection from ischemia/reperfusion injury in the hearts of transgenic mice with a tamoxifen-regulated form of ATF6. *Circ Res* **98**, 1186–1193.

357 Peralta C & Brenner C (2011) Endoplasmic reticulum stress inhibition enhances liver tolerance to ischemia/reperfusion. *Curr Med Chem* **18**, 2016–2024.

358 Folch-Puy E, Panisello A, Oliva J, Lopez A, Benítez CC, Adam R & Roselló-Catafau J (2016) Relevance of endoplasmic reticulum stress cell signaling in liver cold ischemia reperfusion injury. *Int J Mol Sci* **17**, 1–12.

359 Kwon SK, Ahn M, Song HJ, Kang SK, Jung SB, Harsha N, Jee S, Moon JY, Suh KS, Do LS *et al.* (2015) Nafamostat mesilate attenuates transient focal

ischemia/reperfusion-induced brain injury via the inhibition of endoplasmic reticulum stress. *Brain Res* **1627**, 12–20.

360 Zhang H, Yue Y, Sun T, Wu X & Xiong S (2017) Transmissible endoplasmic reticulum stress from myocardiocytes to macrophages is pivotal for the pathogenesis of CVB3-induced viral myocarditis. *Sci Rep* **7**, 42162.

361 Rodvold JJ, Chiu KT, Hiramatsu N, Nussbacher JK, Galimberti V, Mahadevan NR, Willert K, Lin JH & Zanetti M (2017) Intercellular transmission of the unfolded protein response promotes survival and drug resistance in cancer cells. *Sci Signal* **10**, eaah7177. https://doi.org/10.1126/scisignal.aah7177

362 Brownlie RJ, Myers LK, Wooley PH, Corrigall VM, Bodman-Smith MD, Panayi GS & Thompson SJ (2006) Treatment of murine collagen-induced arthritis by the stress protein BiP Via interleukin-4 – producing regulatory t cells a novel function for an ancient protein. *Arthritis Rheumatol* **54**, 854–863.

363 Kirkham B, Chaabo K, Hall C, Garrood T, Mant T, Allen E, Vincent A, Vasconcelos JC, Prevost AT, Panayi GS *et al.* (2016) Safety and patient response as indicated by biomarker changes to binding immunoglobulin protein in the phase I/IIA RAGULA clinical trial in rheumatoid arthritis. *Rheumatology (United Kingdom)* **55**, 1993–2000.

364 Axten JM, Romeril SP, Shu A, Ralph J, Medina JR, Feng Y, Li WHH, Grant SW, Heerding DA, Minthorn E *et al.* (2013) Discovery of GSK2656157: an optimized perk inhibitor selected for preclinical development. *ACS Med Chem Lett* **4**, 964–968.

365 Boyce M, Bryant KF, Jousse C, Long K, Harding HP, Scheuner D, Kaufman RJ, Ma D, Coen DM, Ron D *et al.* (2005) A selective inhibitor of eIF2alpha dephosphorylation protects cells from ER stress. *Science* **307**, 935–939.

366 Saxena S, Cabuy E & Caroni P (2009) A role for motoneuron subtype-selective ER stress in disease manifestations of FALS mice. *Nat Neurosci* **12**, 627–636.

367 Colla E, Coune P, Liu Y, Pletnikova O, Troncoso JC, Iwatsubo T, Schneider BL & Lee MK (2012) Endoplasmic reticulum stress is important for the manifestations of α-synucleinopathy *in vivo*. *J Neurosci* **32**, 3306–3320.

368 Wang L, Popko B, Tixier E & Roos RP (2014) Guanabenz, which enhances the unfolded protein response, ameliorates mutant SOD1-induced

amyotrophic lateral sclerosis. *Neurobiol Dis* **71**, 317–324.

369 Das I, Krzyzosiak A, Schneider K, Wrabetz L, D'Antonio M, Barry N & Sigurdardottir ABA (2015) Preventing proteostasis diseases by selective inhibition of a phosphatase regulatory subunit. *Science* **348**, 239–242.

370 Lee A-H, Iwakoshi NN & Glimcher LH (2003) XBP-1 regulates a subset of endoplasmic reticulum resident chaperone genes in the unfolded protein response. *Mol Cell Biol* **23**, 7448–7459.

371 Ghosh R, Wang L, Wang ES, Perera BGK, Igbaria A, Morita S, Prado K, Thamsen M, Caswell D, Macias H *et al.* (2014) Allosteric inhibition of the IRE1α RNase preserves cell viability and function during endoplasmic reticulum stress. *Cell* **158**, 534–548.

372 Kawamura T, Tashiro E, Shindo K & Imoto M (2008) SAR study of a novel triene-ansamycin group compound, quinotrierixin, and related compounds, as inhibitors of ER stress-induced XBP1 activation II. Structure elucidation. *J Antibiot (Tokyo)* **61**, 312–317.

373 Chen D, Landis-Piwowar KR, Chen MS & Dou QP (2007) Inhibition of proteasome activity by the dietary flavonoid apigenin is associated with growth inhibition in cultured breast cancer cells and xenografts. *Breast Cancer Res* **9**, R80.

374 Zhu M, Rajamani S, Kaylor J, Han S, Zhou F & Fink AL (2004) The flavonoid baicalein inhibits fibrillation of alpha-synuclein and disaggregates existing fibrils. *J Biol Chem* **279**, 26846–26857.

375 Kim D-S, Ha K-C, Kwon D-Y, Kim M-S, Kim H-R, Chae S-W & Chae H-J (2008) Kaempferol protects ischemia/reperfusion-induced cardiac damage through the regulation of endoplasmic reticulum stress. *Immunopharmacol Immunotoxicol* **30**, 257–270.

376 Plate L, Cooley CB, Chen JJ, Paxman RJ, Gallagher CM, Madoux F, Genereux JC, Dobbs W, Garza D, Spicer TP *et al.* (2016) Small molecule proteostasis regulators that reprogram the ER to reduce extracellular protein aggregation. *Elife* **5**, e15550.

377 Higa A, Taouji S, Lhomond S, Jensen D, Fernandez-Zapico ME, Simpson JC, Pasquet JM, Schekman R & Chevet E (2014) Endoplasmic reticulum stress-activated transcription factor atf6α requires the disulfide isomerase PDIA5 to modulate chemoresistance. *Mol Cell Biol* **34**, 1839–1849.

Chapter 12

Measuring the Activation of Cell Death Pathways upon Inhibition of Metabolism

Franziska Püschel and Cristina Muñoz-Pinedo

Abstract

Nutrient starvation or inhibition of cellular metabolism can induce cancer cell death. This can be measured by a variety of methods. We describe here four simple methods to measure cell death in culture by using microscopy, western blot, and flow cytometry. We also provide tools to differentiate between different forms of cell death like apoptosis and necrosis by using chemical inhibitors.

Key words Cell death, Necrosis, Apoptosis, Necroptosis

1 Introduction

Inhibition of Cancer Metabolism Promotes Cell Death: Cancer cells demand a high level of energy and metabolites to maintain high proliferation rates through increased glucose uptake and increased metabolic activity. Energy and metabolites can be provided through extracellular nutrients like glucose, amino acids or lipids, as well as through intracellular recycling pathways like autophagy or lysosomal and proteasomal degradation [1]. Upon transient nutrient deprivation, cancer cells are frequently able to resolve metabolic stress. However, sustained stress or treatment with drugs that inhibit metabolism leads to permanent cell cycle arrest or induction of cell death [2].

Cell Death: Cell death occurs in different forms classified by their morphology and biochemical criteria. The two main forms are designated as apoptosis and necrosis. The traditional view indicates that apoptosis is an autonomous, programmed cell death form whereas the latter is a passive process induced through cell injuries by external factors. However, some forms of non-apoptotic cell death like necroptosis, pyroptosis, and ferroptosis are regulated by signaling pathways [3]. Necrosis is morphologically characterized through cell swelling and the rupture of the plasma membrane,
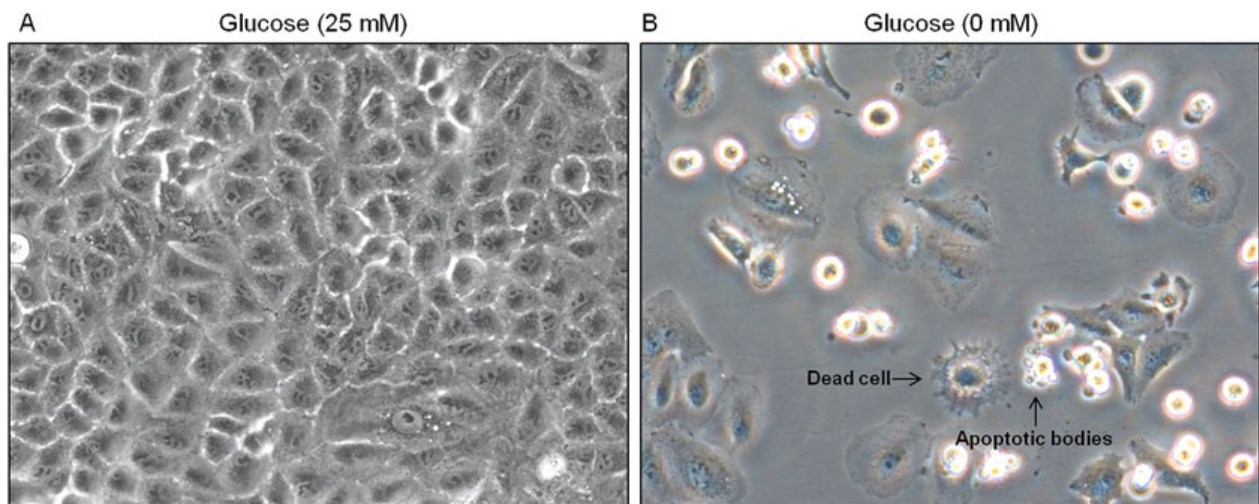
Fig. 1 Dead A549 cells. Cells were incubated for 48 h in DMEM with 25 mM or 0 mM glucose. Arrows show dying or dead cells. To verify that cells are dying via apoptosis, the use of inhibitors is recommended rather than morphology-based assays

which involves the liberation of cytoplasmic contents. The hallmarks of apoptosis are the detachment, rounding, and shrinking of the cell accompanied by chromatin condensation. In cell cultures, shrunk cells and apoptotic bodies accumulate; the latter consist out of cytoplasm containing a high content of organelles as well as nuclear fragments. In animals, the apoptotic bodies are recycled by being phagocytized by macrophages that degrade them. These morphological changes are visible under the microscope (Fig. 1).

The cellular mechanism of apoptosis is different from other forms of cell death because it involves activation and cleavage of caspases, which are in an inactive form as pro-caspases present in the cell. Upon activation they auto-cleave and activate further downstream caspases, which cleave numerous substrates that lead to morphological changes. Morphological criteria are useful to count dead cells; however, they are not recommended to distinguish apoptosis from other forms of cell death as inhibition of metabolism may change cellular morphology and cause detachment of cells.

Microscopical analysis of cell death allows a quantitative analysis by taking photographs at an inverted microscope, as well as by staining with Trypan Blue Solution. These methods provide an easy and quick approach with little expenses. A more precise and reproducible method is the cell death analysis by Flow Cytometry or Fluorescence-Activated Cell Sorting (FACS) and the use of fluorescent markers. These methods allow quantitative as well as qualitative analysis of cell death since different cell death forms can be distinguished through co-treatment with drugs inhibiting specific cell death forms as well as through specific staining methods.
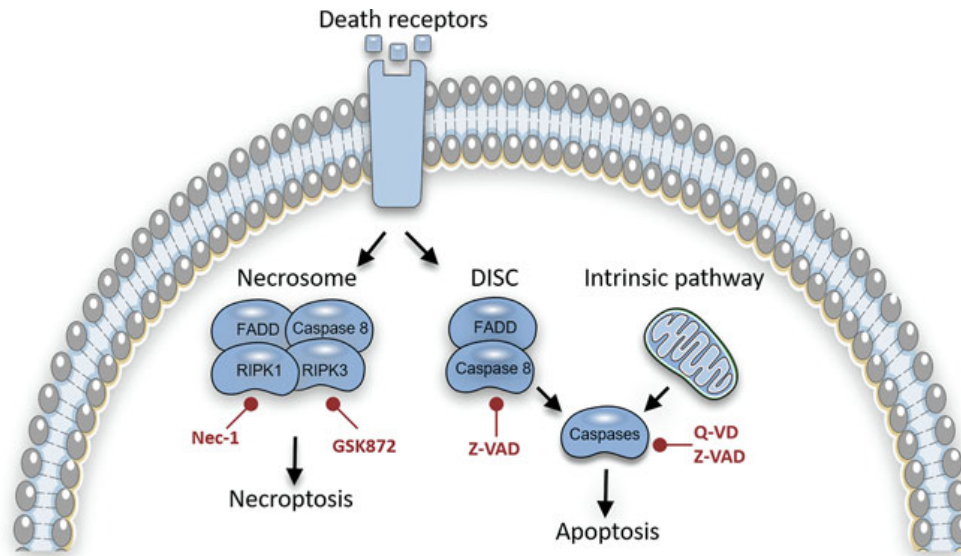
Fig. 2 Inhibitors targeting cell death machineries. Cell death receptor activation leads to the formation of the necrosome which induces necroptosis. GSK872 inhibits RIPK3 whereas Nec-1 blocks RIPK1. Formation of the DISC (Death Inducing Signaling Complex) leads to activation of caspases and induces apoptosis. Z-VAD and QVD are caspase inhibitors

Compared to the microscope, FACS is more costly and results could be affected due to a longer cell processing.

Drugs that can inhibit cell death are pan-caspase inhibitors like Q-VD-OPH (QVD) and Z-VAD-fmk (Z-VAD) (which block apoptosis), or Ac-Y-VAD-cmk (Y-VAD), the caspase-1 inhibitor that inhibits pyroptosis. Necroptosis is a specific form of necrosis mediated by RIP kinases and the pore-forming protein MLKL, and can be prevented by using Necrostatin-1 (Nec-1) or RIPK3 inhibitors (GSK872) [3] (Fig. 2). Other forms of cell death like ferroptosis and mitochondrial permeability transition-mediated can be prevented by ferrostatins and cyclosporin A, respectively.

The different approaches summarized in Fig. 3 will be described in the following chapter. Methods widely used to measure proliferation like MTT-like assays are based on metabolic measurements. We strongly advise against the use of these tools to analyze cell death, especially when the stimulus used to induce cell death disturbs metabolic parameters.

2   Materials

Prior to the start of the experiments all the reagents have to be cooled down or warmed up to room temperature except it is indicated differently. Antibodies and drugs were prepared according to the manufacturer's instructions.
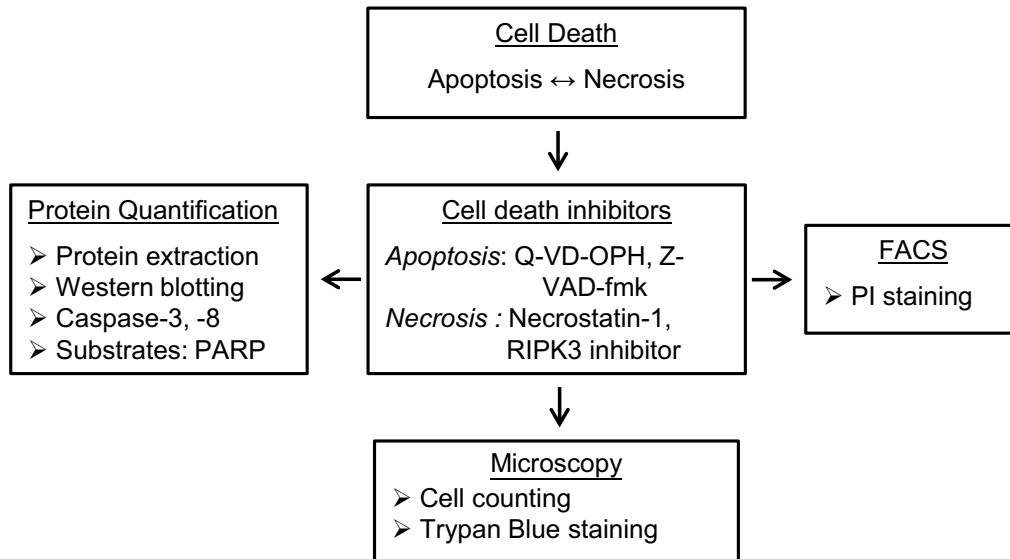
```
                      ┌─────────────────────────┐
                      │       Cell Death        │
                      │   Apoptosis ↔ Necrosis  │
                      └─────────────────────────┘
                                  │
                                  ▼
┌──────────────────────┐  ┌─────────────────────────┐  ┌──────────────────┐
│ Protein Quantification│ │   Cell death inhibitors │  │      FACS        │
│ ➤ Protein extraction  │←│ Apoptosis: Q-VD-OPH, Z- │→ │ ➤ PI staining    │
│ ➤ Western blotting    │ │         VAD-fmk         │  └──────────────────┘
│ ➤ Caspase-3, -8       │ │ Necrosis : Necrostatin-1,│
│ ➤ Substrates: PARP    │ │     RIPK3 inhibitor     │
└──────────────────────┘  └─────────────────────────┘
                                  │
                                  ▼
                      ┌─────────────────────────┐
                      │        Microscopy       │
                      │ ➤ Cell counting         │
                      │ ➤ Trypan Blue staining  │
                      └─────────────────────────┘
```

Fig. 3 Overview of methods for cell death analysis: Cell death can be classified into two main routines: apoptosis and necrosis, which can be blocked by specific inhibitors. The detection can be facilitated through FACS, microscopy, or protein cleavage quantification

2.1 Cell Culture

1. Fetal bovine serum (FBS).

2. Phosphate-buffered saline (PBS).

3. Dialysing membrane (MWCO 7000).

4. Syringe filter (0.22 μm).

5. DMEM: pyruvate-free, 25 mM Glucose, supplemented with 2 mM L-glutamine.

6. DMEM: pyruvate-free, 0 mM Glucose, supplemented with 2 mM L-glutamine.

2.2 Drugs

1. 2-Deoxyglucose (2-DG).

2. Q-VD-OPH (Q-VD).

3. Z-VAD-fmk (Z-VAD).

4. Ac-Y-VAD-cmk (Y-VAD).

5. Necrostatin-1 (Nec-1).

6. GSK 872 (RIPK3 inhibitor).

7. Trypan Blue Solution.

8. Inverted Microscope.

9. Neubauer cell counting chamber.

10. Software ImageJ.

2.3 Materials for Western Blot Analysis

2.3.1 Reagents

1. Phosphate-Buffered Saline (PBS).

2. Trypsin-EDTA (0.05%).

3. RIPA buffer: 25 mmol/L Tris–HCl (pH 7.6), 150 mM NaCl, 1% NP-40, 1% sodium deoxycholate, 0.1% SDS supplemented with protease inhibitors and phosphatase inhibitors.

4. 4× Laemmli buffer: 63 mM Tris–HCl; 10% glycerol; 2% SDS; 0.01% bromophenol blue; 5% β-mercaptoethanol.

5. BCA Protein Assay.

6. SDS-PAGE Running buffer: 0.025 M Tris–HCl, 0.192 M glycine, 0,1% SDS.

7. Western blot Transfer buffer: 0.025 M Tris–HCL 0.192 M glycine, 20% methanol.

8. Tris-buffered saline containing 0.05% Tween-20 (TBST): 0.01 M Tris–HCl, 0.15 NaCl.

9. Nitrocellulose membrane.

10. Ponceau S. staining.

11. Odyssey blocking solution.

2.3.2 Antibodies

Primary: Caspase-3, Caspase-8, PARP.
  Secondary: Rabbit Alexa Fluor 568, Mouse Alexa Fluor 647.

2.4 Materials for FACS

1. Phosphate-buffered saline (PBS).

2. Trypsin-EDTA (0.05%).

3. Propidium Iodide.

4. Gallios Flow Cytometer Beckman Coulter.

5. Software Flow Jo.

3 Methods

3.1 Dialyzing FBS

1. Inactivate FBS by heating up to 57 °C for 30 min. Allow it to cool down to room temperature.

2. Warm up the dialyzing membrane to 60 °C for 30 min in a water bath or wash as recommended by the manufacturer.

3. Close the membrane with a knot or an appropriate clip at one side and add 100 mL of inactivated FBS in the pipe. Close the other end of the pipe with a further knot or clip (*see* **Note 1**).

4. Wash the pipe twice for one hour in 1 L PBS at 4 °C while stirring. Afterward, wash another time with PBS overnight at 4 °C, stirring.

5. Filtrate dialyzed FBS (dFBS) sterile using a 0.22 μm syringe filter.

3.2 Glucose Deprivation

1. Plate A549 cells (300,000 cells/well) in a 6-well plate in pyruvate-free DMEM containing 25 mM glucose, 10% FBS and supplemented with 2 mM L-glutamine.

2. Treat cells at a confluence of 80% 24 h after plating (*see* **Note 2**). Wash cells twice with pyruvate-free DMEM without glucose to remove remaining glucose.

3. Add 2 mL of pyruvate-free DMEM without glucose containing 10% FBS and supplement with 2 mM L-glutamine and incubate for up to 72 h at 37 °C in the incubator. Long term experiments would require plating the cells at low concentrations to avoid overgrowth in the controls. Alternatively, a low-density control culture should be used in parallel.

3.3 Treatment with Metabolic Drugs

1. Plate cells as described above and treat them 24 h after plating with 2-DG (*see* **Note 3**) in pyruvate-free DMEM containing 25 mM glucose, 10% FBS and supplemented with 2 mM L-glutamine.

2. Analyze cell death up to 72 h post-treatment with methods indicated below.

3.4 Treatment with Cell Death Inhibiting Drugs

1. Plate and treat cells upon glucose deprivation as described above.

2. Add the inhibitor of interest at the same time point as the glucose deprivation treatment. If cell death is fast (less than 12 h), the inhibitors can be preincubated for 1 h.

3. Use Q-VD at a concentration of 10 μM and Z-VAD at 20 μM.

4. Use Nec-1 at 40 and 100 μM and the GSK 872 at a concentration of 1 and 3 μM (*see* **Note 4**).

5. Analyze cell death between 48 and 72 h after treatment with methods indicated below.

3.5 Cell Death Analysis by Microscopy

Cell death is detectable through different approaches (Fig. 3). The easiest and fastest method to detect cell death in a cell population is by using the microscope. Dying cells are clearly distinguishable from healthy cells through their morphology which is characterized by the appearance of apoptotic bodies, rounding, detachment, and loss of refringent appearance (Fig. 1). Furthermore, counting dead cells by microscopic examination is the more precise method to analyze cell death in adherent cell cultures. The reason is cells do not have to be harvested and cell death induced by the protocol is excluded. Additional staining of cells with Trypan Blue Solution after trypsinization dyes dead cells blue and cell death can be quantified by counting total and dead cells with a Neubauer cell counting chamber. Use positive controls for cell death induction (*see* **Note 5**).

1. Plate cells in 6-well plates the day before treatment and let them grow to 80% confluence (described above).

2. Treat cells (described above) and take at least three pictures of different areas of the culture plate.

3. Use ImageJ software or count detached cells manually and calculate the corresponding percentage.

   Alternatively, or in parallel, use Trypan Blue Staining:

4. Transfer the supernatant to a tube.

5. Wash attached cells with PBS. Incubate attached cells for 5 min with 500 μL Trypsin-EDTA (0.05%) and resuspend cells in 1 mL of DMEM (pyruvate-free, 10% FBS, supplemented with 2 mM L-glutamine).

6. Combine supernatant and trypsinized cells and centrifuge for 5 min at 450 rcf and room temperature.

7. Resuspend cell pellet in 1 mL DMEM containing 10% FBS, 25 mM glucose and supplement with 2 mM L-glutamine.

8. Dilute 10 μL of cell suspension in 10 μL of Trypan Blue Solution and use a Neubauer cell counting chamber according to the manufacturer's instructions. If needed, adjust cell number by diluting cell suspension.

9. Total cell number and blue stained cells are counted and percentage of cell death is calculated.

3.6 Cell Death Analysis by Western Blot of Caspases or Caspase Substrates

Another approach is to analyze caspase cleavage through performance of western blots and further quantification of the protein expression of pro-caspase 3 or 8 and their cleaved forms as well as by detecting the cleaved form of the caspase substrate Poly (ADP-ribose) polymerase (PARP).

Before starting the experiment prepare complete RIPA lysis buffer by adding protease and phosphatase inhibitors according to the manufacturer's instructions.

1. Treat and harvest cells as described above. Wash once with PBS.

2. Resuspend cell pellet in 30 μL RIPA buffer completed with protease and phosphatase inhibitors.

3. Sonicate cell lysate to guarantee complete cell membrane rupture and DNA disruption.

4. Quantify protein concentration by BCA or Bradford Protein Assay according to the manufacturer's instructions.

5. Heat samples containing 40 μg of protein in a final volume of 40 μL in 4× Laemmli Buffer up to 95 °C for 10 min.

6. Load samples on a 12% SDS gel (10% recommended for PARP) and add 500 mL of Running buffer.

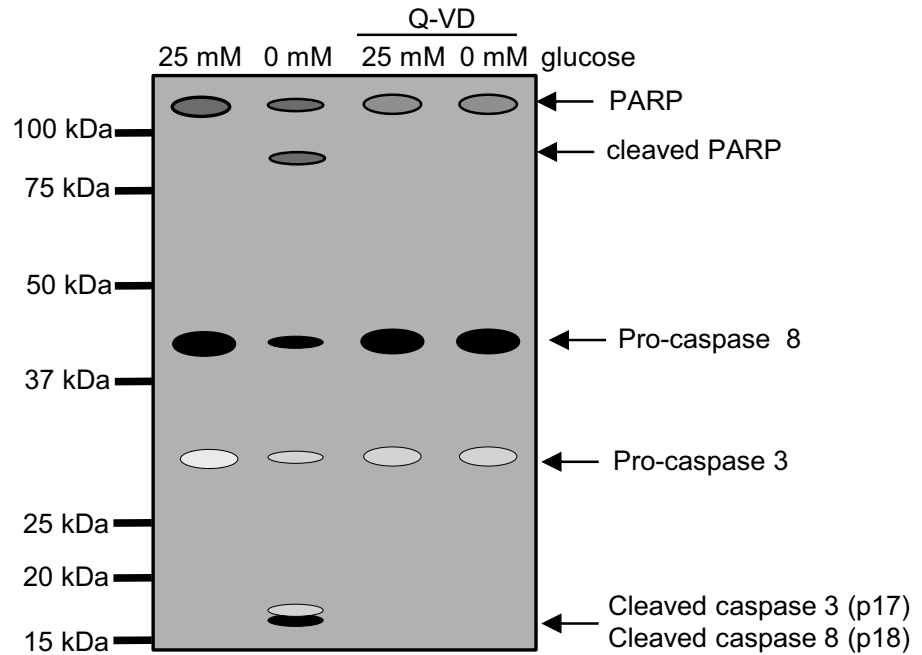7. Run SDS PAGE at 120 V for 1.5 h.

Fig. 4 Schematic representation of western blot for Caspase-8, -3 and its substrate PARP. Cells were incubated for 48 h in DMEM with 25 mM or 0 mM glucose. Right lanes, cells incubated in the presence of Q-VD 20 μM

8. Transfer proteins to nitrocellulose membrane using Transfer buffer.

9. Check quantitative protein transfer by incubating membrane for 2 min with Ponceau S. Staining.

10. Remove dye by washing several times for 5 min with TBST. Repeat until dye is completely removed.

11. Block membrane in 5% milk and TBST for 1 h at room temperature.

12. Incubate with primary antibody diluted 1:1000 in Blocking buffer overnight at 4 °C while shaking.

13. Wash membranes 3 times for 5 min with TBST.

14. Incubate with fluorescent secondary antibodies diluted 1:15,000 with TBST and 5% milk for 1–2 h at room temperature in agitation.

15. Wash membranes 3 times for 10 min with TBST and develop them using the *Odyssey Infrared Imaging System* (Fig. 4) (*see* **Note 6**).

3.7 Cell Death Analysis by FACS

Another possibility to measure quantitative cell death is to detect membrane alterations like the phosphatidylserine translocation which can be detected by Annexin-V binding, as described elsewhere [4] Alternatively, using propidium iodide (PI) would allow cell death measurement thanks to its ability to intercalate in the DNA of dying cells. The resulting emission can be detected
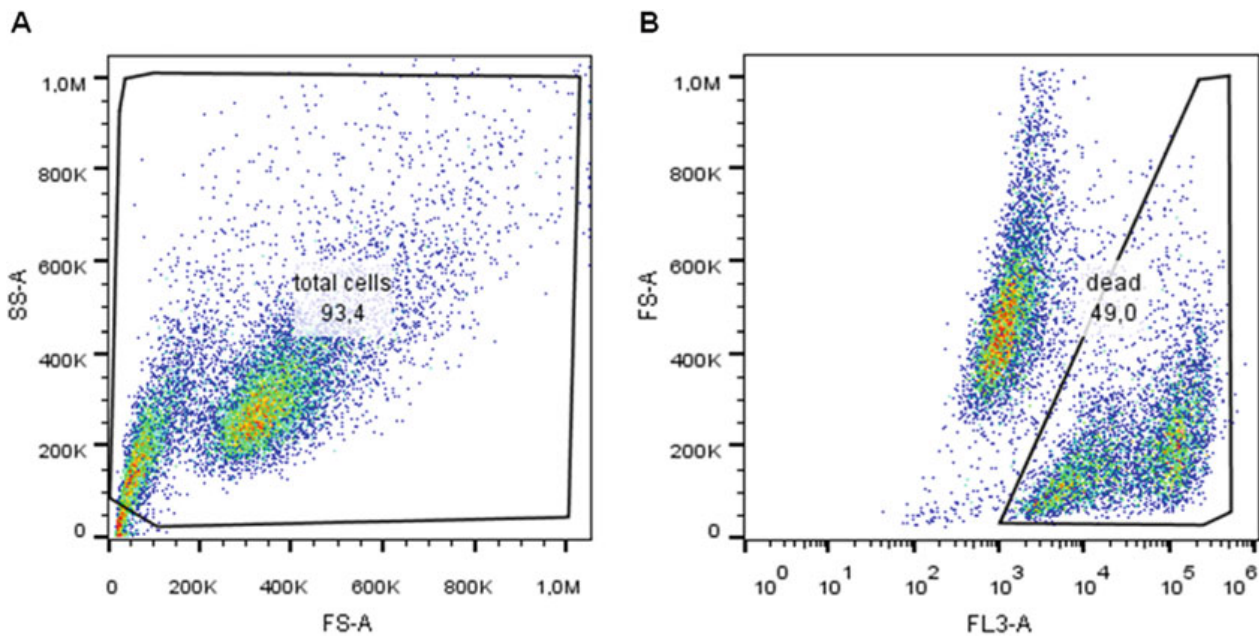
Fig. 5 Flow Jo analysis of cell death by PI staining. (**a**) Total cell population presented as SS-A versus FS-A. (**b**) FS-A is plotted versus FL-3 and dead cell population is gated

through a photodetector between 550 and 700 nm at the fluorescence-activated cell sorter (FACS). Since PI can only cross the permeable membranes of dead cells, quantification can be done through measuring total cell count and PI positive cells. This form of cell death analysis is very accurate, reproducible and allows detecting even small amounts of dead cells.

1. Treat cells as described above.

2. Wash cells once with PBS and trypsinize with 500 μL of 0.05% of Trypsin-EDTA.

3. Combine supernatant and cell suspension in a FACS tube and centrifuge for 7 min at 450 rcf at room temperature.

4. Discard the supernatant and resuspend cell pellet in 300 μL of PBS containing 0.5 μg/mL PI.

5. Measure cell death after 10 min incubation using the *Gallios Flow Cytometer Beckman Coulter.*

6. Analyze data using *FlowJo* (Fig. 5).

7. Plot data side scattered (SS-A) versus foward scattered (FS-A) and gate the total cell population excluding cell debris (particles approximately 10 times smaller than untreated cells) (Fig. 5a). Apply the gate to all samples.

8. Plot FS-A versus FL3-A (red-channel) and measure dead cells (Fig. 5b). Apply for all samples.

4   Notes

1. Avoid bubbles to guarantee a complete dialysis.

2. Keep the cell concentration consistent. Starvation can induce very different cell numbers when cells are grown at high or low density.

3. 2-DG concentrations for treatment range between 2 and 10 mM depending on the cell line.

4. Effective inhibitor concentrations can vary between different cell lines.

5. Use positive controls when measuring cell death. Classical apoptotic inducers are serum removal and most chemotherapeutic drugs. Classical necrotic inducers are freeze-thaw and high H_2O_2 (between 33 and 66 μM) [5].

6. Other bands may appear due to internal caspase cleavage. Depending on the stimulus, QVD may not protect fully from the production of the small fragment of caspase-3 and other bands accumulate instead at 19–20 kDa apparent molecular weight.

References

1. Villa E, Ricci JE (2016) How does metabolism affect cell death in cancer? FEBS J 283 (2016):2653–2660

2. Caro-Maldonado A, Muñoz-Pinedo C (2011) Dying for Something to Eat: How Cells Respond to Starvation. Open Cell Signal J 3:42–51

3. Galluzzi L, Bravo-San Pedro JM, Vitale I et al (2015) Essential versus accessory aspects of cell death: Recommendations of the NCCD 2015. Cell Death Differ 22:58–73

4. Logue SE, Elgendy M, Martin SJ (2009) Expression, purification and use of recombinant annexin V for the detection of apoptotic cells. Nat Protoc 4:1383–1395

5. Leõn-Annicchiarico CL, Ramírez-Peinado S, Domínguez-Villanueva D et al (2015) ATF4 mediates necrosis induced by glucose deprivation and apoptosis induced by 2-deoxyglucose in the same cells. FEBS J 282:3647–3658

Spotlight

In the Hunger Games, the Winner Takes Everything

Franziska Püschel[1] and Cristina Muñoz-Pinedo[1],*,@

Entosis is an atypical form of cell death that occurs when a cell engulfs and kills another cell. A recent article by Overholtzer and colleagues indicates that glucose deprivation promotes entosis. AMP-activated protein kinase (AMPK) activation in the loser cells triggers their engulfment and elimination by winner cells, which endure starvation.

Cells in our bodies are constantly dying and being replaced by new cells. The best understood form of regulated cell death is apoptosis. However, other forms of cell death are pathologically and physiologically relevant in certain contexts. In some cases, cell death is actively engaged from within the cell, which senses that it is damaged or aged. These subroutines of cell death include the mitochondrial apoptotic pathway and can be called suicide. In other cases, cells die when they are attacked by the immune system that senses that they are infected, and are, thus, usually, 'murdered'. This includes granzyme- and death-receptor-mediated apoptosis, and perforin-mediated necrosis. However, other intriguing and understudied cell death routines involve the killing of living cells that are selected and phagocytosed by professional phagocytes (phagoptosis, [1]) or by a neighboring epithelial cell (entosis). These forms of cell death could be labeled as 'cannibalism'.

Entosis is a particularly intriguing process by which a perfectly viable living cell is eaten and killed by an epithelial cell [2]. Entotic structures are detected in human carcinomas, and this observation suggested that entosis could represent a form of competition between cancer cells. This competition involves a winner and a loser cell, and the winner status has been shown to be conferred by oncogenes such as *KRas* [3]. The winner versus loser status is dictated by mechanical deformability, with the loser cell being stiffer and becoming entrapped by the softer cell that engulfs it.

In a recent article, Hamann *et al.* examined whether the frequency of entotic events in culture could be enhanced by starvation [4]. The group had previously shown that during entosis, recovery of amino acids from entotic corpses contributes to nutrient balance [5]. However, amino acid deprivation did not promote entosis. In contrast, the authors now show that glucose deprivation greatly increased the number of entotic events. Moreover, the time between engulfment and death of the internalized cells was reduced under glucose deprivation.

Glucose deprivation has been shown to induce cell death in several manners, and in many cases simultaneously. Indeed, in the culture conditions employed by Hamann *et al.* [4], some MCF-7 cells died by apoptosis or necrosis along with entosis. However, inhibition of entosis by deleting *E-cadherin*, which had been shown to mediate this process, reduced the total number of dead cells. Deletion of *E-cadherin* or inhibition of rho-associated protein kinase (ROCK) also increased the percent of necrotic versus apoptotic cells, which suggests interplay between necrosis and entosis. As shown before for spontaneous entosis, LC3, which is involved in autophagy and in phagocytosis of corpses, decorated entotic vesicles. Another similarity with autophagy was that silencing ATG5, a protein involved in autophagy vesicle formation, reduced the number of engulfed cells that could not escape and underwent cell death.

Although the effects of silencing ATG5 on the percent cell death in the whole population were not addressed, this reinforces the notion that macroautophagy does not promote survival of glucose-deprived cells [6]. Interestingly, however, entosis did support proliferation of the winner cells. Moreover, entosis promoted multinucleation and aneuploidy in the population (Figure 1), suggesting that starvation can promote aneuploidy by inducing entosis, and thus contribute to tumor promotion.

Perhaps the most intriguing finding is what determines whether a cell eats or gets eaten. The authors investigated AMPK, the ATP/AMP sensor, and found that the cells that activate it are the ones that turn 'stiffer' and get eaten as a consequence [4]. In fact, activation of AMPK is sufficient to enhance the frequency of entosis in the presence of glucose. The question remains whether, under glucose deprivation, the cells that activate AMPK are more stressed; perhaps because of the cell cycle stage that they are in – or whether both populations, winners and losers, undergo the same levels of energetic stress but stochastically activate AMPK differently. Even clonal cell populations in culture are heterogeneous, and in this case, detecting energy failure is lethal.

Several questions arise regarding the evolution and consequences of entosis in this context. Why does AMPK activation promote entosis: is this somehow linked to phagocytosis? It should be mentioned that AMPK is an evolutionarily conserved signal of infection: numerous publications link AMPK activation to viral infection, while AMPK is activated via transforming growth factor β-activated kinase 1 (TAK1) downstream of immune cytokines [7]. This suggests that detection of loss of ATP could be evolutionarily linked to detection of infection, and to immune function, and perhaps it is a signal that promotes phagocytosis by neighboring cells. Follow-up questions in the
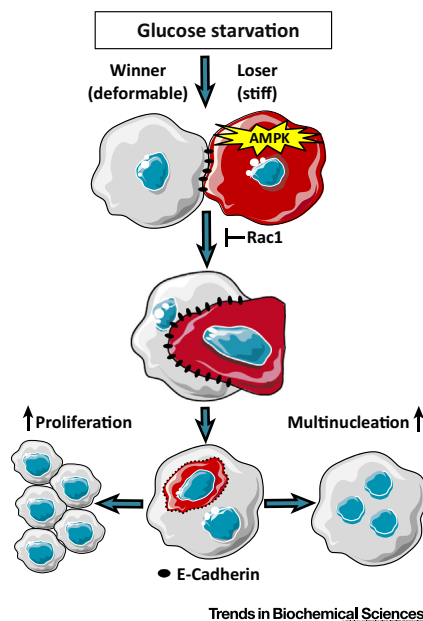
Figure 1. Glucose Starvation Promotes Entosis Mediated by AMPK Induction. Metabolic stress induced by glucose starvation results in induction of entosis. This is mediated by activation of the energy sensor AMPK in the loser cells accompanied by a stiffer cell phenotype. In contrast, winner cells show a more deformable phenotype after glucose starvation. Entosis is facilitated by ROCK signaling and can be blocked by Rac1 induction. Subsequent engulfment of loser cells supports winner cells with nutrients promoting multinucleation, proliferation and survival. AMPK, AMP-activated protein kinase; ROCK, rho-associated protein kinase.

context of entosis include: does AMPK promote exposure and/or secretion of 'eat me' signals? Which classical eat me signals are associated with entosis? How is AMPK linked to the mechanical changes involved in entosis? The recent finding that AMPK participates in mechanotransduction should help clarify mechanistic details [8].

Metabolic stress, and particularly, glucose starvation, has been shown to promote several different forms of cell death, ranging from necrosis to atypical necroptosis or mitochondrial apoptosis, and more recently, death-receptor-mediated apoptosis [9,10]. We should now add cannibalism to the list of typical and atypical cell death subroutines engaged by lack of nutrients.

[1]Cell Death Regulation Group, Oncobell Program, Bellvitge Biomedical Research Institute (IDIBELL), Barcelona, Spain
@Twitter: @apoptosislab

*Correspondence: cmunoz@idibell.cat (C. Muñoz-Pinedo).

References
1. Brown, G.C. and Neher, J.J. (2012) Eaten alive! Cell death by primary phagocytosis: 'phagoptosis'. *Trends Biochem. Sci.* 37, 325–332
2. Overholtzer, M. *et al.* (2007) A Nonapoptotic cell death process, entosis, that occurs by cell-in-cell invasion. *Cell* 131, 966–979
3. Sun, Q. *et al.* (2012) Competition between human cells by entosis. *Cell Res.* 24, 1299–1310
4. Hamann, J.C. *et al.* (2017) Entosis is induced by glucose starvation. *Cell Rep.* 20, 201–210
5. Krajcovic, M. *et al.* (2013) mTOR regulates phagosome and entotic vacuole fission. *Mol. Biol. Cell* 24, 3736–3745
6. Ramirez-Peinado, S. *et al.* (2013) Glucose-starved cells do not engage in prosurvival autophagy. *J. Biol. Chem.* 288, 30387–30398
7. Hardie, D.G. (2011) AMP-activated protein kinase: an energy sensor that regulates all aspects of cell function. *Genes Dev.* 25, 1895–1908
8. Bays, J.L. *et al.* (2017) Linking E-cadherin mechanotransduction to cell metabolism through force-mediated activation of AMPK. *Nat. Cell Biol.* 19, 724–731
9. Ding, B. *et al.* (2016) Sestrin2 is induced by glucose starvation via the unfolded protein response and protects cells from non-canonical necroptotic cell death. *Sci. Rep.* 6, 22538
10. Iurlaro, R. *et al.* (2017) Glucose deprivation induces ATF4-mediated apoptosis through TRAIL death receptors. *Mol. Cell Biol.* 37, e00479–16